

UCLA

UCLA Electronic Theses and Dissertations

Title

Modifiable and Protein-Stabilizing Polymers Prepared Using Controlled Polymerization Techniques

Permalink

<https://escholarship.org/uc/item/6zp0m84g>

Author

Pelegri-O'Day, Emma

Publication Date

2018

Peer reviewed|Thesis/dissertation

UNIVERSITY OF CALIFORNIA

Los Angeles

Modifiable and Protein-Stabilizing Polymers Prepared
Using Controlled Polymerization Techniques

A dissertation submitted in partial satisfaction of the
requirements for the degree Doctor of Philosophy
in Chemistry

by

Emma Pelegri-O'Day

2018

© Copyright by
Emma Pelegri-O'Day
2018

ABSTRACT OF THE DISSERTATION

Modifiable and Protein-Stabilizing Polymers Prepared
Using Controlled Polymerization Techniques

by

Emma Pelegri-O'Day

Doctor of Philosophy in Chemistry

University of California, Los Angeles, 2018

Professor Heather D. Maynard, Chair

Even after significant advances in polymerization and protein modification chemistries, the majority of polymeric biomaterials focus on poly(ethylene glycol) (PEG)-based monomers. Despite their widespread use, these polymers present concerns due to their non-biodegradable nature, the possibility of toxicity and immunogenicity, and their limited chemical functionality. Therefore, there is significant interest in the rational design of alternative polymers with specific chemical or biological properties. Specifically, approaches that allow for the rapid and divergent synthesis of a large number of biodegradable polymeric materials capable of functionalization would be broadly applicable. This dissertation focuses on novel degradable and modifiable polymers with applications in protein conjugation and stabilization.

In Chapter 1, the history of protein-polymer conjugates for therapeutic use is outlined, from PEGylation techniques to next-generation conjugation strategies. Alternative polymer

technologies and future directions of the field are also presented. In Chapter 2, the synthesis and biological application of a degradable trehalose glycopolymer is described. The polymer is shown to stabilize the therapeutic protein granulocyte colony stimulating factor (G-CSF) against heat stress. While the polymer was noncytotoxic, its degradation products inhibited cell proliferation at high concentrations.

Chapter 3 details the development of poly(caprolactone)-based polyesters for protein stabilization. An alkene-substituted polyester was synthesized and modified using thiol-ene chemistry with thiols containing glucose, lactose, trehalose, PEG, and carboxybetaine units. The relative stabilizing ability of these side-chains toward G-CSF was assessed. Trehalose and carboxybetaine were found to maintain the most protein activity upon exposure to heat stress. We varied the size of these polymers and found a dependence on molecular weight, where longer polymers were more effective protein stabilizers. These materials and their degradation products were cytocompatible, yet exhibited minimal degradation in aqueous conditions. Chapter 4 describes the synthesis of trehalose- and carboxybetaine-functionalized polyesters and polycarbonates with tunable degradability, with half-lives from 10 hours to over 4 months. We expect these materials will be useful in the development of novel protein-polymer therapeutics.

We also describe the development of novel PEG analogs using ring-opening metathesis polymerization (ROMP). Chapter 5 describes the synthesis of these PEG analogs and subsequent conjugation to the model protein lysozyme. Exploration of post-polymerization modifications to install thiols onto the unsaturated polymer backbone are also described.

The dissertation of Emma Pelegri-O'Day is approved.

Timothy J. Deming

Stephanie K. Seidlits

Heather D. Maynard, Committee Chair

University of California, Los Angeles

2018

*If you don't have time to do it right,
when will you have time to do it over?*

- John Wooden

TABLE OF CONTENTS

Abstract of the Dissertation.....	ii
Table of Contents.....	vi
List of Figures.....	x
List of Tables.....	xvi
List of Schemes	xvii
List of Abbreviations	xviii
Acknowledgements.....	xxiii
Vita.....	xxvi

Chapter 1. Rational Design for the Improvement of Therapeutic Protein Delivery:

Advancing Beyond PEG	1
1.1. Introduction.....	2
1.2. PEG Conjugates	2
1.3. Advances in Protein Conjugation Chemistry.....	4
1.3.1. Straight-Chain PEG Conjugates	4
1.3.2. New Polymeric Methods for Bioconjugation.....	7
1.4. Alternatives to PEG in Development	11
1.4.1. Known Biocompatible Polymers.....	12
1.4.2. Degradable PEG Alternatives	13
1.4.3. PEG Alternatives with Varied Architectures	16
1.5. Protein Therapeutics of the Future	18

1.5.1. Biomimetic Polymer Design	18
1.5.2. Precise Sequence Control and Monodispersity	21
1.5.3. Protein-‘Polymer’ Conjugates by Genetic Fusion.....	22
1.6. Summary.....	23
1.7. References.....	24

Chapter 2. Synthesis of Degradable Trehalose Polymers via Copolymerization of Cyclic

Ketene Acetals.....	36
2.1. Introduction.....	37
2.2. Results	38
2.2.1. Polymer Synthesis and Characterization	38
2.2.2. Cytocompatibility of Degradable Trehalose Polymers.....	42
2.2.3. Stabilization of Granulocyte Colony Stimulating Factor.....	45
2.3. Conclusions.....	48
2.4. Experimental	49
2.4.1. Materials.....	49
2.4.2. Analytical Techniques	49
2.4.3. Methods.....	50
2.5. Appendix with Supplementary Figures	55
2.6. References.....	57

Chapter 3. Substituted Polyesters by Thiol–Ene Modification: Rapid Diversification for

Therapeutic Protein Stabilization	61
--	-----------

3.1. Introduction.....	62
3.2. Results	64
3.2.1. Synthesis of a Library of Functionalized Polyesters	66
3.2.2. Assessment of Stabilizing Ability	71
3.2.3. Testing of Different Molecular Weights and Comparison to Common Excipients	74
3.2.4. Degradation, Biological Compatibility, TEM, and DSC Analysis of the Polymers.....	82
3.3. Discussion.....	86
3.4. Conclusions.....	89
3.5. Experimental.....	90
3.5.1. Materials.....	90
3.5.2. Analytical Techniques	90
3.5.3. Methods.....	91
3.6. Appendix with Supplementary Figures.....	101
3.7. References.....	128

Chapter 4. Polymers with Tunable Degradability and Zwitterionic or Trehalose Side

Chains via Ring-Opening Polymerization.....	134
4.1. Introduction.....	135
4.2. Results and Discussion	137
4.2.1. Polymer Synthesis	137
4.2.2. Degradation Studies.....	142
4.3. Conclusions.....	147
4.4. Materials and Methods	149

4.4.1. Materials.....	149
4.4.2. Analytical Techniques	149
4.4.3. Methods.....	150
4.5. Appendix with Supplementary Figures	156
4.6. References.....	165
Chapter 5. Protein-Reactive Unsaturated PEG Analogs by ROMP	168
5.1. Introduction.....	169
5.2. Results and Discussion	171
5.2.1. Polymer Synthesis	171
5.2.2. Protein Conjugation.....	174
5.2.3. Efforts Toward rPEG Chemical Modification	175
5.3. Conclusions.....	179
5.4. Materials and Methods	181
5.4.1. Materials.....	181
5.4.2. Analytical Techniques	181
5.4.3. Methods.....	182
5.5. Appendix with Supplementary Figures	186
5.6. References.....	196

LIST OF FIGURES

Figure 1-1. Advances in protein-polymer conjugation chemistry	4
Figure 1-2. Examples of second-generation site-selective protein PEGylation using oxime “click” chemistry	6
Figure 1-3. Synthetic erythropoiesis protein with a) structure of branched, negatively charged PEG-like polymer b) schematic of resulting PEGylated protein.....	7
Figure 1-4. Schematic presenting significant “grafting from” methods	10
Figure 1-5. PEG-like polymers with degradable backbones	13
Figure 1-6. Examples of alternatives to PEG currently in use and development.	15
Figure 1-7. Examples of stabilizing and biomimetic polymers.....	20
Figure 2-1. Gel permeation chromatograms of p(BMDO-co-bMA), p(BMDO-co-BMA-trehalose-OAc), and p(BMDO-co-BMA-trehalose)	40
Figure 2-2. Degradation of p(BMDO-co-BMA-trehalose) after 0, 24, and 72 hours in 5% KOH	41
Figure 2-3. Structure of control polymer p(styrenyl acetal trehalose).....	42
Figure 2-4. Cytotoxicity assay of p(BMDO-co-BMA-trehalose) before and after degradation and benzyl trehalose in a) HDFs with benzyl trehalose and in NFS-60 cells with p(styrenyl acetal trehalose) based on b) cell viability by LIVE/DEAD assay and c) cell proliferation...	44
Figure 2-5. Bioactivity of G-CSF without any additive or with 1, 10, 100, or 500 weight equivalents of excipient to protein without heating (untreated) and with heating (treated) to 40 °C for 30 minutes.....	46

Figure 2-6. Bioactivity of G-CSF after heating with polymer excipients, p(styrenyl acetal trehalose) and p(BMDO-co-BMA-trehalose), presented as the percent activity relative to the unheated sample containing polymer excipient.....	47
Figure 2-7. ¹ H-NMR spectrum of p(BMDO-co-bMA).....	55
Figure 2-8. ¹ H-NMR spectrum of p(BMDO-co-BMA-trehalose-OAc)	55
Figure 2-9. ¹ H-NMR spectrum of p(BMDO-co-BMA-trehalose).....	56
Figure 3-1. Illustrative scheme of pCL backbone and modification with thiols using thiol-ene chemistry to produce a small library of degradable polymers.....	66
Figure 3-2. Characterization of trehalose modification of pCL using thiol-ene chemistries. a) The ¹ H-NMR traces before and after modification. b) GPC characterization of pCL-allyl40 before and after modification.....	69
Figure 3-3. Effect of side chain identity on stabilization of G-CSF at pH 4.0 to a) storage conditions at 4 °C for 90 minutes and b) thermal stress at 60 °C for 30 minutes.	72
Figure 3-4. Comparison of a) gel permeation chromatogrpahy (DMF) and b) size exclusion chromatography (aqueous) traces for pCL-trehalose ₈₀	76
Figure 3-5. a) Effect of pCL-trehalose molecular weight on G-CSF stabilization at pH 4.0 to storage at 4 °C for 90 minutes. b) G-CSF stabilization to thermal stress at 60 °C for 30 minutes. Data shown as the average of six experimental repeats and six well repeats with standard deviation. c) Effect of pCL-zwitterion molecular weight on G-CSF stabilization at pH 4.0 to storage at 4 °C for 90 minutes. d) G-CSF stabilization to thermal stress at 60 °C for 30 minutes.	77
Figure 3-6. Dependence on G-CSF stabilization on polymeric equivalents of pCL-trehalose ₄₀ and pCL-zwitterion ₄₀ against heating at 60 °C for 30 minutes.....	79

Figure 3-7. Stabilization of G-CSF against thermal stress at 60 °C for 30 minutes and comparison of pCL-trehalose ₈₀ and pCL-zwitterion ₈₀ with relevant small molecule controls ...	80
Figure 3-8. Timecourse of G-CSF activity in the presence of 100 weight equivalents of pCL-trehalose ₈₀ and pCL-zwitterion ₈₀ when heated at 60 °C.....	81
Figure 3-9. Size exclusion chromatogram of the degradation of a) pCL-trehalose ₁₀ and b) pCL-zwitterion ₂₀	82
Figure 3-10. Size exclusion chromatograms of pCL-trehalose ₄₀ and pCL-zwitterion ₄₀ before and after exposure to pH 4.0 at 60 °C for 30 minutes.	83
Figure 3-11. Cytotoxicity assay of pCL-trehalose ₂₀ , pCl-zwitterion ₂₀ , and their basic degradation products with HUVECs.....	84
Figure 3-12. Transmission electron micrographs of a) pCL-trehalose ₈₀ b) pCL-zwitterion ₈₀ c) pCL-trehalose ₈₀ and G-CSF mixture d) pCL-zwitterion ₈₀ and G-CSF mixture.	85
Figure 3-13. ¹ H-NMR spectrum of tosylated trehalose heptaacetate 2	101
Figure 3-14. ¹³ C-NMR spectrum of tosylated trehalose heptaacetate 2	102
Figure 3-15. COSY spectrum of tosylated trehalose heptaacetate 2	102
Figure 3-16. ¹ H-NMR spectrum of thioacetylated trehalose heptaacetate 3	103
Figure 3-17. ¹³ C-NMR spectrum of thioacetylated trehalose heptaacetate 3	103
Figure 3-18. ¹ H-NMR spectrum of crude unpurified thiolated trehalose heptaacetate A	104
Figure 3-19. ¹³ C-NMR spectrum of thiolated trehalose heptaacetate A	104
Figure 3-20. ¹ H-NMR spectrum of pCL-allyl ₁₀	105
Figure 3-21. ¹ H-NMR spectrum of pCL-allyl ₂₀	106
Figure 3-22. ¹ H-NMR spectrum of pCL-allyl ₄₀	107

Figure 3-23. ¹ H-NMR spectrum of pCL-allyl ₈₀	108
Figure 3-24. Gel permeation chromatograms of pCL-allyl ₂₀ , pCL-allyl ₄₀ , pCL-allyl ₈₀	109
Figure 3-25. Matrix-assisted laser desorption/ionization (MALDI) chromatogram of pCL-allyl ₁₀	109
Figure 3-26. ¹ H-NMR spectrum of pCL-trehaloseOAc ₁₀	110
Figure 3-27. ¹ H-NMR spectrum of pCL-trehaloseOAc ₂₀	111
Figure 3-28. ¹ H-NMR spectrum of pCL-trehaloseOAc ₄₀	112
Figure 3-29. ¹ H-NMR spectrum of pCL-trehaloseOAc ₈₀	113
Figure 3-30. ¹ H-NMR spectrum of pCL-glucoseOAc ₄₀	114
Figure 3-31. ¹ H-NMR spectrum of pCL-lactoseOAc ₄₀	115
Figure 3-32. Gel permeation chromatograms of pCL-trehaloseOAc ₁₀ , pCL-trehaloseOAc ₂₀ , pCL-trehaloseOAc ₄₀ , pCL-trehaloseOAc ₈₀	116
Figure 3-33. Gel permeation chromatograms of pCL-glucoseOAc ₄₀ , pCL-lactoseOAc ₄₀ ...	116
Figure 3-34. ¹ H-NMR spectrum of pCL-trehalose ₁₀	117
Figure 3-35. ¹ H-NMR spectrum of pCL-trehalose ₂₀	118
Figure 3-36. ¹ H-NMR spectrum of pCL-trehalose ₄₀	118
Figure 3-37. ¹ H-NMR spectrum of pCL-trehalose ₈₀	119
Figure 3-38. Gel permeation chromatograms of pCL-trehalose ₁₀ , pCL-trehalose ₂₀ , pCL-trehalose ₄₀ , pCL-trehalose ₈₀	119
Figure 3-39. Thermal gravimetric analysis (TGA) chromatogram of pCL-trehalose ₂₀	120
Figure 3-40. ¹ H-NMR spectrum of pCL-glucose ₄₀	121
Figure 3-41. ¹ H-NMR spectrum of pCL-lactose ₄₀	122
Figure 3-42. ¹ H-NMR spectrum of pCL-PEG ₄₀	123

Figure 3-43. ¹ H-NMR spectrum of pCL-zwitterion ₁₀	124
Figure 3-44. ¹ H-NMR spectrum of pCL-zwitterion ₂₀	125
Figure 3-45. ¹ H-NMR spectrum of pCL-zwitterion ₄₀	125
Figure 3-46. ¹ H-NMR spectrum of pCL-zwitterion ₈₀	126
Figure 3-47. Gel permeation chromatograms of pCL-glucose ₄₀ , pCL-lactose ₄₀ , pCL-PEG ₄₀	126
Figure 3-48. Size exclusion chromatograms of pCL-zwitterion ₁₀ , pCL-zwitterion ₂₀ , pCL- zwitterion ₄₀ , pCL-zwitterion ₈₀	127
Figure 4-1. Stability of pLA-allyl after TFA treatment as measured by GPC	141
Figure 4-2. SEC chromatogram of the DPBS degradation of a) and b) pC-zwitterion and c) and d) pLA-zwitterion	144
Figure 4-3. Degradation kinetics of pX-zwitterion polymers as percent original molecular weight over time	145
Figure 4-4. Enzymatic treatment of pCL-zwitterion using immobilized lipase B	146
Figure 4-5. ¹ H-NMR spectrum of zwitterion disulfide 4	156
Figure 4-6. ¹³ C-NMR spectrum of zwitterion disulfide 4	157
Figure 4-7. ¹ H-NMR spectrum of zwitterion thiol 5	157
Figure 4-8. ¹³ C-NMR spectrum of zwitterion thiol 5	158
Figure 4-9. ¹ H-NMR spectrum of pLA-allyl.....	158
Figure 4-10. ¹ H-NMR spectrum of pMAC.....	159
Figure 4-11. ¹ H-NMR spectrum of pC-zwitterion.....	160
Figure 4-12. ¹ H-NMR spectrum of pC-trehalose.....	161
Figure 4-13. ¹ H-NMR spectrum of pLA-zwitterion	162

Figure 4-14. ¹ H-NMR spectrum of pLA-trehalose	163
Figure 4-15. SEC overlays of synthesized polyesters and polycarbonates	164
Figure 4-16. Enzymatic hydrolysis of 4-nitrophenyl acetate by immobilized lipase B.....	164
Figure 5-1. Gel permeation chromatography (GPC) traces for the synthesized rPEGs	173
Figure 5-2. a) Conjugation of rPEG to lysozyme b) SDS-PAGE analysis C) IEX purification and analysis.....	174
Figure 5-3. GPC trace of a) initial successful rPEG modification using thiolated glucose and b) a representative unsuccessful thiol-ene experiment using hexanethiol	176
Figure 5-4. ¹ H-NMR spectrum of 10:1 rPEG polymer	186
Figure 5-5. ¹ H-NMR spectrum of 25:1 rPEG polymer	187
Figure 5-6. ¹ H-NMR spectrum of 50:1 rPEG polymer	188
Figure 5-7. ¹ H-NMR spectrum of 75:1 rPEG polymer	189
Figure 5-8. ¹ H-NMR spectrum of 100:1 rPEG polymer	190
Figure 5-9. ¹ H-NMR spectrum of successful thiol-ene product rPEG-g-glucose	191
Figure 5-10. ¹ H-NMR spectrum of rPEG model 2	192
Figure 5-11. ¹³ C-NMR spectrum of rPEG model 2	192
Figure 5-12. Crude ¹ H-NMR spectrum of model thiol-ene (Table 5-2, entry 1).....	193
Figure 5-13. Crude ¹ H-NMR spectrum of model thiol-ene (Table 5-2, entry 6).....	194
Figure 5-14. DMF GPC trace of rPEG thiol-ene using optimized -78 °C conditions.....	194
Figure 5-15. ¹ H-NMR spectrum of rPEG thiol-ene using optimized -78 °C conditions.....	195

LIST OF TABLES

Table 2-1. Molecular weight and GPC data for degradation of p(BMDO-co-BMA-trehalose)	42
Table 3-1. Molecular weights and GPC data for the library of polyesters (DP40)	71
Table 3-2. Molecular weights and GPC data for the library of pCL-trehalose and pCL- zwitterion polymers with variable DP.....	75
Table 3-3. Changes in melting and crystallization enthalpy of water upon addition of 1 mol% trehalose, trehalose repeating units in pCL-trehalose ₈₀ , betaine, or zwitterionic repeating units in pCL-zwitterion ₈₀	86
Table 4-1. Molecular weights and GPC data for allyl-functional polyesters and polycarbonates	138
Table 4-2. Molecular weights and GPC data for functional zwitterionic and trehalose polymers	142
Table 5-1. Reaction parameters for the synthesis of aldehyde-functional rPEGs	173
Table 5-2. Screen of thiol-ene conditions for the modification of rPEG model compound 2	178

LIST OF SCHEMES

Scheme 2-1 Synthesis of p(BMDO- <i>co</i> -bMA) and modification with thiolated trehalose to yield p(BMDO- <i>co</i> -BMA-trehalose).	39
Scheme 3-1. Synthetic scheme of thiol-ene modification of pCL-allyl polymers with acetyl-trehalose, acetyl-glucose, acetyl-lactose and PEG thiols, followed by deprotection of the acetylated sugars	67
Scheme 3-2. Synthesis of thiolated trehalose	68
Scheme 3-3. Synthetic scheme for the synthesis of zwitterionic polymer pCL-zwitterion _n ...	70
Scheme 3-4. Basic hydrolysis of pCL-trehalose ₁₀ and pCL-zwitterion ₂₀	99
Scheme 4-1. Polymerization of allyl-functionalized lactide, carbonate, and caprolactone polymers	138
Scheme 4-2. Synthesis of cationic thiol 5	139
Scheme 4-3. Synthesis of pCB-zwitterion and pLA-zwitterion using cationic thiol 5	140
Scheme 4-4. Representative modification of pMAC using thiolated trehalose	141
Scheme 5-1. Polymerization of monomer using ROMP.....	172
Scheme 5-2. Reversibility and isomerization of thiol-ene addition.....	176
Scheme 5-3. Synthesis of rPEG model compound 2	177
Scheme 5-4. Thiol-ene modification of rPEG model compound 2 with hexanethiol.....	178

LIST OF ABBREVIATIONS

AIBN	Azobisisobutyronitrile
Anti-TNF α	Anti-tumor necrosis factor α
ATRP	Atom transfer radical polymerization
bFGF	Basic fibroblast growth factor
bMA	Butenyl methacrylate
BMDO	5,6-benzo-2-methylene-2,3-dioxepane
BSA	Bovine serum albumin
CCM	Cell-conditioned media
CKA	Cyclic ketene acetal
CL	Caprolactone
Con A	Concanavalin A
CPMV	Cowpea mosaic virus
CRP	Controlled radical polymerization
CTA	Chain transfer agent
CuAAC	Copper-catalyzed azide-alkyne cycloaddition
DBU	1,8-Diazabicyclo[5.4.0]undec-7-ene
DCM	Dichloromethane
DMF	Dimethylformamide
DMPA	2,2-dimethoxyphenyl acetophenone
DNA	Deoxyribonucleic acid
DP	Degree of polymerization

DPBS	Dulbecco's phosphate buffered saline
DSC	Differential scanning calorimetry
ELISA	Enzyme-linked immunosorbent assay
ELP	Elastin-like peptide
EPO	Erythropoiesis protein
ESI	Electrospray ionization
FDA	Food and drug administration
FPLC	Fast protein liquid chromatography
FT-IR	Fourier-transform infrared spectroscopy
G-CSF	Granulocyte colony-stimulating factor
GFP	Green fluorescent protein
GI	Gastrointestinal
GPC	Gel permeation chromatography
HDFs	Human dermal fibroblasts
HES	Hydroxyethyl starch
HPLC	High-performance liquid chromatography
HPMA	<i>N</i> -(2-Hydroxypropyl)methacrylamide
HRMS	High resolution mass spectrometry
HSA	Human serum albumin
HUVECs	Human umbilical vein endothelial cells
IEX	Ion exchange
IFN α	Interferon-alpha
IL-8	Interleukin-8

MAC	Methyl allyl carbonate
MALDI	Matrix assisted laser desorption/ionization
MALS	Multi-angle light scattering
MBL	Mannose-binding lectin
MDO	2-methylene-1,3-dioxepane
MeOH	Methanol
MPDL	2-methylene-4-phenyl-1,3-dioxolane
mPEG	Monomethoxy poly(ethylene glycol)
MTBD	7-Methyl-1,5,7-triazabicyclo[4.4.0]dec-5-ene
MWCO	Molecular weight cutoff
NHS	<i>N</i> -hydroxysuccinimidyl
NMR	Nuclear magnetic resonance
PC	Poly(carbonate)
PCB	Poly(carboxybetaine)
PEG	Poly(ethylene glycol)
PEGMA	Poly(ethylene glycol) methyl ether methacrylate
PEP	Proline-specific endopeptidase
PG	Poly(glycerol)
PGA	Polyglutamic acid
PLA	Poly(lactide)
PLP	Pyridoxal-5-phosphate
PMMA	Poly(methyl methacrylate)
PNAs	Peptide nucleic acids

PNAcM	Poly(<i>N</i> -acryloyl morpholine)
POZ	Poly(oxazoline)
pPEGMA	Poly(poly(ethylene glycol)methyl ether methacrylate)
PSA	Polysialic acid
PTMC	Poly(trimethylene carbonate)
PVP	Poly(vinylpyrrolidone)
RAFT	Reversible addition-fragmentation chain transfer
RALS	Right-angle light scattering
rhEGF	Recombinant human epidermal growth factor
rh-GH	Recombinant human growth hormone
ROMP	Ring-opening metathesis polymerization
ROP	Ring-opening polymerization
SAv	Streptavidin
sCT	Salmon calcitonin
SDS-PAGE	Sodium dodecyl sulfate polyacrylamide gel electrophoresis
SEC	Size exclusion chromatography
siRNA	Small interfering ribonucleic acid
SPR	Surface plasmon resonance
SS	Styrene sulfonate
TBD	1,5,7-Triazabicyclo[4.4.0]dec-5-ene
TEM	Transmission electron microscopy
THF	Tetrahydrofuran
TMS	Trimethylsilyl

UV

Ultraviolet

ACKNOWLEDGEMENTS

First I thank my advisor, Professor Heather Maynard, for giving me advice, mentorship, and opportunities during my graduate career at UCLA. I truly became a scientist during these past 5 years and I will be always grateful for my time in the Maynard lab. I also thank my committee, Professor Ken Houk, Professor Tim Deming, and Professor Stephanie Seidlits, for their advice and guidance at UCLA. I also thank Professor Patrick Theato for welcoming me into his lab during my Fulbright year and for inspiring me to become a polymer chemist. I thank Professors Lee Park, Sarah Goh, and my undergraduate thesis advisors David Richardson and Jay Thoman for giving me a strong background in chemistry and for inspiring me to love research.

I have been so lucky to work alongside my favorite scientists in the Maynard lab. I thank past Maynard lab members, including Dr. En-Wei Lin, Dr. Nicolas Matsumoto, Dr. Juneyoung Lee, Dr. Kathy Nguyen, Dr. Muhammet Kahveci, Dr. Caitlin Decker, Dr. Uland Lau, Dr. Liang Sun, Dr. Natalie Boehnke, Dr. Samantha Paluck, Eric Raftery, Peter Nauka, and Maltish Lorenzo as well as present members: Dr. Jacquelin Kammeyer, Jeong Hoon Ko, Marco Messina, Prieria Panescu, Kyle Tamshen, Kathryn Mansfield, Madeline Gelb, Doug Rose, Neil Forsythe, Kathleen Chen, Arvind Bhattacharya, Warrick Ma, and Omar Ebrahim. I say it after every presentation and mean it every time; you have all been amazing people to work with and I have learned something from each of you!

I am also specifically grateful for the collaborative assistance of many colleagues at UCLA. I thank En-Wei Lin for her mentorship throughout my first year in graduate school and for her help writing the review that was adapted for Chapter 1. I thank Uland Lau for working together on the BMDO-project incorporated into Chapter 2, as well as the use of the protein he expressed for the

caprolactone project that was discussed in Chapter 3. Samantha Paluck was invaluable for her experimental help and scientific advice throughout my PhD and I was thrilled to be able to work with her on Chapter 3. I thank Arvind Bhattacharya for his perfectly timed assistance in completing Chapter 4. I also thank Nic Matsumoto, Eric Raftery, Uland Lau, and Kyle Tamshen for their collaboration on the ROMP PEG project that is discussed in Chapter 5; it takes a village to complete a project. Finally, I thank Jeong Hoon Ko for sharing every day of the last 5 years in lab and for (almost) never being too busy to talk about science.

I am additionally grateful to the generous funding sources who have supported me during my graduate research. I thank the National Science Foundation Graduate Research Fellowship Program (DGE-1144087). I also thank UCLA Graduate Division for a Dissertation Year Fellowship. I thank the UCLA Chemistry & Biochemistry Department for a Graduate Dean's Fellowship, the Departmental Leadership Award, and the Thomas L. and Ruth F. Jacobs Award. I thank the Organic Division for a Christopher S. Foote Senior Fellowship.

Finally, I gratefully acknowledge the support of my friends and family outside of UCLA; I appreciate the opportunity to talk about something other than science and I also appreciate their patience when I inevitably do discuss my research. I thank my friends for a supportive community of amazing people. I thank my parents, my grandma, and my brother for knowing when to ask about research progress and when to change the subject. And finally, I thank Brett Beekley for his constant love and support; I wouldn't have made it without you.

Chapter 1 is reproduced with permission from Pelegri-O'Day, E. M., Lin, E.-W.; Maynard, H. D. Therapeutic Protein-Polymer Conjugates: Advancing Beyond PEGylation. *J. Am. Chem. Soc.* **2014**, *136*, 14323. 10.1021/ja504390x. Copyright 2014 American Chemical Society. Chapter 2 is reproduced with permission from Lau, U. Y.; Pelegri-O'Day, E. M.; Maynard, H. D. Synthesis

and Biological Evaluation of a Degradable Trehalose Glycopolymer Prepared by RAFT Polymerization. *Macromol. Rapid Commun.* **2018**, *39*, 1700652. 10.1002/marc.201700652. Copyright 2018 John Wiley Sons, Inc. Chapter 3 is reproduced with permission from Pelegri-O'Day, E. M.; Paluck, S. J.; Maynard, H. D. Substituted Polyesters by Thiol–Ene Modification: Rapid Diversification for Therapeutic Protein Stabilization. *J. Am. Chem. Soc.* **2017**, *139*, 1145. 10.1021/jacs.6b10776. Copyright 2017 American Chemical Society.

VITA

EDUCATION

2012	B.A. Chemistry	Williams College, Williamstown, MA
2015	M.S. Chemistry	University of California, Los Angeles, CA

EXPERIENCE

2013-2018	Graduate Research Assistant, University of California, Los Angeles
2017-2018	Graduate Fellow, UCLA Technology Development Group
2012-2013	Fulbright Student, Universität Hamburg, Germany
2010-2012	Undergraduate Research Assistant, Williams College

PUBLICATIONS

Lau, U.Y.; Pelegri-O'Day, E.M.; Maynard, H.D. Synthesis and Biological Evaluation of a Degradable Trehalose Glycopolymer Prepared by RAFT Polymerization. *Macromol. Rapid Commun.* **2017**, *39*, 1700652.

Pelegri-O'Day, E. M.; Paluck, S. J.; Maynard, H. D. Substituted Polyesters by Thiol–Ene Modification: Rapid Diversification for Therapeutic Protein Stabilization. *J. Am. Chem. Soc.* **2017**, *139*, 1145.

Pelegri-O'Day, E. M.; Maynard, H. D. Controlled Radical Polymerization as an Enabling Approach for the Next Generation of Protein–Polymer Conjugates. *Acc. Chem. Res.* **2016**, *49*, 1777.

Pelegri-O'Day, E. M.; Lin, E. W.; Maynard, H. D. Therapeutic Protein–Polymer Conjugates: Advancing Beyond PEGylation. *J. Am. Chem. Soc.* **2014**, *136*, 14323.

PRESENTATIONS

“Synthesis of a Library of Degradable and Protein-Stabilizing Polyesters using Thiol-Ene Post-Polymerization Modification,” 253rd National Meeting of the American Chemical Society, Polymers & Biomimicry, San Francisco, CA, April 2017.

"Biodegradable Trehalose Glycopolymers for Protein Stabilization," 251st National Meeting of the American Chemical Society, 13th International Symposium on Biorelated Polymers, San Diego, CA, March 2016.

"Biodegradable Trehalose Glycopolymers for the Stabilization of Therapeutic Proteins," 14th Pacific Polymer Conference National Meeting & Exposition, Bio-Conjugates Symposium, Lihue, HI, December 2015.

HONORS AND AWARDS

2018	Thomas L. and Ruth F. Jacobs Award
2018	Departmental Leadership Award
2017-2018	UCLA Dissertation Year Fellowship
2015-2017	Christopher S. Foote Senior Fellowship
2014-2017	NSF Graduate Research Predoctoral Fellowship
2013-2015	UCLA Graduate Dean's Scholar Award
2012-2013	Fulbright Student Fellowship
2012	Class of 1925 Scholar-Athlete Award
2009-2012	DIII NCAA Champion (rowing)

Chapter 1

Rational Design for the Improvement of Therapeutic Protein

Delivery: Advancing Beyond PEG¹

1.1. Introduction

Protein-polymer conjugates display a unique combination of properties derived from the biologic and synthetic materials, which can be individually tuned to elicit a desired effect. Proteins can be used in therapies to replace deficient or absent natural proteins, upregulate existing metabolic pathways, or inhibit molecular targets.² Proteins may function in chemotherapeutic delivery devices as targeting agents. Additionally, enzymes can be used to catalyze chemical reactions both *in vivo* and *in vitro*. Synthetic polymers exhibit high thermal and chemical stabilities and can be synthesized with controlled molecular weight and low dispersity (i.e. narrow molecular weight distribution). Moreover, synthetic polymers allow for the incorporation of desired functional groups and can be designed to respond to biological and non-biological stimuli including changes in pH, temperature, redox potential, or analyte concentration. This fusion of biological properties and chemical stability or reactivity gives protein-polymer conjugates a unique position at the intersection of chemistry, biotechnology, nanotechnology, and medicine.

The subject of protein-polymer conjugates has been extensively reviewed,³⁻¹⁰ with details on synthetic methods and comprehensive summaries of reported work. This introduction chapter will provide a brief overview on the history of poly(ethylene glycol) (PEG) conjugates, current status of therapeutic protein-polymer conjugates, advanced conjugates for biomedical use, and an outlook to the future of next-generation therapeutics.

1.2. PEG Conjugates

In 1977, Abuchowski and coworkers demonstrated the first conjugation of monomethoxy PEG (mPEG) to bovine serum albumin (BSA) through the use of a cyanuric chloride coupling agent.¹¹ This BSA-PEG conjugate displayed a lower immunogenic response in animal models

relative to the native protein. They later reported that PEGylated proteins increased circulation times in animal models relative to native proteins.¹¹⁻¹² Two years later, Kanamaru and coworkers reported the increased biocirculation of the chromoprotein neocarzinostatin when covalently coupled to a polystyrene-maleimide copolymer.¹³ Together, these discoveries prompted a flurry of interest in conjugating polymers to proteins for therapeutic use (**Figure 1-1**). In Japan, the protein-polymer conjugate SMANCS (zinostatin stimalamer), which is made up of the anti-tumor chromoprotein neocarzinostatin and a styrene-maleic acid copolymer, was approved for the treatment of hepatocellular cancer.¹⁴ However, the majority of the focus for medical use has been on the conjugation of PEG to proteins, also known as PEGylation, and only PEG has been attached in all of the Food and Drug Administration (FDA)-approved protein conjugates.⁵

PEG is generally regarded as safe by the FDA and is known to increase protein half-life through multiple mechanisms. Conjugation of PEG to protein or small-molecule therapeutics increases their molecular weight, which reduces kidney clearance and increases biocirculation time. PEG is also well-known as a “stealth” molecule; this allows PEG therapeutic conjugates to avoid phagocytosis and removal from the bloodstream. One process for clearing foreign material from the body requires opsonization, or the coverage of exogenous particles by opsonin proteins, and subsequent activation of phagocytes, which then remove the foreign body *via* endocytosis and degradation.¹⁵ Opsonization relies on attractive forces between the exogenous body and the opsonins, and is increased for hydrophobic particles¹⁶⁻¹⁷ and charged species¹⁸ due to enhanced adsorbability. Because PEG is a hydrophilic, neutral, and non-fouling molecule, it exhibits low opsonization rates and longer biocirculation.¹⁶ Additionally, PEGylation adds steric bulk and nonfouling properties, which may reduce the immunological response to a protein by disruption of antibody binding or breakdown of the molecule by enzymes. There are currently ten FDA-

approved PEG-protein conjugates and one PEG-aptamer conjugate with diverse applications as therapeutics.¹⁹⁻²⁰ These conjugates function as replacement therapies for native enzyme deficiencies, stimulate immune responses, increase production of red or white blood cells, or neutralize overactive cytokines or receptors.⁵ They have been used to treat diseases such as Hepatitis C or Crohn's disease, or to stimulate regrowth of white blood cells after chemotherapy. As a result, protein-polymer conjugates are an important class of biologics, generating more than 7.5 billion dollars annually.

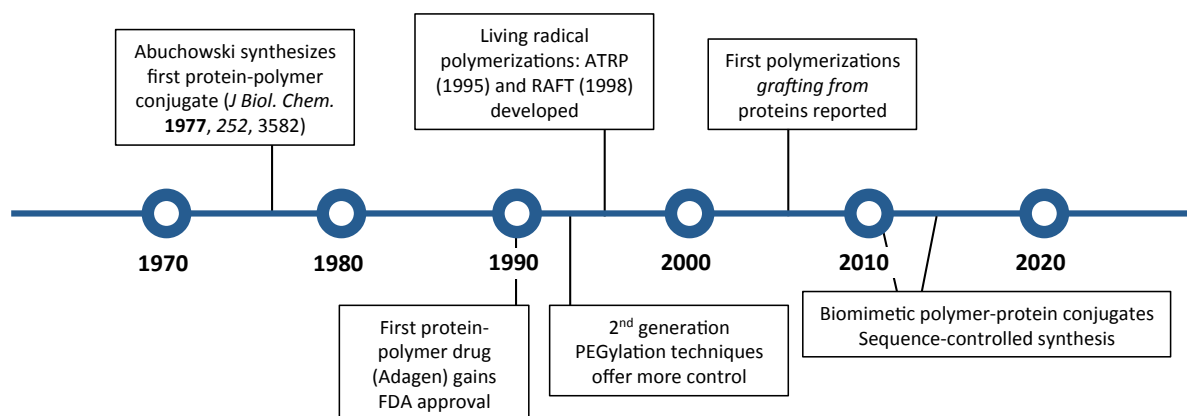


Figure 1-1. Advances in protein-polymer conjugation chemistry

1.3. Advances in Protein Conjugation Chemistry

1.3.1. Straight-chain PEG Conjugates

PEG conjugation techniques have greatly improved over the past 40 years. First-generation PEGylation methods used semitelechelic mPEG to modify lysine side chains. The mPEG hydroxyl groups were activated through formation of derivatives such as mPEG dichlorotriazine, mPEG succinimidyl carbonate, mPEG benzotriazol and mPEG tresylate, but these methods were inefficient.³ They suffered from crosslinking due to contamination with bisfunctional PEG,

unstable and easily cleavable protein-polymer linkages, alterations in protein charges, and lack of selectivity, which all led to heterogeneity of the PEGylated proteins.^{6,21} Most of these early protein conjugations relied on post-polymerization modifications or coupling reactions with the terminal hydroxyl group of PEG that required multiple steps or difficult purification procedures.^{11,22}

Second-generation techniques focused on chemical transformations of mPEG to derivatives such as mPEG-propionaldehyde, which could produce more stable linkages as well as more selective PEGylation, resulting in increased bioactivity. For example, Neulasta was prepared by PEGylation of the N-terminus of granulocyte colony-stimulating factor (G-CSF) utilizing this chemistry.⁵ In other examples, it was shown that the N-terminal amine of interleukin 8 (IL-8) may be selectively oxidized with sodium periodate under mild conditions to form a glyoxyl group, which can subsequently react with an aminoxy PEG to form a conjugate *via* oxime bond formation (**Figure 1-2a**).²³ A transamination reaction was introduced wherein the N-terminus could be selectively modified with pyridoxal-5-phosphate (PLP) to yield an oxoamide (**Figure 1-2b**).²⁴ A variety of hydroxylamine-functionalized molecules or polymers including PEG were conjugated to the resulting N-terminus carbonyls *via* an oxime bond. However, the downsides of these techniques are the possibility of nonselective oxidation affecting other amino acids and low yields in the transamination reaction. Second-generation techniques can also minimize the negative effects on biological activity caused by conjugation. For instance, PEGylation of G-CSF and other proteins resulted in less protein aggregation when the positive charge on the N-terminal methionine residue was retained after conjugation.²⁵

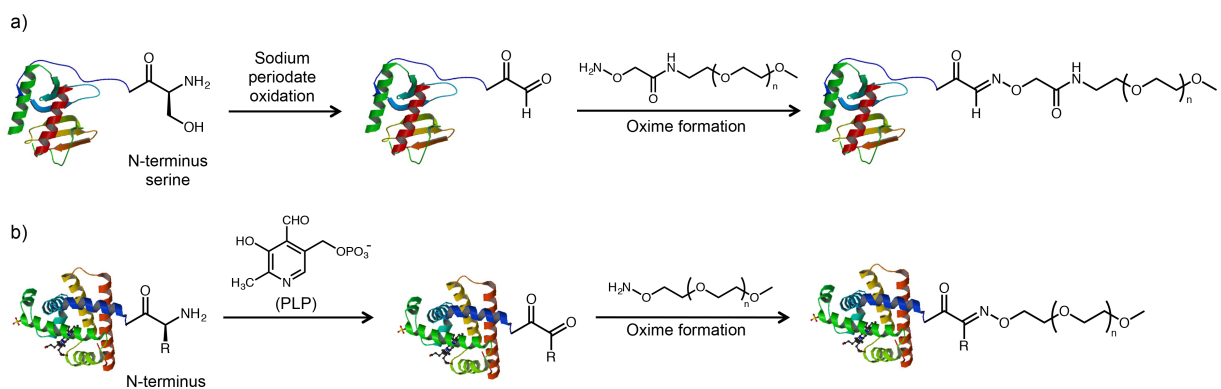


Figure 1-2. Examples of second-generation site-selective protein PEGylation using oxime "click" chemistry a) Gaertner et al.²³b) Gilmore et al.²⁴ (Protein structure of interleukin 8 from PDB #1IL8. Protein structure of myoglobin from PDB #1WLA)

Free cysteines in the desired protein have also been targeted using thiol-reactive groups such as maleimide, vinylsulfone, iodoacetamide, and pyridyl disulfide.²⁶⁻²⁸ FDA-approved CIMZIA was prepared utilizing maleimide PEG addition to antitumor necrosis factor α (anti-TNF α).⁵ Recently, newer chemistries to target free cysteines have been reported. For instance, disulfide bridges may be reduced and conjugated *in situ* with a bridging moiety to retain tertiary structure while incorporating a linear or comb PEG chain.²⁹⁻³¹ In another example, cross-metathesis was utilized to functionalize a protein with a short ethylene glycol. Specifically, a native cysteine was modified to contain an *S*-allyl group, which was then able to undergo cross-metathesis with a variety of alkenes, including carbohydrate groups and an alkene-functionalized tetra-(ethylene glycol).³⁰

For proteins that do not contain free cysteines or where non-natural amino acids are desired, they can be inserted through genetic engineering.³²⁻³³ Other ways to incorporate reactive handles include the preparation of synthetic proteins using native chemical ligation³⁴. For example,

erythropoiesis protein (EPO) was prepared by synthesizing polypeptide chains containing levulinyl ester-modified lysine residues (**Figure 1-3**).³⁵ Branched PEG-like polymers with negatively charged end-groups were then site-specifically conjugated *via* oxime chemistry, and the resulting PEGylated EPO had similar bioactivity to the native protein with enhanced pharmacokinetics. The inclusion of reactive functional groups in the peptide sequence allows for site-specific PEGylation as well as retention of native protein bioactivity provided that the conjugated polymer does not inhibit access to the active site. However, of these above-mentioned PEGylation techniques, only five linker chemistries have been utilized in the FDA-approved protein conjugates: activated carbonyls such as *N*-hydroxysuccinimidyl (NHS) ester, *p*-nitrophenol carbonate, and NHS carbonate, as well a thiol-reactive maleimide and amine-reactive aldehyde.⁵

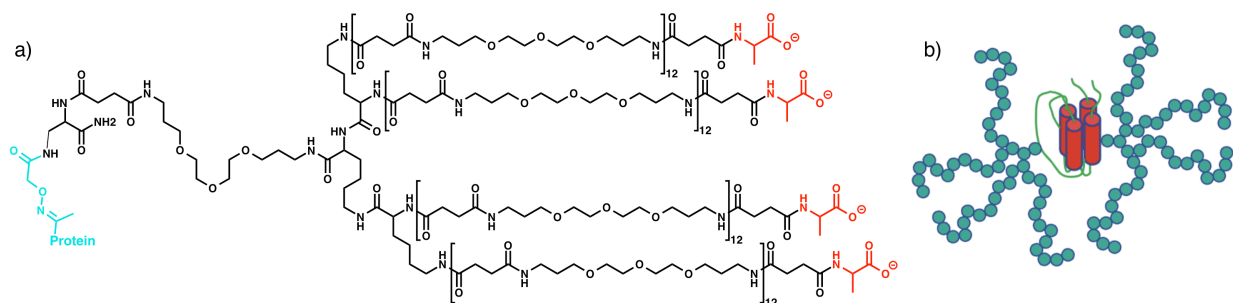


Figure 1-3. Synthetic erythropoiesis protein with a) structure of branched, negatively charged PEG-like polymer b) schematic of resulting PEGylated protein.³⁵ From Kochendoerfer et al *Science* **2003**, 299, 884. Reprinted with permission from AAAS.

1.3.2. New Polymeric Methods for Bioconjugation

Just as the development of novel techniques for PEG conjugation has greatly improved the field of PEGylated conjugates, the development and use of novel monomers and new

polymerization methods have greatly enhanced the field of protein-polymer conjugates. Controlled radical polymerization (CRP) is currently the most popular technique to prepare conjugates with polymers other than PEG. Atom transfer radical polymerization (ATRP), in which a halogenated initiator undergoes a reversible redox reaction mediated by a transition metal catalyst,³⁶⁻³⁷ and reversible addition-fragmentation chain transfer (RAFT) polymerization, which utilizes a chain transfer agent (CTA) to mediate the reversible chain-transfer process,³⁸ are the two CRP techniques commonly used for this purpose. However, other methods have been used, including ring opening metathesis polymerization (ROMP),³⁹⁻⁴⁰ ring opening polymerization (ROP)⁴¹ and anionic polymerization, as in the case of PEG. These controlled polymerization techniques tolerate a wide range of functional groups, solvents, reaction conditions, and allow for the introduction of functional end-groups. Importantly for therapeutic applications, these techniques provide polymers with narrow molecular weight distributions. This can be important for FDA approval as well as for uniformity in resulting properties.

New polymerization techniques have also led to new methods of protein conjugation.^{4, 9, 42} *Grafting to* is the covalent attachment of a synthetic polymer to a protein using a protein-reactive handle. CRP techniques using protein-reactive initiators or CTAs can eliminate post-polymerization modifications and facilitate more efficient conjugations. For example, pyridyl disulfide and maleimide are commonly incorporated directly into initiators and CTAs, resulting in protein-reactive polymers by ATRP or RAFT without post-polymerization modification.⁴³⁻⁴⁴ *Grafting from* involves the polymerization of monomers from an initiating site on the protein, which offers clear benefits in minimal steric hindrance and higher efficiency in the initiator-protein conjugation, as well as easier purification and characterization. Initial reports focused on biotinylated ATRP initiators that could bind streptavidin non-covalently and generate a protein

macroinitiator upon association with streptavidin.⁴⁵ After polymerization of various monomers, the protein was modified at the biotin binding sites. Shortly thereafter, pyridyl disulfide- and maleimide-functionalized ATRP initiators⁴⁶ and RAFT agents⁴⁷⁻⁴⁸ were used and conjugated to free cysteines of BSA and T4 lysozyme to generate protein macroinitiators. ATRP initiators have also been introduced in proteins through other chemistries such as oxime formation, genetic encoding of unnatural amino acids, and intein-mediated attachment.⁴⁹⁻⁵¹ *Grafting from* can also be carried out using ROMP; Grubbs III was conjugated to lysozyme and the resulting protein macroinitiator was used to polymerize water-soluble norbornene monomers.⁵² **Figure 1-4** outlines a representative sampling of significant *grafting from* CRP methods that have been developed in this past decade.

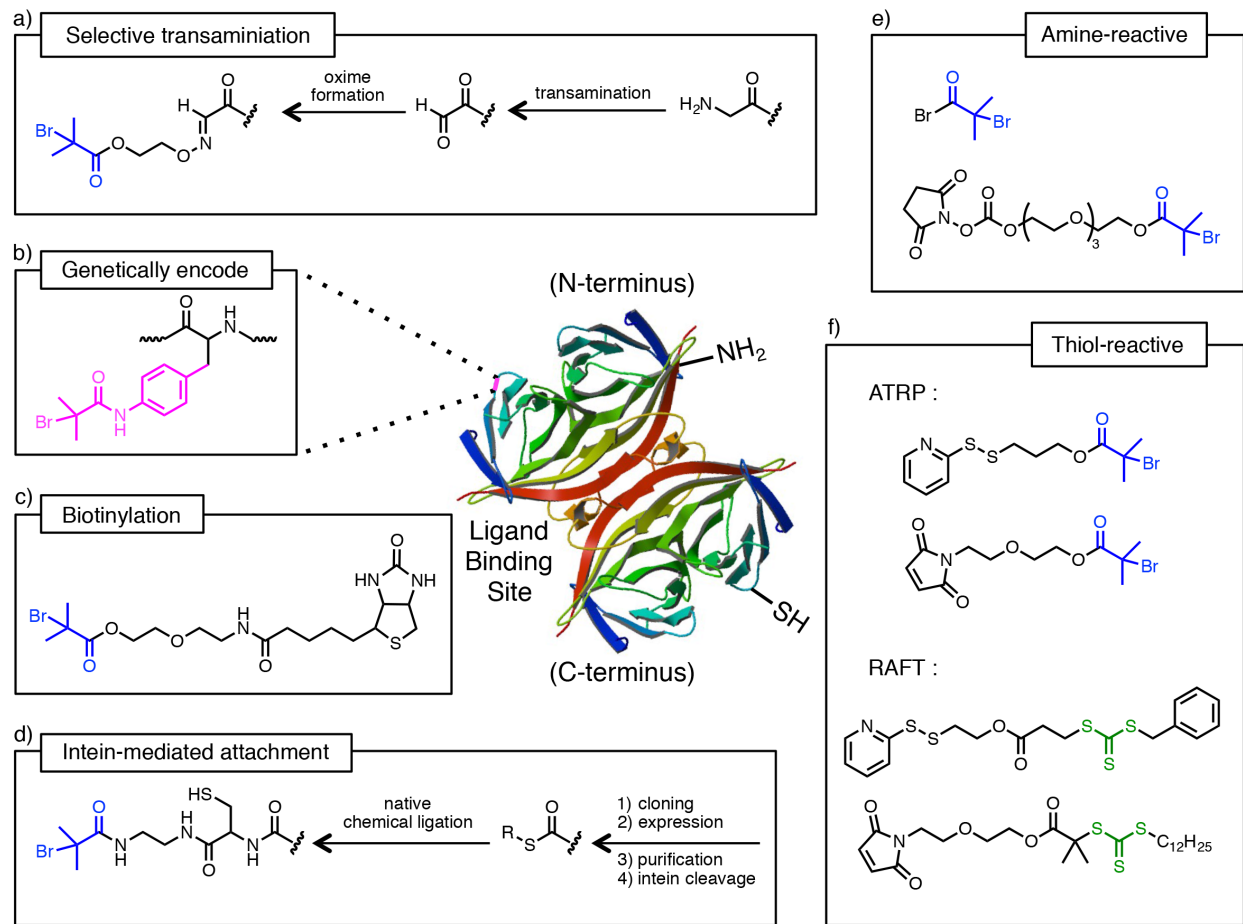


Figure 1-4. Schematic presenting significant “grafting from” methods (Protein structure of Streptavidin from PDB #1N4J). References: a) Gao et al.,⁵⁰ b) Peeler et al.,⁴⁹ c) Bontempo et al.,⁴⁵ d) Gao et al.,⁵¹ e) Lele et al.,⁵³ Magnusson et al.,⁵⁴ f) Heredia et al.,⁴⁶ Liu et al.,⁴⁷ De et al.,⁵⁵

Together, these new polymeric methods greatly enhance the available chemical space of the polymers while minimizing the number of synthetic steps. But a drawback to the use of CRP methods is the possibility of cytotoxicity: ATRP uses copper catalysts and the trithiocarbonate and dithioester moieties found in RAFT CTAs have shown degradation and cytotoxicity *in vitro*.⁵⁶ However, both of these issues can be solved by removal of the metal or by postpolymerization modification steps to remove the end groups. Additionally, at this stage there is a general lack of

long-term studies on the fate of these synthetic polymers in the body. Limited *in vivo* studies have showed promise as to the safety and efficacy of CRP polymer-protein conjugates^{50-51, 54, 57-62} but more thorough studies will need to be conducted. For example, little is known about their pharmacokinetic properties, safety, and long-term fate in the body.

1.4. Alternatives to PEG in Development

An advantage of the new polymer and conjugation chemistries described above is the ability to prepare alternative polymers to PEG; this is especially important because of the potential side effects of the polymer that have been observed. PEG has been shown to cause hypersensitivity and immunological responses, accumulation in tissues, and accelerated blood clearance upon repeated exposure. The recognition of PEG by the body and the formation of anti-PEG antibodies were first reported in 1984.⁶³ Reports of differing levels of PEG antibodies in the general population vary widely with detection technique, from 4% using general enzyme-linked immunosorbent assay (ELISA)⁶⁴ up to 25% using a combination of serology and flow cytometry.⁶⁵ These PEG antibodies increased clearance rates of PEGylated conjugates.⁶⁶⁻⁶⁷ Since the goal of protein PEGylation is to reduce immunogenicity and increase biocirculation time, the occurrence of these antibodies detracts from their utility in protein therapies. Hypersensitivity has been observed in other cases; potential allergic reactions to PEG detract from its usefulness in some patient populations.⁶⁸ The non-biodegradability of PEG is another main drawback; PEG has been shown to form vacuoles in organs such as the liver, kidney, and spleen after protein-PEG conjugate administration.⁶⁹⁻⁷³ While non-biodegradable, PEG has shown degradation under light, heat, and mechanical stress with the possibility of toxic side product buildup during storage.⁷⁴ These deficiencies have led researchers to investigate alternative polymers for protein conjugation.

1.4.1. Known Biocompatible Polymers

While PEG remains the only polymer conjugate to be FDA approved, many other polymers are widely recognized as biocompatible in other contexts (such as small-molecule drug carriers) and have been used to produce protein-polymer conjugates with improved *in vitro* and *in vivo* properties.

Statistical copolymers of *N*-(2-Hydroxypropyl)methacrylamide (HPMA) and a monomer containing a pendant drug-reactive group (such as an ester or carboxylic acid) have been thoroughly studied in many clinical trials.⁷⁵ Although this polymer is well-established as a biocompatible drug carrier and promising as a PEG replacement, protein conjugates of HPMA are less developed. HPMA conjugates have demonstrated improved stability against heat and autolysis with model⁷⁶⁻⁷⁸ and therapeutically relevant proteins.⁷⁹⁻⁸¹ The synthesis of end-functionalized HPMA by CRP using a protein-reactive thiazolidine-2-thione functionalized CTA has been reported.^{58, 76-77}

Poly(vinylpyrrolidone) (PVP) has also been explored *in vivo* as a nontoxic and hydrophilic PEG alternative for conjugation to proteins⁸²⁻⁸³ and has been synthesized by RAFT polymerization.⁸⁴ Studies comparing the immune response of protein conjugates revealed that both PVP and poly(*N*-acryloyl morpholine) (PNAcM) conjugates with uricase stimulated antibody production after the first dose.⁸⁵ This result underscores the effect of conjugation on the immunological response to polymers and may limit the use of these polymers, since antibody production is already a concern in the use of PEG.

A set of promising alternatives are poly(2-oxazolines), which exhibit similar stealth behavior to PEG.⁸⁶⁻⁸⁷ These polymers are easily modifiable and thermoresponsive, and they have been widely promoted as biocompatible PEG alternatives for use as polyplexes, conjugates, and

micelles.⁸⁸⁻⁹⁰ Experiments have shown that the conjugation of poly(2-ethyl-2-oxazoline) to G-CSF through reductive amination or enzyme-mediated acyl transfer resulted in conjugates that are bioactive *in vivo*.⁹¹

1.4.2. Degradable PEG Alternatives

The polymers above share with PEG the disadvantage of non-biodegradability. For those patients that use protein conjugates as replacement therapies, these polymers, like PEG, may accumulate in the body. This provides a strong reason to develop polymers that can eventually degrade. Degradable main-chain PEG-like polymers have been developed that offer exciting alternatives to existing PEGylation strategies (**Figure 1-5**). For example, redox sensitive degradable PEG has been produced by the introduction of disulfide bridges between oligomeric units.⁹²⁻⁹⁵ And more recently, poly[(ethylene oxide)-*co*-(methylene ethylene oxide)] was prepared through post-polymerization elimination of epichlorohydrin monomer.⁹⁶ The resulting copolymer was degradable at physiological pH and temperature yet stable to storage at 6 °C. Acid-labile acetals have also been incorporated into the backbone of functional PEGs.⁹⁷ These polymers have not yet been conjugated to proteins or biologically evaluated, although the approach of preparing main-chain-degradable PEGs is promising.

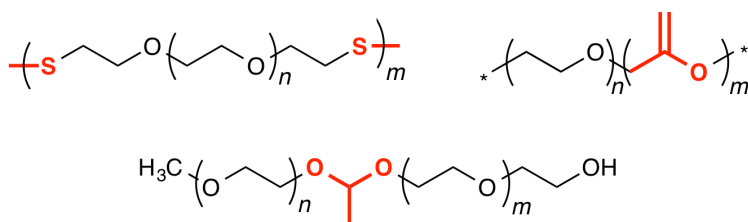


Figure 1-5. PEG-like polymers with degradable backbones

Other degradable PEG alternatives in development have been studied *in vivo*, including hydroxyethyl starch (HES), polysialic acid, and dextrin (**Figure 1-6**). HES polymer conjugates are one of the most advanced of these alternatives.⁹⁸ HESylation of EPO by the pharmaceutical company Fresenius-Kabi showed *in vivo* and *in vitro* bioactivities comparable to Mircera® (the PEGylated protein currently on the market) with a threefold increase in half-life over the wild type protein.⁹⁸ Other proteins, including G-CSF and interferon-alpha (IFN α), have also been HESylated with comparable results.⁹⁸ HES has the advantage that it can be degraded by α -amylase, although degradation slows with increasing hydroxyethylation.⁹⁸ While HES was commonly used as a volume expander for patients with severe blood loss, currently the safety of HES is under controversy. On the scale used for fluid therapy, HES has been shown to accumulate in the liver, kidney, and bone marrow, leading to increased risk of kidney injury and death for critically ill patients.⁹⁹ While HESylated proteins exhibit good pharmacokinetic properties, the side effects associated with the repeated use of HES may be a hindrance to their widespread adoption as conjugates.

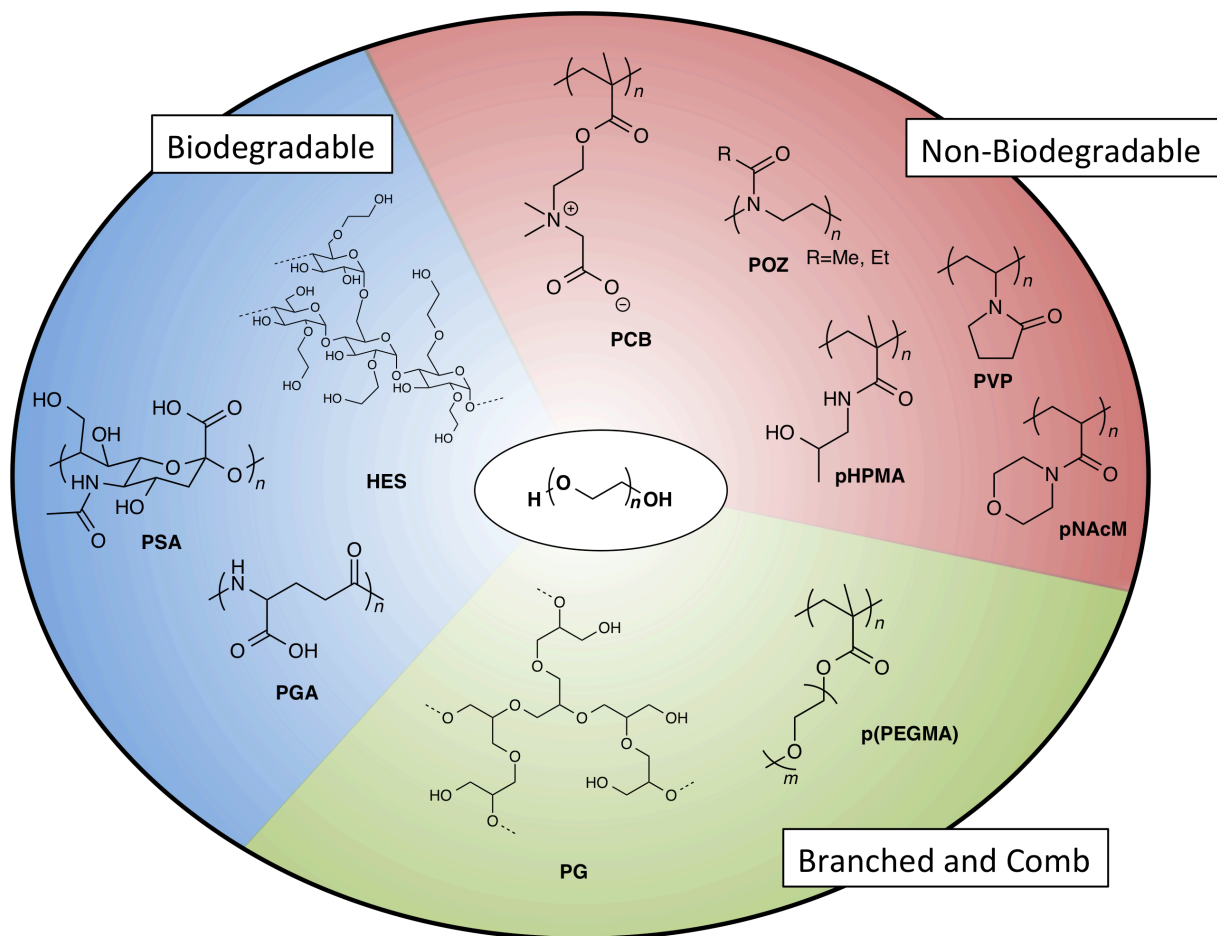


Figure 1-6. Examples of alternatives to PEG currently in use and development. PCB: poly(carboxybetaine). POZ: poly(2-oxazoline). PVP: poly(vinylpyrrolidone). pHPMA: poly(*N*-hydroxypropyl)methacrylamide). pNAcM: poly(*N*-acryloylmorpholine). pPEGMA: poly(poly(ethylene glycol)methyl ether methacrylate). PG: poly(glycerol). PGA: polyglutamic acid. PSA: polysialic acid. HES: hydroxyethyl starch.

Conjugates utilizing dextrin, polysialic acid, and other biodegradable polymers have demonstrated improved therapeutic properties in animal studies.¹⁰⁰ A recombinant human epidermal growth factor (rhEGF)-dextrin conjugate demonstrated greater wound healing *in vivo* than free rhEGF.¹⁰¹ Studies in rat models have reported that conjugation of polysialic acid to

insulin prolonged the reduction of glucose levels.¹⁰² Drug conjugates containing the enzymatically degradable poly(glutamic acid) (PGA) have been prepared and shown to increase tumor exposure to chemotherapeutics,¹⁰³ but its conjugation to proteins has not yet been extensively explored.

1.4.3. PEG Alternatives with Varied Architectures

Polymer architecture is an important consideration when designing protein conjugates, with branched¹⁰⁴⁻¹⁰⁵ or dendritic¹⁰⁶ PEG-like polymers generally displaying improved biocirculation and stability. A notable example of branched PEG is the synthetic erythropoiesis protein described above (see **Figure 1-3**).³⁵ Branching can also reduce the solution viscosity at high concentrations.¹⁰⁷ Since PEG-containing protein conjugates must be injected, a decrease in viscosity for PEG alternatives would be especially important in increasing the ease of injection for patients. Furthermore, branched polymers may be able to mimic the glycosylation patterns on native proteins. These covalent glycans can be important for stability and signaling yet are missing from proteins expressed from *Escherichia coli*. Therefore, the exploration of PEG alternatives with disparate architectures will be important. A major recent focus in the field has been on comb-like PEG polymers because of their ease of synthesis and potential for low dispersity enabled by CRP techniques. These polymers can also be made degradable by including cyclic ketene acetals (CKAs) in the reaction mixture,¹⁰⁸⁻¹¹⁰ and the degradable comb PEGs have been conjugated to proteins.¹¹¹ Although more intensive studies need to be undertaken to verify the validity of these polymers as potential therapeutics, there are several that have shown promise *in vivo*; these examples are summarized below.

An early study involved site-specific conjugation of aldehyde pPEGMA to salmon calcitonin (sCT) through reductive amination.¹¹² *In vivo*, the conjugate displayed 72% of the native

activity while displaying an extended half-life in rats.⁵⁷ *Grafting from* recombinant human growth hormone (rh-GH) was shown to produce conjugates with improved properties.⁵⁴ The initiator, NHS bromoisobutyrate was coupled to free amine groups on rh-GH and polymerization of PEGMA was conducted. The conjugate showed higher stability to denaturation and proteolysis compared to unmodified rh-GH. The *in vivo* efficacy of the hormone also improved, as confirmed by monitoring of weight growth in administrated female rats. Polymerization of PEGMA from the N-terminus of myoglobin and C-terminus of genetically modified green fluorescent protein (GFP) was also shown.⁵⁰⁻⁵¹ In mice, these conjugates displayed improved pharmacokinetics compared to unmodified protein. These examples clearly demonstrated that similar to PEG conjugates, pPEGMA conjugates significantly extend the circulation lifetime of the protein and are effective *in vivo*.

Polyglycerols (PGs) are structurally similar to PEG and have been prepared in both linear form and with tunable branching. While linear PGs have recently been reviewed as alternatives for PEG,¹¹³ polymers are often designed to mimic the typically branched structures of proteoglycans. For example, a library of linear, mid-functional, hyperbranched, and linear-hyperbranched PG conjugates were synthesized to assess the effect of structure on conjugate activity.¹¹⁴ Using BSA and lysozyme as model proteins, the mid-functional PG-lysozyme conjugates displayed higher activity than conjugates using linear PG, while hyperbranched PG conjugates displayed decreased activity. More recently, it was reported that PG could be *grafted from* BSA using kinetic control to control the degree of branching.¹¹⁵ Using ring-opening polymerization with a tin triflate catalyst, short polymers were obtained *in situ* with relatively low polydispersity index (1.25-1.36) and low dendritic unit composition. These polyglycerols offer promising alternatives to PEGylation.

Significant progress has been made in the synthesis of polymers that mimic natural glycans, especially in the area of ligands that exhibit biological functions,¹¹⁶⁻¹¹⁷ and some of these have been conjugated to proteins. For example, an alkyne end-functionalized glycopolymer synthesized *via* ATRP was conjugated to a cowpea mosaic virus (CPMV) modified with an azide group.¹¹⁸ This virus-glycopolymer conjugate interacted with Concanavalin A (Con A) and could potentially be used to target cancer cells for drug delivery. A maleimide end-functionalized glycopolymer with mannose pendent groups was prepared by a combination of ATRP and Cu-catalyzed azide-alkyne cycloaddition (CuAAC) “click” chemistry.¹¹⁹ The polymer was then site-specially grafted to BSA, a non-glycosylated model protein. Surface plasmon resonance (SPR) studies showed binding of the BSA conjugates to a recombinant rat mannose-binding lectin (MBL). In addition, some groups have synthesized branched glycopolymers in order to better mimic proteoglycans. Highly branched carbohydrate structures are able to display more potent effects. For instance, a galactose dendrimer and subtilisin, a protease, were conjugated to construct a glycodendrioprotein.¹²⁰ This synthetic glycoprotein demonstrated nanomolar inhibition of gram-positive bacteria aggregation. This work presents well-defined and synthetically designed glycoprotein mimics that exhibit combined features of the original protein component and the lectin binding properties of the glycopolymer.

1.5. Protein Therapeutics of the Future

1.5.1. Biomimetic Polymer Design

While PEG substitutes have been discovered and developed, there remains a need for protein-polymer conjugates that exhibit specific desirable properties. Ideally, the attached polymer should improve existing functions or introduce new properties to the protein. This section details

the purposeful synthesis and design of biomimetic, biodegradable, and biocomplementary polymer systems. As with any new entity, these polymers would have to clear a large number of experimental hurdles prior to FDA approval and use as therapeutics, and many of these examples have not yet been tested *in vivo*. However, these approaches may significantly improve the properties of protein therapeutics beyond an enhancement in pharmacokinetics, and thus innovation in this area should not be deterred.

Polymers with stabilizing properties offer the possibility of not only increasing the circulation lifetime but also increasing the stability of the protein to storage, transport, and other stresses. Such materials could be superior analogs to PEG if both the pharmacokinetic properties and stability outside of the body are improved, particularly since the majority of protein therapeutics need to be refrigerated.¹²¹ To this end, glycopolymers with pendant trehalose side chains have been utilized as conjugates and excipients to increase protein stability to common environmental stressors (**Figure 1-7a**).¹²²⁻¹²⁷ The polymers significantly enhanced the protein stability to lyophilization and high temperatures. The polymer combines two important classes of stabilizers, namely the osmolytes and nonionic surfactants, providing a superior stabilization compared with PEG and trehalose alone.

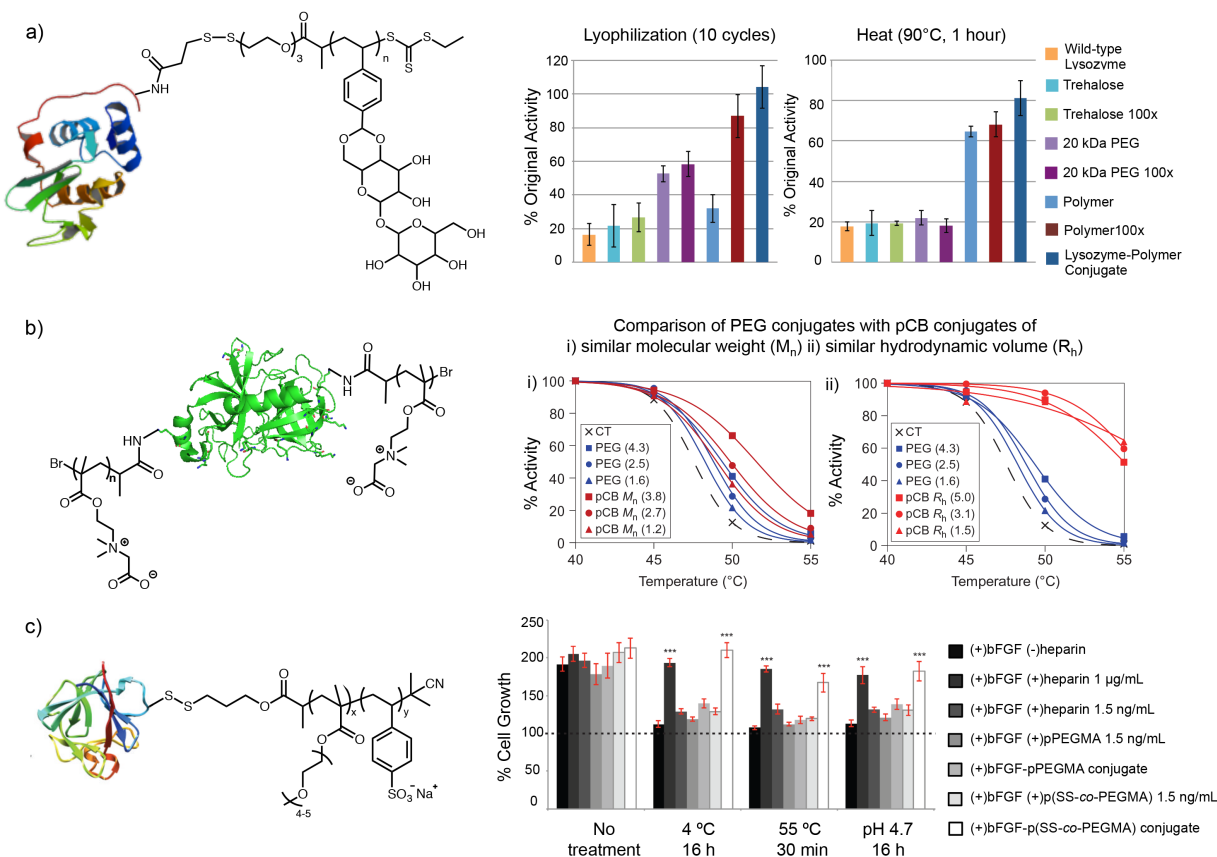


Figure 1.7. Examples of stabilizing and biomimetic polymers. References: a) Adapted with permission from Mancini et al *J Am Chem Soc* 2012, 134, 8474.¹²³ Copyright 2012 American Chemical Society. b) Adapted by permission from Macmillan Publishers Ltd: *Nature Chemistry*¹²⁸, copyright 2011 (Protein structure of α -Chymotrypsin from PBD #4CHA) c) Adapted by permission from Macmillan Publishers Ltd: *Nature Chemistry*¹³⁵, copyright 2013.

Poly(zwitterionic) protein conjugates were also recently reported (**Figure 1-7b**). Specifically, poly(carboxybetaine) was coupled to α -chymotrypsin, and the protein displayed higher activity than the comparable PEGylated conjugate or native protein at elevated temperatures.¹²⁸ Polyionic conjugates that can stabilize proteins in the gut have also been reported; the covalent attachment of a cationic dendronized polymer to a proline-specific endopeptidase

(PEP) maintained enzyme activity in the stomach of rats for more than three hours, while control linear mPEG-PEP conjugates were inactive in the harsh environment.⁵⁹ This is important because the conjugate has to pass through the stomach to enter the intestine to be active against coeliac disease. Other polymers such as anionic polyacrylate, PGA, and carboxylated polyamidosaccharides, as well as block copolymers of PEG and poly(histidine) have shown to stabilize a variety of proteins to stressors such as heat, aggregation, and lyophilization.¹²⁹⁻¹³⁴ In another example, a heparin-mimicking polymer, poly(styrene sulfonate-*co*-PEGMA) (p(SS-*co*-PEGMA)), was conjugated to basic fibroblast growth factor (bFGF) (**Figure 1-7c**).¹³⁵ The p(SS-*co*-PEGMA)-bFGF conjugate exhibited superior stability to heat, acidic and proteolytic conditions, and storage when compared to the native protein which was inactivated by these conditions, while maintaining *in vitro* activity. This example in particular demonstrates that rationally designing a polymer to mimic a known biological stabilizer can result in conjugates with superior properties, and further development of heparin-mimicking polymers has since been carried out.¹³⁶⁻¹³⁸

1.5.2. Precise Sequence Control and Monodispersity

Another area of promise is to precisely control the order of different monomer units within a polymer (sequence control) and to obtain absolutely monodisperse conjugates. The former is important for dialing in properties and the latter is advantageous for FDA approval and precise control over properties. This has been recently accomplished for polymers, but has not yet been applied to conjugates. For example, through the use of DNA-templated synthesis, the order of monomer addition can be selectively controlled. Sequence-controlled alkene-linked amino acid oligomers have been synthesized through sequential Wittig reactions.¹³⁹ To prepare these

oligomers, each amino acid was first functionalized with ylide and aldehyde groups, then coupled with DNA to yield ylide-aldehyde DNA macromonomers. Strand association brought macromonomers into contact, assisting Wittig reactions between complementary strands. Subsequent strand exchanges introduced new amino acids into the growing oligomer chain. A DNA template was also used to synthesize sequence-defined polymers of PEG, as well as alpha- and beta-peptides.¹⁴⁰⁻¹⁴¹ In a method designed to be analogous to translation, a series of azide- and alkyne-containing monomeric units were functionalized with peptide nucleic acids (PNAs), through cleavable disulfide linkers. The substrates could then site-specifically hybridize to DNA strands, undergo inter-monomer CuAAC coupling, and then cleave the PNA-monomer linker to free the sequence-controlled polymer from the DNA template. The polymers produced by this method were up to 26kD in size.

1.5.3. Protein-‘Polymer’ Conjugates by Genetic Fusion

A novel approach toward the synthesis of protein-polymer conjugates is the expression of fusion proteins to increase serum-half life.¹⁴² One approach is fusion of a protein of interest to antibodies or other biomolecules that undergo a biological recycling mechanism in order to increase biocirculation time, and 11 of these constructs have already been FDA-approved.¹⁴² More interestingly, amino acid sequences have been designed to mimic PEG by increasing hydrodynamic volume and blocking proteolysis *in vivo*.¹⁴³⁻¹⁴⁴ These constructs have the advantage that they do not require chemical conjugation and have the potential to decrease production, purification, and heterogeneity in conjugate design. Furthermore, they are degradable due to the presence of amide bonds in the resulting polypeptide sequence. One of the most established of these methods is a sequence of aspartic acid, glutamic acid, glycine, proline, serine, and threonine,

named XTEN.¹⁴⁵ This technology has been demonstrated on glucagon¹⁴⁶, glucagon-like-peptide 2¹⁴⁷, human growth hormone¹⁴⁸, and an antiretroviral peptide¹⁴⁹, among others. Other designed amino acid sequences have been shown to have similar benefits to biocirculation, such as conjugation of sequences containing proline, alanine, and serine residues (PASylation).¹⁵⁰ Fusion of elastin-like-peptide (ELP) to an anti-TNF α fragment resulted in improved pharmacokinetic properties in humanized mice.¹⁵¹ Amino acid sequences can also be designed for enhanced stability; zwitterionic sequences of amino acids consisting of alternating glutamic acid and lysine residues have been appended to lactamase and the fusion protein demonstrated increased stability against environmental stressors such as heat and high-salt solutions.¹⁵²

1.6. Summary

Outstanding progress has been made in the past four decades on protein-PEG conjugate drugs for use in medicine. Currently there are 10 PEGylated protein therapeutics that are used clinically to treat a range of diseases, with many more currently under investigation. However, room for improvement still remains. Many conjugates, while improving half-life circulation, exhibit decreased biological activity compared to the native protein. It has been shown that by rational design of the conjugation site and the use of site-selective conjugation reactions, the activity of the protein can be fully retained. Also, the toolbox of protein conjugation techniques is steadily growing with the addition of *grafting from* methods, genetic engineering, highly efficient conjugation chemistries, and new approaches to synthesize end-functional polymers for conjugation. This has led to PEG alternatives that are degradable and new biomimetic strategies to increase stability and activity of native proteins. There are many more possibilities in the future, including polymers with precise sequence control and monodispersity and those that increase the

activity of the protein by specific orthogonal biological function. Protein-polymer conjugation will continue to be an exciting field requiring scientists with expertise in different disciplines including protein biologists, polymer, organic, and computational chemists, physicists, and pharmacologists.

1.7. References

1. Portions of this chapter have been previously published as Pelegri-O'Day, E. M.; Lin, E. W.; Maynard, H. D. *J. Am. Chem. Soc.* **2014**, *136*, 14323.
2. Dimitrov, D. S., *Methods Mol. Biol.* **2012**, *899*, 1.
3. Heredia, K. L.; Maynard, H. D., *Org. Biomol. Chem.* **2007**, *5*, 45.
4. Grover, G. N.; Maynard, H. D., *Curr. Opin. Chem. Biol.* **2010**, *14*, 818.
5. Alconcel, S. N. S.; Baas, A. S.; Maynard, H. D., *Polym. Chem.* **2011**, *2*, 1442.
6. Duncan, R., *Nat. Rev. Drug Discovery* **2003**, *2*, 347.
7. Haag, R.; Kratz, F., *Angew. Chem. Int. Ed.* **2006**, *45*, 1198.
8. Gauthier, M. A.; Klok, H.-A., *Chem. Commun.* **2008**, 2591.
9. Canalle, L. A.; Lowik, D. W. P. M.; van Hest, J. C. M., *Chem. Soc. Rev.* **2010**, *39*, 329.
10. Borchmann, D. E.; Carberry, T. P.; Weck, M., *Macromol. Rapid Commun.* **2014**, *35*, 27.
11. Abuchowski, A.; Vanes, T.; Palczuk, N. C.; Davis, F. F., *J. Biol. Chem.* **1977**, *252*, 3578.
12. Abuchowski, A.; McCoy, J. R.; Palczuk, N. C.; Vanes, T.; Davis, F. F., *J. Biol. Chem.* **1977**, *252*, 3582.
13. Maeda, H.; Takeshita, J.; Kanamaru, R., *Int. J. Pept. Protein Res.* **1979**, *14*, 81.
14. Greish, K.; Fang, J.; Inutsuka, T.; Nagamitsu, A.; Maeda, H., *Clin. Pharmacokinet.* **2003**, *42*, 1089.
15. Owens, D. E.; Peppas, N. A., *Int. J. Pharm.* **2006**, *307*, 93.
16. Norman, M. E.; Williams, P.; Illum, L., *Biomaterials* **1992**, *13*, 841.
17. Carstensen, H.; Muller, R. H.; Muller, B. W., *Clin. Nutr.* **1992**, *11*, 289.
18. Roser, M.; Fischer, D.; Kissel, T., *Eur. J. Pharm. Biopharm.* **1998**, *46*, 255.
19. Pfister, D.; Morbidelli, M., *J. Controlled Release* **2014**, *180*, 134.

20. Besheer, A.; Liebner, R.; Meyer, M.; Winter, G. In *Tailored Polymer Architectures for Pharmaceutical and Biomedical Applications*; Scholz, C., Kressler, J., Eds.; ACS Symposium Series, Vol. 1135; American Chemical Society: Washington, DC, **2013**; p 215.
21. Roberts, M. J.; Bentley, M. D.; Harris, J. M., *Adv. Drug Delivery Rev.* **2002**, *64*, 116.
22. Veronese, F. M.; Largajolli, R.; Boccú, E.; Benassi, C. A.; Schiavon, O., *Appl. Biochem. Biotechnol.* **1985**, *11*, 141.
23. Gaertner, H. F.; Offord, R. E., *Bioconj. Chem.* **1996**, *7*, 38.
24. Gilmore, J. M.; Scheck, R. A.; Esser-Kahn, A. P.; Joshi, N. S.; Francis, M. B., *Angew. Chem. Int. Ed.* **2006**, *45*, 5307.
25. Kinstler, O. B.; Brems, D. N.; Lauren, S. L.; Paige, A. G.; Hamburger, J. B.; Treuheit, M. J., *Pharm. Res.* **1996**, *13*, 996.
26. Kogan, T. P., *Synth. Commun.* **1992**, *22*, 2417.
27. Woghiren, C.; Sharma, B.; Stein, S., *Bioconj. Chem.* **1993**, *4*, 314.
28. Morpurgo, M.; Veronese, F. M.; Kachensky, D.; Harris, J. M., *Bioconj. Chem.* **1996**, *7*, 363.
29. Jones, M. W.; Strickland, R. A.; Schumacher, F. F.; Caddick, S.; Baker, J. R.; Gibson, M. I.; Haddleton, D. M., *J. Am. Chem. Soc.* **2012**, *134*, 1847.
30. Shaunak, S.; Godwin, A.; Choi, J. W.; Balan, S.; Pedone, E.; Vijayarangam, D.; Heidelberger, S.; Teo, I.; Zloh, M.; Brocchini, S., *Nat. Chem. Biol.* **2006**, *2*, 312.
31. Smith, M. E. B.; Schumacher, F. F.; Ryan, C. P.; Tedaldi, L. M.; Papaioannou, D.; Waksman, G.; Caddick, S.; Baker, J. R., *J. Am. Chem. Soc.* **2010**, *132*, 1960.
32. Goodson, R. J.; Katre, N. V., *Bio-Technology* **1990**, *8*, 343.

33. Dieterich, D. C.; Link, A. J.; Graumann, J.; Tirrell, D. A.; Schuman, E. M., *Proc. Natl. Acad. Sci. U. S. A.* **2006**, *103*, 9482.
34. Dawson, P. E.; Muir, T. W.; Clarklewis, I.; Kent, S. B. H., *Science* **1994**, *266*, 776.
35. Kochendoerfer, G. G.; Chen, S. Y.; Mao, F.; Cressman, S.; Traviglia, S.; Shao, H. Y.; Hunter, C. L.; Low, D. W.; Cagle, E. N.; Carnevali, M.; Gueriguian, V.; Keogh, P. J.; Porter, H.; Stratton, S. M.; Wiedeke, M. C.; Wilken, J.; Tang, J.; Levy, J. J.; Miranda, L. P.; Crnogorac, M. M.; Kalbag, S.; Botti, P.; Schindler-Horvat, J.; Savatski, L.; Adamson, J. W.; Kung, A.; Kent, S. B. H.; Bradburne, J. A., *Science* **2003**, *299*, 884.
36. Kato, M.; Kamigaito, M.; Sawamoto, M.; Higashimura, T., *Macromolecules* **1995**, *28*, 1721.
37. Wang, J. S.; Matyjaszewski, K., *J. Am. Chem. Soc.* **1995**, *117*, 5614.
38. Chiefari, J.; Chong, Y. K.; Ercole, F.; Krstina, J.; Jeffery, J.; Le, T. P. T.; Mayadunne, R. T. A.; Meijs, G. F.; Moad, C. L.; Moad, G.; Rizzardo, E.; Thang, S. H., *Macromolecules* **1998**, *31*, 5559.
39. Carrillo, A.; Gujraty, K. V.; Rai, P. R.; Kane, R. S., *Nanotechnology* **2005**, *16*, S416.
40. Chen, B. Z.; Metera, K.; Sleiman, H. F., *Macromolecules* **2005**, *38*, 1084.
41. Liu, Z.; Dong, C.; Wang, X.; Wang, H.; Li, W.; Tan, J.; Chang, J., *ACS Appl. Mater. Interfac.* **2014**, *6*, 2393.
42. Gauthier, M. A.; Klok, H. A., *Chem. Commun.* **2008**, 2591.
43. Bontempo, D.; Heredia, K. L.; Fish, B. A.; Maynard, H. D., *J. Am. Chem. Soc.* **2004**, *126*, 15372.
44. Boyer, C.; Liu, J.; Wong, L.; Tippett, M.; Bulmus, V.; Davis, T. P., *J Polym Sci Pol Chem* **2008**, *46*, 7207.

45. Bontempo, D.; Maynard, H. D., *J. Am. Chem. Soc.* **2005**, *127*, 6508.
46. Heredia, K. L.; Bontempo, D.; Ly, T.; Byers, J. T.; Halstenberg, S.; Maynard, H. D., *J. Am. Chem. Soc.* **2005**, *127*, 16955.
47. Liu, J. Q.; Bulmus, V.; Herlambang, D. L.; Barner-Kowollik, C.; Stenzel, M. H.; Davis, T. P., *Angew. Chem. Int. Ed.* **2007**, *46*, 3099.
48. Boyer, C.; Bulmus, V.; Liu, J. Q.; Davis, T. P.; Stenzel, M. H.; Barner-Kowollik, C., *J. Am. Chem. Soc.* **2007**, *129*, 7145.
49. Peeler, J. C.; Woodman, B. F.; Averick, S.; Miyake-Stoner, S. J.; Stokes, A. L.; Hess, K. R.; Matyjaszewski, K.; Mehl, R. A., *J. Am. Chem. Soc.* **2010**, *132*, 13575.
50. Gao, W. P.; Liu, W. G.; Mackay, J. A.; Zalutsky, M. R.; Toone, E. J.; Chilkoti, A., *Proc. Natl. Acad. Sci. U. S. A.* **2009**, *106*, 15231.
51. Gao, W.; Liu, W.; Christensen, T.; Zalutsky, M. R.; Chilkoti, A., *Proc. Natl. Acad. Sci. U. S. A.* **2010**, *107*, 16432.
52. Isarov, S. A.; Pokorski, J. K., *ACS Macro Lett.* **2015**, *4*, 969.
53. Lele, B. S.; Murata, H.; Matyjaszewski, K.; Russell, A. J., *Biomacromolecules* **2005**, *6*, 3380.
54. Magnusson, J. P.; Bersani, S.; Salmaso, S.; Alexander, C.; Caliceti, P., *Bioconj. Chem.* **2010**, *21*, 671.
55. De, P.; Li, M.; Gondi, S. R.; Sumerlin, B. S., *J. Am. Chem. Soc.* **2008**, *130*, 11288.
56. Chang, C.-W.; Bays, E.; Tao, L.; Alconcel, S. N. S.; Maynard, H. D., *Chem. Commun.* **2009**, 3580.
57. Ryan, S. M.; Frias, J. M.; Wang, X.; Sayers, C. T.; Haddleton, D. M.; Brayden, D. J., *J. Controlled Release* **2011**, *149*, 126.

58. Tao, L.; Chen, G.; Zhao, L.; Xu, J.; Huang, E.; Liu, A.; Marquis, C. P.; Davis, T. P., *Chem. - Asian J.* **2011**, *6*, 1398.
59. Fuhrmann, G.; Grotzky, A.; Lukic, R.; Matorri, S.; Luciani, P.; Yu, H.; Zhang, B.; Walde, P.; Schlueter, A. D.; Gauthier, M. A.; Leroux, J.-C., *Nat. Chem.* **2013**, *5*, 582.
60. Tsunoda, S.; Kamada, H.; Yamamoto, Y.; Ishikawa, T.; Matsui, J.; Koizumi, K.; Kaneda, Y.; Tsutsumi, Y.; Ohsugi, Y.; Hirano, T.; Mayumi, T., *J. Controlled Release* **2000**, *68*, 335.
61. Lewis, A.; Tang, Y.; Brocchini, S.; Choi, J.-w.; Godwin, A., *Bioconj. Chem.* **2008**, *19*, 2144.
62. Crownover, E. F.; Convertine, A. J.; Stayton, P. S., *Polym. Chem.* **2011**, *2*, 1499.
63. Richter, A. W.; Akerblom, E., *Int. Arch. Allergy Appl. Immunol.* **1984**, *74*, 36.
64. Liu, Y.; Reidler, H.; Pan, J.; Milunic, D.; Qin, D.; Chen, D.; Vallejo, Y. R.; Yin, R., *J. Pharmacol. Toxicol. Methods* **2011**, *64*, 238.
65. Fisher, T. C.; Armstrong, J. K.; Wenby, R. B.; Meiselman, H. J.; Leger, R.; Garratty, G., *Blood* **2003**, *102*, 559A.
66. Schellekens, H.; Hennink, W. E.; Brinks, V., *Pharm. Res.* **2013**, *30*, 1729.
67. Armstrong, J. K. In *PEGylated Protein Drugs: Basic Science and Clinical Applications*; Veronese, F. M., Ed.; Birkhäuser: Basel, Switzerland, **2009**; p 147.
68. Shah, S.; Prematta, T.; Adkinson, N. F.; Ishmael, F. T. *J. Clin. Pharmacol.* **2013**, *53*, 352.
69. Conover, C.; Lejeune, L.; Linberg, R.; Shum, K.; Shorr, R. G. L., *Artif. Cells Blood Sub. Immobil. Technol.* **1996**, *24*, 599.
70. Conover, C. D.; Linberg, R.; Gilbert, C. W.; Sham, K. L.; Shorr, R. G. L., *Artif. Organs* **1997**, *21*, 1066.
71. Conover, C. D.; Gilbert, C. W.; Shum, K. L.; Shorr, R. G. L., *Artif. Organs* **1997**, *21*, 907.

72. Conover, C. D.; Lejeune, L.; Shum, K.; Gilbert, C.; Shorr, R. G. L., *Artif. Organs* **1997**, *21*, 369.
73. Bendele, A.; Seely, J.; Richey, C.; Sennello, G.; Shopp, G., *Toxicol. Sci.* **1998**, *42*, 152.
74. Knop, K.; Hoogenboom, R.; Fischer, D.; Schubert, U. S., *Angew. Chem. Int. Ed.* **2010**, *49*, 6288.
75. Duncan, R.; Vicent, M. J., *Adv. Drug Delivery Rev.* **2010**, *62*, 272.
76. Tao, L.; Liu, J.; Xu, J.; Davis, T. P., *Org. Biomol. Chem.* **2009**, *7*, 3481.
77. Tao, L.; Liu, J.; Davis, T. P., *Biomacromolecules* **2009**, *10*, 2847.
78. Treetharnmathurot, B.; Dieudonne, L.; Ferguson, E. L.; Schmaljohann, D.; Duncan, R.; Wiwattanapatapee, R., *Int. J. Pharm.* **2009**, *373*, 68.
79. Ulbrich, K.; Strohalm, J.; Plocova, D.; Oupicky, D.; Subr, V.; Soucek, J.; Pouckova, P.; Matousek, J., *J. Bioact. Compat. Polym.* **2000**, *15*, 4.
80. Oupicky, D.; Ulbrich, K.; Rihova, B., *J. Bioact. Compat. Polym.* **1999**, *14*, 213.
81. Ulbrich, K.; Subr, V.; Strohalm, J.; Plocova, D.; Jelinkova, M.; Rihova, B., *J. Controlled Release* **2000**, *64*, 63.
82. Lee, W. Y.; Schon, A. H.; Vonspecht, B. U., *Eur. J. Immunol.* **1981**, *11*, 13.
83. Smorodinsky, N.; Vonspecht, B. U.; Cesla, R.; Shaltiel, S., *Immunol. Lett.* **1981**, *2*, 305.
84. Pound, G.; McKenzie, J. M.; Lange, R. F. M.; Klumperman, B., *Chem. Commun.* **2008**, 3193.
85. Caliceti, P.; Schiavon, O.; Veronese, F. M., *Bioconj. Chem.* **2001**, *12*, 515.
86. Zalipsky, S.; Hansen, C. B.; Oaks, J. M.; Allen, T. M., *J. Pharm. Sci.* **1996**, *85*, 133.
87. Gaertner, F. C.; Luxenhofer, R.; Blechert, B.; Jordan, R.; Essler, M., *J. Controlled Release* **2007**, *119*, 291.

88. Hoogenboom, R., *Angew. Chem. Int. Ed.* **2009**, *48*, 7978.
89. Viegas, T. X.; Bentley, M. D.; Harris, J. M.; Fang, Z.; Yoon, K.; Dizman, B.; Weimer, R.; Mero, A.; Pasut, G.; Veronese, F. M., *Bioconj. Chem.* **2011**, *22*, 976.
90. Konradi, R.; Pidhatika, B.; Muehlebach, A.; Textort, M., *Langmuir* **2008**, *24*, 613.
91. Mero, A.; Fang, Z.; Pasut, G.; Veronese, F. M.; Viegas, T. X., *J. Controlled Release* **2012**, *159*, 353.
92. Lee, Y.; Koo, H.; Jin, G. W.; Mo, H. J.; Cho, M. Y.; Park, J. Y.; Choi, J. S.; Park, J. S., *Biomacromolecules* **2005**, *6*, 24.
93. Sun, K. H.; Sohn, Y. S.; Jeong, B., *Biomacromolecules* **2006**, *7*, 2871.
94. Tsarevsky, N. V.; Matyjaszewski, K., *Macromolecules* **2005**, *38*, 3087.
95. Cerritelli, S.; Velluto, D.; Hubbell, J. A., *Biomacromolecules* **2007**, *8*, 1966.
96. Lundberg, P.; Lee, B. F.; van den Berg, S. A.; Pressly, E. D.; Lee, A.; Hawker, C. J.; Lynd, N. A., *ACS Macro Lett.* **2012**, *1*, 1240.
97. Dingels, C.; Mueller, S. S.; Steinbach, T.; Tonhauser, C.; Frey, H., *Biomacromolecules* **2013**, *14*, 448.
98. Hey, T.; Knoller, H.; Vorstheim, P. In *Therapeutic Proteins*; Wiley-VCH: Weinheim, Germany, **2012**; p 117.
99. Lameire, N.; Hoste, E., *Intensive Care Med.* **2014**, *40*, 427.
100. Duncan, R., *Curr. Opin. Biotechnol.* **2011**, *22*, 492.
101. Hardwicke, J. T.; Hart, J.; Bell, A.; Duncan, R.; Thomas, D. W.; Moseley, R., *J. Controlled Release* **2011**, *152*, 411.
102. Jain, S.; Hreczuk-Hirst, D. H.; McCormack, B.; Mital, M.; Epenetos, A.; Laing, P.; Gregoriadis, G., *Biochim. Biophys. Acta, Gen. Subj.* **2003**, *1622*, 42.

103. Chipman, S. D.; Oldham, F. B.; Pezzoni, G.; Singer, J. W. *Int. J. Nanomed.* **2006**, *1*, 375.
104. Veronese, F. M.; Caliceti, P.; Schiavon, O., *J. Bioact. Compat. Polym.* **1997**, *12*, 196.
105. ul-Haq, M. I.; Lai, B. F. L.; Chapanian, R.; Kizhakkedathu, J. N., *Biomaterials* **2012**, *33*, 9135.
106. Khandare, J. J.; Jayant, S.; Singh, A.; Chandna, P.; Wang, Y.; Vorsa, N.; Minko, T., *Bioconj. Chem.* **2006**, *17*, 1464.
107. Kainthan, R. K.; Brooks, D. E., *Biomaterials* **2007**, *28*, 4779.
108. Delplace, V.; Tardy, A.; Harrisson, S.; Mura, S.; Gigmes, D.; Guillaneuf, Y.; Nicolas, J., *Biomacromolecules* **2013**, *14*, 3769.
109. Riachi, C.; Schuwer, N.; Klok, H. A., *Macromolecules* **2009**, *42*, 8076.
110. Siegwart, D. J.; Bencherif, S. A.; Srinivasan, A.; Hollinger, J. O.; Matyjaszewski, K., *J. Biomed. Mater. Res., Part A* **2008**, *87A*, 345.
111. Decker, C. G.; Maynard, H. D., *Eur. Polym. J.* **2015**, *65*, 305.
112. Sayers, C. T.; Mantovani, G.; Ryan, S. M.; Randev, R. K.; Keiper, O.; Leszczyszyn, O. I.; Blindauer, C.; Brayden, D. J.; Haddleton, D. M., *Soft Matter* **2009**, *5*, 3038.
113. Thomas, A.; Mueller, S. S.; Frey, H., *Biomacromolecules* **2014**, *15*, 1935.
114. Wurm, F.; Dingels, C.; Frey, H.; Klok, H. A., *Biomacromolecules* **2012**, *13*, 1161.
115. Spears, B. R.; Waksal, J.; McQuade, C.; Lanier, L.; Harth, E., *Chem. Commun.* **2013**, *49*, 2394.
116. Mortell, K. H.; Weatherman, R. V.; Kiessling, L. L., *J. Am. Chem. Soc.* **1996**, *118*, 2297.
117. Mowery, P.; Yang, Z. Q.; Gordon, E. J.; Dwir, O.; Spencer, A. G.; Alon, R.; Kiessling, L. L., *Chem. Biol.* **2004**, *11*, 725.

118. Sen Gupta, S.; Raja, K. S.; Kaltgrad, E.; Strable, E.; Finn, M. G., *Chem. Commun.* **2005**, 4315.
119. Geng, J.; Mantovani, G.; Tao, L.; Nicolas, J.; Chen, G. J.; Wallis, R.; Mitchell, D. A.; Johnson, B. R. G.; Evans, S. D.; Haddleton, D. M., *J. Am. Chem. Soc.* **2007**, *129*, 15156.
120. Rendle, P. M.; Seger, A.; Rodrigues, J.; Oldham, N. J.; Bott, R. R.; Jones, J. B.; Cowan, M. M.; Davis, B. G., *J. Am. Chem. Soc.* **2004**, *126*, 4750.
121. Leader, B.; Baca, Q. J.; Golan, D. E., *Nat. Rev. Drug Discovery* **2008**, *7*, 21.
122. Lee, J.; Lin, E.-W.; Lau, U. Y.; Hedrick, J. L.; Bat, E.; Maynard, H. D., *Biomacromolecules* **2013**, *14*, 2561.
123. Mancini, R. J.; Lee, J.; Maynard, H. D., *J. Am. Chem. Soc.* **2012**, *134*, 8474.
124. Liu, Y.; Lee, J.; Mansfield, K. M.; Ko, J. H.; Sallam, S.; Wesderniotis, C.; Maynard, H. D., *Bioconj. Chem.* **2017**, *28*, 836.
125. Messina, M. S.; Ko, J. H.; Yang, Z. Y.; Strouse, M. J.; Houk, K. N.; Maynard, H. D., *Polym. Chem.* **2017**, *8*, 4781.
126. Pelegri-O'Day, E. M.; Paluck, S. J.; Maynard, H. D., *J. Am. Chem. Soc.* **2017**, *139*, 1145.
127. Mansfield, K. M.; Maynard, H. D., *ACS Macro Lett.* **2018**, *7*, 324.
128. Keefe, A. J.; Jiang, S., *Nat. Chem.* **2012**, *4*, 59.
129. Martin, N.; Ma, D.; Herbet, A.; Boquet, D.; Winnik, F. M.; Tribet, C., *Biomacromolecules* **2014**, *15*, 2952.
130. Lee, E.-H.; Tsujimoto, T.; Uyama, H.; Sung, M.-H.; Kim, K.; Kuramitsu, S., *Polym. J.* **2010**, *42*, 818.
131. Izaki, S.; Kurinomaru, T.; Handa, K.; Kimoto, T.; Shiraki, K., *J. Pharm. Sci.* **2015**, *104*, 2457.

132. Gombotz, W. R.; Pankey, S. C.; Phan, D.; Drager, R.; Donaldson, K.; Antonsen, K. P.; Hoffman, A. S.; Raff, H. V., *Pharm. Res.* **1994**, *11*, 624.
133. Stidham, S. E.; Chin, S. L.; Dane, E. L.; Grinstaff, M. W., *J. Am. Chem. Soc.* **2014**, *136*, 9544.
134. Taluja, A.; Bae, Y. H., *Mol. Pharmaceutics* **2007**, *4*, 561.
135. Nguyen, T. H.; Kim, S.-H.; Decker, C. G.; Wong, D. Y.; Loo, J. A.; Maynard, H. D., *Nat. Chem.* **2013**, *5*, 221.
136. Nguyen, T. H.; Paluck, S. J.; McGahran, A. J.; Maynard, H. D., *Biomacromolecules* **2015**, *16*, 2684.
137. Paluck, S. J.; Nguyen, T. H.; Lee, J. P.; Maynard, H. D., *Biomacromolecules* **2016**, *17*, 3386.
138. Paluck, S. J.; Maynard, H. D., *Polym. Chem.* **2017**, *8*, 4548.
139. McKee, M. L.; Milnes, P. J.; Bath, J.; Stulz, E.; Turberfield, A. J.; O'Reilly, R. K., *Angew. Chem. Int. Ed.* **2010**, *49*, 7948.
140. Li, X. Y.; Liu, D. R., *Angew. Chem. Int. Ed.* **2004**, *43*, 4848.
141. Niu, J.; Hili, R.; Liu, D. R., *Nat. Chem.* **2013**, *5*, 282.
142. Strohl, W. R., *BioDrugs* **2015**, *29*, 215.
143. Podust, V. N.; Balan, S.; Sim, B. C.; Coyle, M. P.; Ernst, U.; Peters, R. T.; Schellenberger, V., *J. Controlled Release* **2016**, *240*, 52.
144. Despanie, J.; Dhandhukia, J. P.; Hamm-Alvarez, S. F.; MacKay, J. A., *J. Controlled Release* **2016**, *240*, 93.

145. Schellenberger, V.; Wang, C. W.; Geething, N. C.; Spink, B. J.; Campbell, A.; To, W.; Scholle, M. D.; Yin, Y.; Yao, Y.; Bogin, O.; Cleland, J. L.; Silverman, J.; Stemmer, W. P. C., *Nat. Biotechnol.* **2009**, *27*, 1186.
146. Geething, N. C.; To, W.; Spink, B. J.; Scholle, M. D.; Wang, C. W.; Yin, Y.; Yao, Y.; Schellenberger, V.; Cleland, J. L.; Stemmer, W. P. C.; Silverman, J., *PLoS One* **2010**, *5*.
147. Alters, S. E.; McLaughlin, B.; Spink, B.; Lachinyan, T.; Wang, C. W.; Podust, V.; Schellenberger, V.; Stemmer, W. P. C., *PLoS One* **2012**, *7*.
148. Cleland, J. L.; Geething, N. C.; Moore, J. A.; Rogers, B. C.; Spink, B. J.; Wang, C. W.; Alters, S. E.; Stemmer, W. P. C.; Schellenberger, V., *J. Pharm. Sci.* **2012**, *101*, 2744.
149. Ding, S.; Song, M.; Sim, B. C.; Gu, C.; Podust, V. N.; Wang, C. W.; McLaughlin, B.; Shah, T. P.; Lax, R.; Gast, R.; Sharan, R.; Vasek, A.; Hartman, M. A.; Deniston, C.; Srinivas, P.; Schellenberger, V., *Bioconj. Chem.* **2014**, *25*, 1351.
150. Schlapschy, M.; Binder, U.; Borger, C.; Theobald, I.; Wachinger, K.; Kisling, S.; Haller, D.; Skerra, A., *Protein Eng., Des. Sel.* **2013**, *26*, 489.
151. Conrad, U.; Plagmann, I.; Malchow, S.; Sack, M.; Floss, D. M.; Kruglov, A. A.; Nedospasov, S. A.; Rose-John, S.; Scheller, J., *Plant Biotechnol. J.* **2011**, *9*, 22.
152. Liu, E. J.; Sinclair, A.; Keefe, A. J.; Nannenga, B. L.; Coyle, B. L.; Baneyx, F.; Jiang, S. Y., *Biomacromolecules* **2015**, *16*, 3357.

Chapter 2

Synthesis of Degradable Trehalose Polymers via Copolymerization of Cyclic Ketene Acetals¹

2.1. Introduction

Poly(ethylene glycol) (PEG) is widely used in polymer-based therapeutics to improve the pharmacological properties of protein therapeutics. Decades of clinical experience and product development for PEG-based materials have both illustrated benefits and revealed shortcomings. Side effects include hypersensitivity and immunogenicity against PEG, accumulation of PEG in organs, and non-biodegradability.²⁻⁴ In addition, protein-PEG conjugates are known to be unstable to increased temperatures.⁵ These disadvantages provide a strong motivation for the development of PEG alternatives.

In recent years, synthesis of polymers with additional benefits other than improved pharmacokinetic properties is of great interest.⁶⁻⁸ For example, polymers that stabilize proteins against environmental stressors can be used to eliminate the loss of protein activity associated with storage and handling.⁹ Charged materials such as poly(sulfonates), poly(carboxybetaines), and cationic dendronized polymers have protected conjugates against environmental and thermal stressors.¹⁰⁻¹³ Additionally, synthetic carboxylated polyamidosaccharides have been shown to retain lysozyme activity after multiple lyophilization cycles.¹⁴ And our group has previously reported on glycopolymers with trehalose side chains for enhancing stability of a wide range of proteins against lyophilization, mechanical, and heat stress.¹⁵⁻¹⁸ Yet, most of the reported stabilizers are not degradable.

Hydrolytically or enzymatically degradable alternatives have been used but may present difficulties such as undesired biological side effects or difficulty in attaching protein-reactive units. For instance, hydroxyethyl starch has been extensively used for the preparation of protein conjugates with increased half-lives, but may accumulate in some organs increasing risk of death for critically ill patients.¹⁹⁻²⁰ To address this need, we recently described stabilizing polymers with

polyester backbones.¹⁸ Specifically, polycaprolactone was prepared with zwitterionic and trehalose side chains. These polymers were highly effective protein stabilizers and also degraded through ester hydrolysis. We were thus interested to investigate other degradable protein stabilizers, specifically, those that could be made by controlled radical polymerizations (CRP). We had previously prepared degradable comb PEG polymers by CRP and conjugated them to proteins.²¹ However, these polymers were not protein stabilizers.

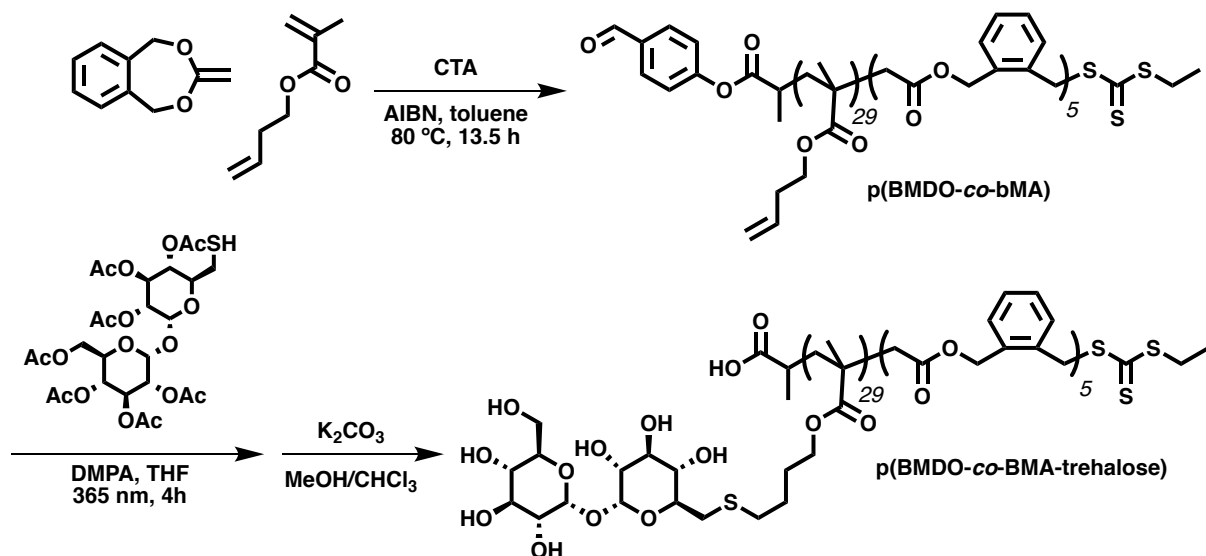
An effective method of introducing degradable units by CRP is by copolymerization of cyclic ketene acetals (CKAs).²²⁻²⁴ This class of monomers undergoes radical ring-opening polymerization to insert degradable esters into the growing polymer chain and is compatible with various CRP techniques. In particular, 5,6-benzo-2-methylene-1,3-dioxepane (BMDO) has been extensively employed,²⁵⁻²⁷ including in degradable glycopolymers. For example, Lu and coworkers described the synthesis of a styrenyl galactopyranose-based copolymer,²⁸ and recently Stenzel and coworkers copolymerized BMDO with an acryloyl fructopyranose monomer.²⁹ Herein, we describe the synthesis and initial biological evaluation of trehalose side chain polymers with BMDO units incorporated in the backbone by reversible addition-fragmentation chain transfer (RAFT) polymerization.

2.2. Results and Discussion

2.2.2. Polymer Synthesis and Characterization

Initial attempts to copolymerize BMDO with a trimethylsilyl (TMS)-protected trehalose monomer were unsuccessful, presumably due to steric hindrance between bulky protected trehalose units (data not shown). Therefore, a system of post-polymerization modification was employed. First, RAFT polymerization was performed with a trithiocarbonate chain transfer agent

(CTA)¹⁷, but-3-enyl methacrylate (bMA), BMDO, and azobisisobutyronitrile (AIBN) to yield p(BMDO-*co*-bMA) (see **Scheme 2-1** for synthetic steps and **Figure 2-7** for ¹H NMR characterization). The final polymer contained 29 bMA units and 5 BMDO units, with a number-average molecular weight (M_n) of 5200 by ¹H-NMR and 2900 by gel permeation chromatography (GPC) and a molecular weight dispersity (\mathcal{D}) of 1.76.



Scheme 2-1. Synthesis of p(BMDO-*co*-bMA) and modification with thiolated trehalose to yield p(BMDO-*co*-BMA-trehalose).

Consistent with the literature,³³ no crosslinking of alkene units was observed and there was no consumption of alkene protons (5.81 ppm) compared to methylene protons (4.06 ppm) in the ¹H-NMR spectrum (**Figure 2-7**). The incomplete control over the polymerization is hypothesized to be due to the mismatch between BMDO and the activated bMA monomer. Thiolated trehalose¹⁸ was then coupled *via* thiol-ene chemistry to prepare p(BMDO-*co*-BMA-trehalose-OAc). GPC analysis revealed a clean increase in molecular weight ($M_n = 20,900$) and decrease in \mathcal{D} to 1.22, consistent with attachment of trehalose side chains (**Figure 2-1**).

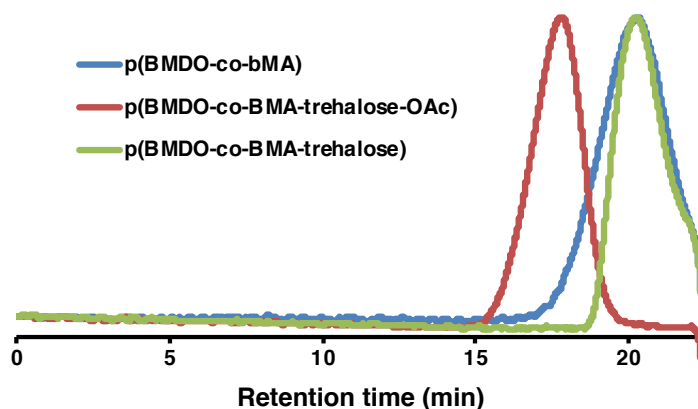


Figure 2-1. Gel permeation chromatograms of p(BMDO-*co*-bMA), p(BMDO-*co*-BMA-trehalose-OAc), and p(BMDO-*co*-BMA-trehalose).

The acetyl groups were then removed with K_2CO_3 to yield p(BMDO-*co*-BMA-trehalose) (see **Figure 2-8** and **Figure 2-9** for 1H NMR characterization). By GPC the M_n shifted to a value of 3300 Da and \mathcal{D} of 1.29. ($M_n = 4600$ and $\mathcal{D} = 1.30$ by aq. SEC), which is smaller than would be anticipated. The M_n by 1H -NMR could not be determined accurately because a complete loss of the aldehyde end group was observed. However, we believe the low molecular weight was not due to cleavage of the backbone during these mild deprotection conditions because treatment with KOH further reduces the molecular weight (**Figure 2-2**) and we have previously shown that BMDO copolymers are stable for greater than 7 days in carbonate solution.²¹ Instead, the low M_n is likely a result of interactions of the polymer with the GPC column, as we have previously observed with other trehalose polymers.³⁴

Degradation of p(BMDO-*co*-BMA-trehalose) was evaluated by exposure to a 5% KOH solution. KOH is commonly used to accelerate conditions for polymer degradation.^{21, 25-26, 35} The trehalose copolymer was found to be hydrolytically degradable, and degradation was observed

within 24 hours as demonstrated by a decrease in GPC molecular weight to 1900 Da (**Figure 2-2**). No further degradation was observed upon longer incubation in KOH. The degraded products were neutralized and dialyzed in water to remove salts for cytotoxicity evaluation. Hydrolytic degradation in cell-conditioned media and upon esterase exposure was also explored (**Table 2-1**), but no decrease in molecular weight was observed on the time scale tested (3 weeks). Slight increases in observed M_n were hypothesized to be due to overlap between biomolecule peaks and p(BMDO-co-BMA-trehalose) in the SEC trace.

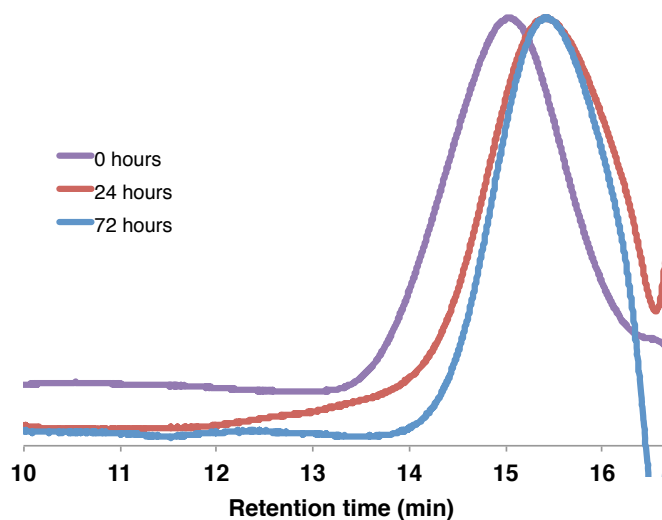


Figure 2-2. Gel permeation chromatograms demonstrating degradation of p(BMDO-co-BMA-trehalose) after 0, 24, and 72 hours in 5% KOH.

Table 2-1. Molecular weight and GPC data for degradation of p(BMDO-co-BMA-trehalose)

	Time	Mn	D
KOH	0 h	4600	1.30
	24 h	1900	1.70
Cell-conditioned media	0h	4800	1.34
	192 h	5300	1.78
	504 h	5800	1.99
1 wt% esterase	0h	4700	1.30
	18 h	4900	1.37
	72 h	5000	1.42
	120 h	5000	1.40

2.2.2. Cytocompatibility of Degradable Trehalose Polymers

Cytotoxicity assessment of the degraded and non-degraded products of p(BMDO-co-BMA-trehalose) from 0.01 to 1 mg/mL concentrations was carried out in NFS-60 cells and human dermal fibroblasts (HDFs) using a LIVE/DEAD assay. Benzyl trehalose and p(styrenyl acetal trehalose) (**Figure 2-3**) both previously shown to be non-cytotoxic,¹⁶ were included in the assays as controls; benzyl trehalose was selected to be analogous with the degraded trehalose fragments.

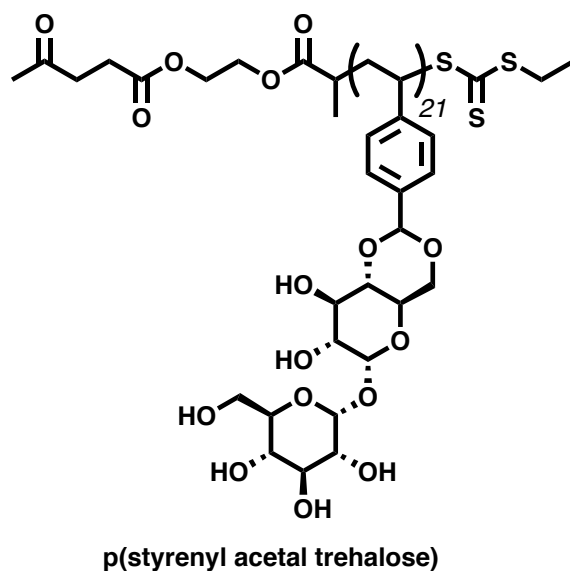


Figure 2-3. Structure of control polymer p(styrenyl acetal trehalose).

In HDFs, degraded p(BMDO-*co*-BMA-trehalose) products were shown to reduce cell viability to 74% at 1 mg/mL, the highest concentration tested, while the non-degraded polymer and benzyl trehalose was shown to be non-cytotoxic at that concentration (**Figure 2-4**). These results indicate that the degraded BMDO unit, and not the trehalose monomer unit, is most likely associated with the observed cytotoxicity. Similar effects were observed in NFS-60 cells. p(Styrenyl acetal trehalose) exhibited no cytotoxicity (100% cell viability relative to no excipient), p(BMDO-*co*-BMA-trehalose) was 95%, and the degraded polymer fragments dropped to 90% cell viability at a concentration of 1 mg/mL (**Figure 2-4b**). Again, degraded p(BMDO-*co*-BMA-trehalose) had a significantly greater adverse effect on cells compared to the non-degraded polymer, which suggests that the degraded products are cytotoxic at high concentrations. To our knowledge, no previous investigation of BMDO degradation product cytocompatibility at concentrations above 0.2 mg/mL has been carried out. At lower concentrations of degraded fragments, p(BMDO-*co*-BMA-trehalose) is equivalent to those previously described.^{26, 29}

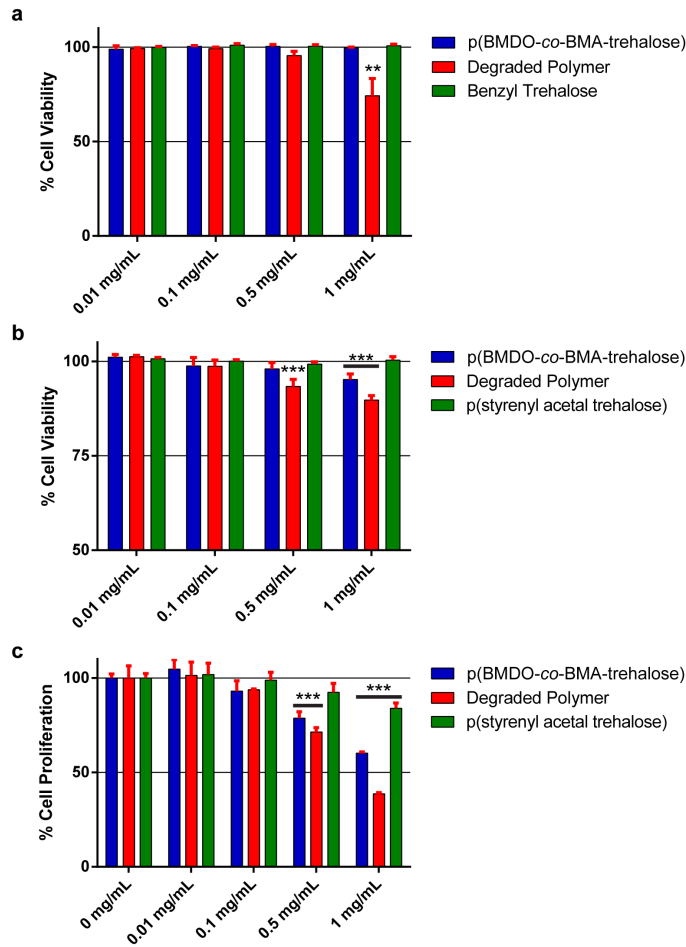


Figure 2-4. Cytotoxicity assay of p(BMDO-co-BMA-trehalose) before and after degradation and benzyl trehalose in a) HDFs by LIVE/DEAD assay (n = 4), and of the non-degraded, degraded products and p(styrenyl acetal trehalose) in NFS-60 cells based on b) cell viability by LIVE/DEAD assay (n = 4), and c) cell proliferation (n = 6). Results are shown as the average with standard deviation and normalized to 100% to the condition of no excipients. ** = $p < 0.01$, *** = $p < 0.005$ relative to no excipients.

The effects of p(BMDO-co-BMA-trehalose) and p(styrenyl acetal trehalose) on cell proliferation were evaluated at concentrations up to 1 mg/mL in NFS-60 cells (**Figure 2-4c**). At the highest concentration, the percent cell proliferation was reduced to 84% for the control

trehalose polymer, 60% for p(BMDO-*co*-BMA-trehalose), and 38% for degraded polymer relative to no additive control. Because these values are significantly higher than the decreases in cell viability previously observed, this indicates that the nondegraded polymers are inhibiting NFS-60 cell growth rather than killing the cells. This combination of inhibition and slight cytotoxicity observed for both p(BMDO-*co*-BMA-trehalose) and the degraded products resulted in a significant decrease in NFS-60 cell proliferation at higher polymer concentrations.

2.2.3. Stabilization of Granulocyte Colony Stimulating Factor (G-CSF)

Next, the trehalose glycopolymers were evaluated for their ability to stabilize the purified G-CSF protein to heat stress. G-CSF was heated at 40 °C for 30 minutes with and without excipients and the bioactivity was assayed by NFS-60 cell proliferation. The excipients included PEG, trehalose, p(BMDO-*co*-BMA-trehalose), and p(styrenyl acetal trehalose), and were screened with weight equivalents from 1 to 500 relative to G-CSF. The resulting G-CSF bioactivities with and without excipients are shown in **Figure 2-5**.

The activity of G-CSF was reduced to about 30% following heat treatment. The addition of PEG did not stabilize G-CSF as the activity levels ($37\% \pm 3.8$) were similar to the negative control (**Figure 2-5a**). In the presence of trehalose, $77\% \pm 7.6$ activity was retained at 500 wt. eq. relative to G-CSF, which showed moderate stabilization (**Figure 2-5b**). Moderate stabilization of G-CSF was also observed with the addition of p(BMDO-*co*-BMA-trehalose) showing $66\% \pm 4.6$ and $51\% \pm 5.9$ of the original activity with 10 and 500 wt. eq., respectively (**Figure 2-5c**). P(styrenyl acetal trehalose), especially at 500 wt. eq., showed full retention of activity (**Figure 2-5d**). In all of the trehalose glycopolymers, even at the lowest concentration of 1 wt. eq., stabilization with statistical significance was observed compared to the negative control.

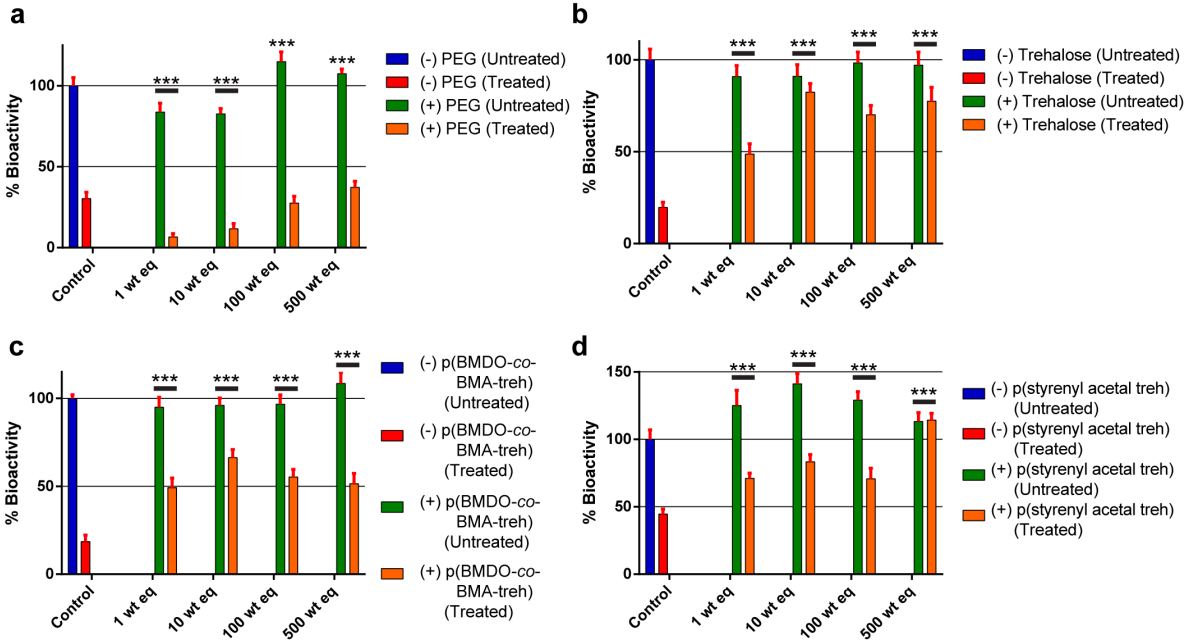


Figure 2-5. Bioactivity of G-CSF without any additive or with 1, 10, 100, or 500 weight equivalents of excipient to protein without heating (untreated) and with heating (treated) to 40 °C for 30 minutes. Excipients shown are a) 20 kDa PEG, b) trehalose, c) p(BMDO-*co*-BMA-trehalose), and d) p(styrenyl acetal trehalose). Data shown as the average (n = 6) and standard deviation. *** = $p < 0.005$ relative to heated G-CSF control.

Additionally, the excipients were added without heating the protein to determine any inherent effects the additives had on GCSF activity. With PEG, trehalose, and p(BMDO-*co*-BMA-trehalose), no significant change in activity was observed. However, the addition of the control p(styrenyl acetal trehalose) increased G-CSF activity to over 100% relative to the positive control. This result in enhancing activity has been observed with other proteins,¹⁶ and suggests that the polymer may help with enhancing protein/substrate binding or stabilization of the active site as does trehalose.³⁶ We then calculated the percent decrease of the degradable and control polymers and found the values to be similar until 500 wt. eq. (**Figure 2-6**). This suggests that the ability of

the trehalose polymers to stabilize GCSF are similar at 1-100 weight equivalents, but GCSF with p(styrenyl acetal trehalose) starts at a higher activity leading to higher overall retention of activity upon heat stress.

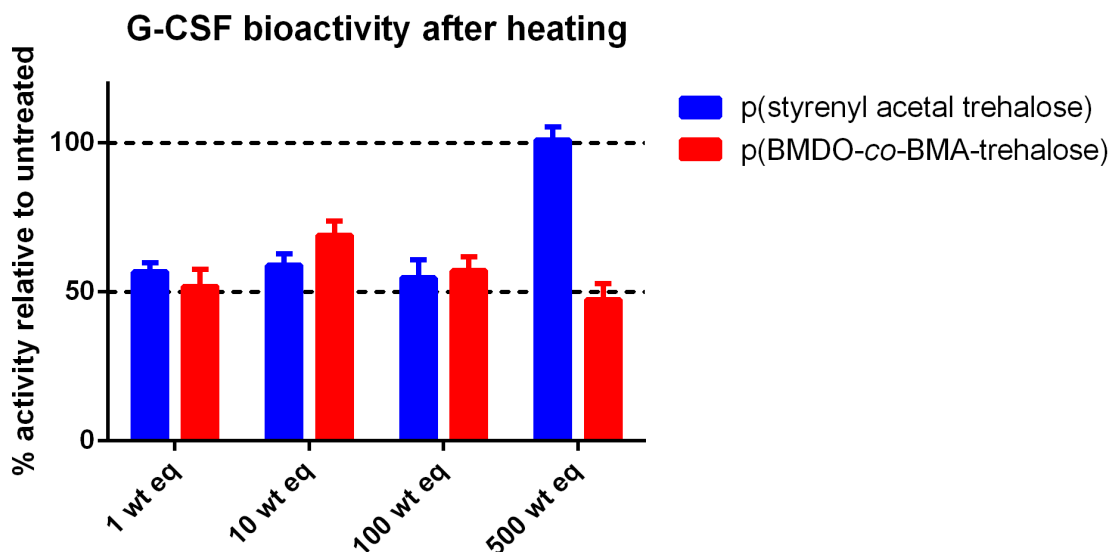


Figure 2-6. Bioactivity of G-CSF after heating with polymer excipients, p(styrenyl acetal trehalose) and p(BMDO-co-BMA-trehalose), presented as the percent activity relative to the unheated sample containing polymer excipient.

This work demonstrates evaluation of a hydrolytically degradable trehalose glycopolymer containing BMDO units. p(BMDO-co-BMA-trehalose) stabilized G-CSF against heat stress similar to the non-degradable control until the highest concentration tested; although the actual percent bioactivities were lower overall. The polymer itself was non-cytotoxic. However, the degradation products demonstrated slight cytotoxicity at higher concentrations and inhibition of cell growth, likely due to the BMDO units. Further optimization of CKA structure may decrease this observed incompatibility. For instance, 2-methylene-1,3-dioxepane (MDO) ring opens into the well-known and FDA-approved poly(caprolactone).³⁷ Alternatively, 2-methylene-4-phenyl-

1,3-dioxolane (MPDL) could be used.³⁸⁻³⁹ These data provide important information about the allowable working concentrations of this polymer within cells.

2.3. Conclusions

A degradable trehalose copolymer was synthesized by CRP. The copolymer was prepared by copolymerizing but-3-enyl methacrylate with BMDO by RAFT polymerization to obtain hydrolysable esters in the backbone followed by thiol-ene modification with trehalose on the side chains. The therapeutic protein G-CSF was expressed and purified. Stability screening with G-CSF with p(BMDO-*co*-BMA-trehalose) showed 66% retention of activity after heat stress. Characterization of the polymer confirmed that the BMDO-containing polymer was degraded within 1 day. Although the parent polymer was non-cytotoxic at the concentrations tested, the degraded fragments exhibited cytotoxicity at a concentration of 1 mg/mL.

2.4. Experimental

2.4.1. Materials

All chemicals and reagents were purchased from Sigma-Aldrich or Fisher Scientific and used as received unless otherwise indicated. Butenyl methacrylate (bMA) was synthesized as previously described.³³ 5,6-benzo-2-methylene-1,3-dioxepane (BMDO) was synthesized as previously described.⁴⁰ Nondegradable p(styrenyl acetal trehalose) glycopolymer, (M_n (GPC) = 9.5 kDa and $\bar{D} = 1.14$), was synthesized as previously described.¹⁷ G-CSF was expressed as described.⁴¹ SDS-PAGE analysis was performed using Bio-Rad Any kD Mini-PROTEAN TGX precast protein gels. Endotoxin removal spin columns (Pierce) were purchased from ThermoFisher Scientific. Enterokinase was purchased from GenScript. Human G-CSF DuoSET ELISA kit was purchased from R&D Systems. LIVE/DEAD Viability/Cytotoxicity assay kit and CellTiter-Blue cell viability assay were purchased from Invitrogen and Promega, respectively.

2.4.2. Analytical Techniques

NMR spectra were obtained on Bruker AV 500 and DRX 500 MHz spectrometers. ¹H-NMR spectra were acquired with a relaxation delay of 2 s for small molecules and 30 s for polymers. Repeat units indicated for each polymer structure was calculated from the NMR spectrum. Infrared absorption spectra were recorded using a PerkinElmer FT-IR equipped with an ATR accessory. High-resolution mass spectra were obtained on Waters LCT Premier with ACQUITY LC and ThermoScientific Exactive Mass Spectrometers with DART ID-CUBE. Gel Permeation Chromatography (GPC) was conducted on a Shimadzu high performance liquid chromatography (HPLC) system with a refractive index detector RID-10A, one Polymer Laboratories PLgel guard column, and two Polymer Laboratories PLgel 5 μ m mixed D columns. Eluent was DMF with LiBr

(0.1 M) at 50 °C (flow rate: 0.80 mL/ min). Calibration was performed using near-monodisperse PMMA standards from Polymer Laboratories. Size Exclusion Chromatography (SEC) was conducted on a Shimadzu HPLC system with a refractive index detector RID-10A, one Tosoh TSKGel guard column, and one Tosoh TSKGel G4000PW column. Eluent was 0.3 M NaNO₃ + 20 mM phosphate buffer pH 7 + 20% MeCN at 25 °C (flow rate 0.7 mL/min). Calibration was performed using near-monodisperse PEG standards from Polymer Laboratories. Fast protein liquid chromatography (FPLC) was performed on a Bio-Rad BioLogic DuoFlow chromatography system equipped with a GE Healthcare Life Sciences size exclusion column (Superdex 75 10/300 GL) in pH 5.0, 25 mM sodium acetate buffer at a flow rate of 0.5 mL/min.

2.4.3. Methods

Polymer Synthesis

Synthesis of poly(5,6-benzo-2-methylene-1,3-dioxepane-co-3-buten-1-yl methacrylate)

Trithiocarbonate CTA³ (6 mg, 0.02 mmol), bMA (96 mg, 0.68 mmol), BMDO (124 mg, 0.76 mmol), and azobisisobutyronitrile (AIBN) (0.63 mg, 0.004 mmol) were added to a dry Schlenk tube. Toluene (1.3 mL) was added, and the tube was subjected to 4 freeze-pump thaw cycles (down to 100 mTorr) followed by immersion in an 80 °C oil bath. After 13.5 h, the polymerization was quenched in liquid N₂, and the conversion was assessed by ¹H NMR. Toluene was removed *in vacuo* and the crude oil was diluted with CH₂Cl₂ and precipitated 3x into cold hexanes to yield **p**(BMDO-*co*-bMA) (86.1 mg). ¹H NMR (500 MHz, CD₃CN): δ 9.96, 7.92, 7.89, 7.87, 7.25, 7.16, 5.81, 5.14, 5.10, 5.08, 4.06, 3.96, 3.27, 2.62, 2.36, 2.13, 1.86, 1.77, 1.45, 1.25, 1.03, 0.97, 0.87, 0.80. *M_n* (¹H NMR) = 5,200, *M_n* (GPC) = 2,900, and Đ = 1.76.

Modification of p(BMDO-co-bMA) with protected trehalose p(BMDO-co-bMA) (15 mg, 94 μ mol allyl groups), thiolated trehalose **4** (305 mg, 467 μ mol), 2,2-dimethoxy-2-phenylacetophenone (DMPA) (12 mg, 47 μ mol) and tetrahydrofuran (THF) (0.9 mL) were mixed in a vial with screw cap. The solution was degassed for 10 min and then irradiated with 365 nm light from a handheld UV lamp. After 4 h, the vial was opened and the solution precipitated into 15 mL cold MeOH to yield p(BMDO-co-BMA-trehalose-OAc) (54.5 mg). ^1H NMR (500 MHz, CD_3CN): δ 9.96, 7.93, 7.24, 7.17, 5.38, 5.24, 5.02, 4.87, 4.16, 3.90, 2.66, 2.58, 2.08, 2.04, 2.00, 1.98, 1.95, 1.93, 1.93, 1.92, 1.92, 1.65, 1.59, 1.25, 1.00, 0.78. M_n (^1H NMR) = 28,900, M_n (GPC) = 20,900, and Đ = 1.22.

Deprotection of p(BMDO-co-BMA-trehalose-OAc) p(BMDO-co-BMA-trehalose-OAc) (24.6 mg, 0.9 μ mol) was dissolved in CHCl_3 :MeOH 1:1 (2 mL). K_2CO_3 (26.5 mg, 0.19 mmol, 1 eq. per hydroxyl) was added and the mixture stirred at room temperature. After 1.5 h, the solution was diluted with CHCl_3 , and the precipitate was isolated, diluted with H_2O , and dialyzed against 3.5 kDa MWCO in 50% MeOH: H_2O followed by switching to 100% H_2O . The purified solution was lyophilized to remove water and yield p(BMDO-co-BMA-trehalose). ^1H NMR (500 MHz, $\text{D}_2\text{O}+\text{CD}_3\text{CN}$): 7.27, 7.19, 5.07, 5.04, 3.94, 3.78, 3.72, 3.65, 3.50, 3.31, 3.25, 2.90, 2.57, 1.91, 1.61, 1.15, 0.98, 0.75. M_n (aq SEC) = 4600, and Đ = 1.30.

Degradation of p(BMDO-co-BMA-trehalose) p(BMDO-co-BMA-trehalose) was dissolved in a 5% KOH solution and incubated over the course of 3 days at 23 $^\circ\text{C}$. Samples were taken at 0, 1, and 3 days and lyophilized. After drying, the samples were dissolved in GPC mobile phase (20% MeCN, 0.3 M NaNO_3 , 20 mM phosphate buffer), neutralized with concentrated HCl, filtered through a 0.20 μm filter, and analyzed by GPC. Additionally, cell-conditioned media (CCM) and esterase incubation were tested. Fibroblast growth medium (Promocell) containing 2% fetal calf

serum (FCS), 1 ng/mL basic fibroblast growth factor (bFGF), 5 µg/mL insulin, and 1% penicillin-streptomycin (see Section 1.3.4) was used to incubate human dermal fibroblasts (HDFs) for 3 days and then used to dissolve p(BMDO-co-BMA-trehalose) at a concentration of 10 mg/mL. To assess degradation, aliquots (15 µL) were removed, diluted with SEC mobile phase (1:10), and filtered (0.22 µm) before analysis by aqueous SEC. For enzymatic degradation, p(BMDO-co-BMA-trehalose) was dissolved in MilliQ water at a concentration of 10 mg/mL. Esterase from porcine liver (Sigma-Aldrich) was dissolved in MilliQ water at a concentration of 16.5 mg/mL. Esterase stock solution was added to the polymer solution (2% v/v) and incubated at 37 °C. To assess degradation, aliquots (12 µL) were diluted with SEC mobile phase (1:10) and filtered (0.22 µm) before analysis by aqueous SEC.

Cytocompatibility

Cytotoxicity Assay in HDF Cells The cell compatibility of the trehalose glycopolymers to human dermal fibroblasts (HDFs, Promocell GmbH) were evaluated using a LIVE/DEAD viability/cytotoxicity assay (Invitrogen). Cytotoxicity of p(BMDO-co-BMA-trehalose), degraded p(BMDO-co-BMA-trehalose), and benzyl trehalose was analyzed in HDF cells. HDF cells were cultured in fibroblast growth medium (Promocell) containing 2% fetal calf serum (FCS), 1 ng/mL basic fibroblast growth factor (bFGF), 5 µg/mL insulin, and 1% penicillin-streptomycin. The cells were seeded in 48-well plates (BD Falcon) at a density of 5×10^3 cells per well. After 24 h, culture media were replaced with 200 µL of the working medium containing known polymer concentrations of 0.01, 0.1, 0.5, and 1 mg/mL. After incubation for 48 h, the cells were gently washed twice with pre-warmed D-PBS, and stained with the LIVE/DEAD reagent (2 µM calcein AM and 4 µM ethidium homodimer-1). Fluorescent images of each well were captured on an Axiovert 200 microscope with an AxioCam MRm camera and FluoArc mercury lamp. The number

of live and dead cells was counted, and percent cell viability was calculated by dividing the number of live cells by the total number of cells. All experiments were conducted with four repetitions. The percent viability was calculated as $100 \times (\text{number of live cells}/\text{total number of cells})$. The data is provided by normalizing each set to the control without any additives. Statistical analysis and calculation of *p*-values were performed using independent Student's *t*-test assuming unequal variances.

Cytotoxicity Assay with NFS-60 Cells Effects of trehalose, p(BMDO-co-BMA-trehalose), degraded p(BMDO-co-BMA-trehalose), and p(styrenyl acetal trehalose) on NFS-60 cells were evaluated by cell proliferation and LIVE/DEAD assay. The polymers were dissolved in working media containing growth factors (RPMI-1640) + 10% FBS + 2 ng/mL IL-3) and sterile filtered. NFS-60 cells were plated in 96-well plates at a cell density of 20,000 cells/well. The polymers were diluted and added to the wells at a final concentration of 0, 0.01, 0.1, 0.5, and 1 mg/mL. The plates were incubated at 37 °C/5% CO₂. After 48 h incubation, CellTiter-Blue viability assay was performed to measure cell proliferation. LIVE/DEAD assay was performed as described above. Statistical analysis and calculation of *p*-values were performed using independent Student's *t*-test assuming unequal variances.

G-CSF Activity Assay

Excipient Stabilization of G-CSF Against Heat Stress Stock solutions of sterile filtered G-CSF in 10 mM acetic acid buffer at a concentration of 500 ng/mL was used. Excipients of 20 kDa PEG, trehalose, p(BMDO-co-BMA-trehalose), and p(styrenyl acetal trehalose) was added at 1, 10, 100, or 500 weight equivalents to G-CSF. Samples were heated in a water bath at 40 °C for 30 minutes.

The samples were then diluted in cold working media and added to plated NFS-60 cells in a 96-well plate (cell density of 20,000 cells/well) at a final concentration of 0.25 ng/mL. The plate was incubated at 37 °C/5% CO₂. After 48 h incubation, cell proliferation was measured by CellTiter-Blue reagent. Data is normalized to 100% as untreated G-CSF control.

2.5. Appendix with Supplementary Figures

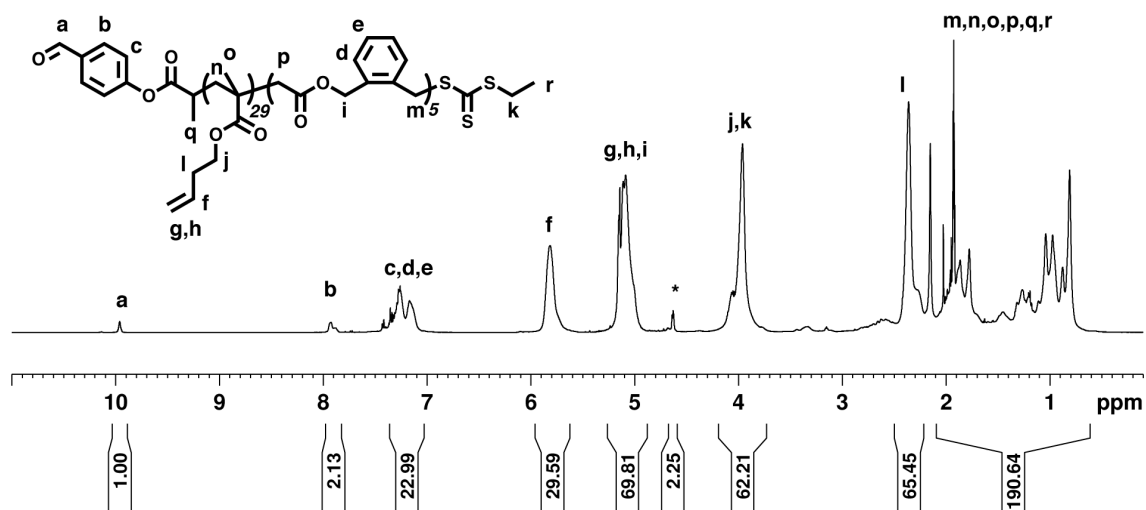


Figure 2-7. ^1H NMR spectrum of **p(BMDO-co-bMA)** (CD_3CN , 500 MHz). * = protons from terminal repeat unit on polymer.

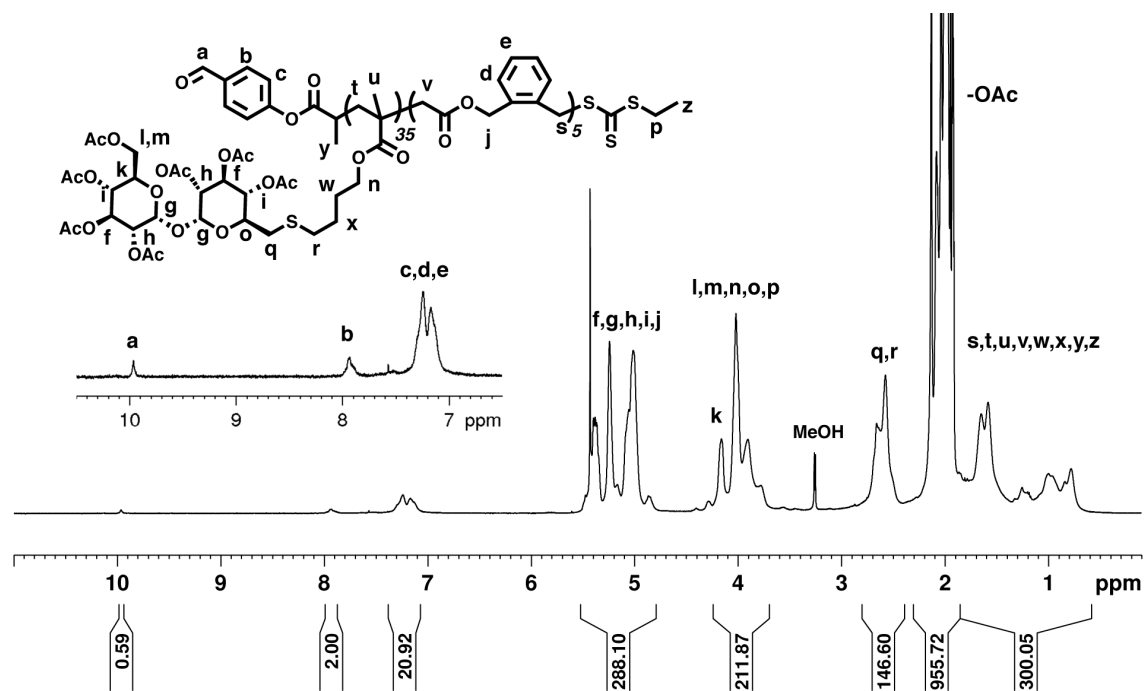


Figure 2-8. ^1H NMR spectrum of **p(BMDO-co-BMA-trehalose-OAc)** (CD_3CN , 500 MHz).

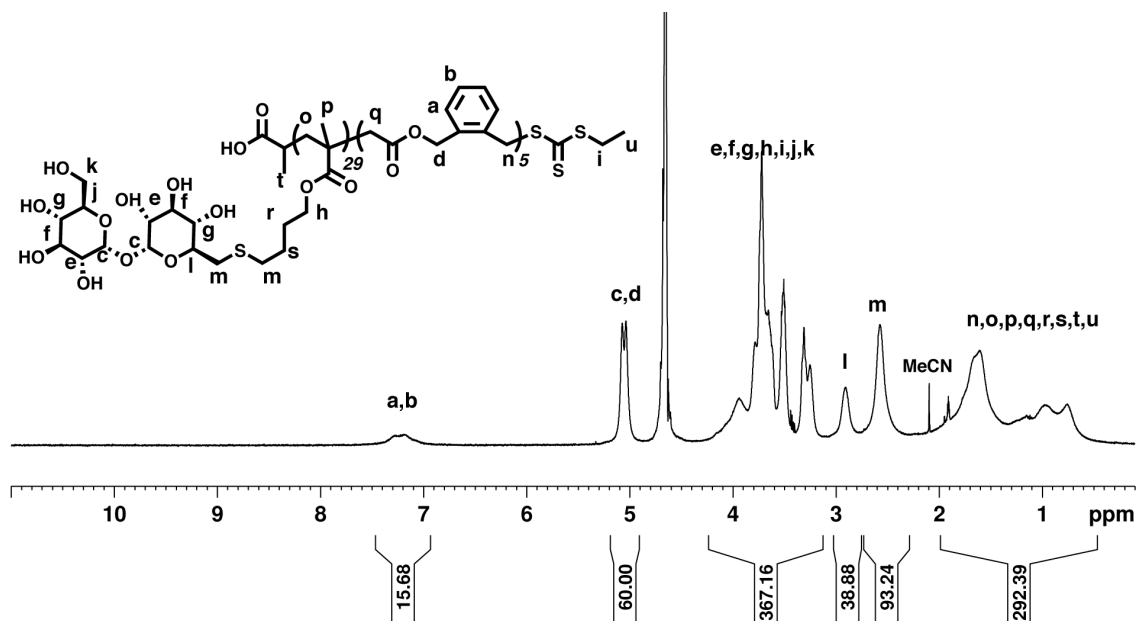


Figure 2-9. ¹H NMR spectrum of p(BMDO-co-BMA-trehalose) (D₂O + CD₃CN, 500 MHz).

2.6. References

1. This chapter previously published as Lau, U.Y.; Pelegri-O'Day, E.M.; Maynard, H.D. *Macromol. Rapid. Commun.*, **2018**, *39*, 1700652.
2. Knop, K.; Hoogenboom, R.; Fischer, D.; Schubert, U. S., *Angew. Chem. Int. Ed.* **2010**, *49*, 6288.
3. Garay, R. P.; El-Gewely, R.; Armstrong, J. K.; Garratty, G.; Richette, P., *Expert Opin. Drug Delivery* **2012**, *9*, 1319.
4. Webster, R.; Elliott, V.; Park, B. K.; Walker, D.; Hankin, M.; Taupin, P. In *PEGylated Protein Drugs: Basic Science and Clinical Applications*; Veronese, F. M., Ed. Birkhäuser, Basel, Switzerland **2009**, p. 127.
5. Leader, B.; Baca, Q. J.; Golan, D. E., *Nat. Rev. Drug Discov.* **2008**, *7*, 21.
6. Qi, Y.; Chilkoti, A., *Curr. Opin. Chem. Biol.* **2015**, *28*, 181.
7. Pelegri-O'Day, E. M.; Lin, E. W.; Maynard, H. D., *J. Am. Chem. Soc.* **2014**, *136*, 14323.
8. Besheer, A.; Liebner, R.; Meyer, M.; Winter, G. In *Tailored Polymer Architectures for Pharmaceutical and Biomedical Applications*; Scholz, C., Kressler, J., Eds.; ACS Symposium Series, Vol. 1135; American Chemical Society: Washington, DC, **2013**; p 215.
9. Pelegri-O'Day, E. M.; Maynard, H. D., *Acc. Chem. Res.* **2016**, *49*, 1777.
10. Nguyen, T. H.; Kim, S. H.; Decker, C. G.; Wong, D. Y.; Loo, J. A.; Maynard, H. D., *Nat. Chem.* **2013**, *5*, 221.
11. Keefe, A. J.; Jiang, S., *Nat. Chem.* **2012**, *4*, 59.
12. Zhang, P.; Sun, F.; Tsao, C.; Liu, S.; Jain, P.; Sinclair, A.; Hung, H.-C.; Bai, T.; Wu, K.; Jiang, S., *Proc. Natl. Acad. Sci. U. S. A.* **2015**.

13. Fuhrmann, G.; Grotzky, A.; Lukic, R.; Matoori, S.; Luciani, P.; Yu, H.; Zhang, B.; Walde, P.; Schlueter, A. D.; Gauthier, M. A.; Leroux, J. C., *Nat. Chem.* **2013**, *5*, 582.
14. Stidham, S. E.; Chin, S. L.; Dane, E. L.; Grinstaff, M. W., *J. Am. Chem. Soc.* **2014**, *136*, 9544.
15. Mancini, R. J.; Lee, J.; Maynard, H. D., *J. Am. Chem. Soc.* **2012**, *134*, 8474.
16. Lee, J.; Lin, E. W.; Lau, U. Y.; Hedrick, J. L.; Bat, E.; Maynard, H. D., *Biomacromolecules* **2013**, *14*, 2561.
17. Liu, Y.; Lee, J.; Mansfield, K. M.; Ko, J. H.; Sallam, S.; Wesderniotis, C.; Maynard, H. D., *Bioconj. Chem.* **2017**, *28*, 836.
18. Pelegri-O'Day, E. M.; Paluck, S. J.; Maynard, H. D., *J. Am. Chem. Soc.* **2017**, *139*, 1145.
19. Hey, T.; Knoller, H.; Vorstheim, P. In *Therapeutic Proteins*; Wiley-VCH: Weinheim, Germany, **2012**; p 117
20. Lameire, N.; Hoste, E., *Intensive Care Med.* **2014**, *40*, 427.
21. Decker, C. G.; Maynard, H. D., *Eur. Polym. J.* **2015**, *65*, 305.
22. Agarwal, S., *Polym. Chem.* **2010**, *1*, 953.
23. Delplace, V.; Nicolas, J., *Nat Chem* **2015**, *7*, 771.
24. Tardy, A.; Nicolas, J.; Gigmes, D.; Lefay, C.; Guillaneuf, Y., *Chem. Rev.* **2017**, *117*, 1319.
25. Delplace, V.; Tardy, A.; Harrisson, S.; Mura, S.; Gigmes, D.; Guillaneuf, Y.; Nicolas, J., *Biomacromolecules* **2013**, *14*, 3769.
26. Siegwart, D. J.; Bencherif, S. A.; Srinivasan, A.; Hollinger, J. O.; Matyjaszewski, K., *J. Biomed. Mater. Res., Part A* **2008**, *87*, 345.
27. He, T.; Zou, Y.-F.; Pan, C.-Y., *Polym. J.* **2002**, *34*, 138.

28. Xiao, N.; Liang, H.; Lu, J., *Soft Matter* **2011**, *7*, 10834.
29. Ganda, S.; Jiang, Y.; Thomas, D. S.; Eliezar, J.; Stenzel, M. H., *Macromolecules* **2016**, *49*, 4136.
30. Gomez d'Ayala, G.; Malinconico, M.; Laurienzo, P.; Tardy, A.; Guillaneuf, Y.; Lansalot, M.; D'Agosto, F.; Charleux, B., *J. Polym. Sci., A, Polym. Chem.* **2014**, *52*, 104.
31. Grover, G. N.; Alconcel, S. N. S.; Matsumoto, N. M.; Maynard, H. D., *Macromolecules* **2009**, *42*, 7657.
32. Yin, L.; Dalsin, M. C.; Sizovs, A.; Reineke, T. M.; Hillmyer, M. A., *Macromolecules* **2012**, *45*, 4322.
33. Campos, L. M.; Killops, K. L.; Sakai, R.; Paulusse, J. M. J.; Damiron, D.; Drockenmuller, E.; Messmore, B. W.; Hawker, C. J., *Macromolecules* **2008**, *41*, 7063.
34. Messina, M. S.; Ko, J. H.; Yang, Z. Y.; Strouse, M. J.; Houk, K. N.; Maynard, H. D., *Polym. Chem.* **2017**, *8*, 4781.
35. Lutz, J. F.; Andrieu, J.; Uzgun, S.; Rudolph, C.; Agarwal, S., *Macromolecules* **2007**, *40*, 8540.
36. Paz-Alfaro, K. J.; Ruiz-Granados, Y. G.; Uribe-Carvajal, S.; Sampedro, J. G., *J. Biotechnol.* **2009**, *141*, 130.
37. Bailey, W. J.; Ni, Z.; Wu, S. R., *J. Polym. Sci., Part A: Polym. Chem.* **1982**, *20*, 3021.
38. Delplace, V.; Guegain, E.; Harrisson, S.; Giggmes, D.; Guillaneuf, Y.; Nicolas, J., *Chem. Commun.* **2015**, *51*, 12847.
39. Hill, M. R.; Guégain, E.; Tran, J.; Figg, C. A.; Turner, A. C.; Nicolas, J.; Sumerlin, B. S., *ACS Macro Lett.* **2017**, *6*, 1071.
40. Bailey, W. J.; Ni, Z.; Wu, S. R., *Macromolecules* **1982**, *15*, 711.

41. Lau, U. Y.; Pelegri-O'Day, E. M.; Maynard, H. D., *Macromol. Rapid Commun.* **2018**, *39*, 1700652.
42. Sizovs, A.; Xue, L.; Tolstyka, Z. P.; Ingle, N. P.; Wu, Y.; Cortez, M.; Reineke, T. M., *J. Am. Chem. Soc.* **2013**, *135*, 15417.
43. Johnson, D. A., *Carbohydr. Res.* **1992**, *237*, 313.

Chapter 3

Substituted Polyesters by Thiol–Ene Modification: Rapid Diversification for Therapeutic Protein Stabilization¹

3.1. Introduction

Due to their substrate specificity and biological function, proteins have unique and essential roles in various industries. For example, proteins are used as reagents for improving chemical transformations, as cosmetic additives, as supplements for improving nutrition of animal feed, and as biological therapeutics. However, the stabilization of certain proteins during storage and transport, especially those used as therapeutics, can be critical to maintain structure and activity. Conditions such as UV exposure,² heat,³ lyophilization,⁴ and excessive agitation⁵ can lead to protein unfolding, aggregation, or loss of biological activity. Measures to prevent this loss of activity, such as the maintenance of a refrigeration chain for delicate protein therapeutics, increase costs and may still result in inactivated protein.

As a result, a number of compounds are used as excipients or additives to maintain protein activity.⁶ For instance, osmolytes and carbohydrates such as trehalose, sorbitol, and sucrose have been shown to maintain protein activity through preferential hydration or protein interactions.⁷ Arginine, histidine, and other amino acids have also been shown to stabilize proteins through binding interactions, buffering, or hydration mechanisms.⁸⁻¹⁰ Moreover, proteins such as human serum albumin (HSA), have been used as bulking agents or to prevent protein adsorption.⁶ Furthermore, surfactants such as polysorbate (Tween) or modified polysaccharides such as hydroxyethyl starch (HES) have been employed to prevent protein unfolding and aggregation.^{6, 11-12} Excipients have also been used in nonbiological therapeutics. For instance, the recently-approved hyperkalemia drug patiomer includes sorbitol in its formulation to improve stability.¹³ However, therapeutics still suffer from activity loss despite the presence of these excipients, prompting further development of improved materials.

Synthetic polymers comprise another promising class of excipients used to stabilize proteins against environmental stressors. Polymers such as anionic polyacrylate, poly(glutamic acid), carboxylated polyamidosaccharides and block copolymers of poly(ethylene glycol (PEG) and poly(histadine) have been shown to stabilize a variety of proteins to stressors such as heat, aggregation, and lyophilization.¹⁴⁻¹⁹ Other charged polymers such as poly(ethylenimine) or heparin mimicking polymers can stabilize a variety of enzymes or growth factors using electrostatic interactions.²⁰⁻²³ Zwitterions have also been shown to have significant stabilizing ability due to their hydration and protein repulsion properties.²⁴ Additionally, thermoresponsive copolymers have been used for refolding denatured proteins.²⁵ We have previously developed styrene- and methacrylate- based polymers with trehalose side chains and shown that these polymers protect lysozyme, horseradish peroxidase (HRP), and glucose oxidase (GOX) against elevated temperatures both as excipients and as protein-polymer conjugates.²⁶⁻²⁷ And others have investigated the use of trehalose in polyacrylamide polymers to inhibit amyloid protein aggregation and in polycationic nanoparticles for delivery of siRNA.²⁸⁻²⁹

Though synthetic polymers show promise in stabilization of proteins, most are nondegradable and thus will not be cleared from biological systems or will persist in the environment. For instance, poly(ethylene glycol) (PEG) is the most widely used biocompatible polymer, but has been shown to induce the formation of antibodies in 32-46 % of patients during a clinical trial because of its persistence *in vivo*.³⁰⁻³¹ Additionally, vacuolation in rats has been reported upon injection with high molecular weight (40 kDa) PEG.³² Small-molecule excipients that have been widely used for therapeutic formulation present other disadvantages. For instance, sorbitol is widely used and effectively maintains protein activity, yet has been shown to result in GI tract complications such as bleeding, ulcers, and necrosis.³³ Other high-performing excipients

include the nonionic surfactants Tween 20 and Tween 80, which effectively prevent protein aggregation but have been shown to undergo auto-oxidation, resulting in the formation of damaging peroxides.³⁴ Therefore, the development of novel, degradable and functional polymers has been a subject of recent interest, especially for biological applications.³⁵⁻³⁶ Degradable polymers might alleviate immunogenic responses, while also enabling the use of higher molecular weight polymers, which typically cannot be employed due to difficulty in clearance. In addition, enzymes are widely employed in applications such as in detergents or animal feed, where the use of any protein stabilizers must be biodegradable to avoid unwanted environmental buildup. Therefore, there is significant need for well-controlled, homogeneous, and degradable synthetic materials for biological and environmental concerns.

Herein we report the synthesis of degradable stabilizing polyesters using ring-opening polymerization (ROP). The polymers were prepared by first synthesizing alkene-functionalized polycaprolactones, followed by the installation of desired side chains using high-yielding thiol-ene reactions. A variety of materials were easily synthesized by varying mercaptan identity and the resulting materials protected granulocyte colony-stimulating factor (G-CSF) against loss of biological activity when added as excipients. We expect that these polymers can function as protein stabilizers in a variety of fields due to their combination of biodegradability and stabilization abilities.

3.2. Results

The nature of the degradable polymer backbone was an important consideration in the design of a modular system for protein stabilization. We have previously observed that trehalose polymers with hydrophobic backbones have demonstrated good protein stabilization²⁷ and

hypothesized that the nonionic surfactant character of these materials was an important contributor to their desirable properties.⁶ Therefore, the FDA-approved polymer poly(caprolactone) (pCL) was selected because of its hydrophobic and biodegradable nature. Previous examples have introduced functional side chains onto pCL using a variety of post-polymerization click chemistries to avoid chemical incompatibilities with ROP conditions and also to minimize steric interference during polymerization. For instance, aminoxy-functionalized PEG chains have been added to ketone-modified pCL through oxime click chemistry, resulting in graft copolymers.³⁷ Alkyne- and alkene-functionalized valero- and caprolactone monomers have been synthesized and polymerized to yield polyesters with reactive handles for later installation of PEG and peptide side-chains.³⁸⁻³⁹ We chose to synthesize our polyester backbone with reactive alkene side chains and use it as a common precursor to introduce stabilizing functionalities via postpolymerization thiol-ene reactions. Thiol-ene is a particularly attractive type of “click” modification because it combines efficiency, a metal-free nature, and a tolerance of both water and oxygen.⁴⁰⁻⁴¹ Using this type of chemistry allows for the ready introduction of different functional, potentially stabilizing moieties onto the polymer side-chains by using a variety of mercaptans (**Figure 3-1**). Additionally, with this post polymerization approach, the backbone length would be the same between the different classes to rule out differences in stabilizing ability due to changes in degree of polymerization.

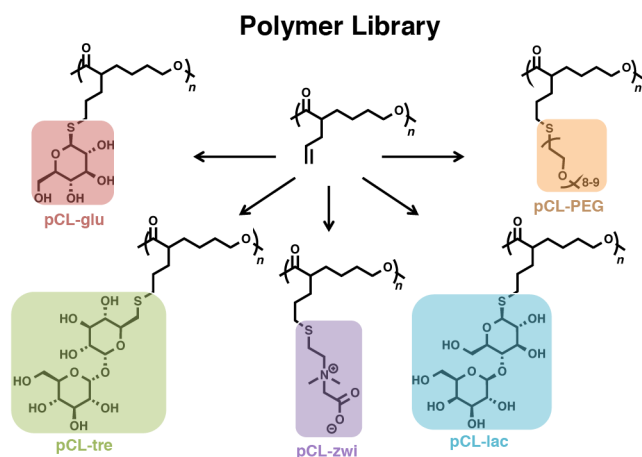
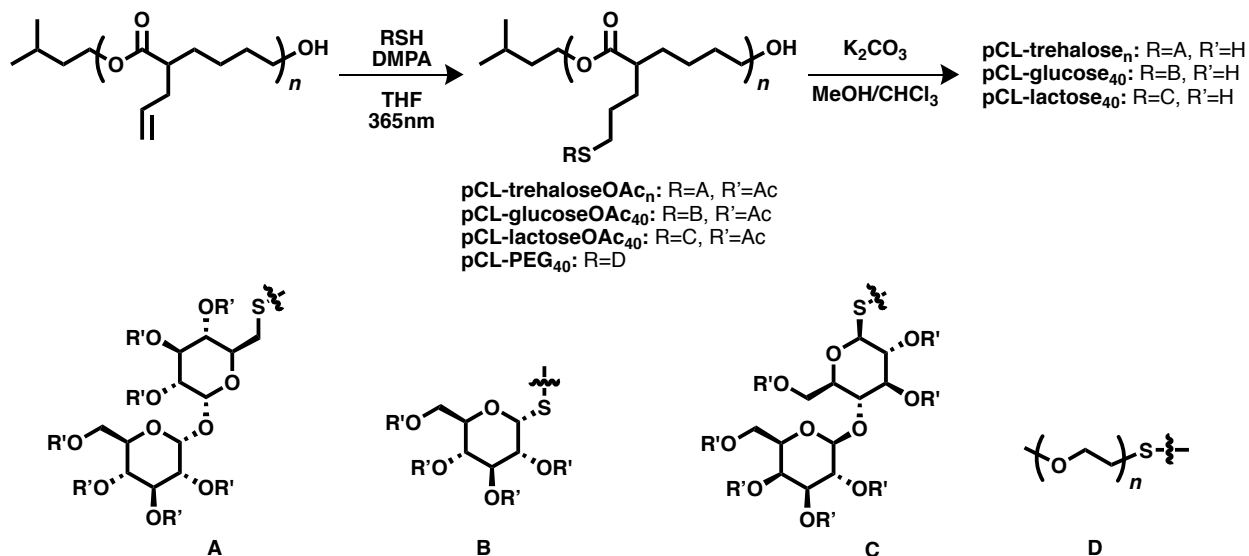


Figure 3-1. Illustrative scheme of pCL backbone and modification with thiols using thiol-ene chemistry to produce a small library of degradable polymers.

3.2.1. Synthesis of a Library of Functionalized Polyesters

The desired alkene-functionalized caprolactone monomer was synthesized by adding allyl bromide to CL in the presence of lithium diisopropylamide following a literature procedure³⁸ and polymerized using ROP to produce polymers. A degree of polymerization (DP) of 40 was targeted because it would result in functionalized polymers with molecular weights between 20.9 and 12.8 kDa. The organic catalyst 1,5,7-triazabicyclo[4.4.0]dec-5-ene (TBD) was used due to its fast polymerization kinetics at room temperature and narrow dispersity (D) for the ROP of functional lactones.⁴²⁻⁴⁵ The initiator 3-methyl-1-butanol was employed because its distinctive ¹H-NMR peaks allowed for good characterization.⁴⁶ Using a monomer concentration of 2 M, high conversion and good control over molecular weight were achieved, with $D = 1.08$, a degree of polymerization (DP) of 36, and a number average molecular weight of 5600 Da by ¹H NMR and 5400 by gel permeation chromatography (pCL-allyl₄₀, **Table 3-1**). Initially, polymers were

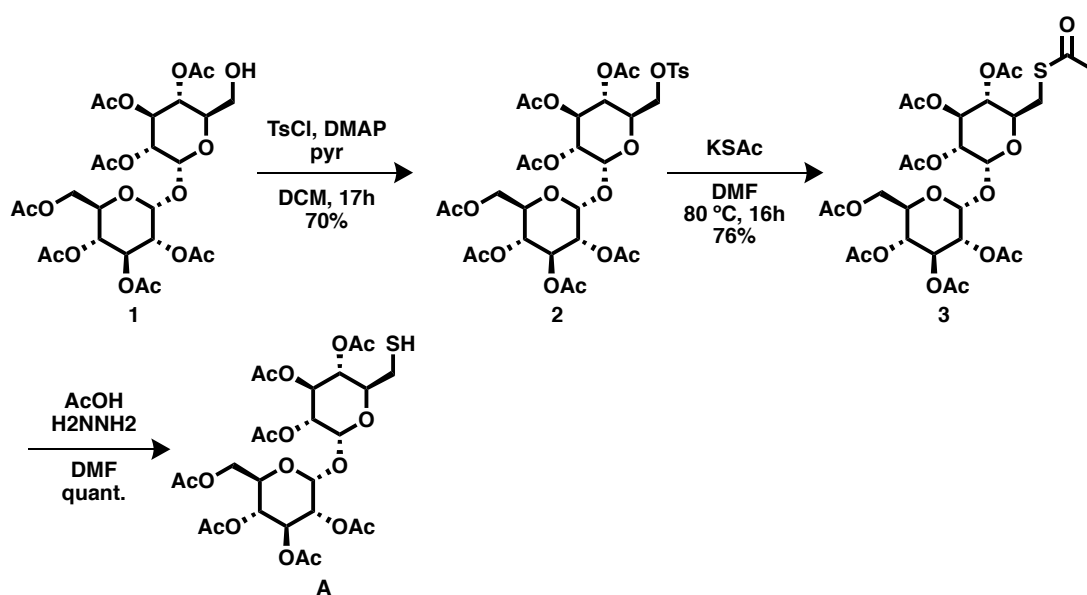
purified by dialysis in DCM/MeOH. However, polymers purified using this method had unidentified impurities, which resulted in significant loss of protein activity in later experiments (data not shown). Purification by silica gel column chromatography successfully removed the impurities, and subsequent polymers were therefore purified using this method.



Scheme 3-1. Synthetic scheme of thiol-ene modification of pCL-allyl polymers with acetyl-trehalose, acetyl-glucose, acetyl-lactose and PEG thiols, followed by deprotection of the acetylated sugars.

The allylated polymers were then used in radical thiol-ene reactions to install the desired pendant stabilizing groups (**Scheme 3-1**). The photoinitiator 2,2-dimethoxyphenylacetophenone (DMPA) was used because of its demonstrated high efficiency in photoinitiated thiol-ene reactions.⁴⁷ A series of easily accessible thiols (**A-D**) were selected containing sugars or oligo(PEG) that as small molecules are known stabilizing excipients.⁶ Thiolated trehalose was synthesized in five steps and 53% overall yield from trehalose using trityl and acetate protecting groups (**Scheme 3-2**). Briefly, monohydroxyl trehalose heptaacetate was synthesized as previously

described.²⁷ A tosylate ester was installed and displaced using potassium thioacetate. Selective cleavage of the thioester using hydrazine acetate then led to thiolated trehalose **A**. Thiolated lactose **C**^{35,48} and thiolated mPEG **D**⁴⁹ were synthesized as previously described.



Scheme 3-2. Synthesis of thiolated trehalose **A**

Use of acetate-protected saccharide mercaptans was found to be important for good miscibility between the pCL backbone and the thiol, giving clean conversion to the acetylated glycopolymers. In all cases, three equivalents of thiol per alkene were used to ensure complete reaction of the alkene side-chains. After polymer modification, removal of the acetate esters using potassium carbonate in MeOH/CHCl₃²⁷ or hydrazine hydrate⁵⁰⁻⁵³ led to the desired glycopolymers without hydrolysis of the polyester backbone. Complete modification was confirmed by disappearance of the alkene peaks in the ¹H-NMR (representative data in **Figure 3-2a**) as well as clean shifts in GPC molecular weight (representative data in **Figure 3-2b**).

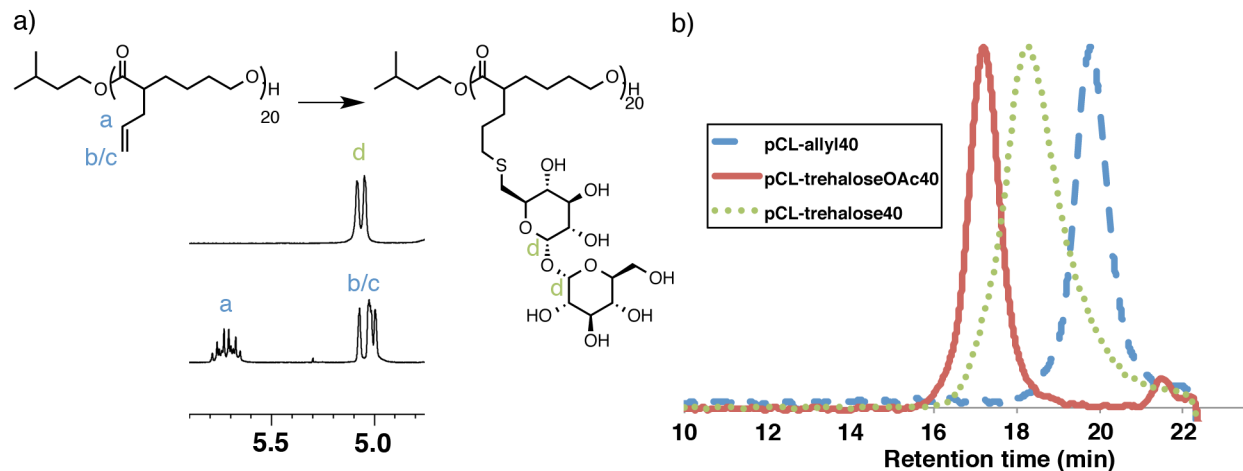
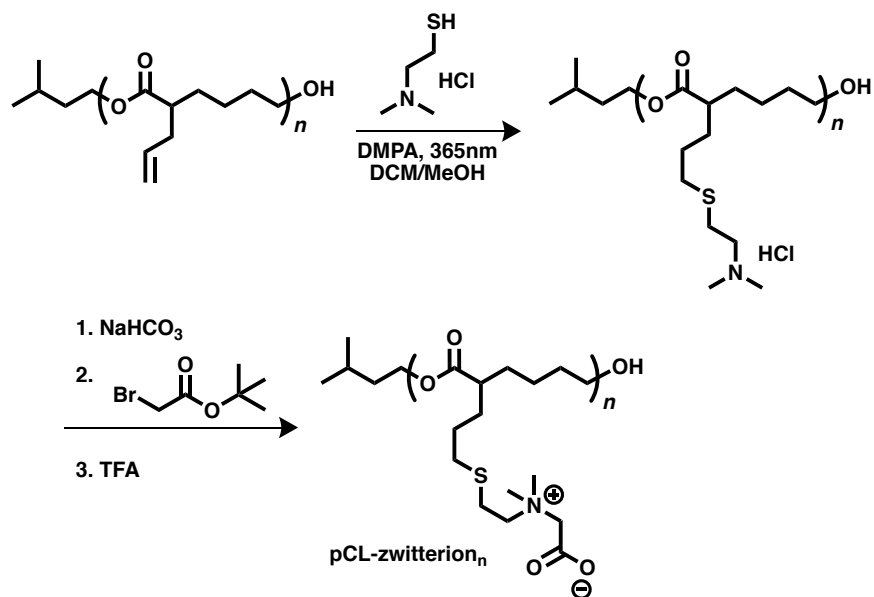


Figure 3-2. Characterization of trehalose modification of pCL using thiol-ene chemistries. a) The ¹H-NMR traces before and after modification showing a disappearance of the alkene resonance peaks at 5.0 and 5.7 ppm and the appearance of resonance peaks corresponding to trehalose anomeric protons. b) GPC characterization of pCL-allyl₄₀ before and after modification showing a shift toward a higher molecular weight species. After deprotection of the trehalose, a shift toward a lower molecular weight species was observed showing complete modification and deprotection of the polymer.

The carboxybetaine zwitterionic pCL polymer was synthesized taking inspiration from a literature procedure for a non-degradable polymer (**Scheme 3-3**).⁵⁴ 2-(Dimethylamino)ethanethiol hydrochloride was added to the pCL-allyl₄₀ backbone polymer using photoinitiated thiol-ene conditions and subsequently treated with sodium bicarbonate to neutralize the hydrochloride salt. Exposure to *t*-butyl bromoacetate quaternized the amine and hydrolysis of the *t*-butyl ester with trifluoroacetic acid led to the formation of the zwitterion. No acidic backbone scission was observed by GPC or ¹H-NMR analysis.



Scheme 3-3. Synthetic scheme for the synthesis of zwitterionic polymer pCL-zwitterion_n.

All polymers were characterized by GPC and ¹H-NMR to determine molecular weight and dispersity (**Table 3-1**). During the deprotection, there was unlikely to be chain scission, as the library of substituted pCL all gave narrow molecular weight distributions between 1.19 and 1.07 and the peak shapes were generally well-defined and symmetrical (**Figures 3-38, 3-47, 3-48**). Using poly(methyl methacrylate) standards, the M_N by GPC for the DMF-soluble polymers varied from 12.7 to 23.6 kDa. The zwitterionic material was not DMF-soluble and was instead analyzed using PEG standards, making direct molecular weight comparison difficult. However, because a postpolymerization approach was used to synthesize these materials, the same backbone was used to construct all polymers in the study. Therefore, while the molecular weight varied due to side chain identity, the DPs of all polymers (i.e. backbone length) compared were identical.

Table 3-1. Molecular weights and GPC data for the library of polyesters (DP40)

	Polymer	M _n (¹ H-NMR)	M _n (GPC)	Đ
	pCL-allyl ₄₀	5600	5400	1.08
protected	pCL-trehalose-OAc ₄₀	34 700	28 400	1.06
	pCL-glucose-OAc ₄₀	20 300	22 300	1.06
	pCL-lactose-OAc ₄₀	29 900	28 900	1.07
deprotected	pCL-trehalose-OH ₄₀	18 500	12 700	1.17
	pCL-glucose-OH ₄₀	11 300	18 300	1.09
	pCL-lactose-OH ₄₀	18 000	16 900	1.17
	pCL-PEG ₄₀	20 400	23 600	1.07
	pCL-zwitterion ₄₀	12 500	5100 ^a	1.19 ^a

^a GPC run in buffer/MeCN with PEG standards.

3.2.2. Assessment of Stabilizing Ability

Next the ability of the polymer to protect protein activity against environmental stressors was assessed. The therapeutic protein granulocyte colony-stimulating factor (G-CSF) was selected to compare excipient efficacy due to its clinical importance. G-CSF is FDA-approved as filgrastim (neupogen) and lenograstim and is used therapeutically to increase neutrophil granulocyte count during chemotherapy.⁵⁵ G-CSF is highly unstable at physiological pH and is therefore stored at pH 4.0; still at this pH the protein readily degrades upon storage or subjection to heat.⁵⁶ The side chain identity was varied to determine the relative stabilizing ability of the functional groups. To investigate storage at refrigeration temperatures, pCL polymers were added to G-CSF at 100 weight equivalents to protein and the protein was stored for 90 minutes at 4 °C at 1 µg/mL and pH

4.0. Protein activity was determined by measuring cell proliferation in murine myeloid leukemia NFS-60 cells, which is enhanced in the presence of G-CSF, and compared to the proliferation of freshly diluted protein.⁵⁷

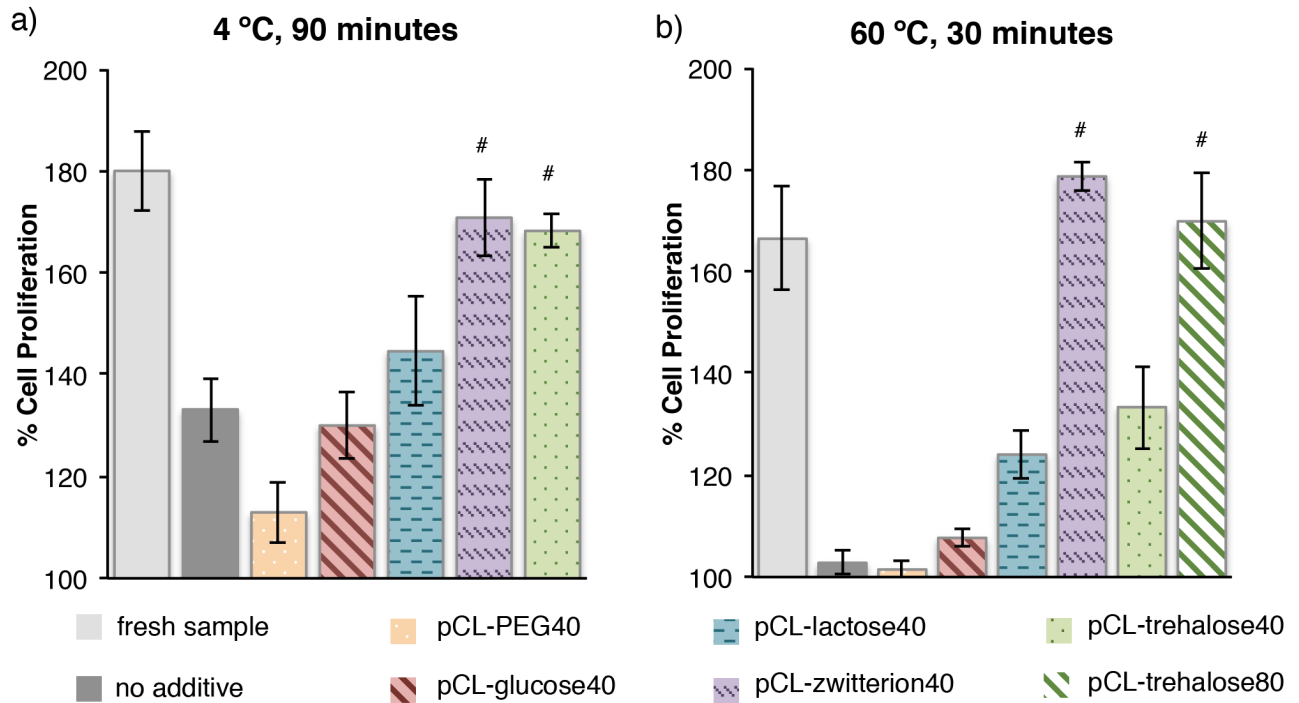


Figure 3-3. Effect of side chain identity on stabilization of G-CSF at pH 4.0 to a) storage conditions at 4 °C for 90 minutes and b) thermal stress at 60 °C for 30 minutes. # = no difference from the fresh sample ($p > 0.01$). Statistical analysis was done by ANOVA with Tukey's HSD post-hoc test. Data shown as the average of six experimental repeats and six well repeats with standard deviation

After stressing at 4 °C, G-CSF with no additive only exhibited $133 \pm 6\%$ cell proliferation, a drastic reduction compared to fresh G-CSF (**Figure 3-3a**). Addition of the pCL-glucose and pCL-lactose polymers was not statistically different than no additive, indicating that for this

protein, the polymers were not effective stabilizers. Interestingly, when the pCL-PEG polymer was added to the G-CSF solution, significantly lower cell proliferation was observed. PEG has been shown to associate with hydrophobic moieties on the protein surface due to its amphiphilic nature,⁵⁸ and has been previously observed to lower protein thermal stability.⁵⁹ A similar mechanism may be a factor for the destabilizing effect of this pCL-PEG polymer. Both the zwitterionic and trehalose side chains significantly outperformed the other polymers, stimulating $171 \pm 7\%$ and $168 \pm 3\%$ cell proliferation respectively. Both stabilizing polymers were not statistically different than the fresh sample, indicating that both are equally effective at preventing G-CSF activity loss under these conditions. G-CSF was also stressed at 60 °C for 30 minutes; this is representative of the maximum temperature inside truck and shipping containers during transport.⁶⁰ As expected, G-CSF lost more than 95% of the native activity after heating; addition of the pCL-PEG polymer was not statistically different than no additive (**Figure 3-3b**). The pCL-glucose and the pCL-lactose polymers were moderately stabilizing. Addition of the trehalose ($133 \pm 8\%$) and zwitterionic ($179 \pm 3\%$) side chain polymers resulted in the highest cell proliferation and the pCL-zwitterion₈₀ was not statistically different than the fresh sample. We observed that the zwitterionic polymers retained greater activity than the trehalose side chain polymers to heat. Since one hypothesis of why trehalose provides stabilization is due to clustering of the sugar around flexible polar residues on the protein surface,⁶¹⁻⁶² we included a larger trehalose CL polymer (preparation vide infra) in the heat study. In this case, a 40 kDa pCL-trehalose₈₀ polymer was statistically the same as the zwitterionic polymer, showing that the larger trehalose pCL stabilizes as well as the zwitterionic polymer and suggesting a molecular weight dependence of the trehalose polymer stabilization ability.

3.2.3. Testing of Different Molecular Weights and Comparison to Common Excipients

To further test this potential molecular weight dependence, various CL trehalose polymer sizes were synthesized. Using previously optimized ROP conditions, well-defined pCL-allyl polymers were synthesized with DP between 10 and 80 and $\bar{D} < 1.25$ (**Table 3-2**). These DPs were selected so that after modification with thiolated trehalose, the molecular weight of the pCL-trehalose polymers would be between 5 and 40 kDa, assuming quantitative conversion. For the smallest pCL-allyl polymer, matrix assisted laser desorption ionization (MALDI) was used to confirm the molecular weight (**Figure 3-25**). Modification was again carried out using photoinitiated thiol-ene chemistry, yielding a series of trehalose-modified pCL polymers. This series demonstrated increased dispersity (\bar{D}) with increasing molecular weight. At high molecular weights (**Table 3-2**, pCL-trehalose₈₀) \bar{D} was increased to 1.39 and the GPC molecular weight was correspondingly lower than that predicted by ¹H-NMR. The peak shape was also asymmetrical and extended toward the low molecular weight side (**Figure 3-4a**). To confirm that this peak broadening was not due to hydrolysis of the backbone esters, the molecular weight of pCL-trehalose₈₀ was also measured on an aqueous size exclusion chromatography (SEC) system (**Figure 3-4b**). In aqueous solution, no asymmetry was observed and the calculated dispersity was lower (1.26). The dragging observed at high molecular weights was therefore hypothesized to be a result of interactions with the stationary phase of the GPC column. Similarly, a series of pCL-zwitterion polymers were synthesized using photoinitiated thiol-ene chemistry on the pCL-allyl backbones. Analysis by GPC showed that they were well-defined and demonstrated clear shifts in molecular weight with increasing pCL-allyl DP (**Table 3-2**).

Table 3-2. Molecular weights and GPC data for the library of pCL-trehalose and pCL-zwitterion polymers with variable DP

	Polymer	M_n (¹H-NMR)	M_n (GPC)	Đ
Starting polymers	pCL-allyl ₁₀	1600	ND ^a	ND ^a
	pCL-allyl ₂₀	3600	2400	1.21
	pCL-allyl ₄₀ ^b	5600	5400	1.08
	pCL-allyl ₈₀	12400	1220	1.08
protected	pCL-trehalose-OAc ₁₀	10 600	9600	1.07
	pCL-trehalose-OAc ₂₀	20 200	15 400	1.06
	pCL-trehalose-OAc ₄₀ ^b	34 700	28 400	1.06
	pCL-trehalose-OAc ₈₀	67 000	53 100	1.06
protected	pCL-trehalose-OH ₁₀	6200	5600	1.09
	pCL-trehalose-OH ₂₀	14 400	8100	1.15
	pCL-trehalose-OH ₄₀ ^b	18 500	12 700	1.17
	pCL-trehalose-OH ₈₀	41 000	17 000	1.39
zwitterions	pCL-zwitterion ₁₀	3200	1700 ^c	1.17 ^c
	pCL-zwitterion ₂₀	6400	3000 ^c	1.12 ^c
	pCL-zwitterion ₄₀ ^b	12 400	5100 ^c	1.19 ^c
	pCL-zwitterion ₈₀	25 400	8900 ^c	1.19 ^c

^a Too small for GPC analysis. ^b Same entry as in Table 3-1. ^c GPC run in buffer/MeCN with PEG standards

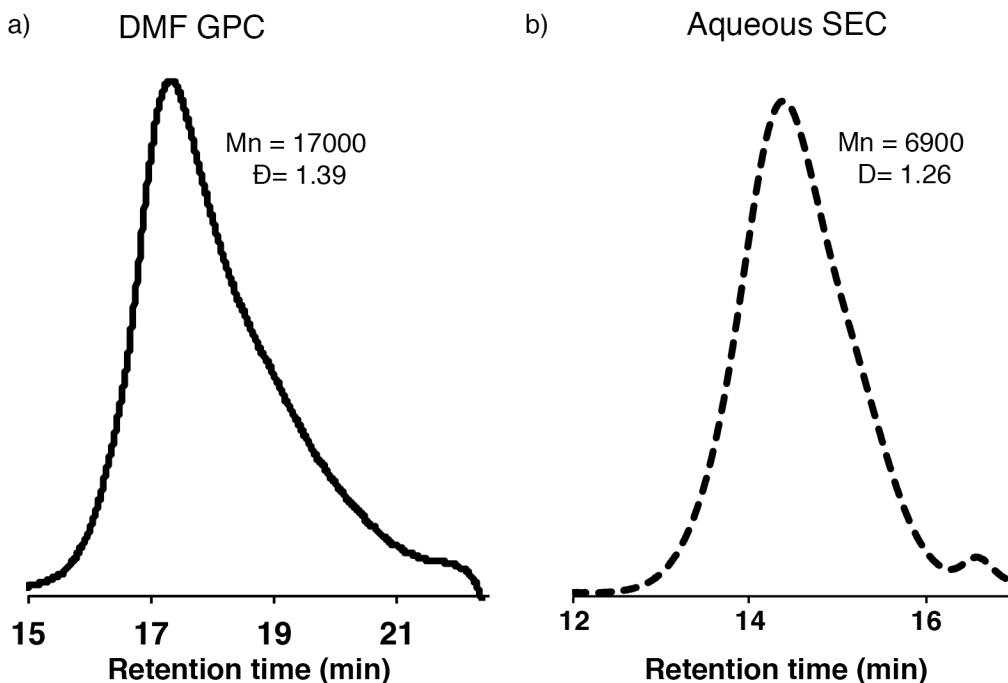


Figure 3-4. Comparison of a) gel permeation chromatography (DMF) and b) size exclusion chromatography (aqueous) traces for pCL-trehalose₈₀.

Both sets of polymeric backbones were then subjected to the same stability tests using 100 weight equivalents of polymer. First the trehalose polymers were tested and a very slight dependence of protein activity on molecular weight was observed upon storage at 4 °C (**Figure 3-5a**). Larger polymers offered improved stabilization compared to smaller polymers, but there was no significant difference between the stabilizing effects of DP40 and DP80 polymers, or between the DP10 and DP20 polymers. The series of pCL-trehalose polymers were also used as stabilizers against 60 °C heating (**Figure 3-5b**). In this case, a drastic molecular weight dependence was observed, with the pCL-trehalose₈₀ polymer exhibiting the highest cell proliferation. It should be noted, that despite the increase in molecular weight, the concentration of stabilizing units in solution remained constant at 69 weight equivalents of trehalose or 190 μM , indicating that the observed changes in stabilizing ability were solely due to the molecular weights of the polymers.

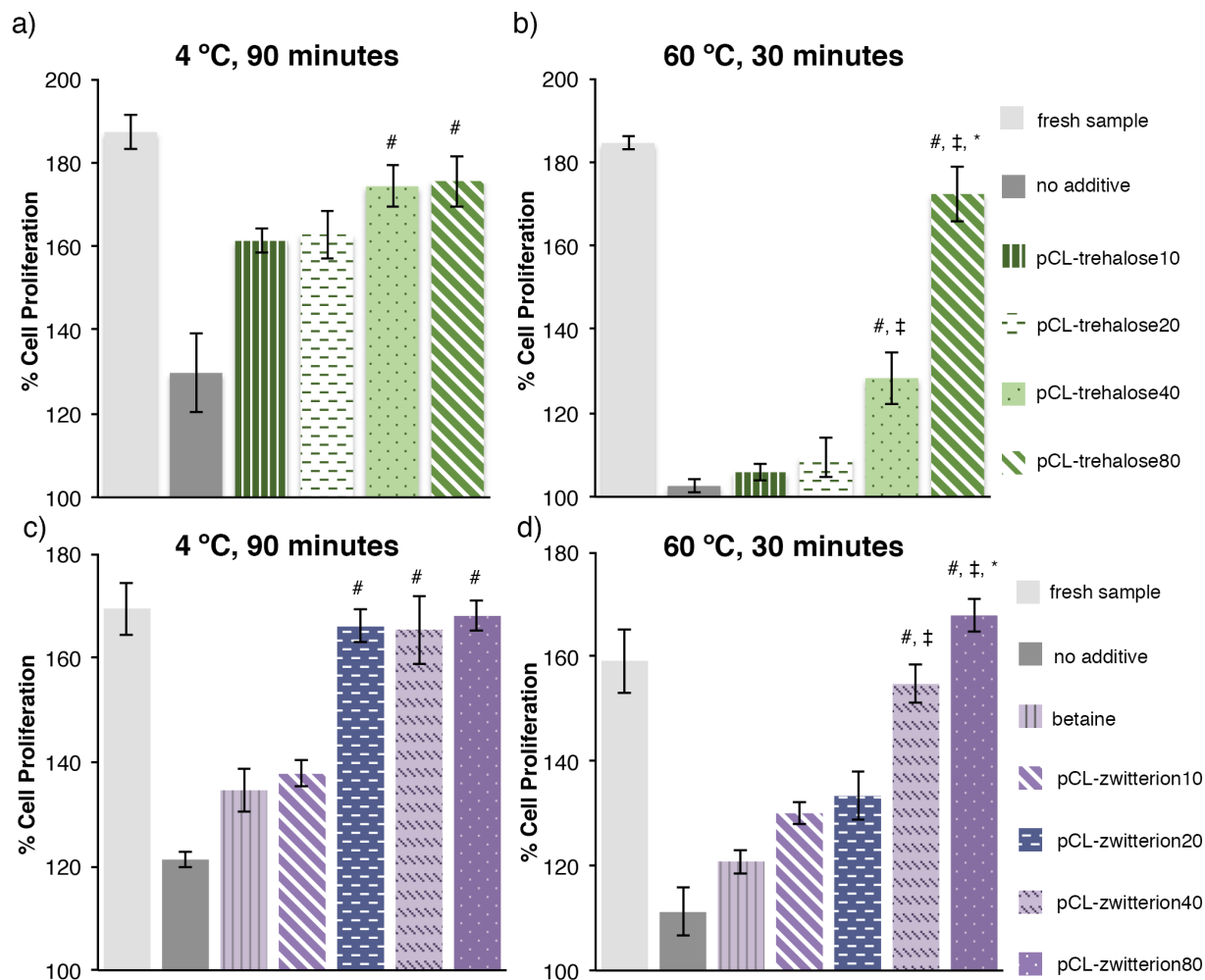


Figure 3-5. A) Effect of pCL-trehalose molecular weight on G-CSF stabilization at pH 4.0 to storage at 4 °C for 90 minutes. B) G-CSF stabilization to thermal stress at 60 °C for 30 minutes. Data shown as the average of six experimental repeats and six well repeats with standard deviation. C) Effect of pCL-zwitterion molecular weight on G-CSF stabilization at pH 4.0 to storage at 4 °C for 90 minutes. D) G-CSF stabilization to thermal stress at 60 °C for 30 minutes. Data shown as the average of four experimental repeats and six well repeats with standard deviation. All polymers other than pCL-trehalose₁₀ and pCL-trehalose₂₀ exhibited statistically significant stabilization ($p < 0.05$) relative to no stabilizing additive. Greater molecular weight polymers showed greater stabilization ($\# = p < 0.01$ relative to DP10 polymers, $\ddagger = p < 0.01$ relative to DP20 polymers, $* =$

$p < 0.01$ relative to DP40 polymers). Statistical analysis was done by ANOVA with Tukey's HSD post-hoc test.

Similar experiments were carried out using the zwitterionic backbone. Upon exposure to the milder 4 °C stressor, only a moderate dependence on molecular weight was observed (**Figure 3-5c**). While the pCL-zwitterion₁₀ polymer sample exhibited reduced cell proliferation, there was no statistical difference between the DP20, DP40, and DP80 polymers. They were statistically the same as the fresh sample, indicating the presence of a molecular weight threshold for complete stabilization ability. However, when the protein was heated to 60 °C for 30 minutes, separation between the polymer additives was observed (**Figure 3-5d**). At this temperature, the performance of the DP20, DP40 and DP80 polymers was significantly different to each other, and only the two largest polymers retained comparable activity to the pristine sample.

Additional experiments were carried out to better understand the observed dependence on molecular weight. To determine if shorter polymers could demonstrate improved stabilization at higher weight equivalents, we stressed G-CSF at 60 °C for 30 minutes and added pCL-trehalose₄₀ and pCL-zwitterion₄₀, varying the amount of polymer in solution between 1 and 500 weight equivalents (**Figure 3-6**). We were curious to determine if the DP40 polymers would match the stabilizing performance of higher molecular weight DP80 polymers when more weight equivalents were used. Instead, there was a distinct plateau, and for both polymers only 100 weight equivalents were required to see the best stabilization, without further improvement at the higher concentrations tested. This is strong evidence that the number of repeat units on the polymer chain has a distinct effect on the polymer's stabilizing ability. Trehalose has been previously shown to demonstrate a clustering effect in computational studies, self-organizing near polar residues on

proteins.⁶² The molecular weight trends observed support a multivalency effect in these materials, where increased equivalents offer inferior protection compared to a preorganized or pre-grouped set of stabilizing units. This sort of molecular weight effect has been previously reported in other systems.⁶³

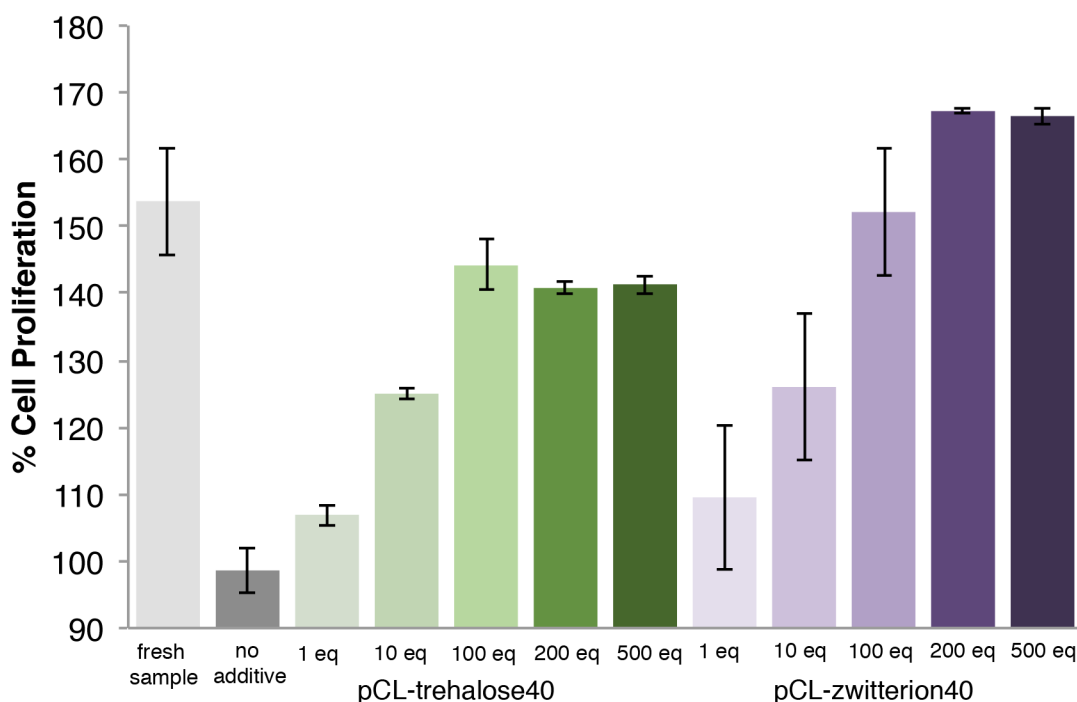


Figure 3-6. Dependence on G-CSF stabilization on polymeric equivalents of pCL-trehalose40 and pCL-zwitterion40 against heating at 60 °C for 30 minutes.

The stabilizing abilities of the pCL polymers to protect G-CSF from 60 °C thermal stress were additionally compared to commonly used small-molecule excipients: sucrose, trehalose, betaine, sorbitol and polysorbate 80 (**Figure 3-7**). These compounds were chosen to represent the materials present in the high-performing pCL scaffolds, with the addition of sorbitol and polysorbate 80 (Tween 80), which are used industrially in the formulation of Neupogen (therapeutic GCSF)⁶⁴ and sucrose, which is a widely used excipient.⁶ The pCL-trehalose₈₀ and pCL-zwitterion₈₀ polymers were selected because they were the highest-performing pCL polymers

in the experiments described above and were added at 100 weight equivalents. Small molecules were added to be equivalent to the concentration of stabilizing units in the pCL-zwitterion₈₀ polymer except for Tween 80, which was added at 100 weight equivalents because of its larger molecular weight, similar to the CL polymers. After heating to 60 °C for 30 minutes, sucrose, betaine and sorbitol had little stabilizing effect and the cell proliferation was low. However, the sorbitol and Tween 80 maintained high protein activity that was statistically equivalent to pCL-trehalose₈₀, and pCL-zwitterion₈₀, respectively. The results show that the degradable polymers with DP of 80 are as good as the currently utilized additives for therapeutic G-CSF and better than other common protein excipients at the concentrations tested.

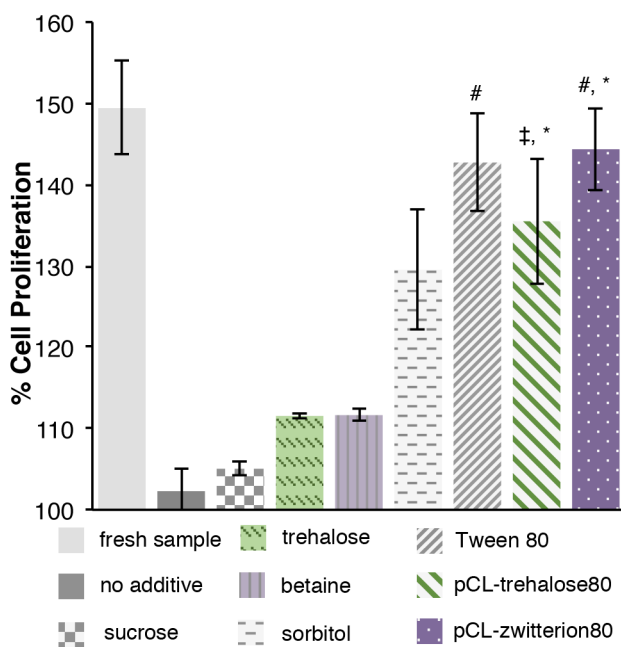


Figure 3-7. Stabilization of G-CSF against thermal stress at 60 °C for 30 minutes and comparison of pCL-trehalose₈₀ and pCL-zwitterion₈₀ with relevant small molecule controls. Data shown as the average of three experimental repeats and six well repeats. # = no statistical difference from the fresh control ($p > 0.05$). ‡ = no statistical difference from sorbitol ($p > 0.05$). * = no statistical

difference from Tween ($p > 0.05$). Statistical analysis done by ANOVA with Tukey's HSD post-hoc test.

Additionally, the half-life of G-CSF at 60 °C was tested with the DP80 polymers as excipients (**Figure 3-8**). When the pCL-trehalose₈₀ polymer was added, G-CSF retained 50% of the native activity until 48 minutes of heating, whereas when the pCL-zwitterion₈₀ polymer was used, the half-life was calculated to be 90 minutes, almost double. In contrast, with no additive G-CSF was already inactive after 30 minutes (first time point tested). These data show that that both pCL scaffolds, especially the zwitterion-substituted polymer, provide a significant increase in thermal stability.

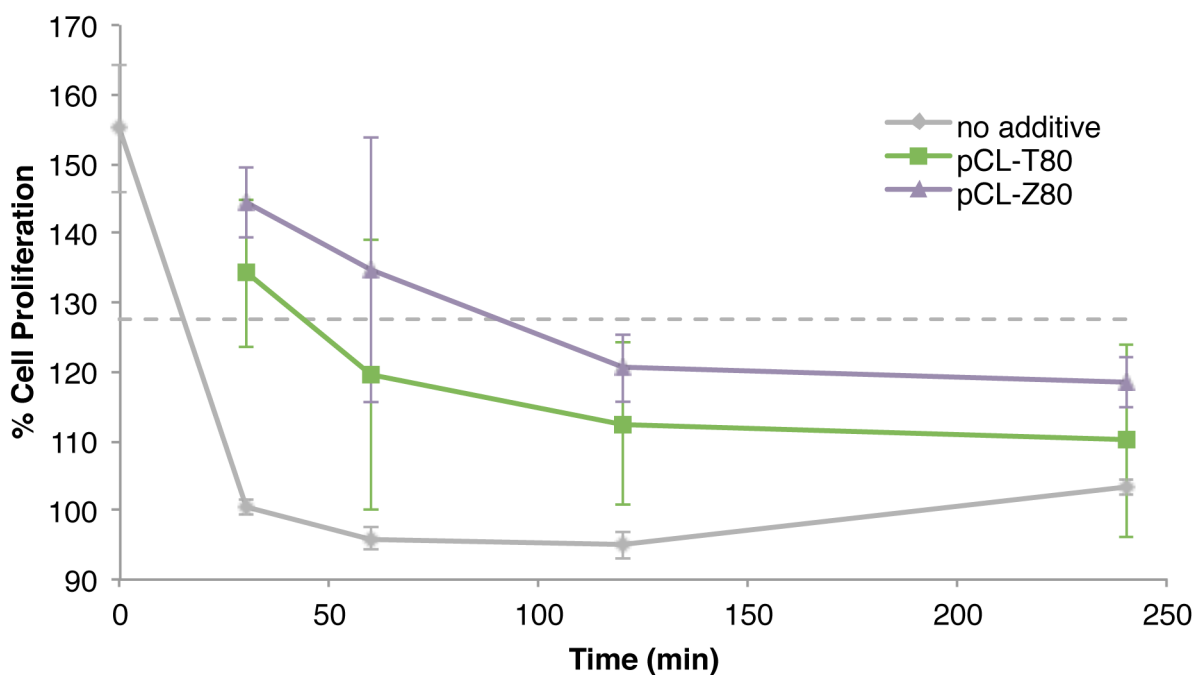


Figure 3-8. Timecourse of G-CSF activity in the presence of 100 weight equivalents of pCL-trehalose₈₀ and pCL-zwitterion₈₀ when heated at 60 °C.

3.2.4. Degradation, Biological Compatibility, TEM, and DSC Analysis of the Polymers

To confirm that the polycaprolactone was still degradable, pCL-trehalose₄₀ and pCL-zwitterion₄₀ were treated with 5% KOH to hydrolytically cleave the backbone esters. The molecular weight of the polymeric materials was determined post cleavage by aqueous SEC (Figure 3-9). In both cases, complete shift in molecular weight towards a lower molecular weight species was observed after 24 hours, confirming hydrolytic degradation. No hydrolytic degradation was observed under more moderate degradation conditions (cell media at 37 °C) for up to 49 days, consistent with the slow hydrolysis rates observed for polycaprolactone in vivo.⁶⁵

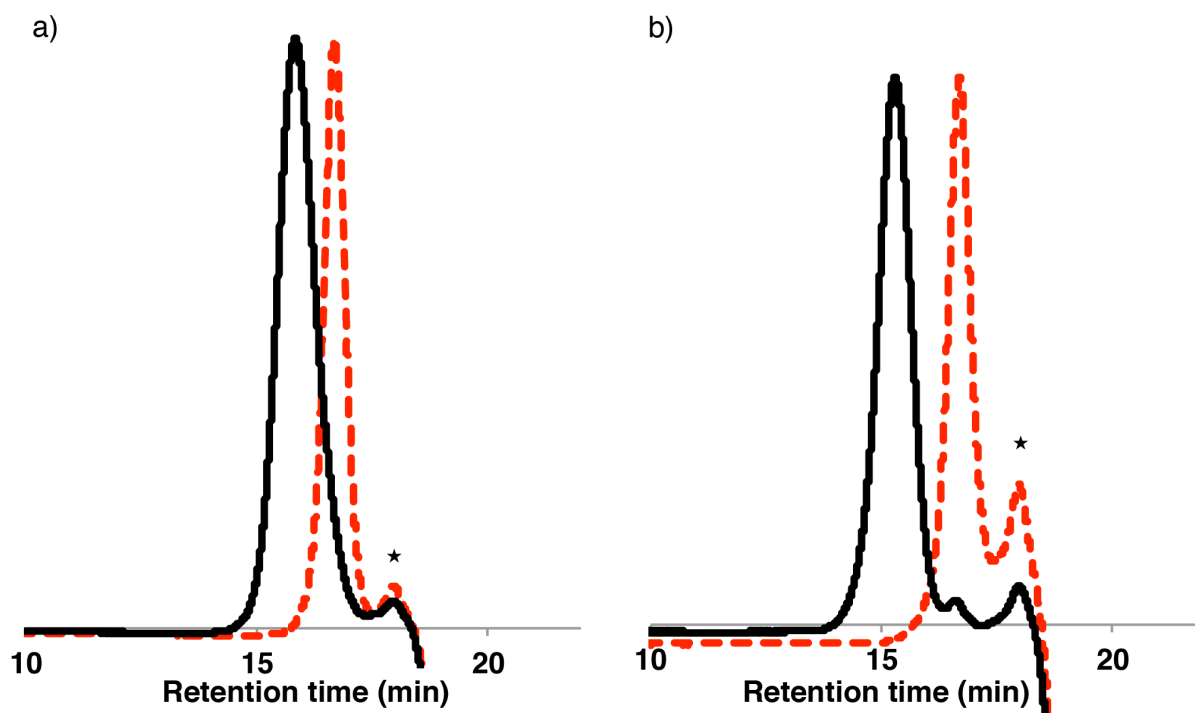


Figure 3-9. Size exclusion chromatogram of the degradation of a) pCL-trehalose₁₀ and b) pCL-zwitterion₂₀. Polymer is indicated by the black solid line and basic degradation products are indicated by the red dashed line. Peaks due to salts in the buffer indicated with ★.

Additionally, experiments were carried out to confirm that the pCL polymers remained stable at the acidic conditions of the cell assay. pCL-trehalose and -zwitterion polymers were heated to 60 °C for 30 minutes to mimic the thermal stress conditions, then buffer was removed and the materials analyzed by GPC (**Figure 3-10**). No shift was observed in the chromatogram, confirming that the polymers were intact throughout the experiment.

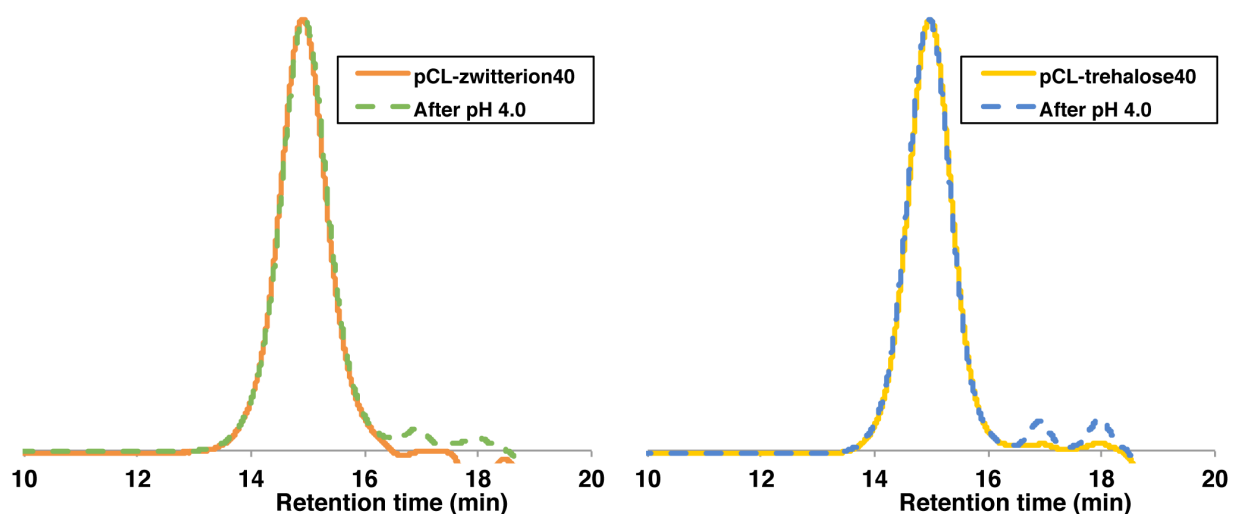


Figure 3-10. Size exclusion chromatograms of pCL-trehalose₄₀ and pCL-zwitterion₄₀ before and after exposure to pH 4.0 at 60 °C for 30 minutes.

Cytotoxicity and biocompatibility of the trehalose and zwitterion based polycaprolactone polymers were also assessed in human umbilical vein endothelial cells (HUVECs) as a primary, non-cancerous cell line. HUVECs were cultured in the presence of pCL-trehalose₂₀, pCL-zwitterion₂₀, and their polymeric degradation products. Compared to the control, no reduction in cell viability was observed upon addition of either polymer (pCL-trehalose and pCL-zwitterion) or polymeric degradation products, up to 1 mg/mL, confirming that the substituted polyesters and their eventual degradation products are noncytotoxic (**Figure 3-11**).

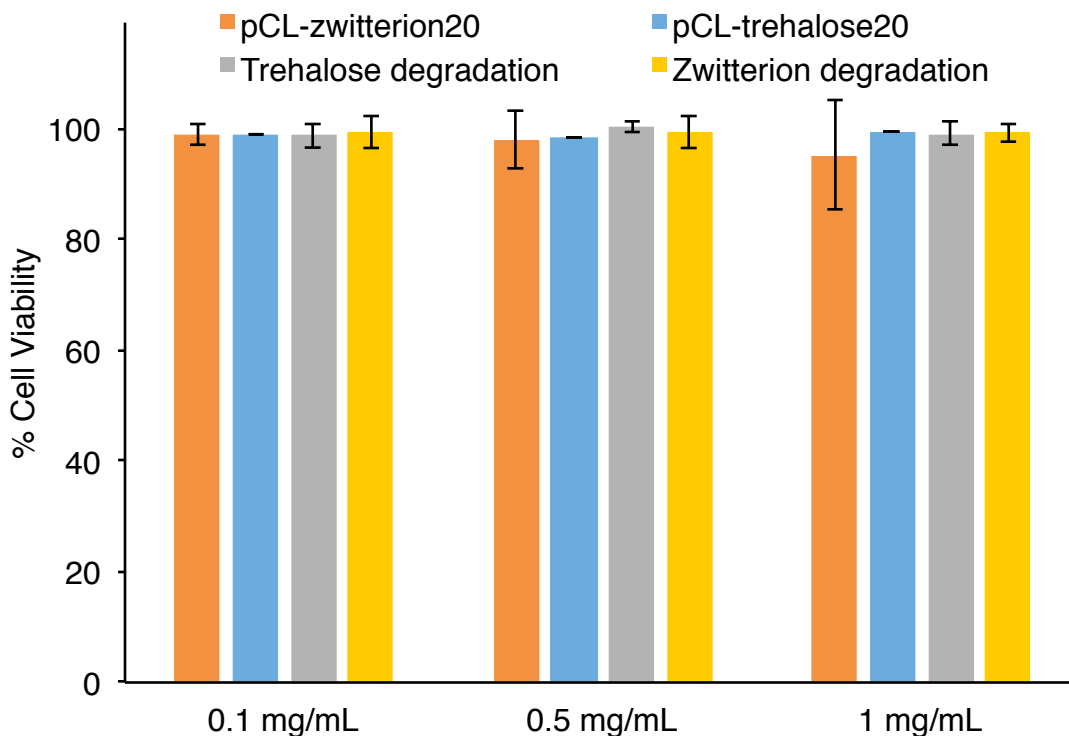


Figure 3-11. Cytotoxicity assay of pCL-trehalose₂₀, pCL-zwitterion₂₀, and their basic degradation products with HUVECs. Data shown as the average of three experimental repeats with standard deviation. There is no statistical difference between groups.

Analysis of the substituted pCL polymers using transmission electron microscopy (TEM) indicated the presence of aggregated structures in both samples of pCL-zwitterion₈₀ and pCL-trehalose₈₀ alone and in the presence of G-CSF (**Figure 3-12**). This self-assembly may play an important role in the mechanism of stabilization and shows that the polymers are nonionic surfactants, an important class of excipients.⁶ Similar aggregates have been observed for tyloxapol, a polymeric material with an aryl backbone and poly(ethylene oxide) side chains that is structurally similar to the pCL polymers.⁶⁶ We additionally investigated the osmolyte character of the synthesized materials using differential scanning calorimetry (DSC). Both polymers changed the

enthalpy of melting and crystallization of water (**Table 3-3**) suggesting the polymers are able to depress ice formation.²⁷

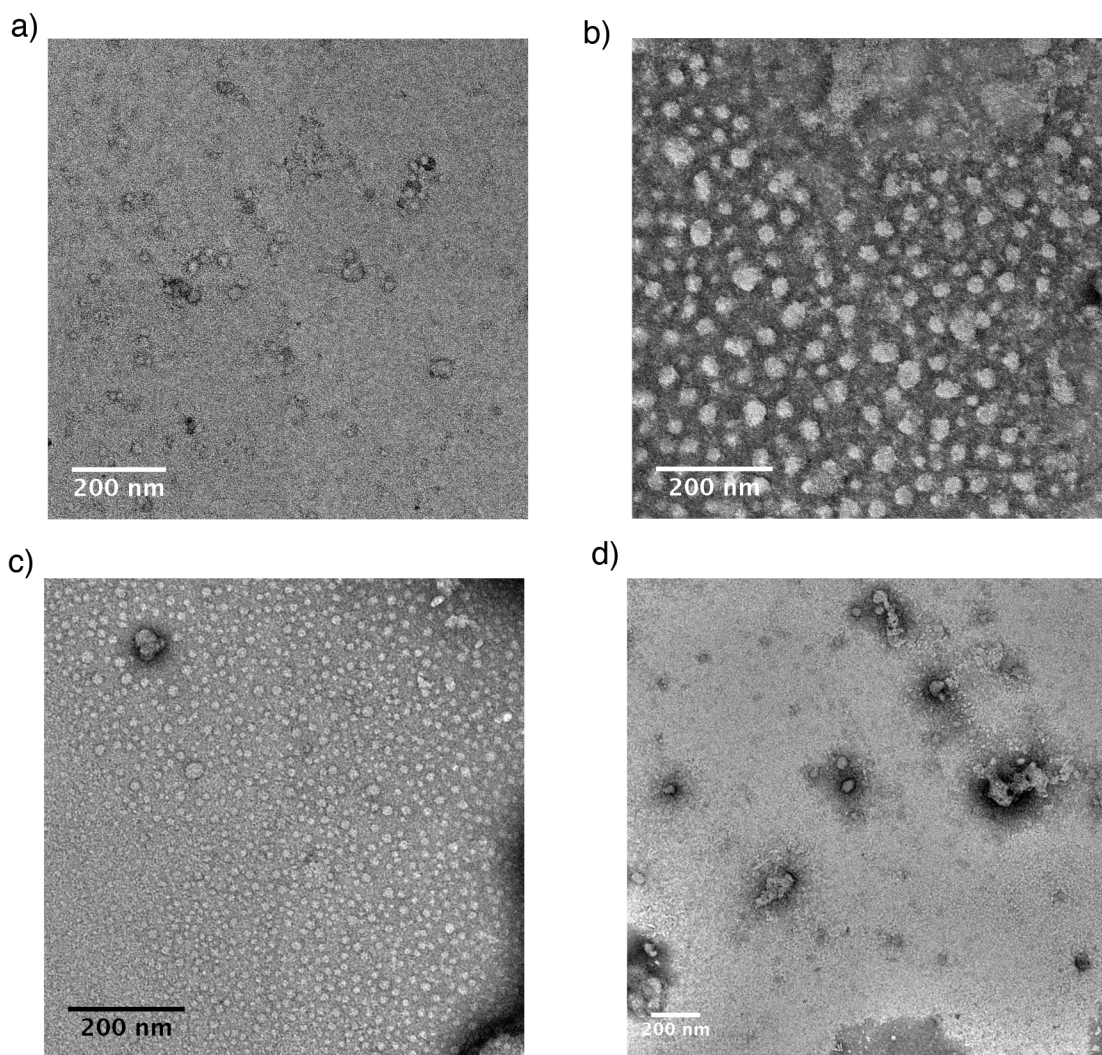


Figure 3-12. Transmission electron micrographs of a) pCL-trehalose₈₀ b) pCL-zwitterion₈₀ c) pCL-trehalose₈₀ and G-CSF mixture d) pCL-zwitterion₈₀ and G-CSF mixture. Solutions contained polymer (1 mg/mL) and G-CSF (0.15 mg/mL) and samples were stained using uranyl acetate as a negative stain.

Table 3-3. Changes in melting and crystallization enthalpy of water upon addition of 1 mol% trehalose, trehalose repeating units in pCL-trehalose₈₀, betaine, or zwitterionic repeating units in pCL-zwitterion₈₀.

Sample	H _m (J/g)	ΔH _m (J/g)	H _c (J/g)	ΔH _c (J/g)
Water	296.5		-252.2	
Trehalose	249.1	-47.4	-229.9	22.3
T80	115.9	-180.6	-96.3	155.9
Betaine	198.1	-98.4	-179	73.2
Z80	16.41	-280.09	-23.4	228.8

3.3. Discussion

We have demonstrated that a biodegradable backbone can be transformed into a library of potential protein stabilizers using thiol-ene chemistry. This approach allows us to survey the effectiveness of various side chains without complications due to differences in the number of backbone repeat units. We tested five relevant side chains: three sugars, oligoPEG and a zwitterion. Yet, one can readily envision that synthesis of larger libraries of side chains using this approach. To investigate side chain effectiveness, the therapeutic protein G-CSF was stabilized against refrigeration and heat, two stresses that are relevant to the storage and shipping of many proteins; for example, nearly 80% of current protein therapeutics need to be refrigerated or frozen.⁶⁷ This temperature requirement causes inconvenience and increased costs to patients and may make some therapeutics impossible for use in parts of the world that do not have an effective

cold chain. In addition, in some industries such as personal care where products are stored at room temperature, the instability of some proteins of interest may preclude their use.

We found that pCL with trehalose- and zwitterion-substituted side chains were the most effective stabilizers to G-CSF to room temperature storage and heating, with the zwitterion polymers as the most effective over different time and molecular weight ranges. Activity loss in G-CSF has been reported to be a result of both methionine oxidation and aggregation.^{56, 68-69} Trehalose as an excipient has been shown to have no effect on methionine oxidation of G-CSF, presumably because it is preferentially excluded from the protein surface, but has been shown to broadly inhibit aggregation of various proteins.⁶⁹⁻⁷⁰ Zwitterionic materials are known to be nonfouling and to repel proteins due to their high hydrophilicity and strong hydration.⁷¹⁻⁷² Additionally, the nonionic surfactant Tween has been shown to reduce G-CSF aggregation through micelle formation.⁷³ Initial analysis by TEM and DSC suggest that the trehalose and zwitterion-substituted polymers form structured aggregates alone and in the presence of G-CSF likely due to the non-ionic surfactant character of the polymers. Additionally, the materials have the capability to reduce the enthalpy of water crystallization and melting, equivalent to the thermodynamic effects that have been previously observed for their constituent side chain materials. Many current studies of osmolyte-protein interactions hypothesize that their stabilizing effect is in fact due to water-osmolyte interactions,⁷⁴⁻⁷⁵ and the pCL materials are likely to be similar to small-molecule osmolytes in this manner. The materials therefore combine two different classes of known excipients. We also found the polymers to be as good as excipients currently used in the formulation for Neulasta, a therapeutic G-CSF. However, as has been previously noted, sorbitol and polysorbate both present downsides to large-scale and repeated applications in therapeutics. Namely, sorbitol has been linked to GI tract problems and polysorbate has been

shown to undergo auto-oxidation.³³⁻³⁴ The substituted pCL polymers offer equivalent stabilities, and may be potential alternatives to the clinically used additives for G-CSF.

Although we looked at G-CSF, it should be possible to utilize this library approach to investigate a wide variety of proteins, and the outcome may be different depending on the individual protein degradation mechanism and the stress imposed. Using the versatile thiol-ene strategy it should be possible to readily alter the polymer side chains to identify stabilizers for a wide variety of stressors. The use of controlled ring-opening polymerization allows for the rapid synthesis of a variety of molecular weights to compare to commercially available additives, which may also be available in multiple molecular weights. As we have demonstrated, the effect of molecular weight on stabilization can be quite important, and the ability to add molecular weight variation to a library of polymeric stabilizers is significant. Additionally, the excellent control provided by ROP conditions allows for delicate tuning of the hydrolytic stability and degradability through selection of a variety of cyclic monomers or even using copolymerization. We anticipate this will greatly expand the possible applications for these materials, and this work is underway.

Polymers have the additional advantage that they may be used as bulk materials for processed materials and are widely used in biomedical applications. For example, polycaprolactone is FDA-approved as a copolymer with glycolide in the absorbable suture Monocryl.⁷⁶ We have previously shown that polystyrene with trehalose side chains stabilizes proteins in the solid state.⁷⁷ Therefore, it may also be possible to utilize these substituted pCL polymers as solid-state protein stabilizers for a myriad of applications where degradability is required. Thermal gravimetric analysis (TGA) has shown that pCL-trehalose₂₀ is stable to over 250 °C when heated (**Figure 3-39**), permitting use of these materials at high temperature. Furthermore, polymers such as PEG have been conjugated to proteins to increase their in vivo

stability via enhanced pharmacokinetic effects.^{35, 78} It should be possible to conjugate these polymers to a variety of proteins to additionally stabilize them to environmental stressors, and this work is underway.

3.4. Conclusions

A series of alkene-functionalized polyesters were synthesized by organocatalyzed ring-opening polymerization. Post-polymerization thiol-ene modification with a series of thiols led to well-defined trehalose-, lactose-, glucose-, PEG- and zwitterion-based biodegradable polyesters. These biodegradable stabilizers were investigated as to their ability to protect the therapeutic protein G-CSF from storage and heat stressors. Side chains containing trehalose and a zwitterionic carboxybetaine were found to be the most effective at maintaining G-CSF activity. Molecular weight studies of pCL-trehalose and pCL-zwitterion were explored and the polymers were shown to have moderate molecular weight dependence to refrigeration, where larger polymers (DP40 and DP80) demonstrated greater protein stabilization to heat. Both high-performing polymer scaffolds and their degradation products were also not cytotoxic up to at least 1 mg/mL. These materials could be used for stabilization of protein activity in therapeutic and industrial applications, leading to improved performance and lowered cost.

3.5. Experimental

3.5.1. Materials

All materials and proteins were purchased from Sigma-Aldrich, Acros, or Fisher Scientific and were used without purification unless noted. Trehalose was purchased from The Healthy Essential Management Corporation (Houston, TX) and dried with ethanol and kept under vacuum before use. Anhydrous toluene was distilled from CaH₂ and stored under argon prior to use. Anhydrous tetrahydrofuran (THF) was distilled from sodium benzophenone and stored under argon prior to use. Allyl-caprolactone was synthesized as previously described³⁸ and purified by distillation under reduced pressure before use. Thiolated methoxy oligo(ethyleneglycol) was synthesized as previously described.⁴⁹ Thiolaactose heptaacetate was synthesized as previously described^{48,79} from commercially available lactosyl bromide. Recombinant human G-CSF (herein called G-CSF) expressed in *E. coli* was expressed as described.⁸⁰

3.5.2. Analytical Techniques

NMR spectra were obtained on Bruker AV 500 and DRX 500 MHz spectrometers. ¹H-NMR spectra were acquired with a relaxation delay of 2 s for small molecules and 30 s for polymers. DP indicated for each polymer structure was calculated from the NMR spectrum. Variations represent instrumental error rather than a change in the polymer backbone length. Infrared absorption spectra were recorded using a PerkinElmer FT-IR equipped with an ATR accessory. High-resolution mass spectra were obtained on Waters LCT Premier with ACQUITY LC and ThermoScientific Exactive Mass Spectrometers with DART ID-CUBE. Gel Permeation Chromatography (GPC) was conducted on a Shimadzu high performance liquid chromatography (HPLC) system with a refractive index detector RID-10A, one Polymer Laboratories PLgel guard column, and two

Polymer Laboratories PLgel 5 μm mixed D columns. Eluent was DMF with LiBr (0.1 M) at 50 °C (flow rate: 0.80 mL/ min). Calibration was performed using near-monodisperse PMMA standards from Polymer Laboratories. Size Exclusion Chromatography (SEC) was conducted on a Shimadzu HPLC system with a refractive index detector RID-10A, one Tosoh TSKGel guard column, and one Tosoh TSKGel G4000PW column. Eluent was 0.3 M NaNO_3 + 20 mM phosphate buffer pH 7 + 20% MeCN at 25 °C (flow rate 0.7 mL/min). Calibration was performed using near-monodisperse PEG standards from Polymer Laboratories. Matrix-assisted laser desorption/ionization (MALDI) was carried out on a Bruker Ultraflex. Solutions of trans-2-[3-(4-tert-butylphenyl)-2-methyl-2-propylidene]malonitrile (DCTB) as a matrix (20 mg/mL in THF), sodium trifluoroacetate (0.33 mg/mL in THF) as a cationizing agent, and polymer (1 mg/mL in THF) were mixed then added to the target to prepare a thin matrix/analyte film.

3.5.3. Methods

Synthesis and Characterization of Small Molecules

Synthesis of tosylated trehalose 2. In a two-neck round bottom flask, monohydroxyheptaacetyltrehalose **1**²⁷ (1.54 g, 2.42 mmol) was dissolved in anhydrous CH_2Cl_2 (15 mL) under argon. 4-Dimethylaminopyridine (59 mg, 0.48 mmol) and anhydrous pyridine (580 μL , 7.26 mmol) were added and the reaction solution cooled to 0 °C in an ice-water bath. Tosyl chloride (1.38 g, 7.26 mmol) was added slowly as a solid and the solution stirred for an additional 20 minutes at 0 °C before warming to room temperature and stirring for 14 hours. The crude mixture was diluted with additional CH_2Cl_2 (40 mL) and washed with water (2x 50 mL) and brine (50 mL). The organic layer was then dried with MgSO_4 and concentrated *in vacuo*. The crude solid was purified by silica gel flash column chromatography (eluent 5:1 CH_2Cl_2 : EtOAc) to obtain a

crispy white solid (1.34 g, 1.70 mmol, 70%). ¹H-NMR (500 MHz in CDCl₃) δ: 7.74 (d, *J* = 8.3 Hz, 2H), 7.34 (d, *J* = 8 Hz, 2H), 5.47-5.41 (m, 2H), 5.14 (d, *J* = 3.9 Hz, 1H), 5.05-5.01 (m, 3H), 4.93-4.89 (m, 2H), 4.21 (dd, *J* = 12.1 Hz, 6.7 Hz, 1H), 4.14-3.94 (m, 5H), 2.44 (s, 3H), 2.09 (s, 3H), 2.06 (s, 3H), 2.05 (s, 3H), 2.03 (s, 3H), 2.02 (s, 3H), 2.01 (s, 3H), 2.00 (s, 3H). ¹³C NMR: (500 MHz in CDCl₃) δ: 169.0, 169.9, 169.6, 169.6, 169.5, 169.5, 145.3, 132.4, 129.9, 128.0, 92.8, 92.3, 70.0, 69.7, 69.7, 69.3, 68.6, 68.4, 68.2, 68.1, 67.5, 61.7, 21.7, 20.7, 20.7, 20.6, 20.6, 20.6, 20.5. IR: ν = 2950, 1744, 1432, 1368, 1221, 1190, 1177, 1138, 1079, 1035, 1016, 988, 911, 862, 805 cm⁻¹. HRMS-ESI (*m/z*) [M+H₂O]⁺ calcd for C₃₃H₄₄O₂₁S, 808.2096; found 808.2226.

Synthesis of thioacetylated trehalose 3. In a two-neck round bottom flask, tosylated trehalose **2** (2.38 g, 3.01 mmol) was dissolved in anhydrous DMF (12 mL) under argon. Potassium thioacetate (1.03 g, 9.03 mmol) was added and the reaction solution heated to 70 °C for 18 hours. After cooling to room temperature, DMF was removed *in vacuo*. The crude brown solid was dissolved in CH₂Cl₂ and washed with water, sat. NaHCO₃ (2x), water, and brine. The organic layer was dried with MgSO₄ and concentrated *in vacuo*. The crude oil was purified by silica gel flash column chromatography (eluent 1:1 hexanes:EtOAc) to obtain **3** as a light tan solid (1.59 g, 2.29 mmol, 76%). ¹H NMR: (500 MHz in CDCl₃) δ: 5.47 (t, *J* = 10 Hz, 2H), 5.28 (dd, *J* = 4, 14 Hz, 2H), 5.07-4.96 (m, 4H), 4.19 (dd, *J* = 6, 12 Hz, 1H), 4.04 (dd, *J* = 2, 12 Hz, 1H), 3.98-3.95 (m, 1H), 3.87 (ddd, *J* = 2.6, 7.8, 10.2 Hz, 1H), 3.17 (dd, *J* = 2.5, 14.5 Hz, 1H), 2.96 (dd, *J* = 8, 14 Hz, 1H), 2.34 (s, 3H), 2.10 (s, 3H), 2.08 (s, 3H), 2.08 (s, 3H), 2.07 (s, 3H), 2.04 (s, 3H), 2.03 (s, 3H), 2.02 (s, 3H). ¹³C NMR: (500 MHz, CDCl₃) δ: 194.7, 170.6, 169.9, 169.9, 169.9, 169.8, 169.7, 169.6, 91.4, 91.2, 70.9, 70.1, 70.0, 69.8, 69.6, 69.3, 68.6, 68.2, 61.8, 30.4, 29.8, 20.7, 20.7, 20.6, 20.6, 20.6. IR:

$\nu = 2957, 1746, 1694, 1431, 1367, 1212, 1161, 1134, 1034, 981, 962, 900, 803 \text{ cm}^{-1}$. HRMS-ESI (m/z) $[M+Na]^+$ calculated for $C_{28}H_{38}NaO_{18}S$, 717.1677, found 717.1650.

Synthesis of selectively deprotected thiolated trehalose A. In a 20 mL screw-top vial, thioacetylated trehalose **3** (1.5 g, 2.16 mmol) was dissolved in DMF (22 mL) under argon. Acetic acid (122 μL , 2.14 mmol) was added and the solution was stirred for 10 minutes. Hydrazine hydrate (70-82% in H_2O , 131 μL , 2.14 mmol) was then added and the reaction solution was stirred at 21 $^\circ\text{C}$ for a further 2 hours. Acetone (200 μL , 2.72 mmol) was added to quench the reaction, and the crude product was poured into H_2O and extracted with EtOAc. The organic layer was washed with brine (2x), dried over $MgSO_4$, and solvent removed in vacuo to obtain **4** as a light tan solid (1.52 g, quantitative yield). 1H NMR: (500 MHz in $CDCl_3$) δ : 5.49 (t, $J = 10$ Hz, 2H), 5.31 (t, $J = 4$ Hz, 2H), 5.11-5.00 (m, 4H), 4.22 (dd, $J = 12, 5.5$ Hz, 1H), 4.03-3.97 (m, 3H), 2.63-2.55 (m, 2H), 2.13 (s, 3H), 2.09 (s, 6H), 2.07 (s, 3H), 2.05 (s, 3H), 2.03 (s, 3H), 2.03 (s, 3H), 1.68 (dd, $J = 10, 7$ Hz, 1H). ^{13}C NMR: (500 Hz, $CDCl_3$) δ : 170.6, 170.0, 169.7, 169.7, 169.6, 92.2, 91.9, 71.2, 70.7, 70.0, 70.0, 69.9, 69.4, 68.6, 68.2, 61.8, 25.8, 21.0, 20.7, 20.7, 20.6, 20.6. IR: $\nu = 2962, 1746, 1669, 1435, 1368, 1215, 1166, 1137, 1033, 984, 964, 904, 804, 722, 659 \text{ cm}^{-1}$. HRMS-ESI (m/z) $[M+Na]^+$ calcd for $C_{26}H_{36}NaO_{17}S$, 675.1571; found 675.1624.

Polymer Synthesis and Characterization

Representative ring-opening polymerization (pCL-allyl₄₀). For the synthesis of pCL-allyl₄₀, a 1.5 mm glass sample vial was equipped with a stir bar and 2-3 4 \AA molecular sieves and the setup was flame-dried. A 0.1 M solution of TBD in toluene (480 μL , 24 μmol , 2.5 mol%) and a solution of 15% v/v 3-methyl-1-butanol in toluene (12.6 μL , 17 μmol , 1 equivalent) were added via nitrogen-purged syringe and the initiator-catalyst mixture was allowed to stir for 30 minutes at 21 $^\circ\text{C}$ before

adding allyl-caprolactone monomer (150 mg, 973 μmol , 56 equivalents) via nitrogen-purged syringe. The reaction mixture was stirred at 21 $^{\circ}\text{C}$ and aliquots were removed for $^1\text{H-NMR}$ analysis via a nitrogen-purged syringe. After the desired conversion was achieved, the reaction was quenched with AcOH and the crude mixture purified by silica gel column chromatography (eluent EtOAc in hexanes 15-50%) to give the polymer as a colorless oil (100.5 mg). M_n (GPC) = 5400 Da, Đ = 1.08. $^1\text{H-NMR}$ (500 MHz in CDCl_3) δ : 5.75-5.67 (m, 36H), 5.06-5.00 (m, 72H), 4.11-4.10 (m, 72H), 3.63-3.61 (m, 2H), 2.44-2.31 (m, 72H), 2.24-2.19 (m, 36H), 1.67-1.45 (m, 144H), 1.36-1.30 (m, 72H), 0.92-0.91 (d, J = 7 Hz, 6H). IR: ν = 3077, 2941, 2863, 1729, 1642, 1444, 1417, 1392, 1364, 1234, 1162, 1135, 1064, 994, 915, 736.

Representative synthesis of functional polyesters via thiol-ene reaction (pCL-trehaloseOAc₄₀). For the synthesis of pCL-trehaloseOAc₄₀, in a 1.5 mm glass sample vial, pCL-allyl₄₀ (12 mg, 2.1 μmol , 77 μmol alkene groups) was dissolved in anhydrous THF (300 μL). Thiolated trehalose A (162 mg, 249 μmol , 3 equivalents per alkene) and 2,2-dimethoxy-2-phenylacetophenone (DMPA) (11 mg, 42 μmol , 0.5 equivalents per alkene) were added and the vial was sealed with a septum, degassed by sparging for 10 minutes, and exposed to a handheld UV lamp (λ = 365 nm) for 4 hours. The crude solution was then precipitated into cold MeOH (protected sugars) or dialyzed in MeOH (PEG and zwitterion precursor) to yield the desired functional polyester (53.1 mg, 1.7 μmol , 79%). M_n (GPC) = 28400 Da, Đ = 1.06. $^1\text{H-NMR}$ (500 MHz in CDCl_3) δ : 5.47 (q, 86H), 5.30-5.26 (m, 86H), 5.13-5.10 (m, 44H), 5.06-4.97 (m, 129H), 4.24-4.20 (m, 43H), 4.06-4.00 (m, 215H), 2.62-2.47 (m, 172H), 2.34-2.27 (m, 43H), 2.15-2.00 (m, 903H), 1.68-1.58 (m, 215H), 1.55-1.42 (m, 172H), 1.34-1.26 (m, 86H), 0.93 (d, J = 6.5 Hz, 6H).

pCL-glucoseOAc₄₀: M_n (GPC) = 22300 Da, \bar{D} = 1.06. ¹H-NMR (500 MHz in CDCl₃) δ : 5.23 (t, 39H), 5.09 (t, 39H), 4.99 (t, 39H), 4.52-4.45 (d, 39H), 4.25 (dd, 39H), 4.16-4.10 (d, 78H), 4.07-3.97 (m, 78H), 3.75-3.69 (m, 39H), 2.73-2.60 (m, 78H), 2.37-2.28 (m, 39H), 2.13-1.97 (m, 468H), 1.70-1.42 (m, 312H), 1.38-1.24 (m, 78H), 0.93 (d, J = 6.5 Hz, 6H).

pCL-lactoseOAc₄₀: M_n (GPC) = 28900 Da, \bar{D} = 1.07. ¹H-NMR (500 MHz in CDCl₃) δ : 5.36 (d, 37H), 5.27 (t, 37H), 5.09 (t, 37H), 4.99-4.86 (m, 74H), 4.53-4.40 (m, 111H), 4.18-3.95 (m, 185H), 3.91-3.84 (t, 37H), 3.82-3.73 (t, 37H), 3.66-3.55 (m, 37H), 2.69-2.56 (m, 74H), 2.35-2.24 (m, 37H), 2.18-1.90 (m, 777H), 1.71-1.40 (m, 370H), 1.34-1.21 (m, 74H), 0.92 (d, J = 6.5 Hz, 6H).

pCL-PEG₄₀: M_n (GPC) = 23600 Da, \bar{D} = 1.07. ¹H-NMR (500 MHz in CDCl₃) δ : 4.11-3.98 (m, 78H), 3.74-3.51 (m, 1225H), 3.38 (s, 117H), 2.69 (t, 78H), 2.53 (t, 78H), 2.36-2.29 (m, 39H), 1.71-1.42 (m, 332H), 1.36-1.25 (m, 78H), 0.93 (d, J = 6.5 Hz, 6H).

Representative deprotection of acetylated glycopolymers (pCL-trehalose₈₀). For the synthesis of pCL-trehalose₈₀, in a 20 mL screw-top vial, pCL-trehaloseOAc₈₀ (16.8 mg, 0.3 μ mol, 145 μ mol acetate groups) was dissolved in CHCl₃:MeOH 1:1 (2 mL). K₂CO₃ (20 mg, 148 μ mol, 1 equivalent per acetate group) was added, and the suspension was let stir at room temperature for 3 hours, during which time a white precipitate formed. The organic solvents were removed and the solid was dissolved in H₂O, neutralized with 2M HCl and dialyzed against 3.5 kD MWCO in 50% MeOH, switching to 100% H₂O after 24 hours. The resulting solution was removed from the dialysis tubing and lyophilized, yielding a fluffy white solid (6.3 mg, 0.16 μ mol, 60% yield). M_n (GPC) = 17000 Da, \bar{D} = 1.39. ¹H-NMR (500 MHz in CDCl₃) δ : 5.12-4.95 (d, 160H), 4.14-3.88 (s, 320H), 3.89-3.56 (m, 400H), 3.54-3.42 (s, 320H), 3.36-3.16 (m, 160H), 2.94-2.78 (s, 80H), 2.65-

2.42 (m, 240H), 2.36-2.22 (s, 80H), 1.78-1.35 (m, 480H), 1.31-1.09 (s, 160H), 0.82 (s, 6H). IR: ν = 3339, 2931, 1726, 1367, 1264, 1146, 1102, 1030, 991, 942, 841, 804, 731.

pCL-glucose₄₀: M_n (GPC) = 18300 Da, \bar{D} = 1.09. ¹H-NMR (500 MHz in CDCl₃) δ : 4.38 (d, 32H), 4.01 (s, 64H), 3.74 (d, 32H), 3.60 (s, 32H), 3.40-2.37 (m, 96H), 3.19 (t, 32H), 2.63 (s, 64H), 2.31 (s, 32H), 1.59-1.42 (m, 256H), 1.29-1.17 (m, 64H), 0.84 (d, J = 6.5 Hz, 6H).

pCL-lactose₄₀: M_n (GPC) = 16900 Da, \bar{D} = 1.17. ¹H-NMR (500 MHz in CDCl₃) δ : 4.38 (dd, 70H), 4.06-3.93 (s, 70H), 3.90-3.78 (m, 70H), 3.74-3.41 (m, 280H), 3.26 (t, 32H), 2.70-2.58 (m, 70H), 2.35-2.27 (m, 35H), 2.04-1.98 (m, 35H), 1.62-1.41 (m, 280H), 1.30-1.19 (m, 70H), 0.84 (d, J = 6.5 Hz, 6H).

Synthesis of pCL-zwitterion₄₀. In a 1.5 mm glass sample vial, pCL-allyl₄₀ (15 mg, 2.5 μ mol, 96 μ mol alkene groups) was dissolved in MeOH:DCM (1:1, 400 μ L total). Dimethylaminoethanethiol hydrochloride (41 mg, 288 μ mol, 3 equivalents per alkene) and DMPA (12 mg, 48 μ mol, 0.5 equivalents per alkene) were added and the vial sealed with a septum, degassed by sparging for 10 minutes, and exposed to a handheld UV lamp (λ = 365 nm) for 4 hours. The crude solution was opened to air and volatiles removed under reduced pressure. A solution of saturated sodium bicarbonate (3 mL) was then added to the vial and let stir for 1 hour. The aqueous layer was extracted with dichloromethane (3x 10 mL) and the organic layers combined and dried using MgSO₄. Solvent was removed in vacuo, and thorough removal of water was ensured by freeze-drying from benzene. The resulting oil was dissolved in anhydrous acetonitrile (2 mL) and t-butyl bromoacetate (57 μ L, 384 μ mol, 4 equivalents per amine) was added. The reaction mixture was stirred at 50 °C for 17 hours. The crude was let cool to room temperature and the acetonitrile was removed in vacuo. Trifluoroacetic acid (TFA, 0.5 mL) was then added and the reaction mixture let

stir at room temperature for 3.5 hours. TFA was removed in vacuo and the crude material was dissolved in MeOH:H₂O 1:1 and dialyzed against 3.5 kD MWCO dialysis tubing, switching to 100% H₂O after 24 hours. The resulting solution was filtered and lyophilized to remove water, yielding a white fluffy solid (18.2 mg, 1.5 μmol, 60% yield). M_n (GPC) = 5100 Da, \bar{D} = 1.19. ¹H-NMR (500 MHz in CDCl₃) δ: 4.07-3.96 (s, 78H), 3.84-3.77 (s, 78H), 3.76-3.65 (m, 78H), 3.23-3.09 (s, 234H), 2.89-2.76 (m, 78H), 2.61-2.47 (m, 78H), 2.39-2.27 (m, 39H), 1.78-1.41 (m, 312H), 1.33-1.16 (s, 78H), 0.84 (d, J = 6 Hz, 6H). IR: ν = 2944, 2861, 1721, 1626, 1457, 1385, 1325, 1250, 1163, 1059, 1006, 960, 886, 799, 715.

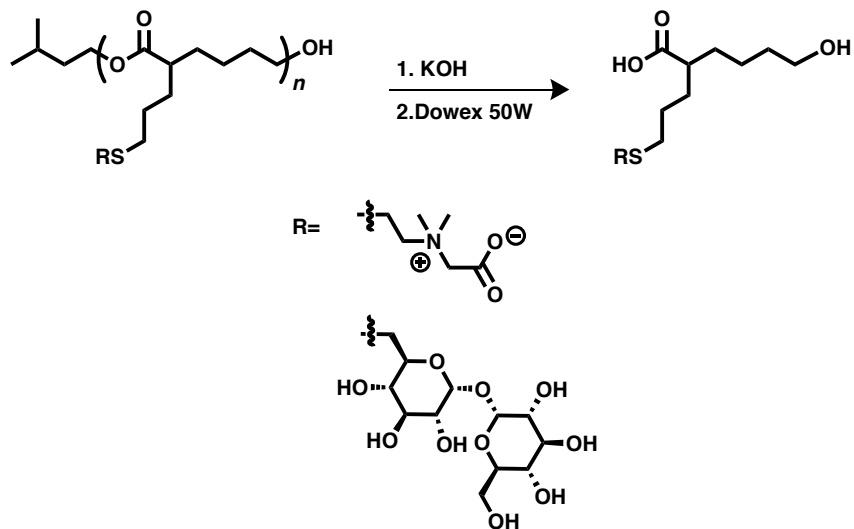
G-CSF Stabilization Studies. G-CSF samples (25 μL) were prepared in 10 mM acetate buffer, pH 4.0 at 1 μg/mL with 100 equivalents polymer additive by weight. Samples were stored at 4 °C for 90 minutes or 60 °C for 30 minutes and then were diluted with cold RPMI-1640 medium + 10% FBS (735 μL). The samples were then further diluted with RPMI-1640 + 10% FBS to a final concentration of 1 ng/mL. G-CSF bioactivity was then assayed in a NFS-60 mouse myelogenous leukemia lymphoblast cell line. NFS-60 cells were cultured in RPMI-1640 medium supplemented with 10% FBS and 2 ng/mL interleukin-3 (IL-3) at 37 °C/5% CO₂. NFS-60 cells were passaged at least three times before use in proliferation experiments. Prior to treating NFS-60 cells with G-CSF samples, NFS-60 cells were collected and resuspended in RPMI-1640 with 10% FBS (without additional growth factors). Cells were plated in the internal wells of a 96 well plate at a density of 20,000 cells per well in 50 μL of medium. G-CSF solution (50 μL) was then added to provide a final concentration of 0.5 ng/mL and total well volume of 100 μL. Following 48 h incubation at 37 °C/5% CO₂, CellTiter-Blue viability assay was performed to measure cell proliferation. All

experimental groups were normalized to the control of media alone without G-CSF addition. All *p* values were calculated using the independent Student's *t* test assuming unequal variances.

Transmission Electron Microscopy (TEM). Solutions were prepared for TEM by preparing polymer solutions (2 mg/mL) and G-CSF solutions (0.3 mg/mL) in 10 mM acetate buffer, pH 4.0. The solutions were mixed 1:1 and 3.0 μ L of the resulting solution was added to TEM grids that had been pre-treated using a glow discharge unit (Pelco easiGlow). Samples were then stained using a 1% uranyl acetate solution, blotted dry, and imaged using a FEI Tecnai T12 cryo-electron microscope. Micrographs were recorded using a Gatan 4 megapixel CCD camera (2k by 2k).

Differential Scanning Calorimetry (DSC). Solutions of trehalose, betaine, pCL-trehalose₈₀, and pCL-zwitterion₈₀ were made at 1 mol% of the stabilizing unit (trehalose or betaine) and analyzed by DSC (TA Instruments Q2000). Runs were carried out using two heat/cool cycles from -40 °C to 40 °C at 10 °C and values were taken from the second run.

Stability to Basic and Acidic Conditions. pCL-trehalose₁₀ or pCL-zwitterion₂₀ (3 mg) were dissolved in 5% aqueous KOH (1 mL) and placed on a rotating plate at 4 °C. Aliquots (300 μ L) were removed after 24 hours, neutralized with a strong cationic resin (Dowex 50W-8x200), lyophilized to remove solvent, and analyzed by aqueous SEC to assess degradation.



Scheme 3-4. Basic hydrolysis of pCL-trehalose₁₀ and pCL-zwitterion₂₀

Cytotoxicity. The cell compatibility of pCL-trehalose₂₀, pCL-zwitterion₂₀, and their KOH-degraded polymeric products was evaluated in human umbilical vein endothelial cells (HUVECs, ATCC) using a LIVE-DEAD viability/cytotoxicity assay (Invitrogen). HUVECs were cultured in endothelial cell growth medium (ATCC) supplemented with 100 unit/mL penicillin and 100 µg/mL streptomycin. At passage 6 the cells were trypsinized and resuspended in supplemented growth medium and then seeded in 48-well plates at a density of 5,000 cells/well in 200 µL medium. After 48 hours, culture medium was replaced with 200 µL of the working medium (endothelial cell growth medium with penicillin and streptomycin) containing polymer concentrations of 0.1, 0.5 and 1 mg/mL. Polymer solutions were sterile filtered prior to use and endothelial cell growth medium without polymers was used as a control. After incubation for 24 hours at 37 °C/5% CO₂, the medium was aspirated out of the wells and 125 µL of the LIVE/DEAD reagent (2 µM calcein AM and 4 µM ethidium homodimer-1) was added. The plate was incubated for 15 minutes and then images were captured on an Axiovert 200 microscope with a AxioCam MRm camera and FluoArc mercury lamp. The number of live and dead cells were counted using

ImageJ software and percent cell viability was calculated by dividing the number of live cells by the total number of cells.

3.6. Appendix with Supplementary Figures

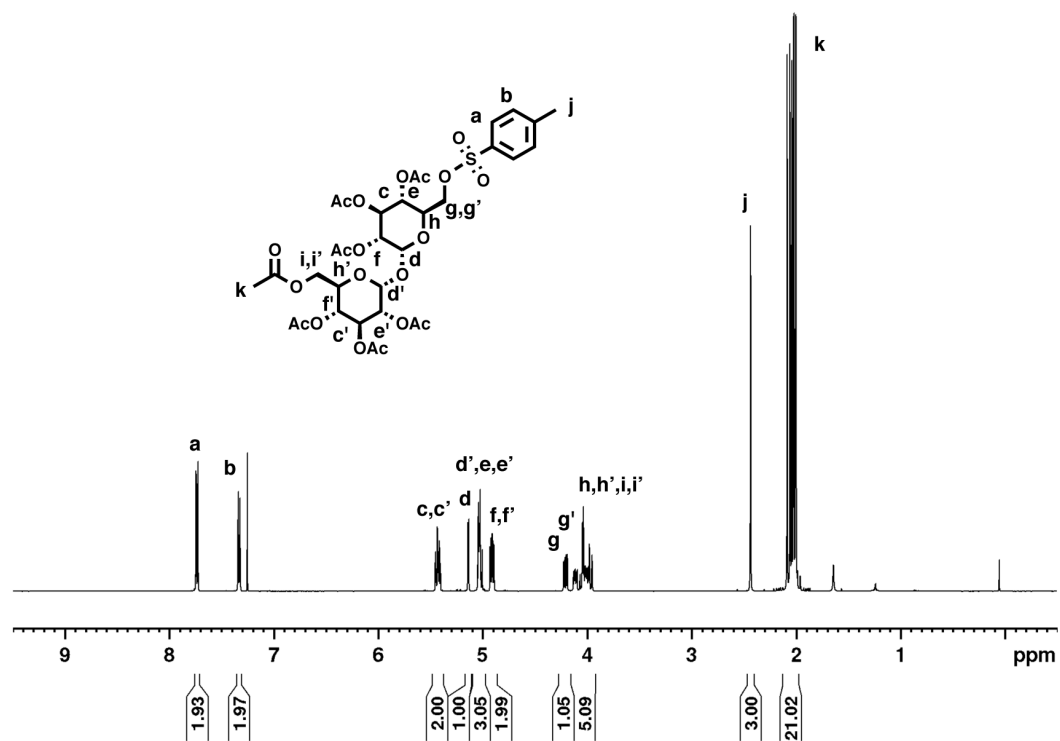


Figure 3-13. ¹H-NMR spectrum of tosylated trehalose heptaacetate **2** (CDCl₃, 500 MHz).

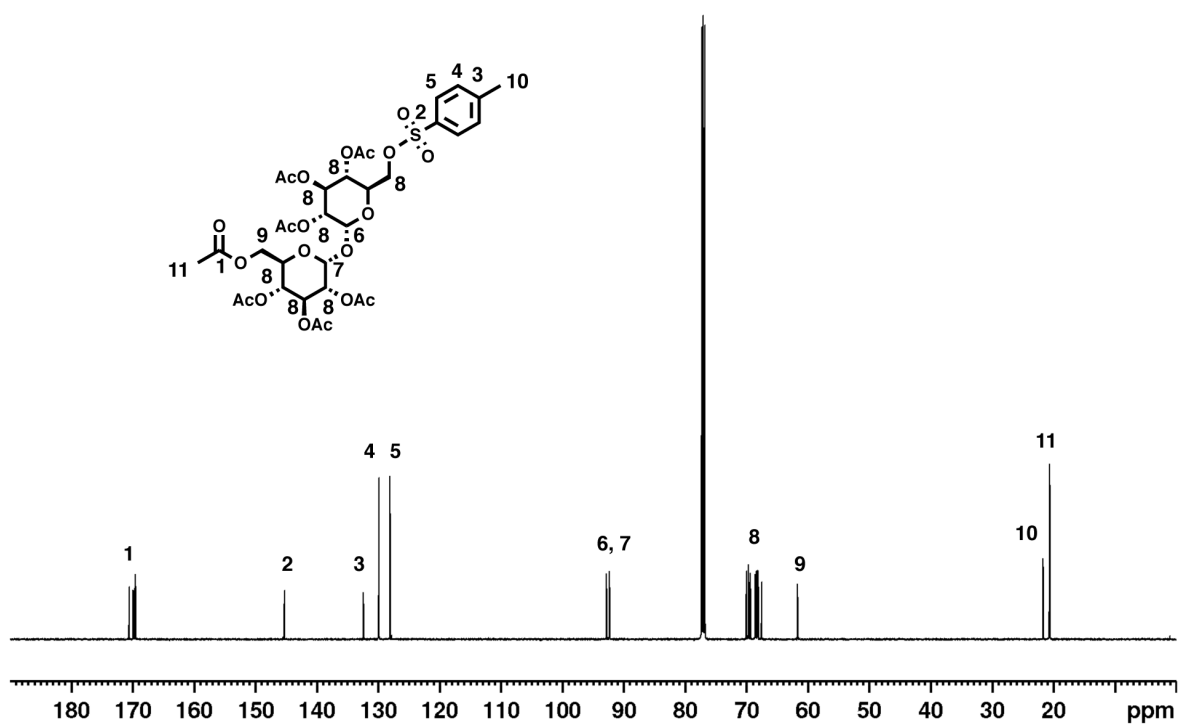


Figure 3-14. ¹³C-NMR spectrum of tosylated trehalose heptaacetate **2** (CDCl₃, 500 MHz).

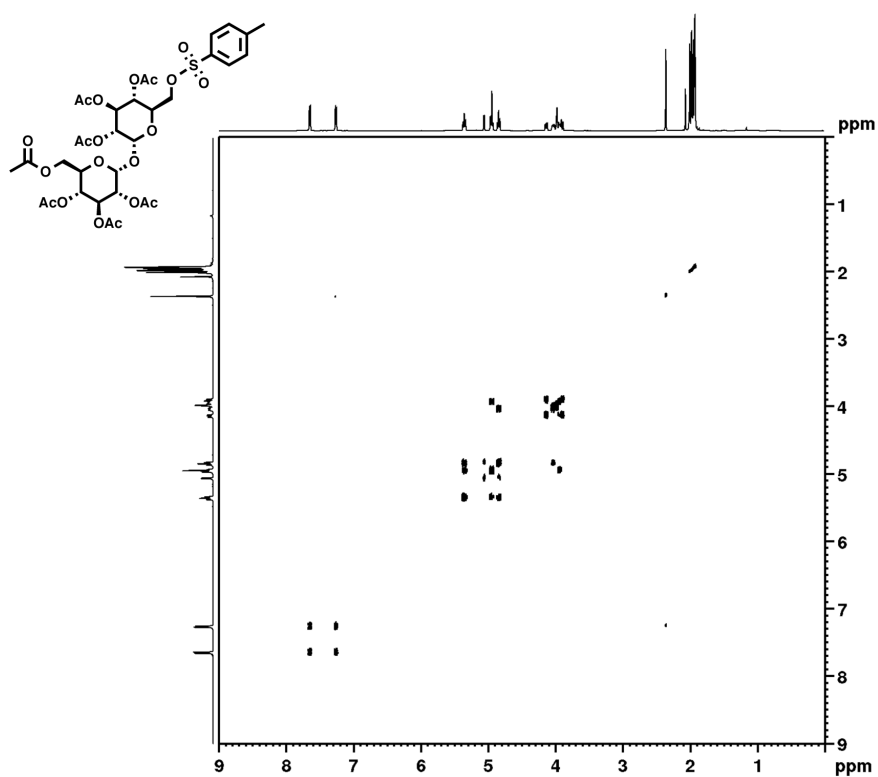


Figure 3-15. COSY spectrum of tosylated trehalose heptaacetate **2** (CDCl₃, 500 MHz).

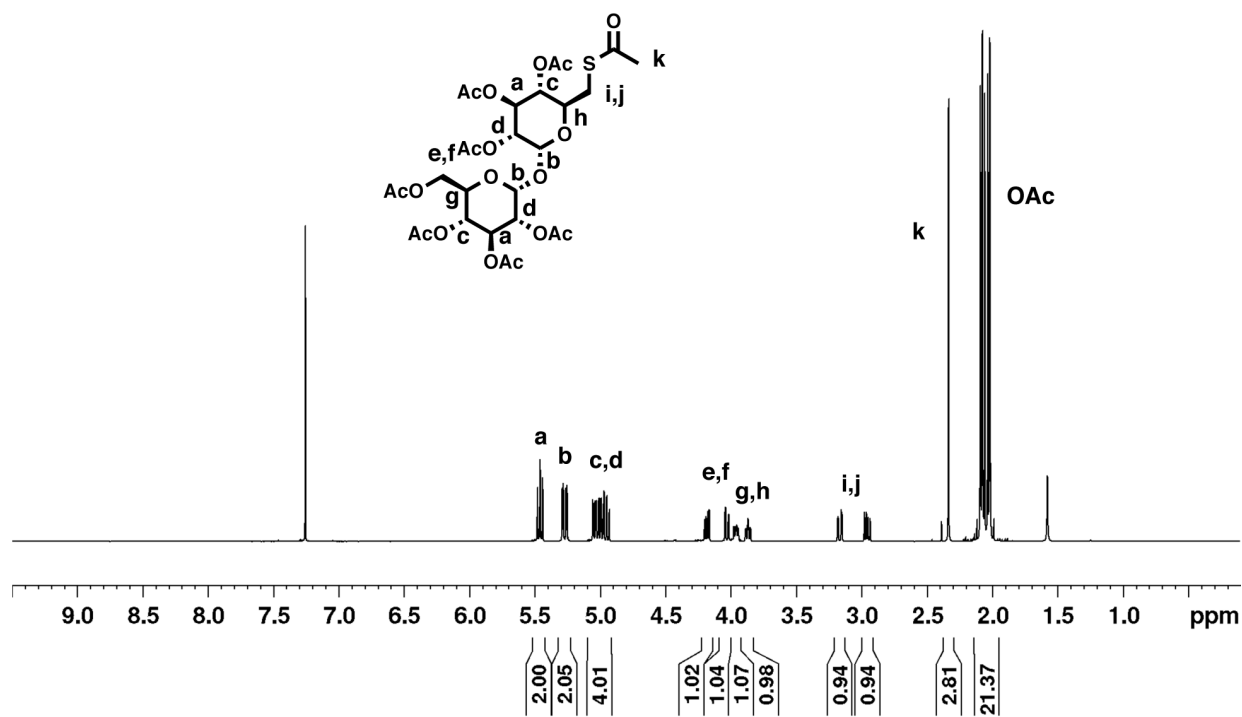


Figure 3-16. ¹H-NMR spectrum of thioacetylated trehalose heptaacetate **3** (CDCl₃, 500 MHz).

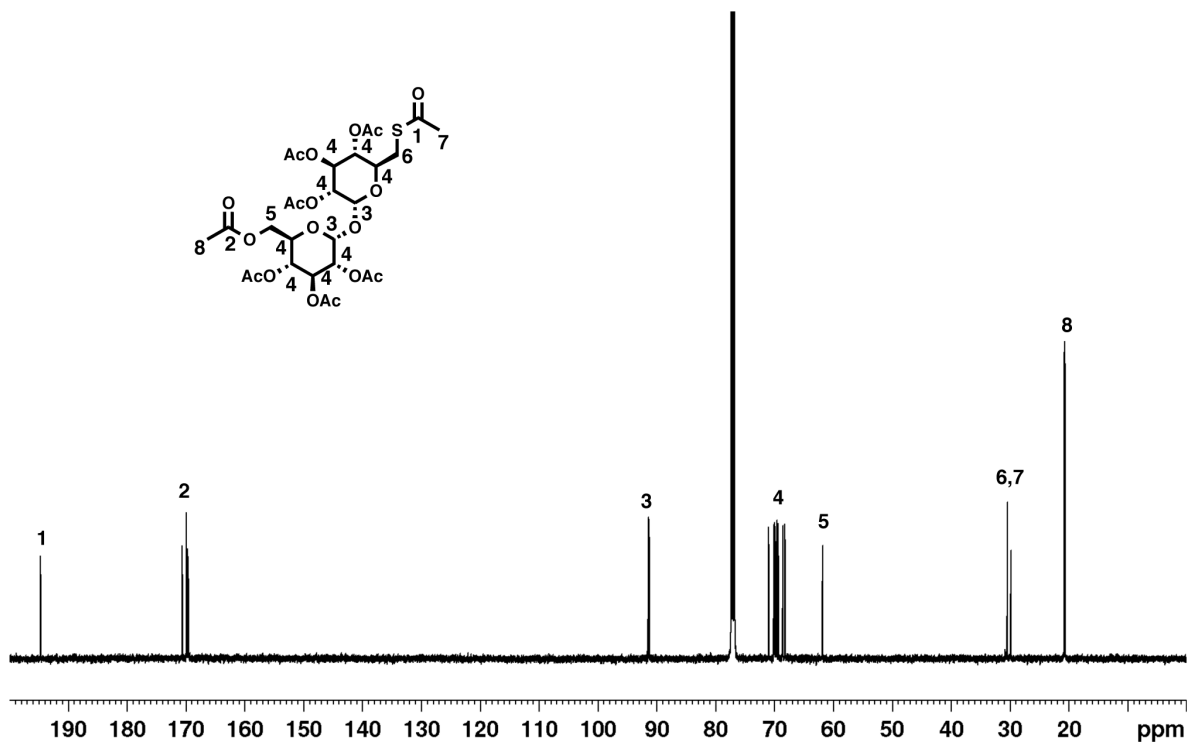


Figure 3-17. ¹³C-NMR spectrum of thioacetylated trehalose heptaacetate **3** (CDCl₃, 500 MHz).

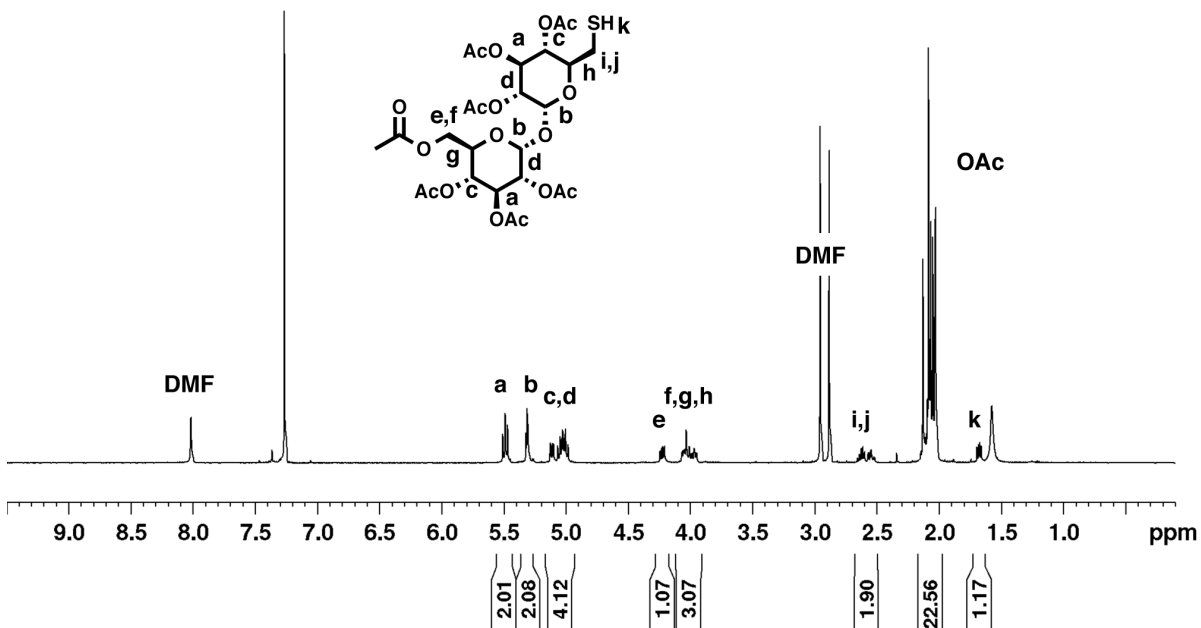


Figure 3-18. ¹H-NMR spectrum of crude unpurified thiolated trehalose heptaacetate A (CDCl₃, 500 MHz).

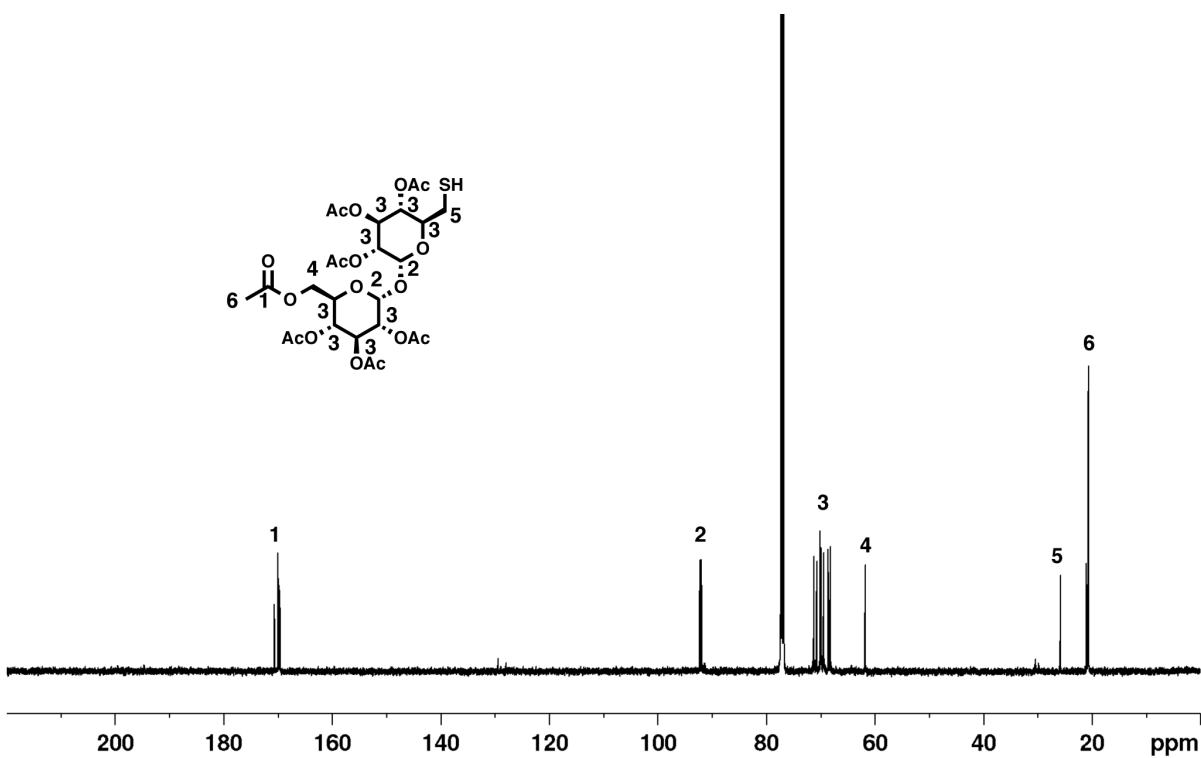


Figure 3-19. ¹³C-NMR spectrum of thiolated trehalose heptaacetate A (CDCl₃, 500 MHz).

Characterization of pCL-allyl_x Polymers

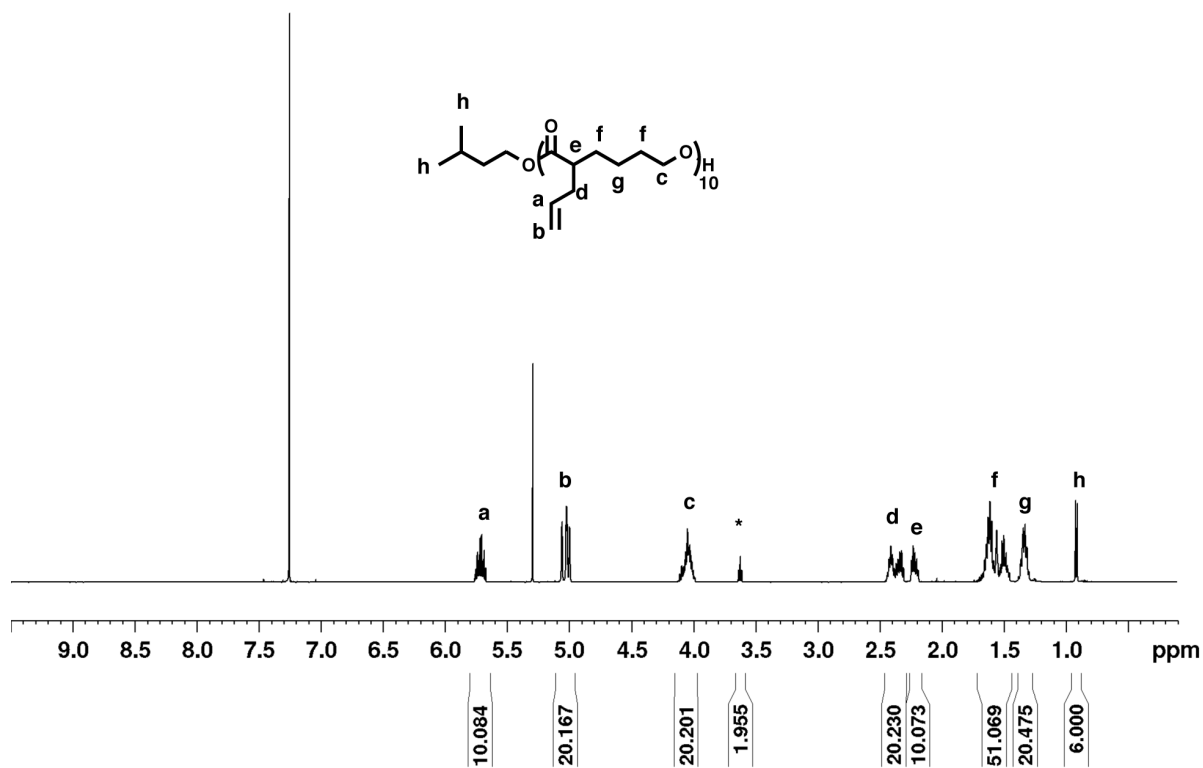


Figure 3-20. ¹H-NMR spectrum of pCL-allyl₁₀ (CDCl₃, 500 MHz). * = protons from terminal repeat unit on polymer.

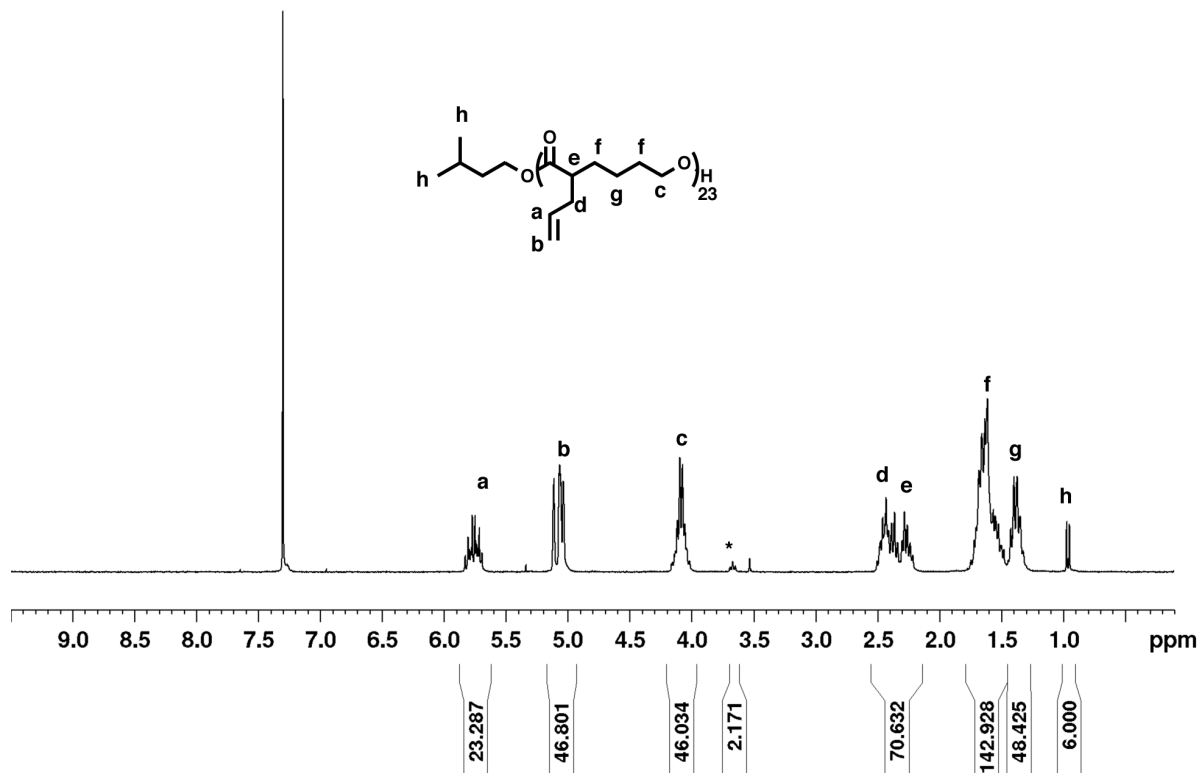


Figure 3-21. ¹H-NMR spectrum of pCL-allyl₂₀ (CDCl₃, 500 MHz). * = protons from terminal repeat unit on polymer.

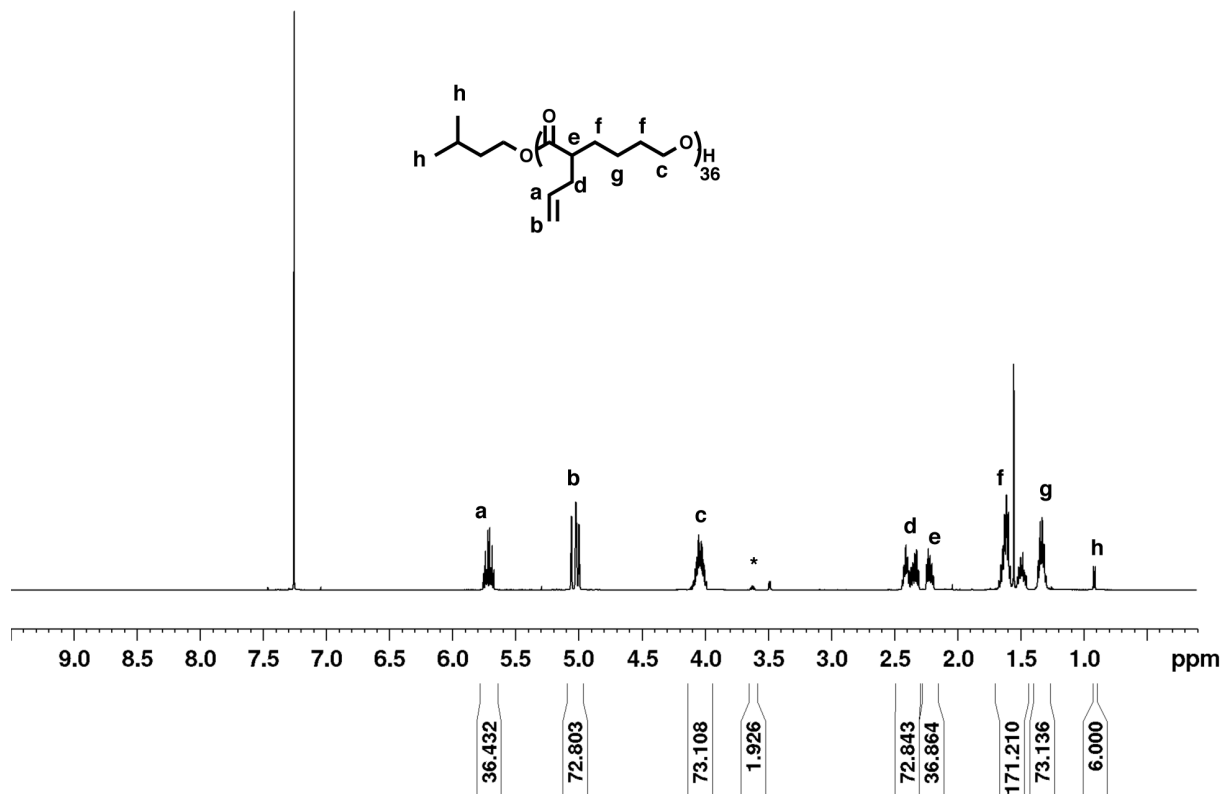


Figure 3-22. ¹H-NMR spectrum of pCL-allyl₄₀ (CDCl₃, 500 MHz). * = protons from terminal repeat unit on polymer.

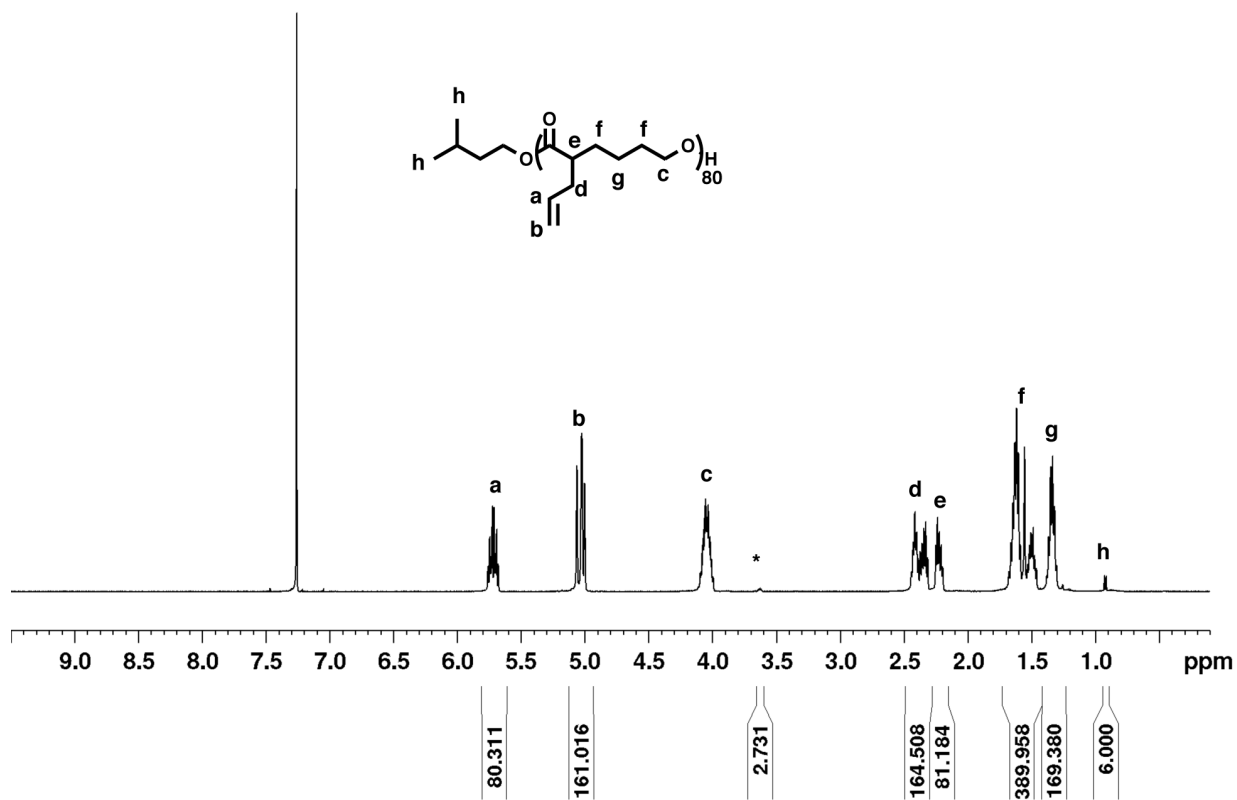


Figure 3-23. ¹H-NMR spectrum of pCL-allyl₈₀ (CDCl₃, 500 MHz). * = protons from terminal repeat unit on polymer.

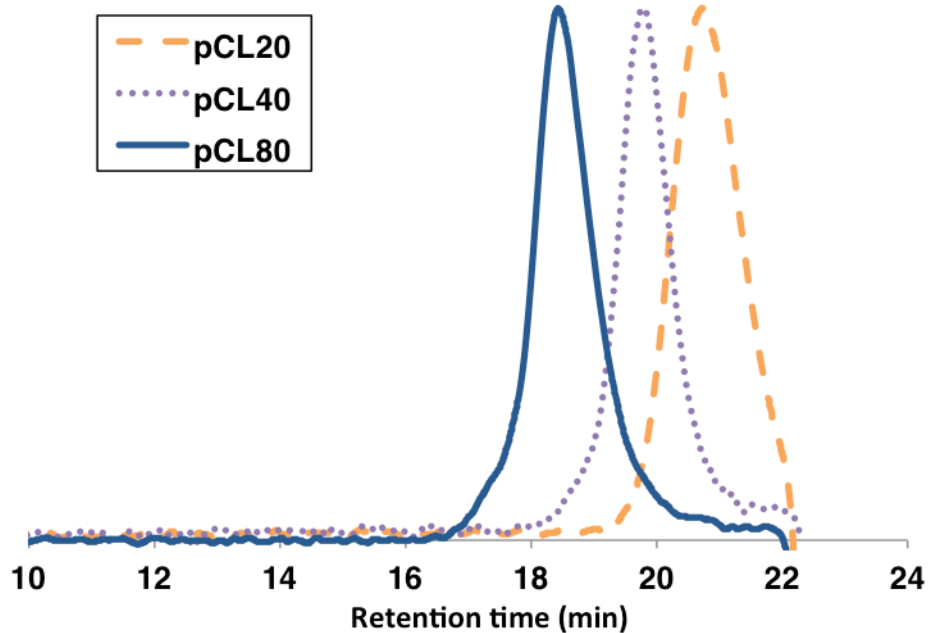


Figure 3-24. Gel permeation chromatograms of pCL-allyl₂₀, pCL-allyl₄₀, pCL-allyl₈₀. pCL-allyl₁₀ overlapped the solvent peak and was not able to be analyzed by GPC.

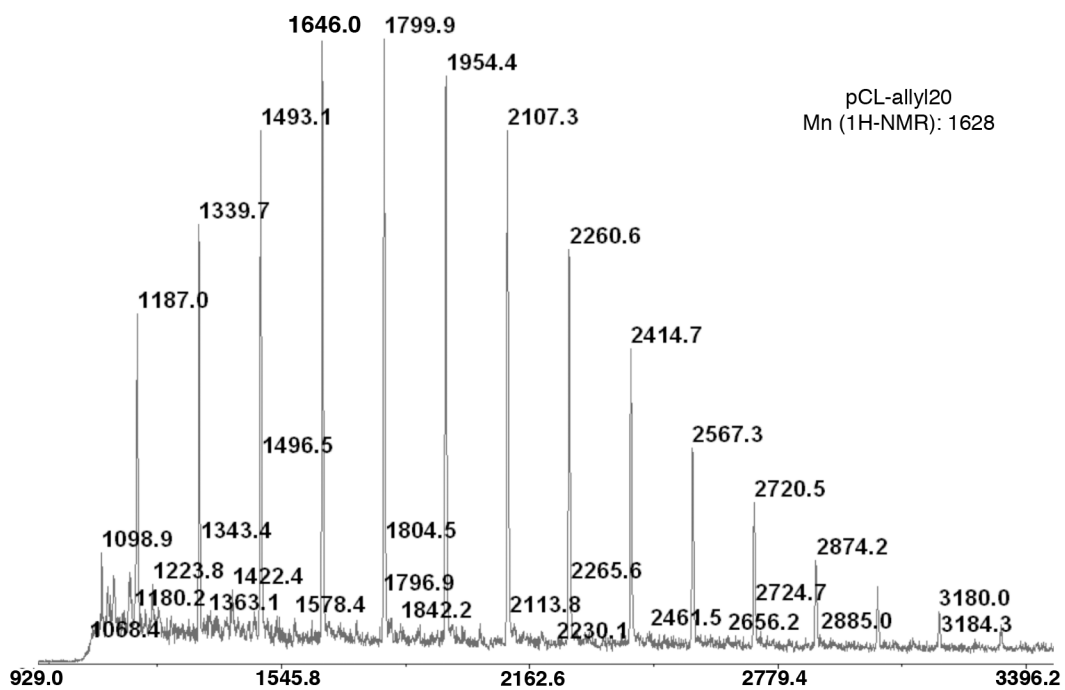


Figure 3-25. Matrix-assisted laser desorption/ionization (MALDI) chromatogram of pCL-allyl₁₀.

Characterization of Protected pCL-Saccharide Polymers

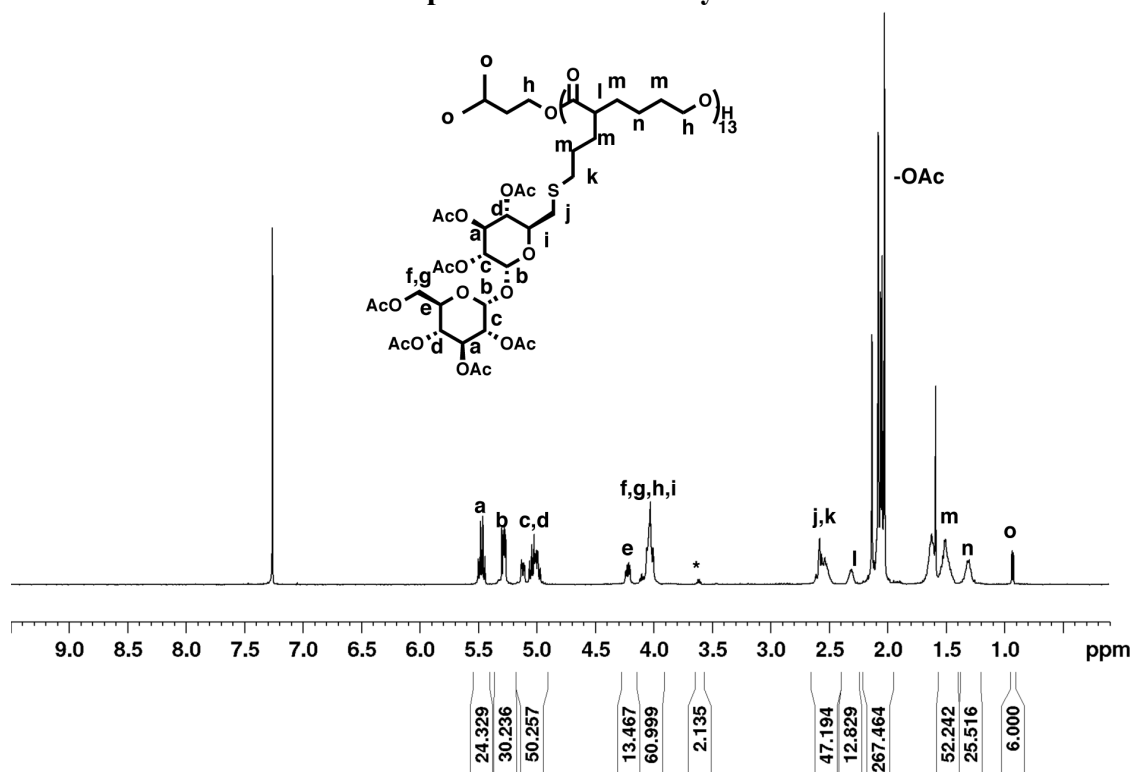


Figure 3-26. ¹H-NMR spectrum of pCL-trehaloseOAc₁₀ (CDCl₃, 500 MHz). * = protons from terminal unit on polymer.

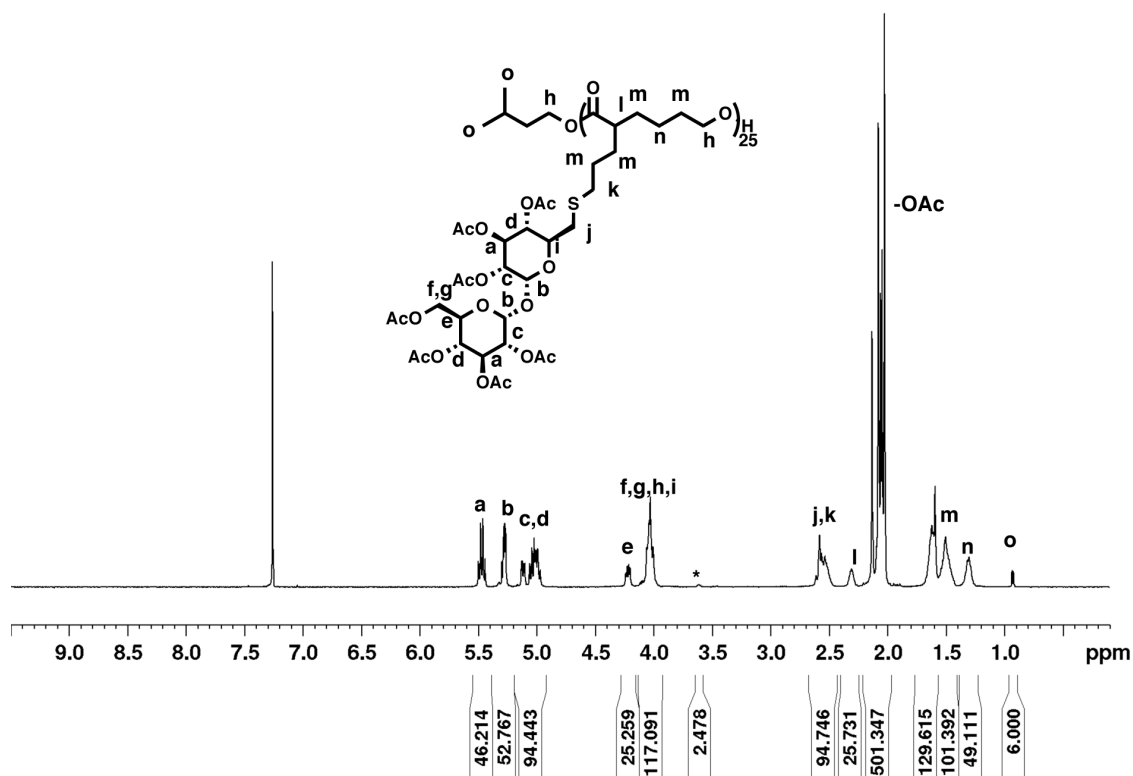


Figure 3-27. ¹H-NMR spectrum of pCL-trehaloseOAc₂₀ (CDCl₃, 500 MHz). * = protons from terminal unit on polymer.

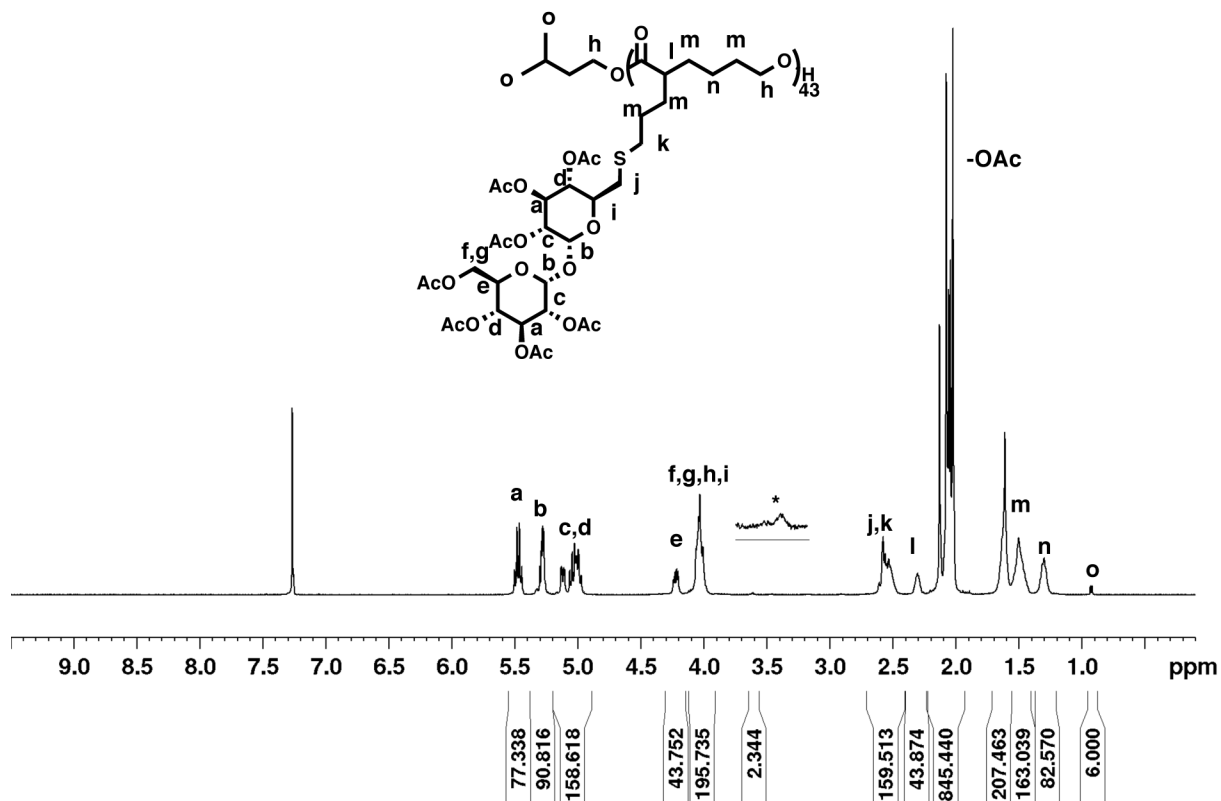


Figure 3-28. ¹H-NMR spectrum of pCL-trehaloseOAc₄₀ (CDCl₃, 500 MHz). * = protons from terminal unit on polymer.

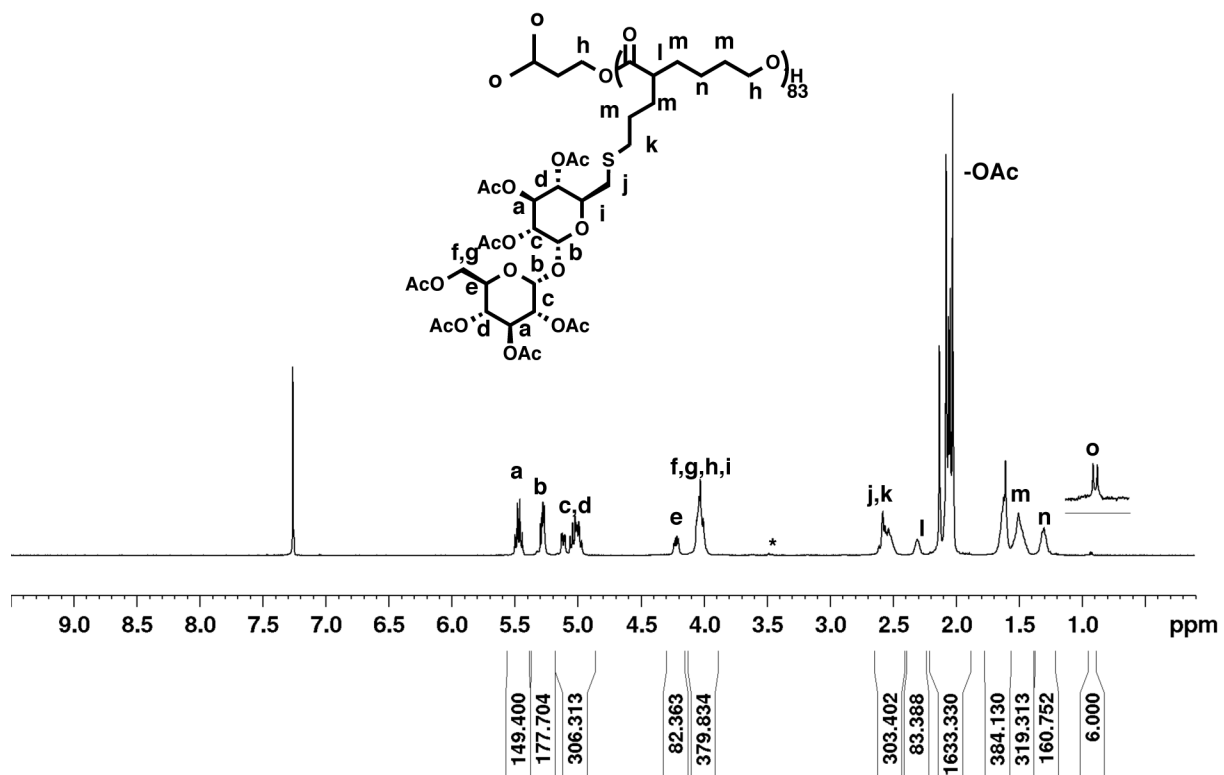


Figure 3-29. ¹H-NMR spectrum of pCL-trehaloseOAc₈₀ (CDCl₃, 500 MHz). * = protons from terminal unit on polymer.

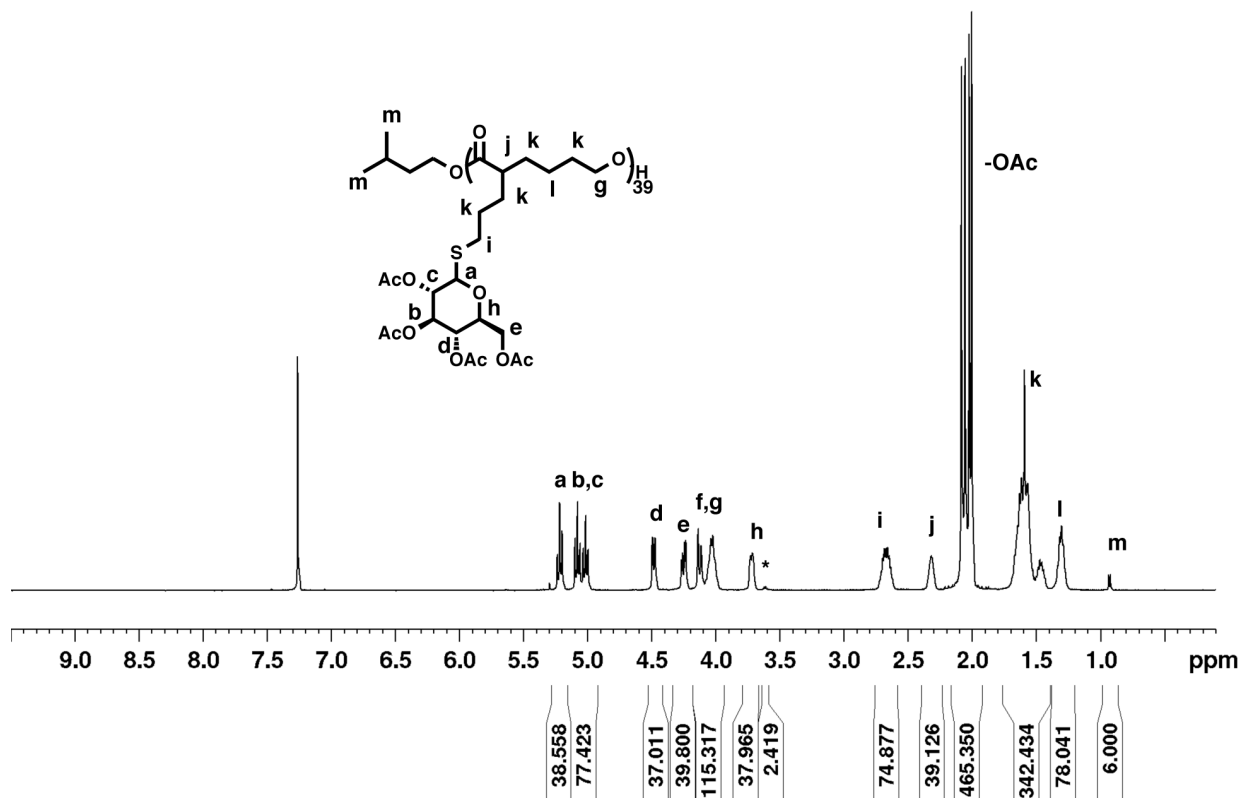


Figure 3-30. ¹H-NMR spectrum of pCL-glucoseOAc₄₀ (CDCl₃, 500 MHz). * = protons from terminal unit on polymer.

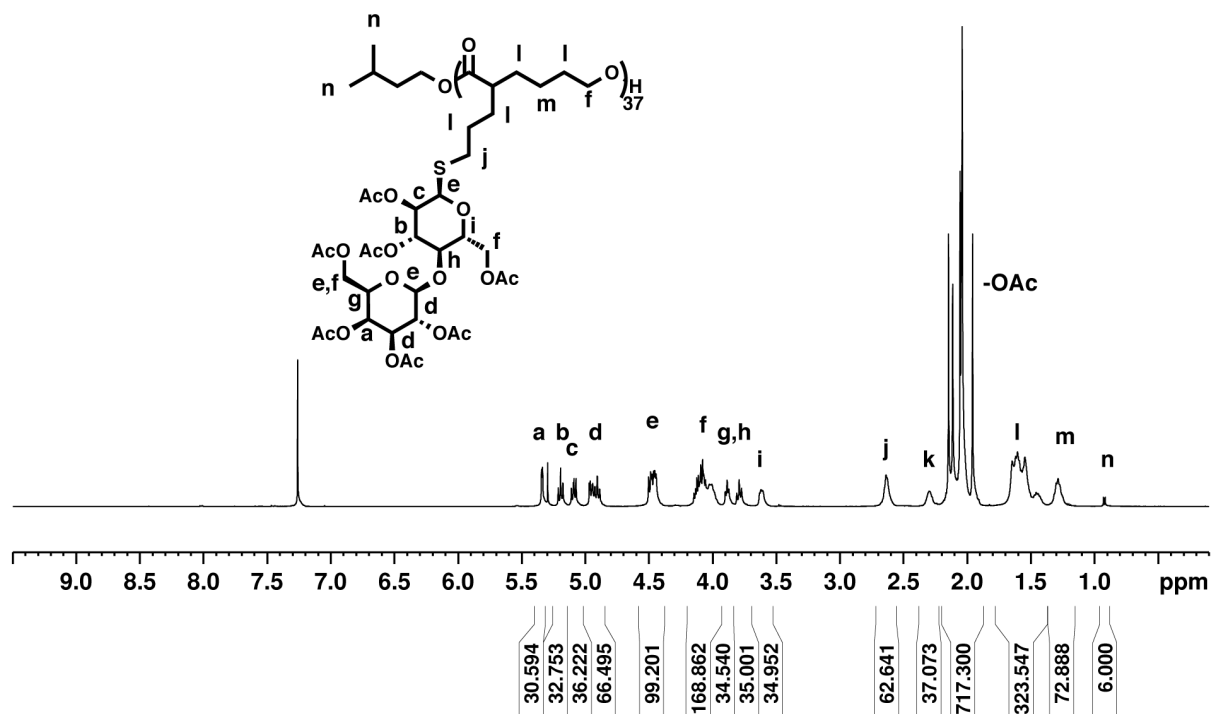


Figure 3-31. ¹H-NMR spectrum of pCL-lactoseOAc₄₀ (CDCl₃, 500 MHz). * = protons from terminal unit on polymer.

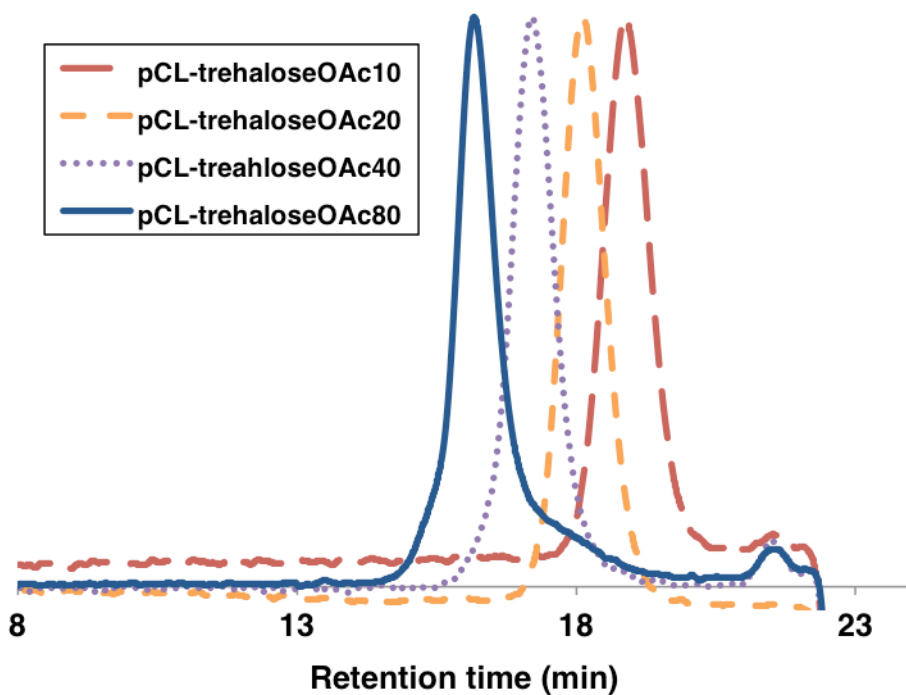


Figure 3-32. Gel permeation chromatograms of pCL-trehaloseOAc₁₀, pCL-trehaloseOAc₂₀, pCL-trehaloseOAc₄₀, pCL-trehaloseOAc₈₀.

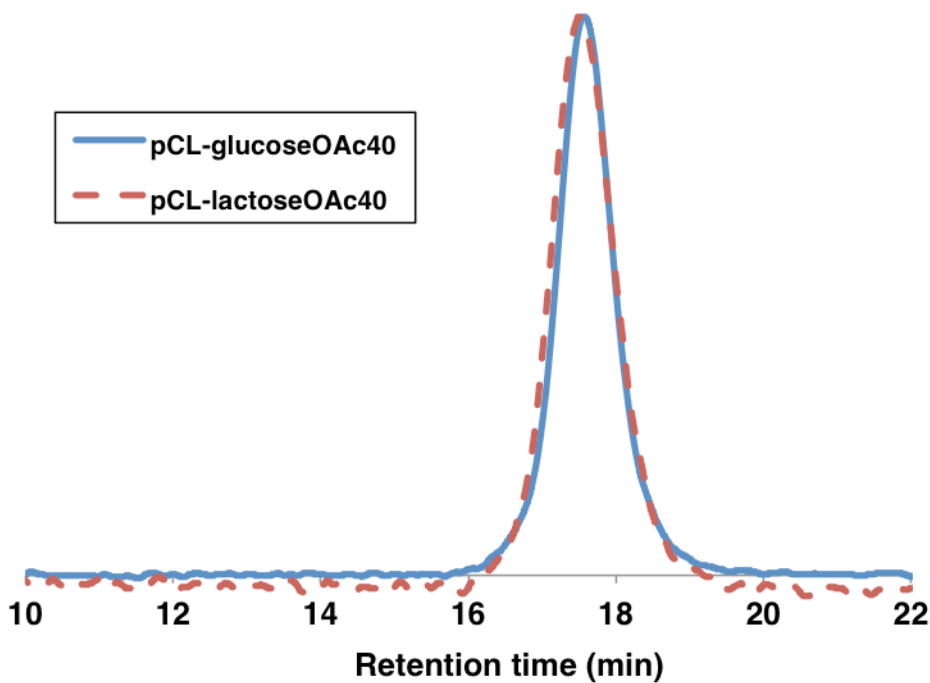


Figure 3-33. Gel permeation chromatograms of pCL-glucoseOAc₄₀, pCL-lactoseOAc₄₀.

Characterization of Substituted pCL Polymers

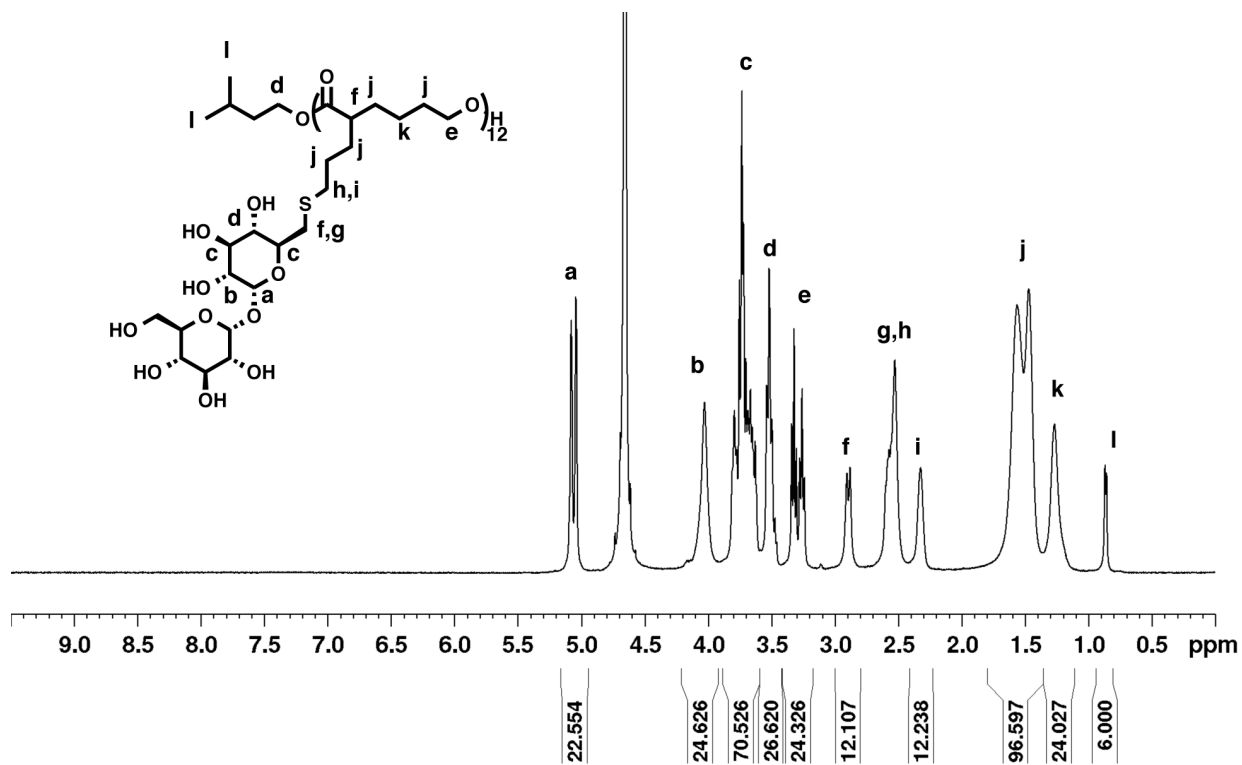


Figure 3-34. ¹H-NMR spectrum of pCL-trehalose₁₀ (D₂O, 500 MHz).

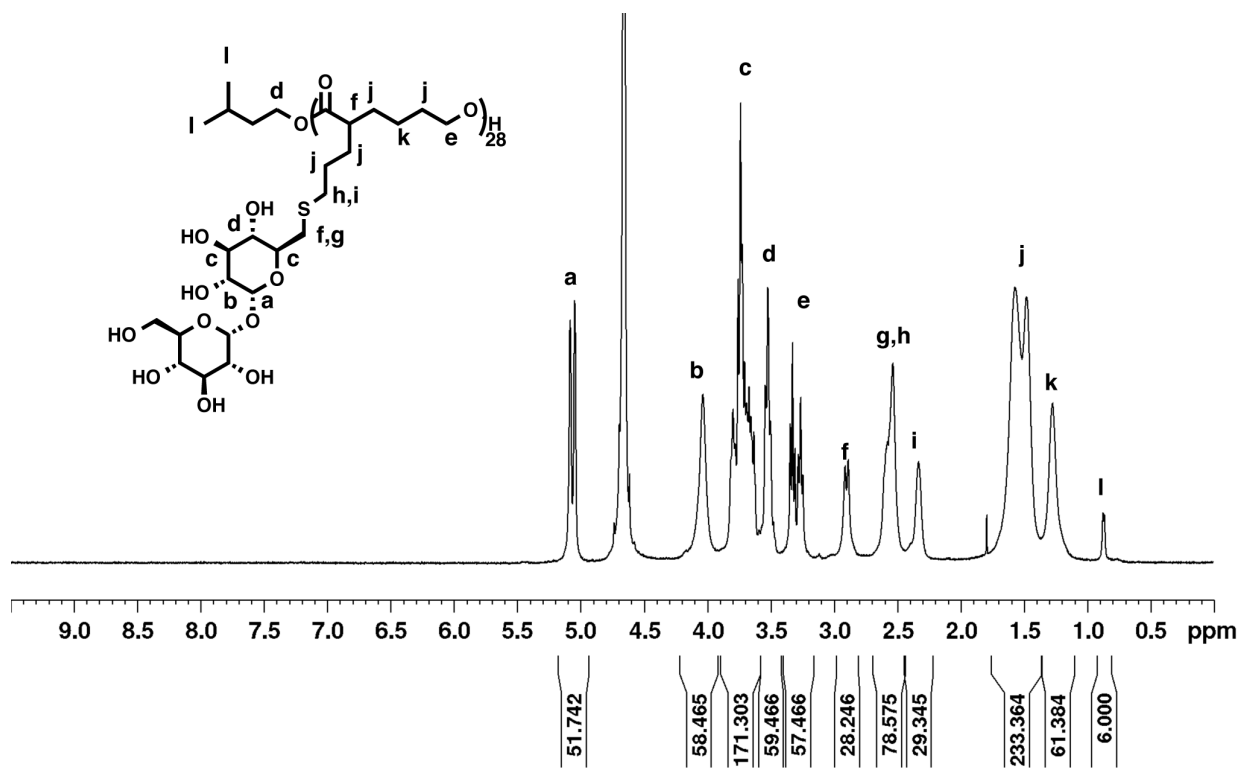


Figure 3-35. ¹H-NMR spectrum of pCL-trehalose₂₀ (D₂O, 500 MHz).

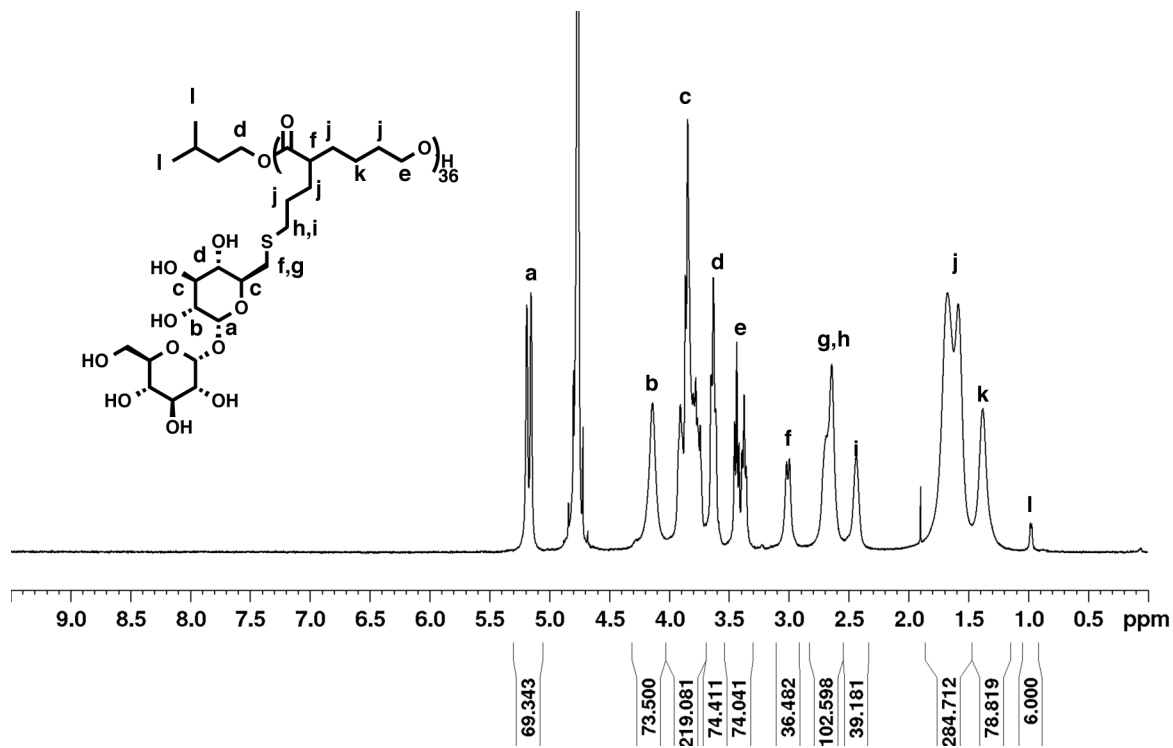


Figure 3-36. ¹H-NMR spectrum of pCL-trehalose₄₀ (D₂O, 500 MHz).

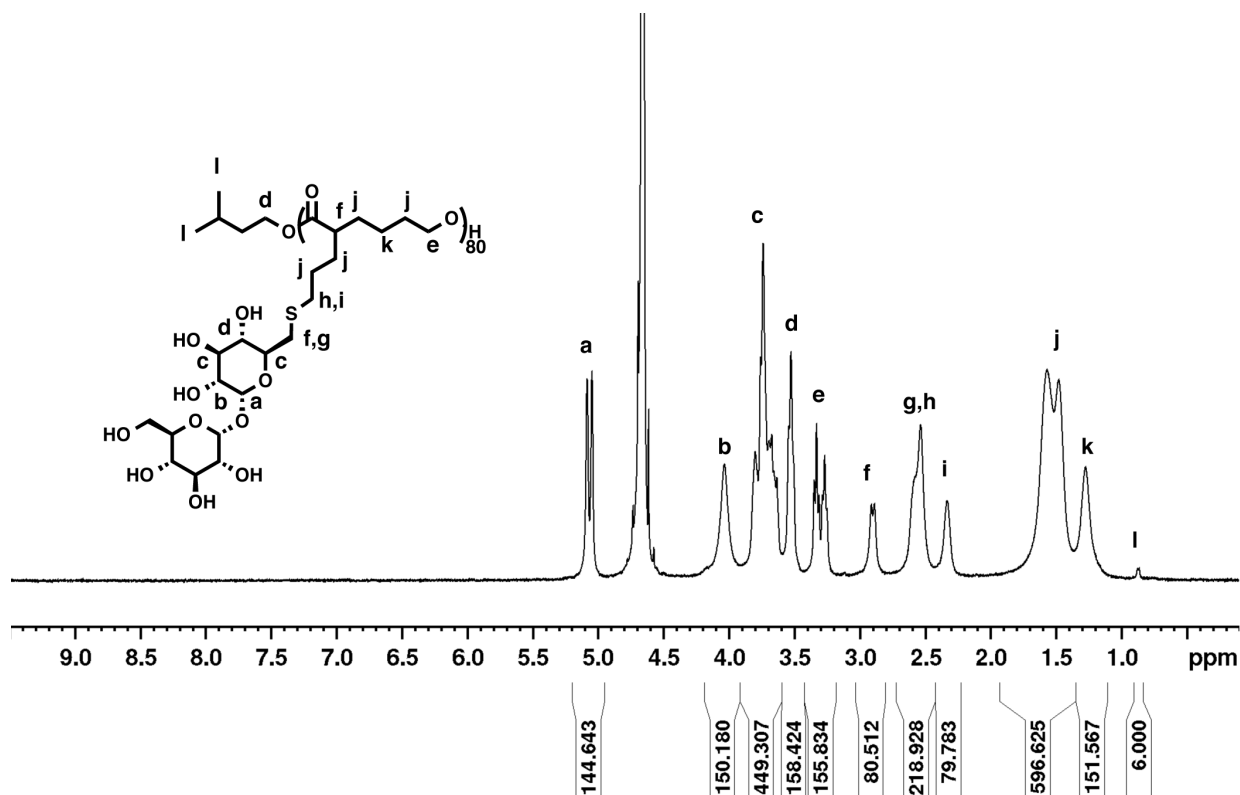


Figure 3-37. ¹H-NMR spectrum of pCL-trehalose₈₀ (D₂O, 500 MHz).

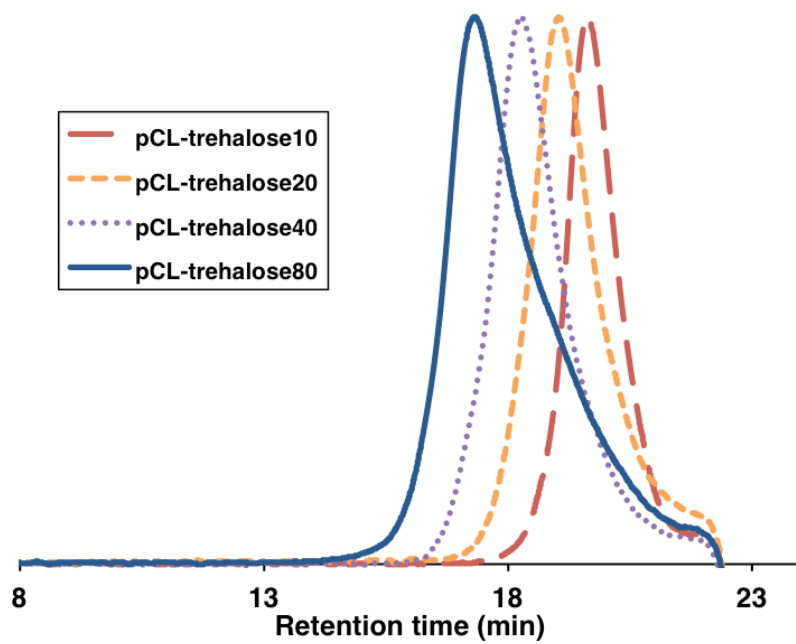


Figure 3-38. Gel permeation chromatograms of pCL-trehalose₁₀, pCL-trehalose₂₀, pCL-trehalose₄₀, pCL-trehalose₈₀.

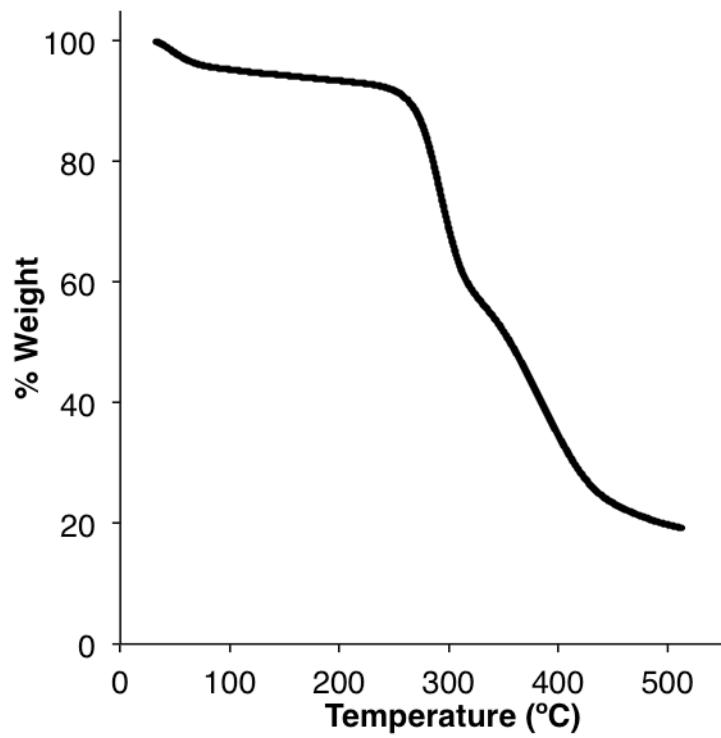


Figure 3-39. Thermal gravimetric analysis (TGA) chromatogram of pCL-trehalose₂₀.

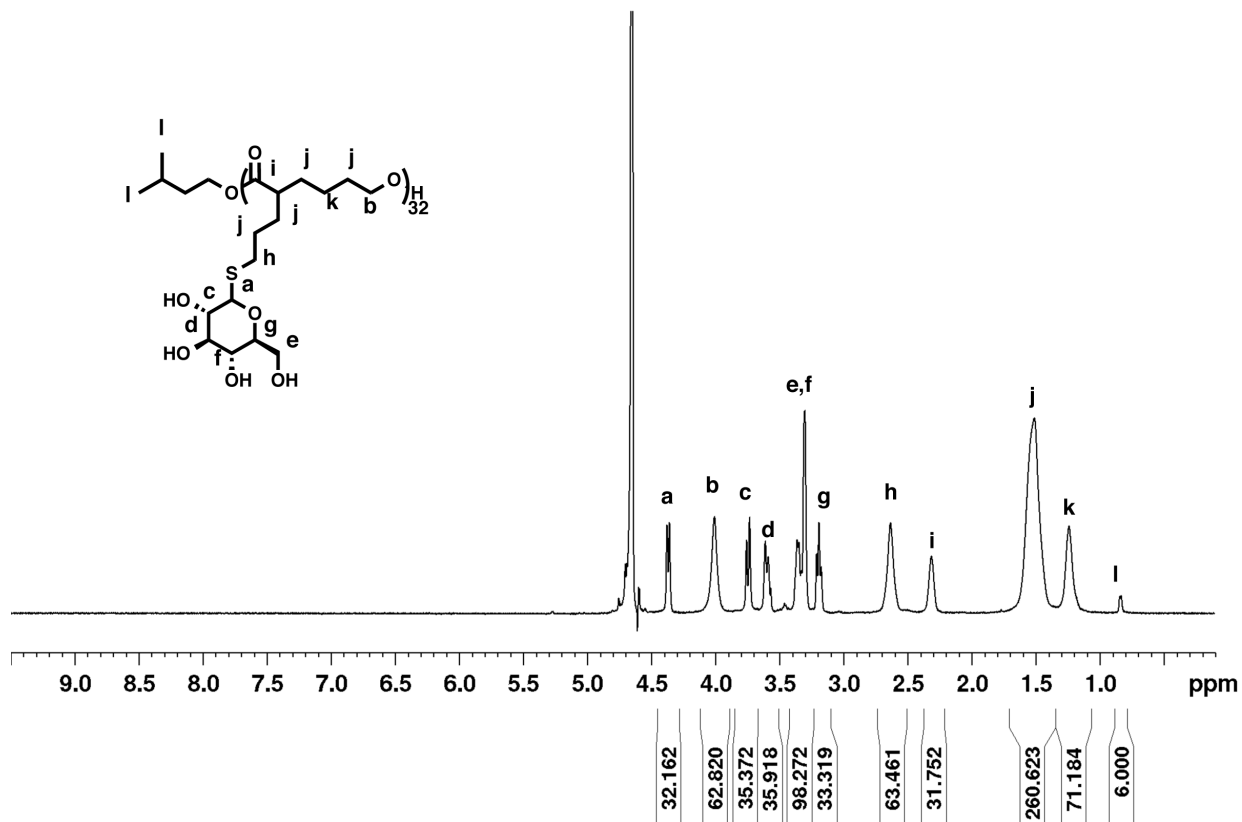


Figure 3-40. $^1\text{H-NMR}$ spectrum of pCL-glucose₄₀ (D_2O , 500 MHz).

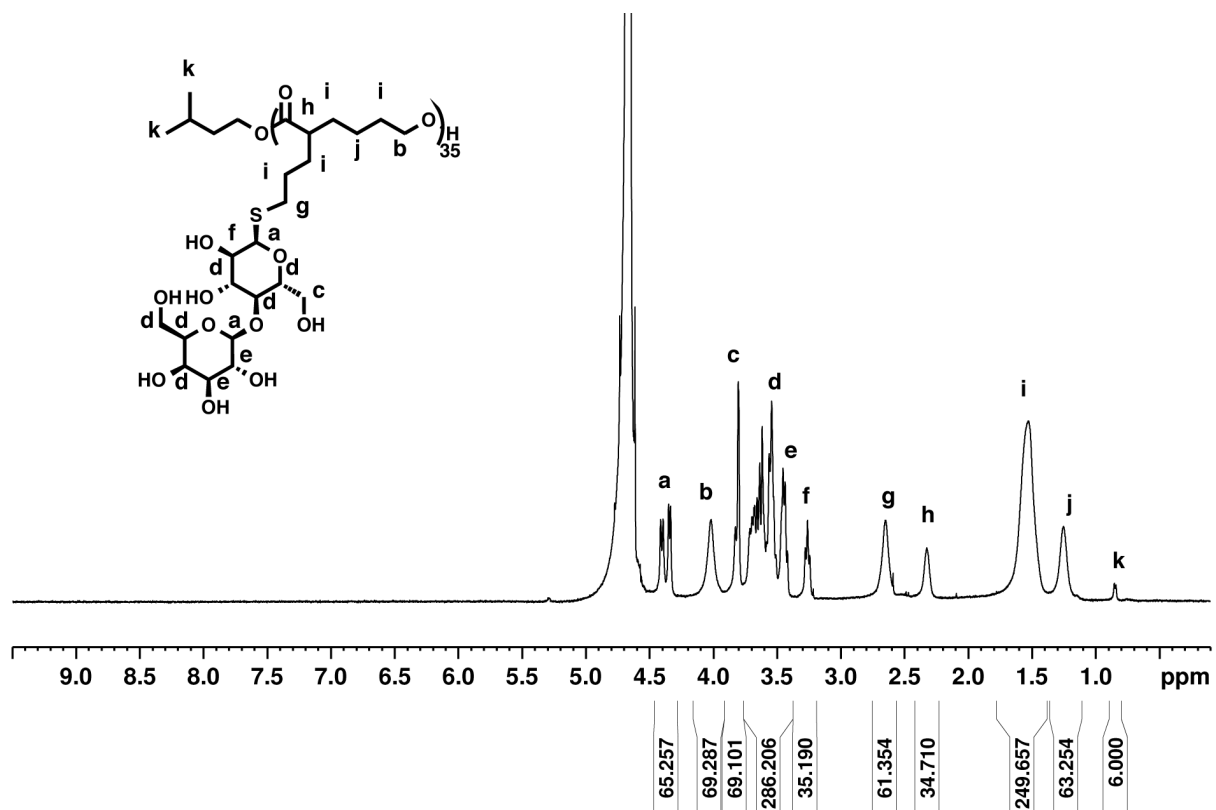


Figure 3-41. ¹H-NMR spectrum of pCL-lactose₄₀ (D₂O, 500 MHz).

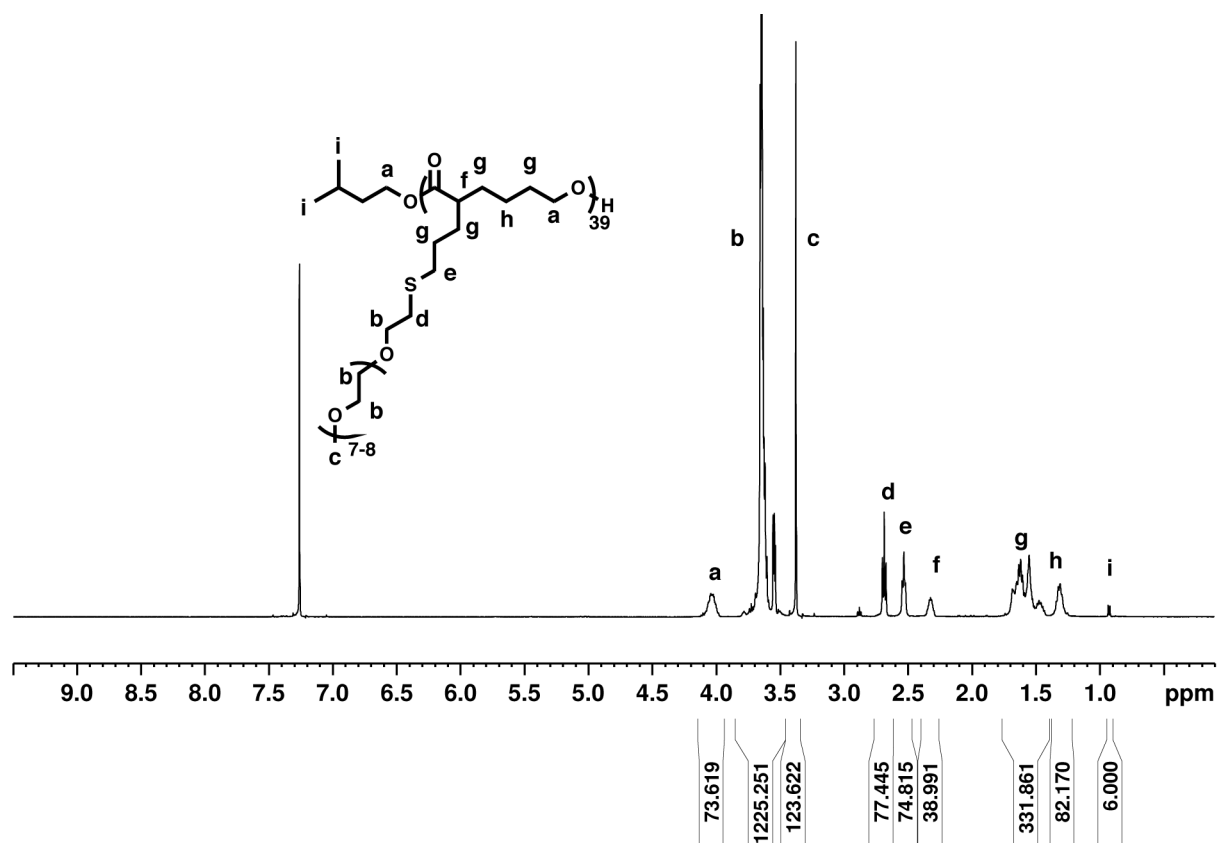


Figure 3-42. ¹H-NMR spectrum of pCL-PEG₄₀ (CDCl₃, 500 MHz).

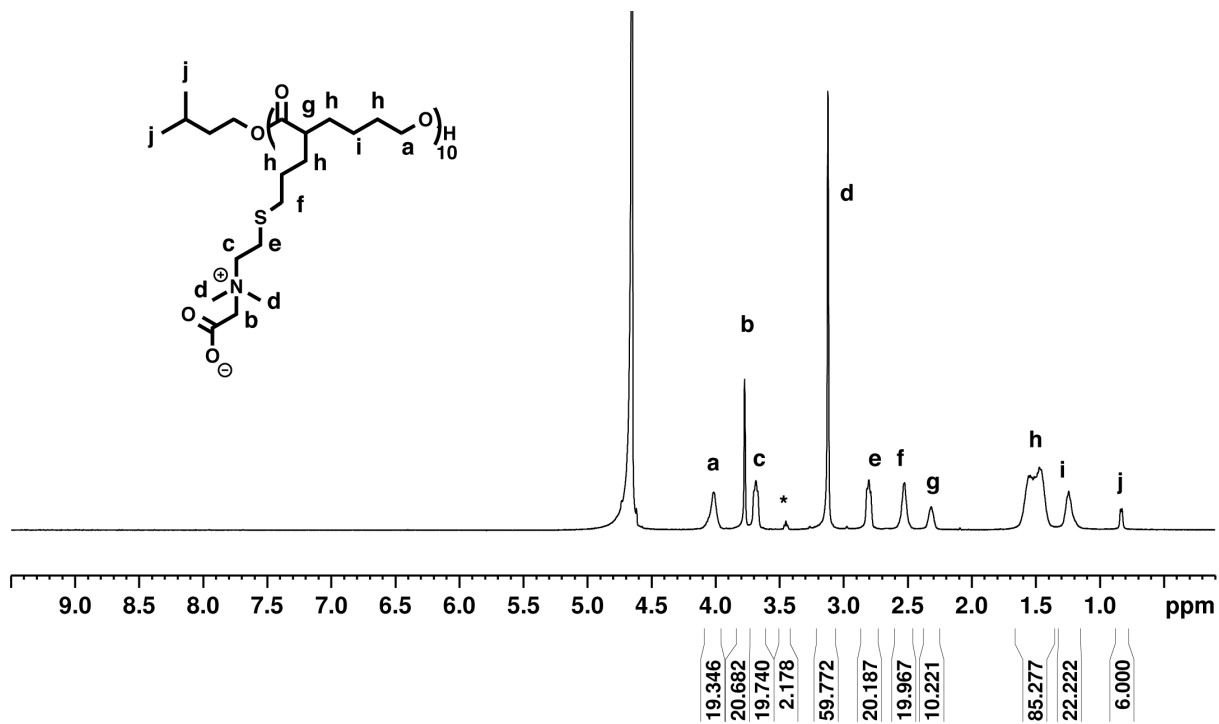


Figure 3-43. ^1H -NMR spectrum of pCL-zwitterion₁₀ (D_2O , 500 MHz). * = protons from terminal unit on polymer.

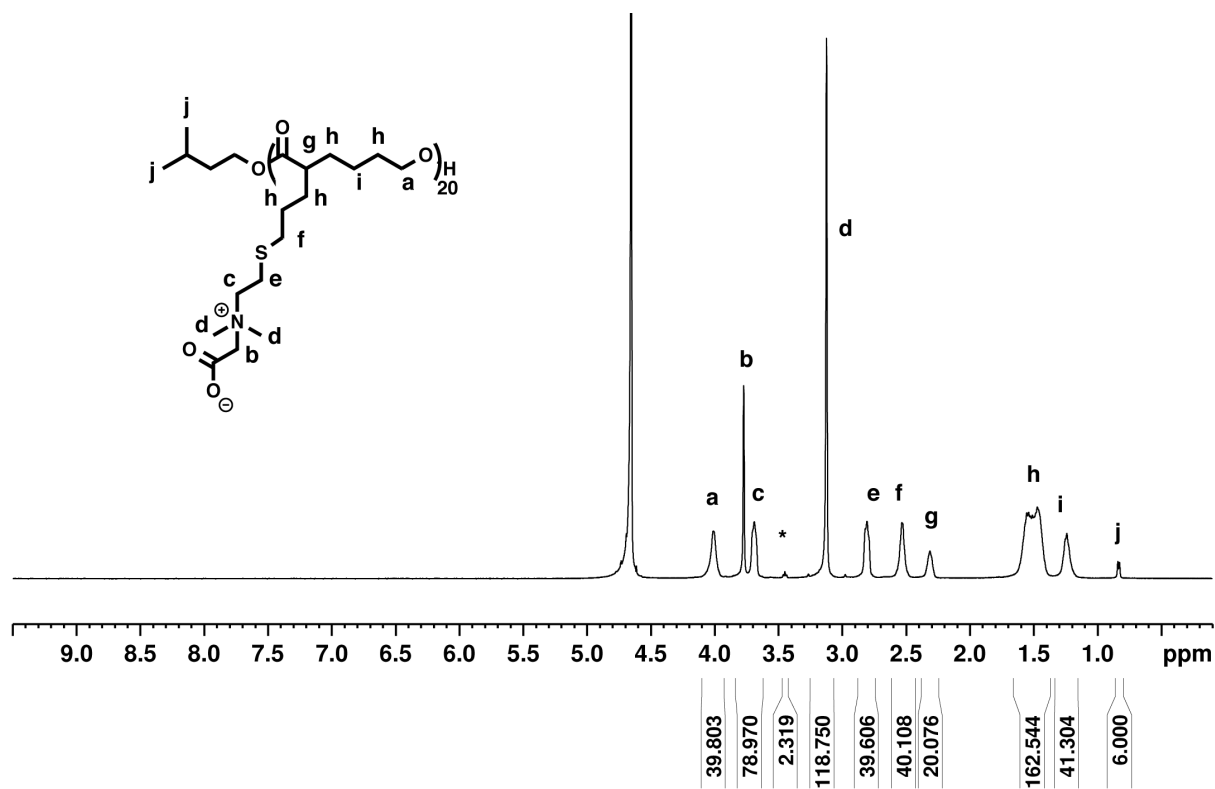


Figure 3-44. ¹H-NMR spectrum of pCL-zwitterion₂₀ (D₂O, 500 MHz). * = protons from terminal unit on polymer.

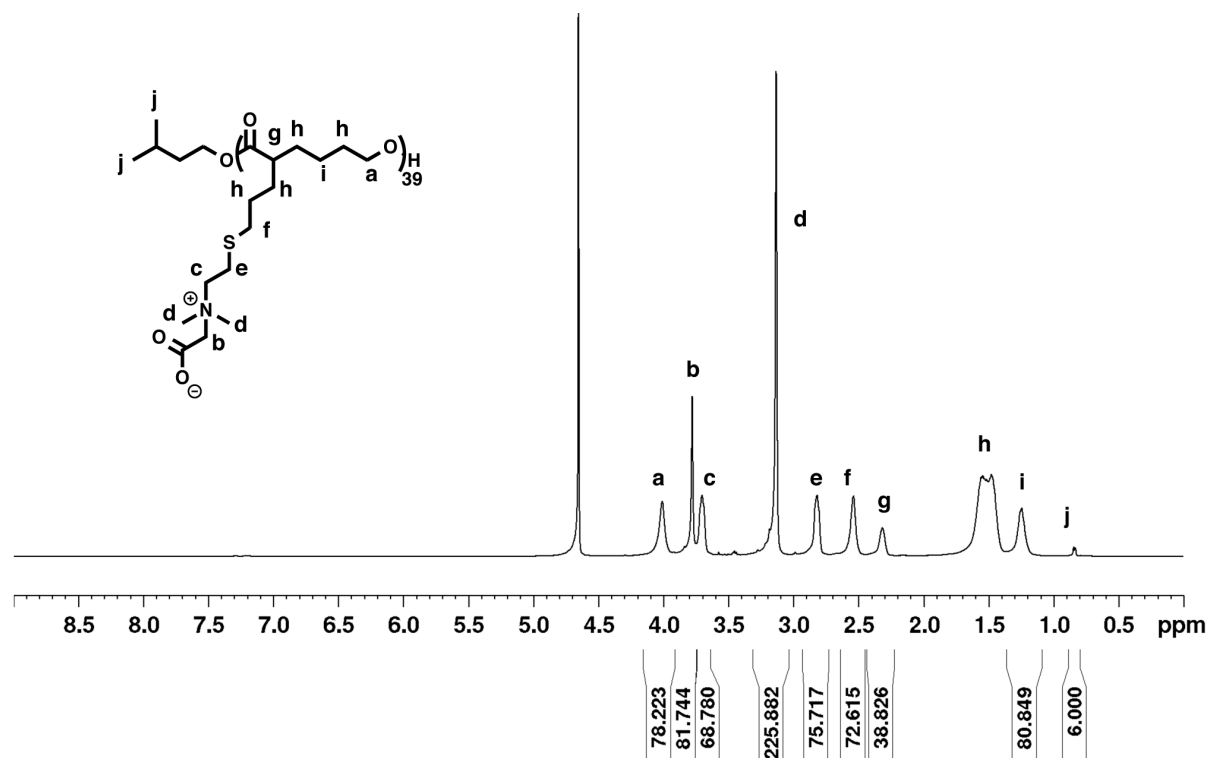


Figure 3-45. ¹H-NMR spectrum of pCL-zwitterion₄₀ (D₂O, 500 MHz).

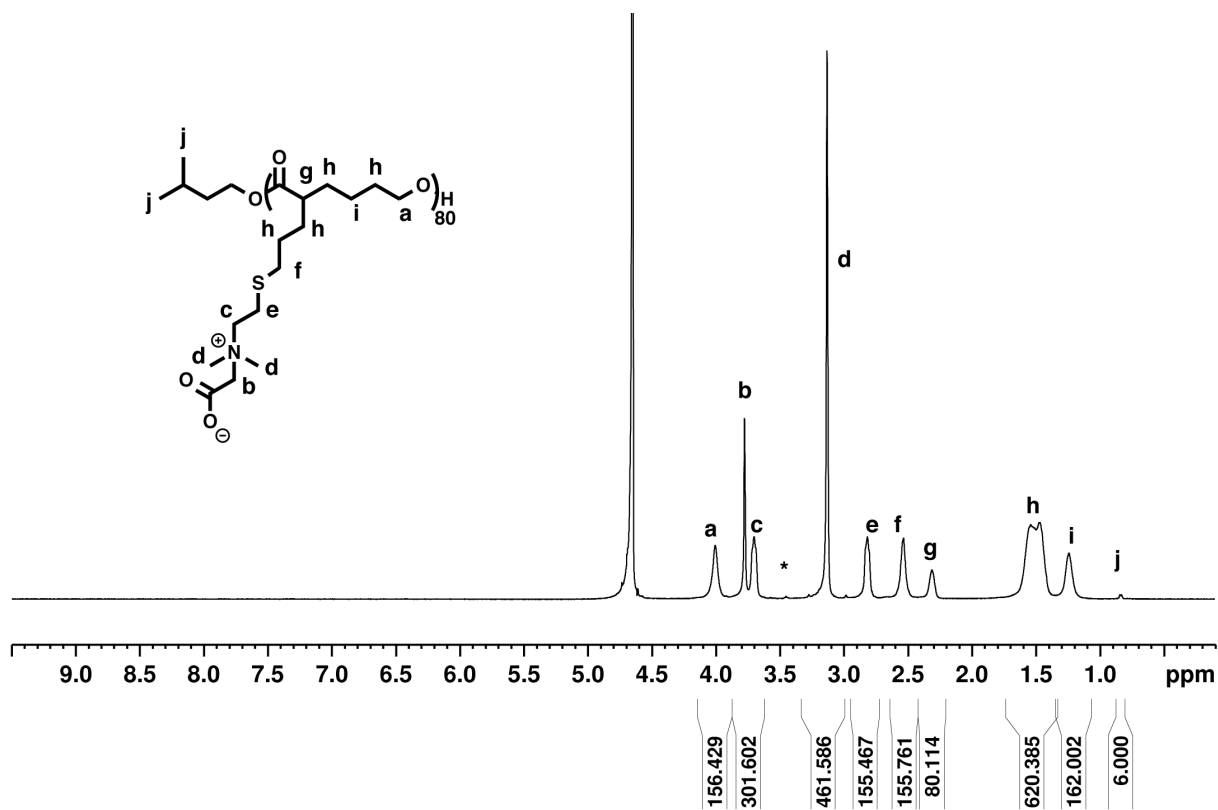


Figure 3-46. ¹H-NMR spectrum of pCL-zwitterion₈₀ (D₂O, 500 MHz). * = protons from terminal unit on polymer.

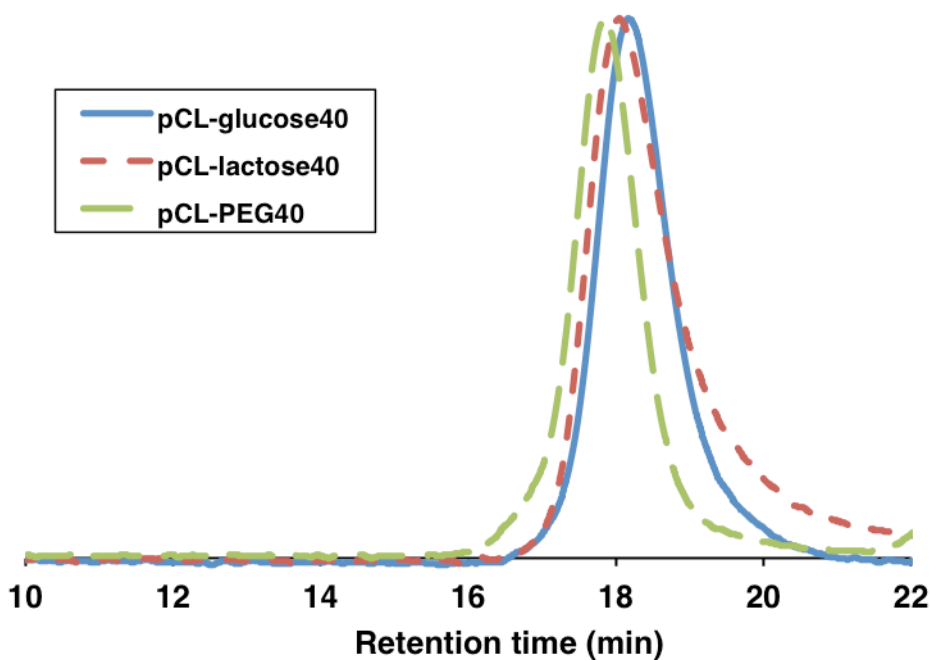


Figure 3-47. Gel permeation chromatograms of pCL-glucose₄₀, pCL-lactose₄₀, pCL-PEG₄₀.

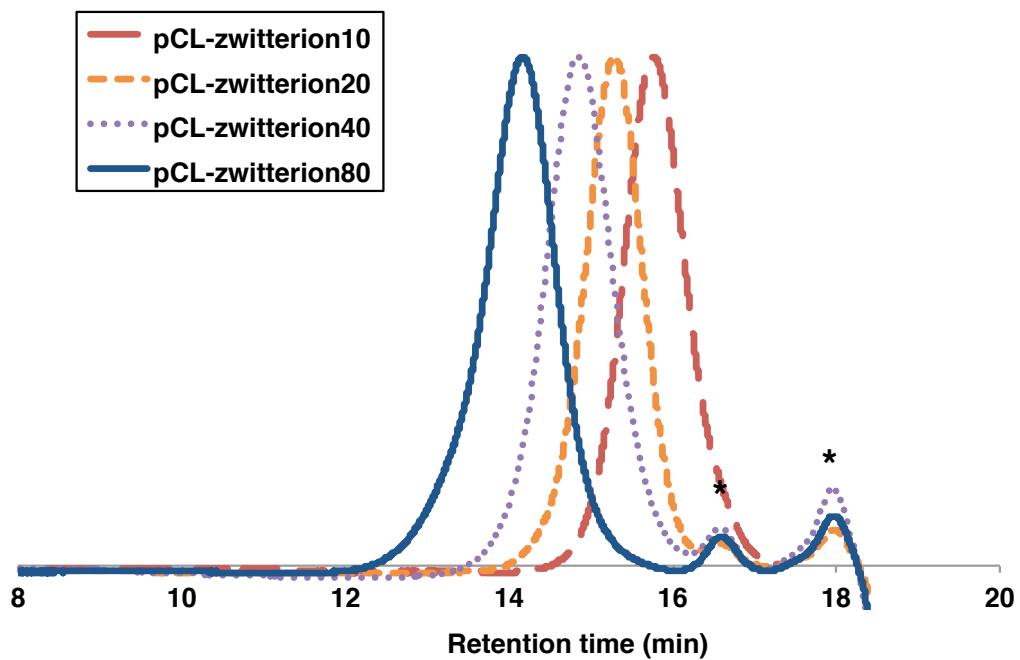


Figure 3-48. Size exclusion chromatograms of pCL-zwitterion₁₀, pCL-zwitterion₂₀, pCL-zwitterion₄₀, pCL-zwitterion₈₀. Peaks due to salts in the buffer indicated with *.

3.7. References

1. This chapter has been previously published as Pelegri-O'Day, E.M.; Paluck, S.J.; Maynard, H.D. *J. Am. Chem. Soc.*, **139**, 1145.
2. Maity, H.; O'Dell, C.; Srivastava, A.; Goldstein, J., *Curr. Pharm. Biotechnol.* **2009**, *10*, 761.
3. Bischof, J. C.; He, X. M. *Ann. N. Y. Acad. Sci.* **2005**, *1066*, 12.
4. Pikal-Cleland, K. A.; Carpenter, J. F., *J. Pharm. Sci.* **2001**, *90*, 1255.
5. Sluzky, V.; Tamada, J. A.; Klibanov, A. M.; Langer, R., *Proc. Natl. Acad. Sci. U. S. A.* **1991**, *88*, 9377.
6. Kamerzell, T. J.; Esfandiary, R.; Joshi, S. B.; Middaugh, C. R.; Volkin, D. B., *Adv. Drug Deliv. Rev.* **2011**, *63*, 1118.
7. Arakawa, T.; Timasheff, S. N., *Biophys. J.* **1985**, *47*, 411.
8. Falconer, R. J.; Chan, C.; Hughes, K.; Munro, T. P., *J. Chem. Technol. Biotechnol.* **2011**, *86*, 942.
9. Arakawa, T.; Tsumoto, K.; Kita, Y.; Chang, B.; Ejima, D., *Amino Acids* **2007**, *33*, 587.
10. Chen, B.; Bautista, R.; Yu, K.; Zapata, G. A.; Mulkerrin, M. G.; Chamow, S. M., *Pharm. Res.* **2003**, *20*, 1952.
11. Fang, W.-J.; Qi, W.; Kinzell, J.; Prestrelski, S.; Carpenter, J. F., *Pharm. Res.* **2012**, *29*, 3278.
12. Garzon-Rodriguez, W.; Koval, R. L.; Chongprasert, S.; Krishnan, S.; Randolph, T. W.; Warne, N. W.; Carpenter, J. F., *J. Pharm. Sci.* **2004**, *93*, 684.
13. Montaperto, A. G.; Gandhi, M. A.; Gashlin, L. Z.; Symoniak, M. R., *Curr. Med. Res. Opin.* **2016**, *32*, 155.

14. Martin, N.; Ma, D.; Herbet, A.; Boquet, D.; Winnik, F. M.; Tribet, C., *Biomacromolecules* **2014**, *15*, 2952.
15. Lee, E.-H.; Tsujimoto, T.; Uyama, H.; Sung, M.-H.; Kim, K.; Kuramitsu, S., *Polym. J.* **2010**, *42*, 818.
16. Izaki, S.; Kurinomaru, T.; Handa, K.; Kimoto, T.; Shiraki, K., *J. Pharm. Sci.* **2015**, *104*, 2457.
17. Gombotz, W. R.; Pankey, S. C.; Phan, D.; Drager, R.; Donaldson, K.; Antonsen, K. P.; Hoffman, A. S.; Raff, H. V., *Pharm. Res.* **1994**, *11*, 624.
18. Stidham, S. E.; Chin, S. L.; Dane, E. L.; Grinstaff, M. W., *J. Am. Chem. Soc.* **2014**, *136*, 9544.
19. Taluja, A.; Bae, Y. H., *Mol. Pharmaceutics* **2007**, *4*, 561.
20. Mazzaferro, L.; Breccia, J. D.; Andersson, M. M.; Hitzmann, B.; Hatti-Kaul, R., *Int. J. Biol. Macromol.* **2010**, *47*, 15.
21. Andersson, M. A.; Hatti-Kaul, R., *J. Biotechnol.* **1999**, *72*, 21.
22. Nguyen, T. H.; Kim, S.-H.; Decker, C. G.; Wong, D. Y.; Loo, J. A.; Maynard, H. D., *Nat. Chem.* **2013**, *5*, 221.
23. Matsusaki, M.; Serizawa, T.; Kishida, A.; Akashi, M., *Biomacromolecules* **2005**, *6*, 400.
24. Keefe, A. J.; Jiang, S., *Nat. Chem.* **2012**, *4*, 59.
25. Yoshimoto, N.; Hashimoto, T.; Felix, M. M.; Umakoshi, H.; Kuboi, R., *Biomacromolecules* **2003**, *4*, 1530.
26. Mancini, R. J.; Lee, J.; Maynard, H. D., *J. Am. Chem. Soc.* **2012**, *134*, 8474.
27. Lee, J.; Lin, E.-W.; Lau, U. Y.; Hedrick, J. L.; Bat, E.; Maynard, H. D., *Biomacromolecules* **2013**, *14*, 2561.

28. Wada, M.; Miyazawa, Y.; Miura, Y., *Polym. Chem.* **2011**, *2*, 1822.
29. Srinivasachari, S.; Liu, Y.; Zhang, G.; Prevette, L.; Reineke, T. M., *J. Am. Chem. Soc.* **2006**, *128*, 8176.
30. Hershfield, M. S.; Ganson, N. J.; Kelly, S. J.; Scarlett, E. L.; Jagers, D. A.; Sundy, J. S., *Arthritis Res. Ther.* **2014**, *16*, R63.
31. Armstrong, J. K.; Hempel, G.; Kolling, S.; Chan, L. S.; Fisher, T.; Meiselman, H. J.; Garratty, G., *Cancer* **2007**, *110*, 103.
32. Rudmann, D. G.; Alston, J. T.; Hanson, J. C.; Heidel, S., *Toxicol. Pathol.* **2013**, *41*, 970.
33. Abraham, S. C.; Bhagavan, B. S.; Lee, L. A.; Rashid, A.; Wu, T. T., *Am. J. Surg. Pathol.* **2001**, *25*, 637.
34. Kerwin, B. A., *J. Pharm. Sci.* **2008**, *97*, 2924.
35. Pelegri-O'Day, E. M.; Lin, E. W.; Maynard, H. D., *J. Am. Chem. Soc.* **2014**, *136*, 14323.
36. Pelegri-O'Day, E. M.; Maynard, H. D., *Acc. Chem. Res.* **2016**, *49*, 1777.
37. Taniguchi, I.; Mayes, A. M.; Chan, E. W. L.; Griffith, L. G., *Macromolecules* **2005**, *38*, 216.
38. Parrish, B.; Quansah, J. K.; Emrick, T., *J. Polym. Sci., Part A: Polym. Chem.* **2002**, *40*, 1983.
39. Parrish, B.; Breitenkamp, R. B.; Emrick, T., *J. Am. Chem. Soc.* **2005**, *127*, 7404.
40. Lowe, A. B., *Polym. Chem.* **2010**, *1*, 17.
41. Hoyle, C. E.; Bowman, C. N., *Angew. Chem. Int. Ed.* **2010**, *49*, 1540.
42. Pratt, R. C.; Lohmeijer, B. G. G.; Long, D. A.; Waymouth, R. M.; Hedrick, J. L., *J. Am. Chem. Soc.* **2006**, *128*, 4556.

43. Lohmeijer, B. G. G.; Pratt, R. C.; Leibfarth, F.; Logan, J. W.; Long, D. A.; Dove, A. P.; Nederberg, F.; Choi, J.; Wade, C.; Waymouth, R. M.; Hedrick, J. L., *Macromolecules* **2006**, *39*, 8574.
44. Silvers, A. L.; Chang, C.-C.; Emrick, T., *J. Polym. Sci., Part A: Polym. Chem.* **2012**, *50*, 3517.
45. Kamber, N. E.; Jeong, W.; Waymouth, R. M.; Pratt, R. C.; Lohmeijer, B. G. G.; Hedrick, J. L., *Chem. Rev.* **2007**, *107*, 5813.
46. Stevens, D. M.; Watson, H. A.; LeBlanc, M.-A.; Wang, R. Y.; Chou, J.; Bauer, W. S.; Harth, E., *Polym. Chem.* **2013**, *4*, 2470.
47. Campos, L. M.; Killops, K. L.; Sakai, R.; Paulusse, J. M. J.; Dameron, D.; Drockenmuller, E.; Messmore, B. W.; Hawker, C. J., *Macromolecules* **2008**, *41*, 7063.
48. Yu, M.; Yang, Y.; Han, R.; Zheng, Q.; Wang, L.; Hong, Y.; Li, Z.; Sha, Y., *Langmuir* **2010**, *26*, 8534.
49. Erdem, S. S.; Nesterova, I. V.; Soper, S. A.; Hammer, R. P., *J. Org. Chem.* **2009**, *74*, 9280.
50. Aoi, K.; Tsutsumiuchi, K.; Okada, M., *Macromolecules* **1994**, *27*, 875.
51. Takasu, A.; Kojima, H., *J. Polym. Sci., Part A: Polym. Chem.* **2010**, *48*, 5953.
52. Dong, C. M.; Faucher, K. M.; Chaikof, E. L., *J. Polym. Sci., Part A: Polym. Chem.* **2004**, *42*, 5754.
53. Takasu, A.; Houjyou, T.; Inai, Y.; Hirabayashi, T., *Biomacromolecules* **2002**, *3*, 775.
54. Cao, Z.; Yu, Q.; Xue, H.; Cheng, G.; Jiang, S., *Angew. Chem. Int. Ed.* **2010**, *49*, 3771.

55. Aapro, M. S.; Cameron, D. A.; Pettengell, R.; Bohlius, J.; Crawford, J.; Ellis, M.; Kearney, N.; Lyman, G. H.; Tjan-Heijnen, V. C.; Walewski, J.; Weber, D. C.; Zielinski, C.; Eortc, G. C., *Eur. J. Cancer* **2006**, *42*, 2433.
56. Krishnan, S.; Chi, E. Y.; Webb, J. N.; Chang, B. S.; Shan, D. X.; Goldenberg, M.; Manning, M. C.; Randolph, T. W.; Carpenter, J. F., *Biochemistry* **2002**, *41*, 6422.
57. Shirafuji, N.; Asano, S.; Matsuda, S.; Watari, K.; Takaku, F.; Nagata, S., *Exper. Hematol.* **1989**, *17*, 116.
58. Wu, J.; Zhao, C.; Lin, W.; Hu, R.; Wang, Q.; Chen, H.; Li, L.; Chen, S.; Zheng, J., *J. Mater. Chem. B* **2014**, *2*, 2983.
59. Jayaraman, S.; Gantz, D. L.; Gursky, O., *Biochemistry* **2004**, *43*, 5520.
60. Young, D. ISTA Temperature Project- Data Summary; International Safe Transit Association: East Lansing, MI, 2002
61. Katyal, N.; Deep, S., *Phys. Chem. Chem. Phys.* **2014**, *16*, 26746.
62. Fedorov, M. V.; Goodman, J. M.; Nerukh, D.; Schumm, S., *Phys. Chem. Chem. Phys.* **2011**, *13*, 2294.
63. Lees, W. J.; Spaltenstein, A.; Kingerywood, J. E.; Whitesides, G. M., *J. Med. Chem.* **1994**, *37*, 3419.
64. Alebouyeh, M.; Tahzibi, A.; Yaghoobzadeh, S.; Zahedy, E. T.; Kiumarsi, S.; Soltanabad, M. H.; Shahbazi, S.; Amini, H., *Biologicals* **2016**, *44*, 150.
65. Woodruff, M. A.; Hutmacher, D. W., *Prog. Polym. Sci.* **2010**, *35*, 1217.
66. Regev, O.; Zana, R., *J. Colloid Interface Sci.* **1999**, *210*, 8.
67. Leader, B.; Baca, Q. J.; Golan, D. E., *Nat. Rev. Drug Discov.* **2008**, *7*, 21.

68. Pan, B.; Abel, J.; Ricci, M. S.; Brems, D. N.; Wang, D. I. C.; Trout, B. L., *Biochemistry* **2006**, *45*, 15430.
69. Yin, J.; Chu, J. W.; Ricci, M. S.; Brems, D. N.; Wang, D. I. C.; Trout, B. L., *Pharm. Res.* **2005**, *22*, 141.
70. Ohtake, S.; Wang, Y. J., *J. Pharm. Sci.* **2011**, *100*, 2020.
71. Chen, S. F.; Zheng, J.; Li, L. Y.; Jiang, S. Y., *J. Am. Chem. Soc.* **2005**, *127*, 14473.
72. Shao, Q.; Jiang, S. Y., *Adv. Mater.* **2015**, *27*, 15.
73. Niven, R. W.; Prestrelski, S. J.; Treuheit, M. J.; Ip, A. Y.; Arakawa, T., *Int. J. Pharm.* **1996**, *127*, 191.
74. Bruzdziak, P.; Panuszko, A.; Stangret, J., *J. Phys. Chem. B* **2013**, *117*, 11502.
75. Street, T. O.; Bolen, D. W.; Rose, G. D., *Proc. Natl. Acad. Sci. U. S. A.* **2006**, *103*, 13997.
76. Bezwada, R. S.; Jamiolkowski, D. D.; Lee, I. Y.; Agarwal, V.; Persivale, J.; Trenkabethin, S.; Ernetta, M.; Suryadevara, J.; Yang, A.; Liu, S., *Biomaterials* **1995**, *16*, 1141.
77. Bat, E.; Lee, J.; Lau, U. Y.; Maynard, H. D., *Nat. Commun.* **2015**, *6*.
78. Caliceti, P.; Veronese, F. M., *Adv. Drug Deliv. Rev.* **2003**, *55*, 1261.
79. Shu, P.; Zeng, J.; Tao, J.; Zhao, Y.; Yao, G.; Wan, Q., *Green Chem.* **2015**, *17*, 2545.
80. Lau, U. Y.; Pelegri-O'Day, E. M.; Maynard, H. D., *Macromol. Rapid Commun.* **2018**, *39*.

Chapter 4

Polymers with Tunable Degradability and Zwitterionic or Trehalose Side Chains via Ring-Opening Polymerization

4.1. Introduction

The current state-of-the-art polymer for biological applications is poly(ethylene glycol) (PEG), which is widely used in drug formulation and conjugation. PEG is used because of its inert backbone, amphiphilic nature, and its nonfouling properties. However, in the human population, PEG antibodies are present prior to and during therapeutic administration¹⁻², with subsequent deleterious effects such as accelerating blood clearance³, and allergic reactions⁴, and a growing body of work corroborates the immunogenicity of this polymer.⁵ Furthermore, PEG is non-biodegradable which can lead to bioaccumulation and the formation of vacuoles.⁶ As a result, there is significant interest in developing novel polymers as PEG replacements that are biodegradable, present reduced immunogenicity, and can offer protein-stabilization properties, especially for protein-replacement therapeutics⁷⁻⁹. We described the synthesis and biological evaluation of novel stabilizing polymers with hydrophobic polyester backbones in Chapter 3.¹⁰ These polycaprolactone-based materials exhibited excellent protein-stabilizing properties, degraded through ester hydrolysis, and were non-cytotoxic both before and after degradation. However, the hydrophobic backbone of these non-ionic surfactants, which we hypothesized was important for their stabilizing properties, resulted in slow degradation at physiological pH.

Tunable and precise degradability is important for biomaterials, and there have been extensive studies of widely-used and FDA-approved polyesters such as polycaprolactone (pCL), poly(lactide-co-glycolide) and copolymers thereof.¹¹⁻¹² However, these materials are not water-soluble and therefore often degrade via surface erosion, where water diffusion into the material is minimal compared to the rate of polymer degradation.¹¹ There have been few studies that thoroughly investigate the tunable degradation of functional and water-soluble polymers. For example, Wurm and coworkers demonstrated that degradation rate of a series of

poly(phosphonate)s could be tuned from 4h to 6 days by adjusting the hydrophobicity and steric bulk of side chains.¹³ Polymers were then conjugated to bovine serum albumin (BSA) and detailed studies of the conjugate's hydrolytic stability were carried out at neutral, acidic, and basic pH.¹⁴ Shokrolahi and coworkers investigated the degradation of polyurethanes consisting of glycolide or caprolactone macroblocks, which exhibited variable degradation rate depending on macroblock composition.¹⁵ Chilkoti and coworkers described the preparation of water-soluble poly(carbonate) and polyphosphonate-based polymers for protein conjugation and described the polymeric degradation under neutral and enzymatic conditions.¹⁶ Alternatively, the degradable monomers cyclic ketene acetals (CKAs) can be incorporated into vinyl polymers at controlled ratios in order to target specific hydrolytic stabilities.¹⁷⁻¹⁹ And we recently showed that the hydrolytic stability of fluorinated BMDO-trehalose triblock copolymers could be tuned by adjusting the fluorine content of the polymers.²⁰ However, none of these materials are designed to have protein-stabilizing properties.

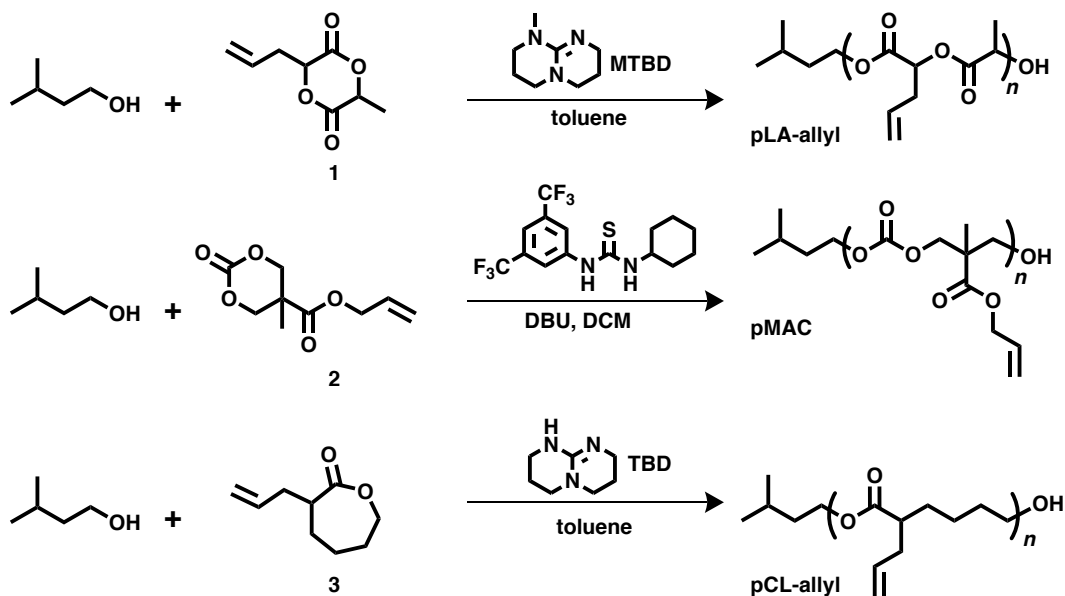
Herein we report the synthesis and evaluation of a series of trehalose- and zwitterionic polymers with tunable degradability that stabilize proteins. Poly(lactide) (pLA), poly(carbonate) (pC) and poly(caprolactone) (pCL)-based materials were polymerized using organocatalysis and modified using postpolymerization thiol-ene reactions in order to install stabilizing trehalose and carboxybetaine side chains onto the degradable backbones. The resulting polymers were characterized for their stability *in vitro*, with hydrolytic half-lives ranging from 12h to more than 4 months. We expect that these degradable and stabilizing polymers will be useful in a variety of biomedical applications.

4.2. Results and Discussion

4.2.1. Polymer Synthesis

We selected three well-characterized polymer backbones with degradation kinetics that were expected to vary significantly. Hydroxylated pLA has been reported to undergo substantial weight within 4 hours²¹, PEG-substituted analogs of carbonate monomer **2** degrade fully in 2 days¹⁶, and we have previously described that substituted and water-soluble pCL polymers are stable for up to 49 days in phosphate-buffered saline.¹⁰ Additionally, all of these polymers can be synthesized through controlled ring-opening polymerization, allowing for good control over dispersity and polymer molecular weight and enabling effective comparison between the polymeric backbones.²²⁻²⁴

A series of allylated polymers were synthesized at degrees of polymerization between 80 and 90 in order to effectively compare backbone identity (**Scheme 4-1**). Allyl lactide²⁵ (LA-allyl) **1** was synthesized as reported and polymerized using 7-methyl-1,5,7-triazabicyclo[4.4.0]dec-5-ene (MTBD).²² Methyl allyl carbonate (MAC) **2** was synthesized as previously described²⁶ and polymerized using 1-(3,5-bis(trifluoromethyl)phenyl)-3-cyclohexylthiourea²³ and 1,8-diazabicyclo[5.4.0]undec-7-ene (DBU). Allylated caprolactone (CL-allyl) **3** was synthesized using literature conditions²⁴ and polymerized using 1,5,7-triazabicyclo[4.4.0]dec-5-ene (TBD) as previously described.¹⁰ In all cases, 3-methyl-butanol was used as an initiator for ease of characterization due to its distinctive ¹H-NMR peaks at 0.92 ppm.²⁷



Scheme 4-1. Polymerization of allyl-functionalized lactide, carbonate, and caprolactone polymers.

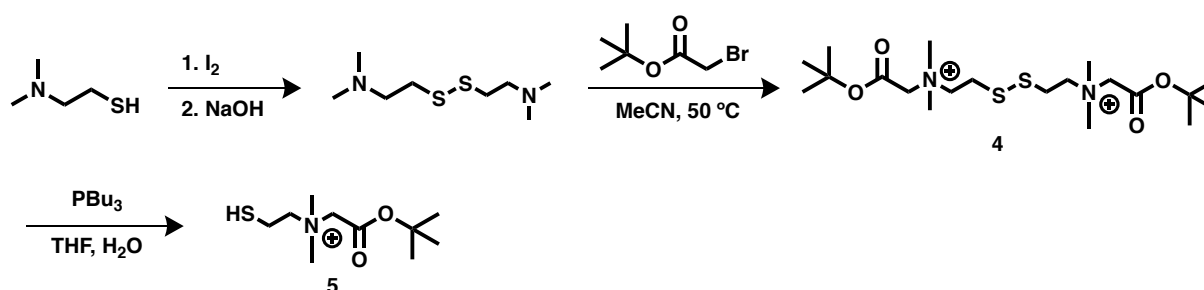
All polymers were characterized by $^1\text{H-NMR}$ and GPC and were shown to be between 80 and 100 DP, with molecular weights ($^1\text{H-NMR}$) varying between 12.3 and 15.4 kDa (**Table 4-1**). The dispersities (Đ) were all below 1.1, indicating that these polymers could be prepared with excellent control. A small high molecular weight shoulder was observed in pMAC, consistent with that previously observed at high [monomer]/[initiator] ratios and hypothesized to be due to undesired monomer self-initiation at high relative concentrations.²⁸

Table 4-1. Molecular weights and GPC data for allyl-functional polyesters and polycarbonates.

polymer	DP	Mn ($^1\text{H-NMR}$)	Mn (GPC) ^b	Đ ^b
pCL-allyl ^a	79	12 300	11 600	1.09
pMAC	75	15 500	20 900	1.09
pLA-allyl	77	13 200	24 100	1.03

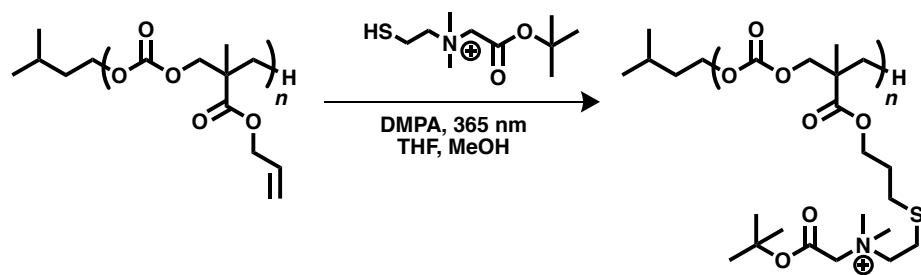
^a Prepared as in ref. 9. ^b Measured in DMF using PMMA standards.

We aimed to use our previously-described conditions (Chapter 3) to install stabilizing zwitterionic carboxybetaine to these polymers in order to prepare degradable protein-stabilizing polymers with tunable hydrolysis rates. These conditions involved installation of a tertiary amine salt onto the polymer backbone, followed by neutralization of the salt with sat. NaHCO₃ and subsequent quaternization using *tert*-butyl bromoacetate.¹⁰ However, polycarbonate (pC-*X*) and polylactide-based backbones (pLA-*X*) were less hydrolytically stable than previous caprolatone-based materials and were susceptible to hydrolysis and degradation upon exposure to the basic bicarbonate solution (data not shown). Therefore, a cationic thiol **5** was synthesized and used to modify the alkene-substituted polymers, avoiding treatment with base (Scheme 4-2).



Scheme 4-2. Synthesis of cationic thiol **5**.

Briefly, dimethylaminoethanethiol hydrochloride was reduced to form the disulfide and then neutralized with aqueous KOH to form tetramethyl cystamine before treating with *tert*-butyl bromoacetate to yield the bis-quaternary amine precursor **4**. The resulting disulfide was then reduced with tributylphosphine to yield cationic thiol **5** that could be used to modify alkene-functional polymers in thiol-ene reactions.



Scheme 4-3. Synthesis of pCB-zwitterion and pLA-zwitterion using zwitterionic thiol **5**.

Both the pC and pLA backbone were then subjected to photoinitiated thiol-ene modification with precursor **5** (**Scheme 4-3**). The polymers with *tert*-butyl ester protecting groups were organic-soluble and could be purified by dialysis in MeOH before removal of the *tert*-butyl esters using dry TFA. After purification, complete conversion to the zwitterion was observed by $^1\text{H-NMR}$ and GPC (**Figure 4-11** and **Figure 4-15**). For the pLA-zwitterion, minimal material was recovered after dialysis purification. At first, it was hypothesized that the backbone was unstable to the TFA deprotection. However, the unsubstituted polymer backbone was tested for stability against acidic conditions and no backbone scission was observed (**Figure 4-1**). It was hypothesized that the material was lost during dialysis purification due to the hydrolytic instability imparted by the water-soluble side chains. Therefore, a different method of purification employing the crosslinked dextran gel Sephadex was undertaken to quickly remove excess thiol and other small-molecule contaminants from the pLA-*X* polymers before lyophilization of the polymer solution to avoid backbone degradation.

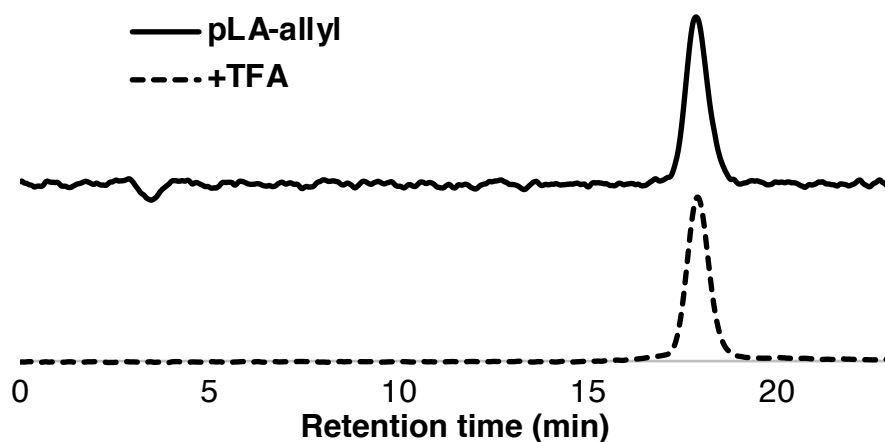
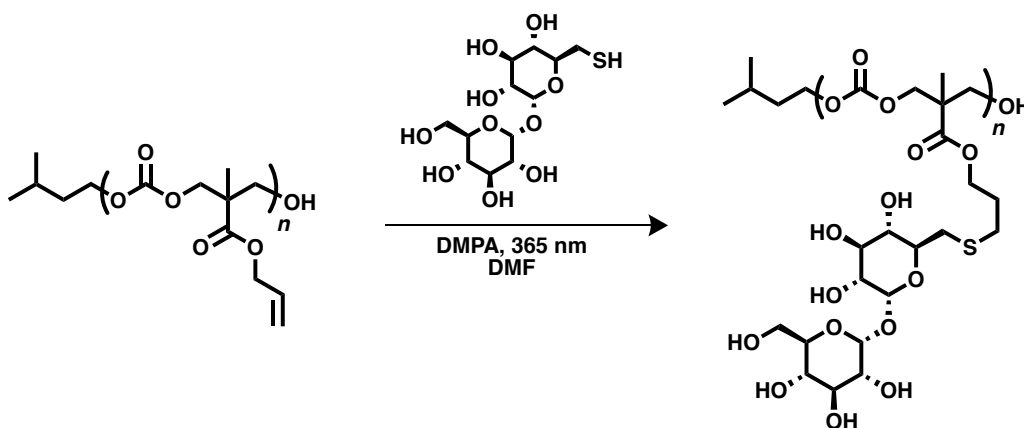


Figure 4-1. Stability of pLA-allyl after TFA treatment as measured by GPC.

For modification of pC and pLA backbones with trehalose, this was initially undertaken as previously described for the polycaprolactone backbone (Chapter 3),¹⁰ with installation of the acetate-protected disaccharide and subsequent deprotection. However, cleavage of the acetate esters using either H_2NNH_2 or K_2CO_3 resulted in hydrolysis and degradation of the resulting polymer, again due to the hydrolytic instability of these backbones. Instead, an unprotected thiolated trehalose was directly installed onto the alkene-substituted polymer. This was undertaken in DMF to solubilize both the polymer and thiolated trehalose (**Scheme 4-4**).



Scheme 4-4. Representative modification of pMAC using thiolated trehalose.

Direct modification of the polymer led to good conversion to the glycopolymer. While the carbonate backbone could be purified by dialysis, lack of stability of the lactide backbone again required use of the Sephadex column to remove excess small molecules. Thus, after adjustment of the thiol-ene conditions to take into account the differing hydrolytic stabilities of the novel backbones, we were able to generate a small library of polyesters and polycarbonates with zwitterionic carboxybetaine and trehalose side chains (**Table 4-2**). All materials were between 15.8 kDa and 30.0 kDa molecular weight as measured by GPC and were well-defined, with $\bar{D} < 1.15$. The pLA-zwitterion polymer was smaller than predicted and could be due to unwanted acidic hydrolysis despite the care taken during handling. TFA treatment could be avoided in the future by exchanging the *t*-butyl ester for a benzylic ester that could be removed using hydrogenation.

Table 4-2. Molecular weights and GPC data for functional zwitterionic and trehalose polymers

polymer	Expected Mn ^b	Mn (¹ H-NMR)	DP	Mn (GPC) ^c	\bar{D}^c
pCL-trehalose ^a	40 500	35 900	72	24 700	1.04
pC-trehalose	42 000	41 900	71	28 000	1.08
pLA-trehalose	40 700	40 200	76	28 800	1.03
pCL-zwitterion ^a	25 100	26 000	82	26 300	1.13
pC-zwitterion	27 200	27 200	74	30 000	1.08
pLA-zwitterion	25 700	22 000	66	15 800	1.06

^a Prepared as in ref. 9. ^b Based on DP of starting allyl-substituted polymer. ^c Measured in MeCN/buffer using RALS-SEC

4.2.2. Degradation Studies

The hydrolytic and enzymatic stability of the zwitterion-substituted polyesters and polycarbonates was then characterized. Polymers were incubated in Dulbecco's phosphate-buffered serum (DPBS) at 37 °C and 250 rpm shaking and time points were removed at intervals

and analyzed by SEC using right-angle light scattering (RALS-SEC). A wide range of hydrolytic stabilities were observed (**Figure 4-2**). As expected due to the difficulty in preparing the lactide backbones, the pLA-zwitterion exhibited fast degradation kinetics when incubated in buffer, with the first time point at 12 hours already showing a 48% decrease in molecular weight. While only a small shift in retention volume was observed, there was significant loss in the light-scattering signal due to decrease of polymer size. Additionally, the measured dispersity (\bar{D}) increased from 1.05 to a maximum of 1.25 at 24 hours. Further increase in \bar{D} was not observed, presumably due to overlap of the polymer peak with the solvent peaks as the retention time increased. A similar trend was observed for the pC-zwitterion polymer, with a 45% decrease in molecular weight between day 1 and day 8. For this experiment, a previously-run polymer sample was used as the initial timepoint for molecular weight calculations (**Figure 4-3**) and therefore no t_0 chromatogram is shown in the overlay of **Figure 4-2**. For the pC-zwitterion backbone, only minimal changes in \bar{D} were measured. No significant change was observed for the pCL-zwitterion polymer, with a slight molecular weight loss from 27.2 kDa to 26.3 kDa over 100 days of incubation (**Figure 4-3**).

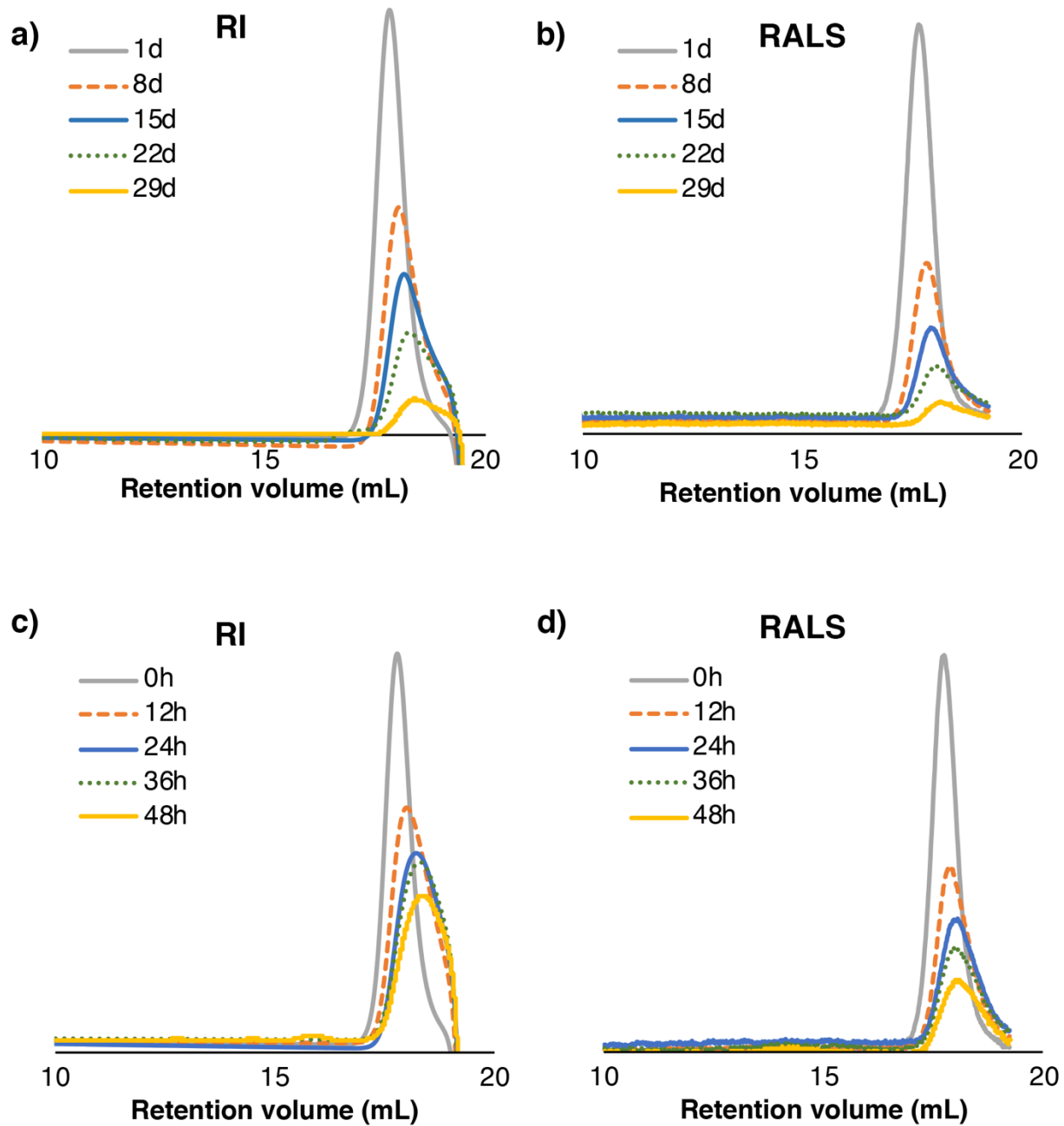


Figure 4-2. SEC chromatogram of the DPBS degradation of a) and b) pC-zwitterion and c) and d) pLA-zwitterion. Chromatograms from the refractive index (RI) and light-scattering detectors are both shown.

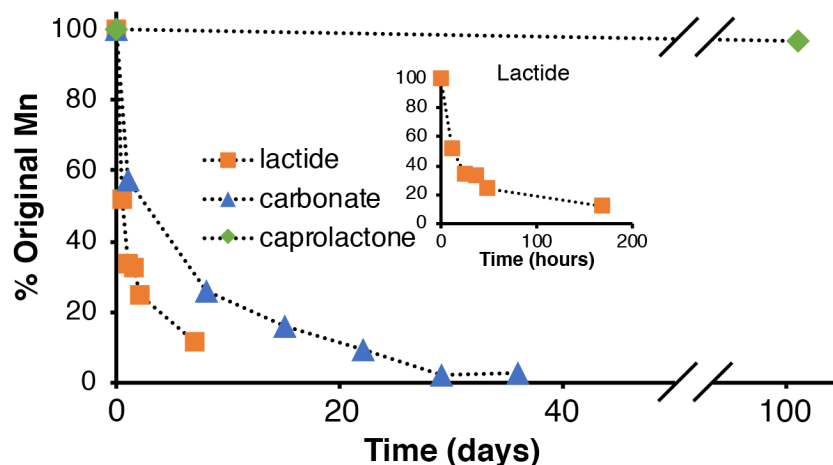


Figure 4-3. Degradation kinetics of pX-zwitterion polymers as percent original molecular weight over time.

To test if the rate of hydrolysis would increase in the presence of enzymes, pCL-zwitterion was incubated with lipase B from *candida antarctica*, a widely used enzyme that has been shown to have degradation activity against polycaprolactone and other synthetic polyesters.¹⁹ While normal lipase levels in healthy adults range from 30-190 U/L²⁹, higher enzyme concentrations were used in this study in order to maximize possible hydrolysis. A resin-immobilized enzyme was used for easy enzyme removal and in order to prevent overlap of the polymer macromolecule signal with protein peaks. However, no degradation was observed within 7 days of incubation (**Figure 4-4**). This may be due to inactivation of the enzyme during this time period or because of steric bulk of the zwitterionic side chain making the ester inaccessible to the enzyme active site. We confirmed that the immobilized lipase was active by monitoring the hydrolysis of the model substrate 4-nitrophenyl acetate to 4-nitrophenol (**Figure 4-16**).³⁰ Therefore, it is more likely that the hydrophilic side chains interfere with substrate binding in the protein active site.

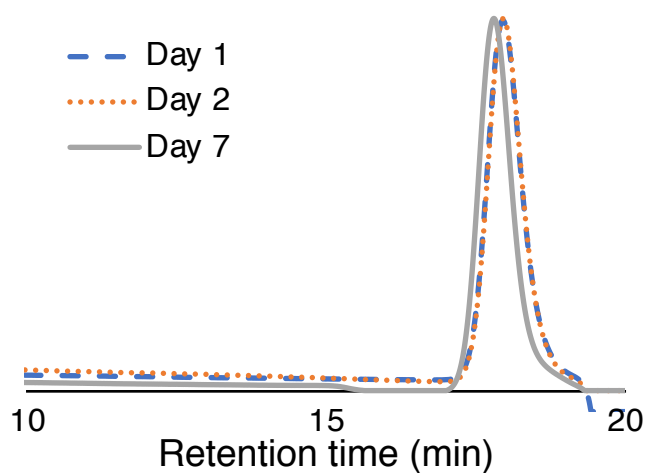


Figure 4-4. Enzymatic treatment of pCL-zwitterion using immobilized lipase B.

In summary, we demonstrated the ring-opening polymerization of allyl polyesters/carbonates, modification with zwitterion or trehalose side chains and degradation of the substituted materials. By tracking the stability in phosphate-buffered saline, we were able to determine the conditions under which these materials might be able to be handled, modified, and then degraded *in vitro* or *in vivo*. However, additional optimization could be carried out for practical stability and degradation of the polymers. Even using high enzyme concentrations and extended time periods (<4 months), no degradation was observed for the polycaprolactone-based material. And surprisingly, the polylactide-based material degraded rapidly, necessitating special purification techniques and perhaps precluding its incorporation into complex biological materials (e.g. protein-polymer conjugates).

Previous reports have mentioned that incorporation of hydrophilic side chains onto these well-known polymer backbones increases hydrolytic susceptibility. Hydroxylated pLA degraded two orders of magnitude faster than the unsubstituted analog.²¹ Poly(trimethylene carbonate) (pTMC), the unfunctionalized analog of MAC, has been reported to degrade very slowly *in vitro*,

with no significant decrease in molecular weight over more than two years.³¹ However, subdermal pTMC implants underwent 25% weight loss in rats after 4 months, indicating susceptibility to enzymatic hydrolysis.³² Our results suggest that addition of zwitterionic carboxybetaine side chains significantly increase hydrolysis rates, perhaps by improving solubility and water penetration to the degradable units. While pCL-zwitterion demonstrated no observable degradation within the time frame studied, we expect that it will be faster than the unmodified hydrophobic polymer, which has been shown to be stable for 2-4 years depending on molecular weight.³³

Copolymerization of the allyl-modified lactide with unfunctional L-lactide might increase the hydrophobicity of the polymer backbone and impart sufficient stability for further handling of the polymer. Similarly, an oxalate unit might be incorporated into the polycaprolactone for improved hydrolytic susceptibility³⁴, or the caprolactone might be replaced with a lactone monomer containing fewer carbons, such as valerolactone or butyrolactone, to decrease the hydrophobicity of the backbone and improve the degradation profile. Alternatively, the alkene-containing monomers studied above could be copolymerized. Copolymers incorporating lactides, carbonates, and/or caprolactone moieties are hypothesized to exhibit intermediate stabilities and monomer ratios could be tuned to target a specific degradation profile.

4.3. Conclusions

Herein, we have described the synthesis of a series of three alkene-containing backbones and their post-polymerization modification with zwitterionic and trehalose thiols. We studied their degradation properties and found them to span a large range of timescales, from hours to greater than four months. We believe that further modification of hydrolytic stability will be possible by

including comonomers to increase or decrease hydrophobicity along the polymer backbone. These materials have potential applications in the protection of proteins from environmental stressors such as heat, lyophilization, or agitation. Further study will focus on their relative stabilizing abilities and toxicities *in vitro* and *in vivo*.

4.4. Materials and Methods

4.4.1. Materials

All materials and proteins were purchased from Sigma-Aldrich, Acros, or Fisher Scientific and were used without purification unless noted. Anhydrous toluene was distilled from CaH₂ and stored under argon prior to use. Anhydrous tetrahydrofuran (THF) was distilled from sodium benzophenone and stored under argon prior to use. Anhydrous dichloromethane (DCM) was distilled from CaH₂ and stored under argon prior to use. Polymerizations were carried out in a Vacuum Atmospheres Genesis stainless steel glove box under anhydrous nitrogen atmosphere. Allyl-caprolactone (CL-allyl) was synthesized as previously described²⁴, purified by distillation under reduced pressure before use, and polymerized as previously described.¹⁰ Methyl allyl carbonate (MAC) was synthesized as previously described.²⁶ Allylated lactide (LA-allyl) was prepared as previously described.²⁵ Thiourea catalyst 1-(3,5-bis(trifluoromethyl)phenyl)-3-cyclohexylthiourea was synthesized as previously described.²³ Thiolated trehalose was a gift of Arvind Bhattacharya (UCLA).

4.4.2. Analytical Techniques

NMR spectra were obtained on Bruker AV 500 and DRX 500 MHz spectrometers. ¹H-NMR spectra were acquired with a relaxation delay of 2 s for small molecules and 30 s for polymers. Infrared absorption spectra were recorded using a PerkinElmer FT-IR equipped with an ATR accessory. High-resolution mass spectra were obtained on Waters LCT Premier with ACQUITY LC and ThermoScientific Exactive Mass Spectrometers with DART ID-CUBE. Gel Permeation Chromatography (GPC) was conducted on a Shimadzu high performance liquid chromatography (HPLC) system with a refractive index detector RID-10A, one Polymer Laboratories PLgel guard

column, and two Polymer Laboratories PLgel 5 μm mixed D columns. Eluent was DMF with LiBr (0.1 M) at 50 $^{\circ}\text{C}$ (flow rate: 0.80 mL/ min). Calibration was performed using near-monodisperse PMMA standards from Polymer Laboratories. RALS size exclusion chromatography (RALS-SEC) was conducted on a Malvern Viscotek VE 2001 GPCmax with a TDA 305 triple detector, with two Viscotek A600M general mixed aqueous columns. Eluent was 200 mM Na_2SO_4 and 20% MeCN. Conventional calibration was performed using near-monodisperse PEG standards from Polymer Laboratories. For zwitterionic polymers, a dn/dc value of 0.15 mL/g was calculated using pCL-zwitterion. For trehalose polymers, a dn/dc value of 0.119 mL/g was calculated using pCL-trehalose.

4.4.3. Methods

Polymerization of allyl-lactide (LA-allyl)

In the glovebox, a dram vial with stir bar was charged with MTBD, 10% v/v in toluene, 8.7 μL , 6.1 μmol and toluene (600 μL). A solution of LA-allyl (103 mg, 0.61 mmol) and 3-methylbutanol (10% v/v in toluene, 6.0 μL , 5.5 μmol) in toluene (600 μL) was added and the polymerization monitored by $^1\text{H-NMR}$. After 75 minutes, the solution was removed from the box and quenched with AcOH and purified by dialysis in acetone using 3.5 kDa MWCO tubing. After 3 days of dialysis, the solution was concentrated and dried in vacuo to yield a colorless oil. Yield: 68.9 mg (66.9 %). M_N ($^1\text{H-NMR}$) = 13.2 kDa, M_N (GPC, PMMA standards) = 22.7 kDa, M_W (GPC) = 23.4 kDa, $\bar{D} = 1.03$. $^1\text{H-NMR}$ (500 MHz in CDCl_3) δ : 5.89-5.69 (m, 90H), 5.34-5.06 (m, 372H), 2.86-2.56 (m, 192H), 1.73-1.40 (m, 394H), 0.91 (d, $J=6.7$ Hz, 6H).

Polymerization of methyl allyl carbonate (MAC)

In the glovebox, a dram vial with stir bar was charged with methyl allyl carbonate (MAC, 200 mg, 1.00 mmol), 3-methylbutanol (10% v/v in toluene, 8.7 μ L, 8.00 μ mol), thiourea catalyst²³ (18.5 mg, 0.05 mmol) and DCM (2 mL) and mixed well to dissolve. Then DBU (7.5 μ L, 0.05 mmol) was added. Conversion was monitored by ¹H-NMR and after 145 minutes the solution was then removed from the box, quenched with AcOH, and precipitated into MeOH, yielding a colorless oil. Yield: 114 mg (76 %). M_N (¹H-NMR) = 15500 kDa, M_N (GPC, PMMA standards) = 20900 kDa, M_W (GPC) = 22700 kDa, D = 1.09. ¹H-NMR (500 MHz in CDCl₃) δ : 5.93-5.83 (m, 75H), 5.35-5.20 (m, 153H), 4.66-4.61 (d, 153H), 4.35-4.26 (m, 303H), 1.27 (s, 234H), 0.92 (d, J = 6.6 Hz, 6H).

Synthesis of zwitterionic disulfide 4

In a 20 mL scintillation vial with stir bar, dimethylaminocystamine³⁵ (132 mg, 0.63 mmol) was dissolved in MeCN (1.5 mL). *t*-butyl bromoacetate (280 μ L, 1.90 mmol) was added and the mixture stirred at 45 °C for 13 hours. The solution was then cooled to room temperature and the solution precipitated into 30 mL diethyl ether. The crude material was then further purified by preparatory HPLC (gradient 10-95 % MeOH in H₂O) to yield an oil, which formed a white solid upon refrigeration (372 mg, 0.62 mmol, 98%). ¹H-NMR (500 MHz in CD₃CN) δ : 4.47 (s, 4H), 4.02 (m, 4H), 3.43 (m, 4H), 3.39 (s, 12H), 1.50 (s, 18H). ¹³C-NMR (500 MHz in CD₃CN) δ : 165.6, 85.8, 64.9, 62.9, 52.7, 32.1, 28.2. IR: 3387, 2977, 2937, 1737, 1639, 1478, 1459, 1396, 1370, 1253, 1153, 1025, 989, 960, 928, 897, 840, 757, 708. MS-QTOF (m/z) [M]⁺ calcd for C₁₆H₃₃N₂O₄S₂ 381.1871; found 381.1913.

Synthesis of zwitterionic thiol 5

In a 20 mL scintillation vial with stir bar, disulfide **4** (372 mg, 0.62 mmol) was dissolved in THF:H₂O (10:1, 700 μ L total). Tributyl phosphine (233 μ L, 0.93 mmol) was then added and the mixture stirred at room temperature for 1 hour. All volatiles were removed in vacuo and the resulting thick oil was dissolved in MeOH and precipitated 2x into Et₂O (30 mL) to yield a white crispy solid (264 mg, 0.88 mmol, 71%). ¹H-NMR (500 MHz in CD₃CN) δ : 4.05 (s, 2H), 3.65 (m, 2H), 3.20 (s, 6H), 2.85 (m, 2H), 1.50 (s, 9H). ¹³C-NMR (500 MHz in CD₃CN) δ : 164.2, 86.1, 67.8, 62.9, 52.5, 28.1, 17.7. IR: 3406, 2977, 2930, 2401, 1727, 1476, 1457, 1426, 1395, 1370, 1292, 1267, 1252, 1218, 1119, 1075, 1057, 1008, 990, 952, 929, 897, 877, 838, 787, 773, 762, 729, 711. MS-QTOF (m/z) [M]⁺ calcd for C₁₀H₂₂NO₂S 220.1366; found 220.1404.

Modification of pMAC with zwitterionic precursor

In a dram vial, reduced thiol **5** (194 mg, 0.88 mmol) was dissolved in MeCN (0.5 mL) and added to a solution of pMAC (30 mg, 0.15 mmol alkene units) and DMPA (19 mg, 0.07 mmol) in THF/MeCN (50%, 0.5 mL total). The mixture was degassed by sparging for 5 minutes, then exposed to 365 nm UV light. After 4 hours, the solution was opened, diluted with MeOH, and dialyzed against 3.5 kDa MWCO in MeOH. After 39 hours, the crude polymer was then removed, solvent removed in vacuo, and TFA (1.5 mL) was added to the crude oil and stirred at room temperature. After 45 minutes, TFA was thoroughly removed in vacuo and the crude oil dissolved in H₂O/MeOH and dialyzed against 3.5 kDa MWCO, switching to 100% H₂O after 24 hours. The resulting solution was then lyophilized to remove solvent to yield a fluffy white solid (45 mg, 84%). M_N (¹H-NMR) = 27200 Da, M_N (RALS GPC) = 30200 Da, M_w (RALS GPC) = 32.6 kDa, Đ = 1.08. ¹H-NMR (500 MHz in D₂O) δ : 4.35-4.02 (m, 441H), 3.86-3.75 (s, 155H), 3.75-3.61 (m,

149H), 3.24-3.05 (s, 455H), 2.93-2.77 (m, 150H), 2.67-2.51 (m, 150H), 1.94-1.76 (m, 147H), 1.23-1.04 (s, 224H), 0.80 (d, $J = 6.2$ Hz, 6H).

Modification of pMAC with thiolated trehalose

In a dram vial with stir bar, pMAC (12.3 mg, 0.080 mmol alkene groups) was dissolved in DMF (500 μ L). Thiotrehalose (86 mg, 0.240 mmol) and DMPA (10.2 mg, 0.040 mmol) were added and the mixture degassed by sparging for 5 minutes. The solution was then exposed to 365 nm light while stirring for 4 hours before being diluted with H₂O and dialyzed against 3.5 kDa MWCO in 50% MeOH, switching to 100% H₂O after 24 hours. The resulted solution was then lyophilized to remove solvent to yield a white fluffy solid (34.6 mg, 77.6%). M_N (¹H-NMR) = 41.9 kDa, M_N (RALS GPC) = 28.0 kDa, M_w (RALS GPC) = 30.1 kDa, $\bar{D} = 1.08$. ¹H-NMR (500 MHz in D₂O) δ : 5.18-4.96 (d, 2H), 4.41-3.96 (m, 6H), 3.86-3.58 (m, 6H), 3.58-3.43 (m, 2H), 3.38-3.18 (m, 2H), 2.67-2.40 (m, 2H), 1.96-1.68 (m, 2H), 1.28-1.02 (s, 3H).

Modification of pLA-allyl with zwitterionic precursor 5

In a dram vial with stir bar, dissolve pLA-allyl (5 mg, 0.029 mmol alkenes), zwitterion precursor thiol **5** (53 mg, 0.176 mmol) and DMPA (3.8 mg, 0.015 mmol) in THF (100 μ L) and MeOH (300 μ L). Degas by sparging for 5 minutes, then expose to 365 nm UV light. After 4 hours, solvent was removed in vacuo and thoroughly dried. The crude was then dissolved in TFA (0.75 mL) and let stir at room temperature for 45 minutes. Then toluene (2 mL) was added and removed in vacuo, and this process was repeated 1x. Diethyl ether (2 mL) was then added to the residual crude, mixed well, and centrifuged to separate. The solution was decanted and repeated until pH test of the ether layer were shown to be not acidic, 3x in total. The crude off-white solid was then dissolved in 2

mL H₂O and purified by passage through a Sephadex PD-10 desalting column. The resulting solution was immediately lyophilized to remove water and stored under reduced pressure to yield a white solid (4.2 mg, 42.9%). M_N (¹H-NMR) = 22.0 kDa, M_N (RALS GPC) = 15.8 kDa, M_W (RALS GPC) = 16.7 kDa, $\bar{D} = 1.06$. ¹H-NMR (500 MHz in D₂O) δ : 5.23-5.02 (m, 2H), 3.89-3.75 (m, 2H), 3.75-2.62 (m, 2H), 3.19-3.08 (s, 6H), 2.91-2.72 (m, 2H), 2.64-2.49 (m, 2H), 2.07-1.83 (m, 2H), 1.75-1.54 (m, 2H), 1.54-1.36 (s, 3H).

Modification of pLA-allyl with thiolated trehalose

In a dram vial with stir bar, pLA-allyl (5 mg, 0.03 mmol alkene units) was dissolved in DMF (400 μ L). Thiotrehalose (42 mg, 0.12 mmol) and DMPA (3.8 mg, 0.01 mmol) were added and stirred well to dissolve. The mixture was degassed by sparging for 5 minutes, then exposed to 365 nm UV light. After 4 hours, DMF was removed in vacuo. The resulting oil was dissolved in H₂O (2 mL) and purified by passage through a Sephadex PD-10 desalting column. The solution was immediately lyophilized to remove water and stored under reduced pressure as a white solid (4 mg, 25%). M_N (¹H-NMR) = 40.2 kDa, M_N (RALS GPC) = 28.8 kDa, M_W (RALS GPC) = 29.7 kDa, $\bar{D} = 1.03$. ¹H-NMR (500 MHz in D₂O) δ : 5.38-5.08 (m, 329H), 4.02-3.73 (m, 488H), 3.71-3.58 (m, 174H), 3.53-3.31 (m, 169H), 3.12-2.93 (m, 76H), 2.84-2.54 (m, 229H), 2.26-1.91 (m, 146H), 1.90-1.67 (m, 155H), 1.67-1.43 (m, 244H), 1.00-0.89 (m, 6H).

Representative hydrolytic degradation of modified polyesters

In an Eppendorf tube, pC-zwitterion (12.5 mg) was dissolved in DPBS (1.25 mL) at a concentration of 10 mg/mL. The tube was then incubated at 37 °C with shaking and time points were removed either every 7 days (pC-zwitterion) or every 12 hours (pLA-zwitterion) for analysis.

Aliquots (100 μ L) were removed, diluted with SEC eluent (0.2 M Na₂SO₄, 20% MeCN, 100 μ L) and filtered before SEC analysis.

Representative enzymatic degradation of modified polyesters

In an Eppendorf tube, pCL-zwitterion (5 mg) was dissolved in DPBS (500 μ L) at a concentration of 10 mg/mL. Lipase B from *Candida antarctica* (immobilized on Immobead 150, 4400 U/g, 12 mg, 52.8 U) was added for a final enzyme concentration of 106 U/mL. The tube was then incubated at 37 °C with shaking and timepoints were removed at 1, 2, and 7 days for analysis. Aliquots (100 μ L) were removed, diluted with SEC eluent (0.2 M Na₂SO₄, 20% MeCN, 100 μ L) and filtered before SEC analysis.

Control enzymatic degradation of 4-nitrophenyl acetate

To confirm that immobilized lipase B (4584 U/g) retained activity under the experimental conditions, the hydrolysis of 4-nitrophenyl acetate was monitored. In a microwell plate, a solution of 5 mM 4-nitrophenyl acetate in DPBS (200 μ L) was treated with lipase (0.73-0.83 U) and incubated at 37 °C with shaking. The concentration of released 4-nitrophenol (4-NP) was determined by measuring absorbance at 410 nm and presented as μ M 4-NP per unit enzyme.

4.5. Appendix with Supplementary Figures

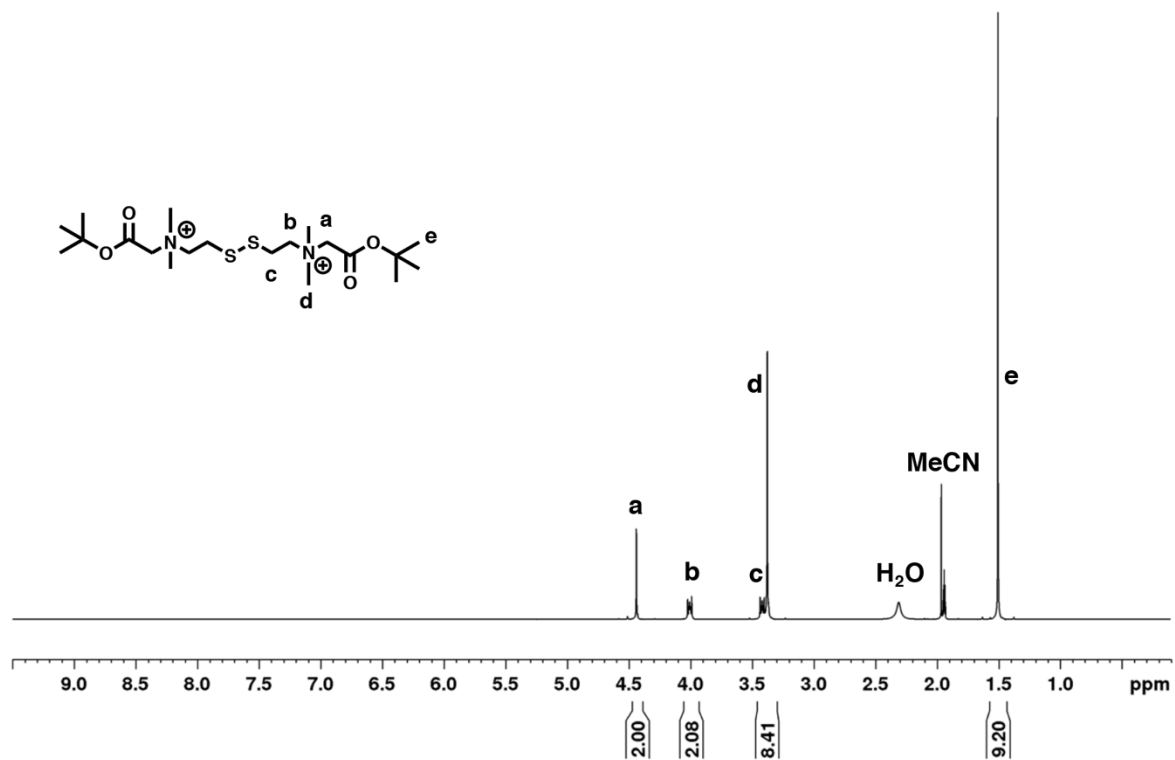


Figure 4-5. ¹H-NMR spectrum of zwitterion disulfide 4 (500 MHz, CD₃CN).

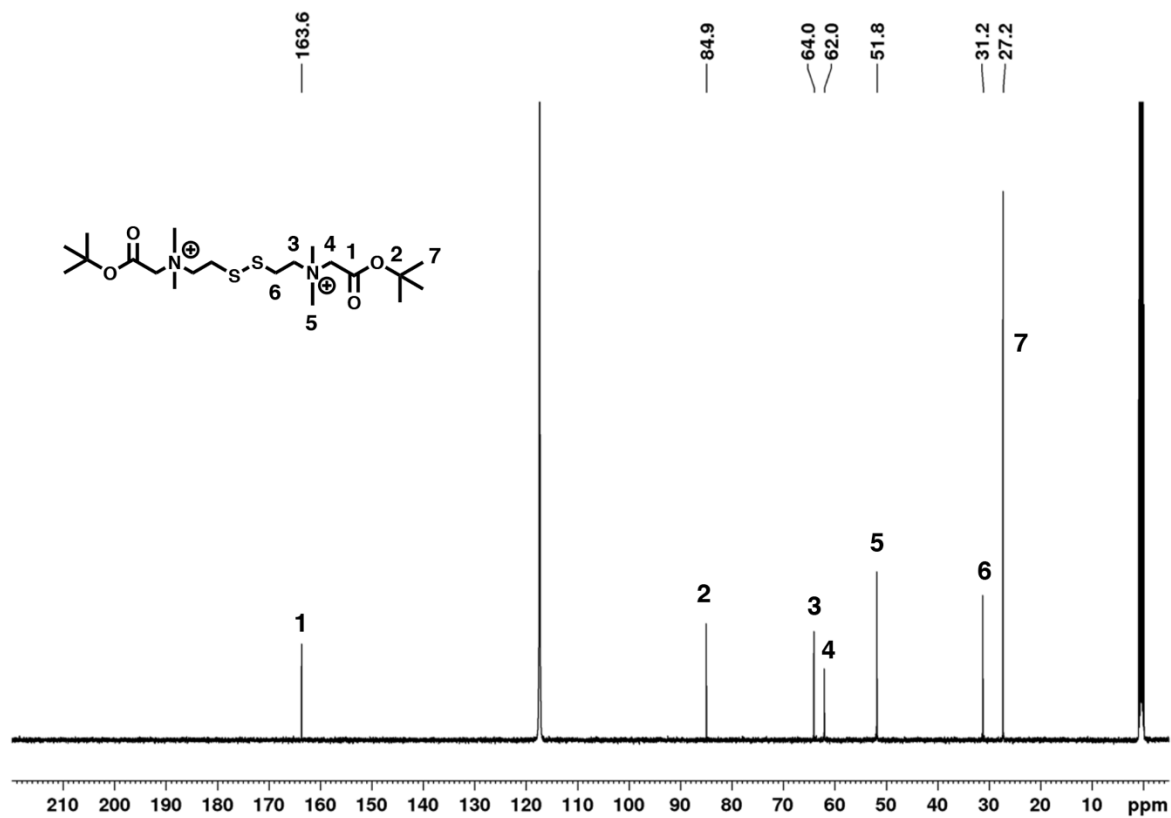


Figure 4-6. ^{13}C -NMR spectrum of zwitterion disulfide **4** (500 MHz, CD_3CN).

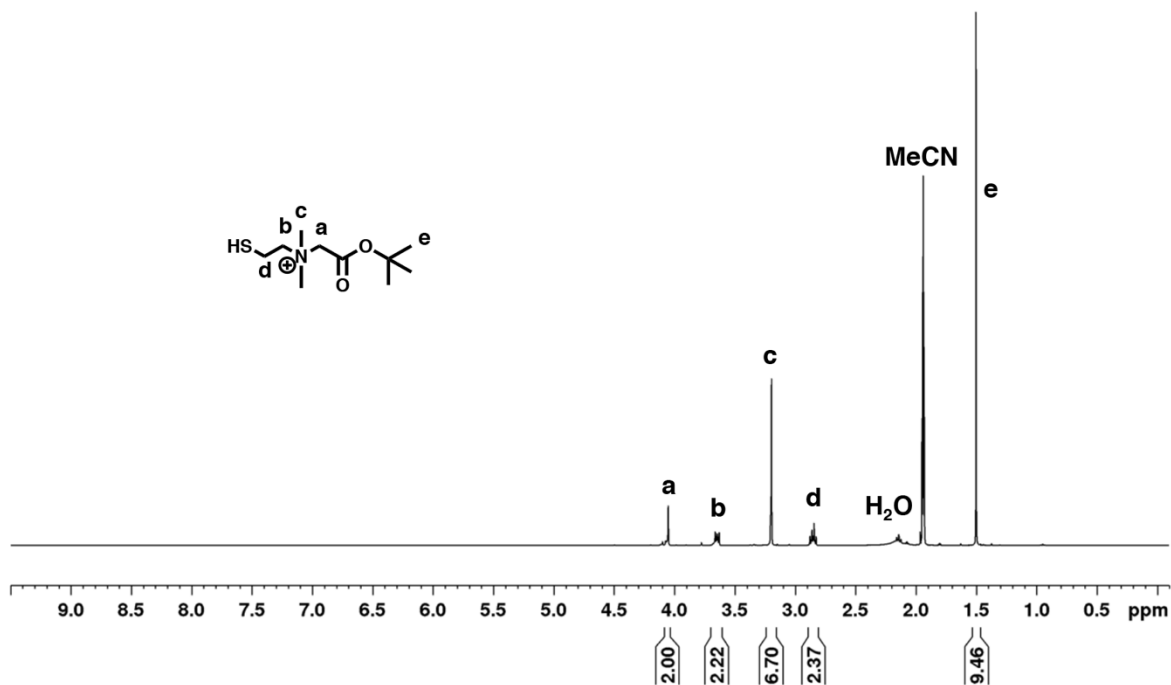


Figure 4-7. ^1H -NMR spectrum of zwitterion thiol **5** (500 MHz, CD_3CN).

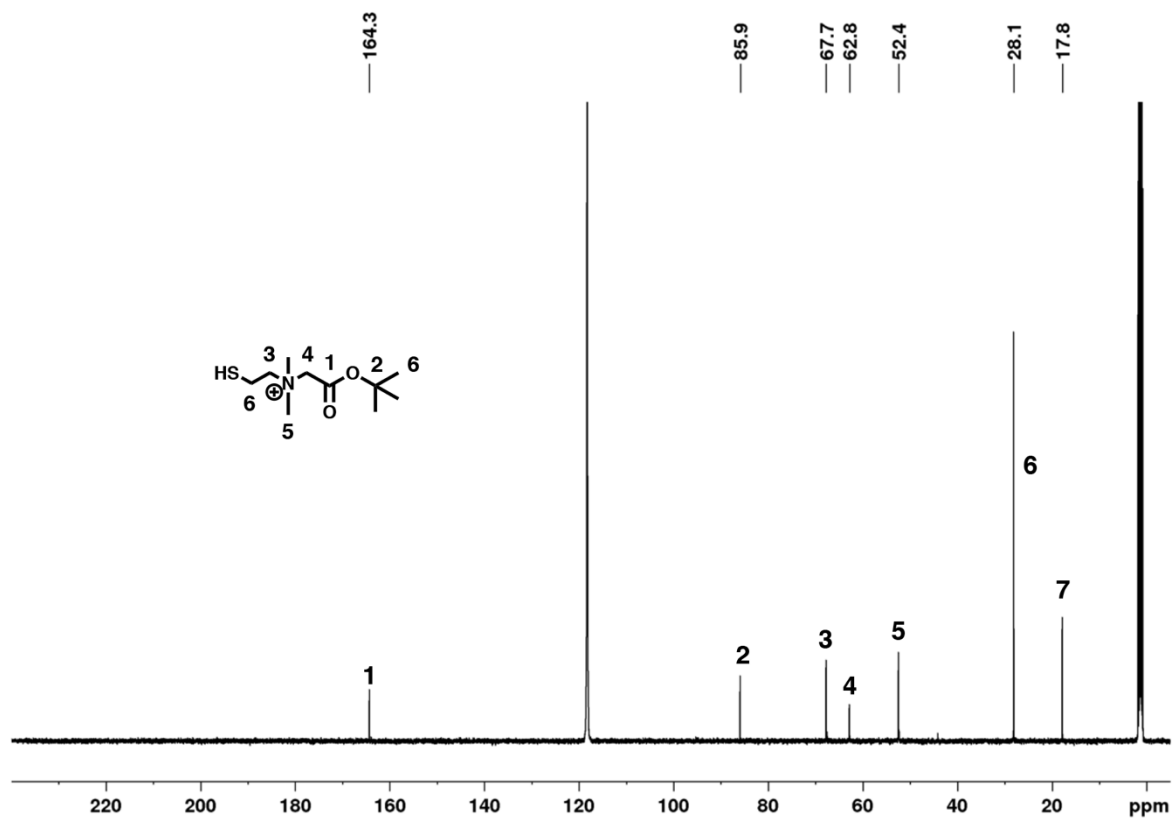


Figure 4-8. ¹³C-NMR spectrum of zwitterion thiol **5** (500 MHz, CD₃CN).

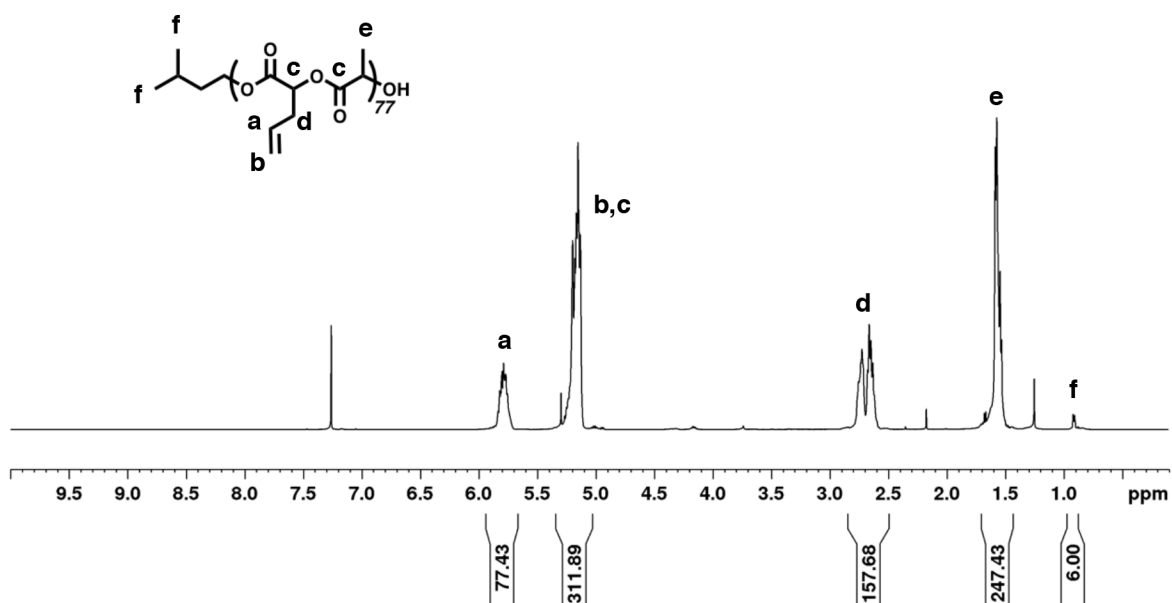


Figure 4-9. ¹H-NMR spectrum of pLA-allyl (500 MHz, CDCl₃).

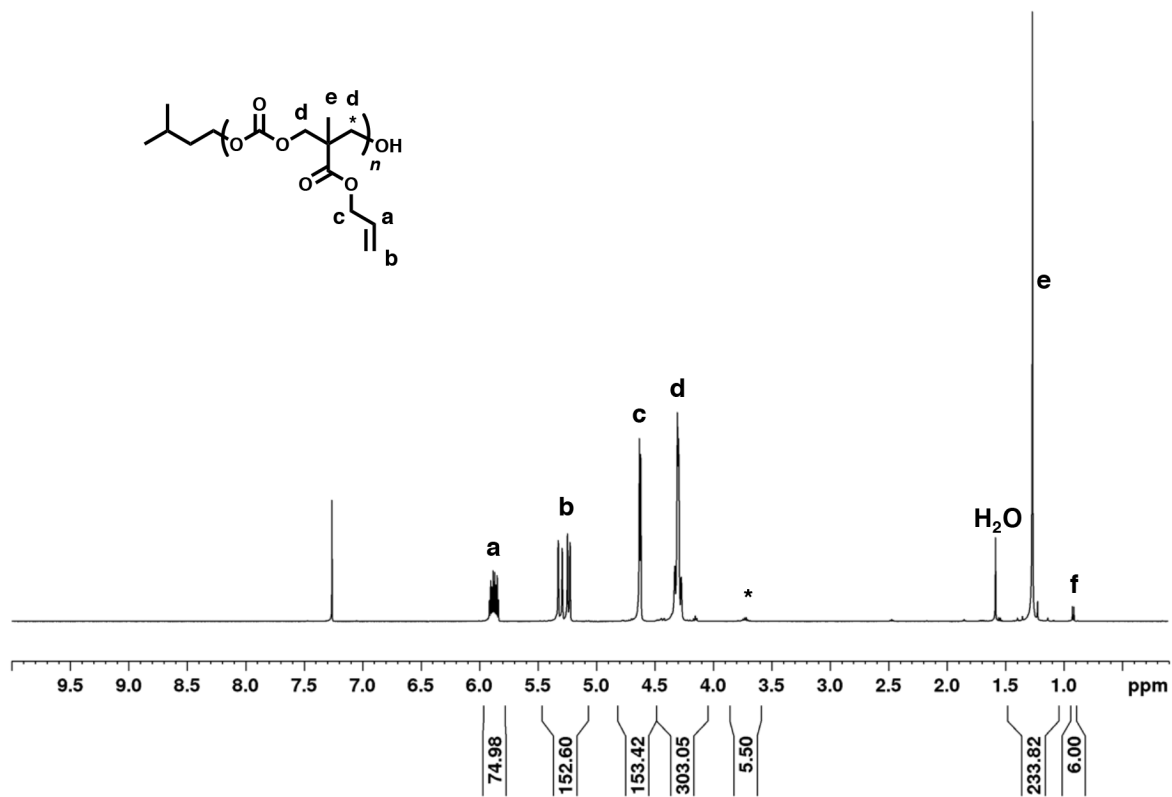


Figure 4-10. ¹H-NMR spectrum of pMAC (500 MHz, CDCl₃). * = protons from terminal unit on polymer.

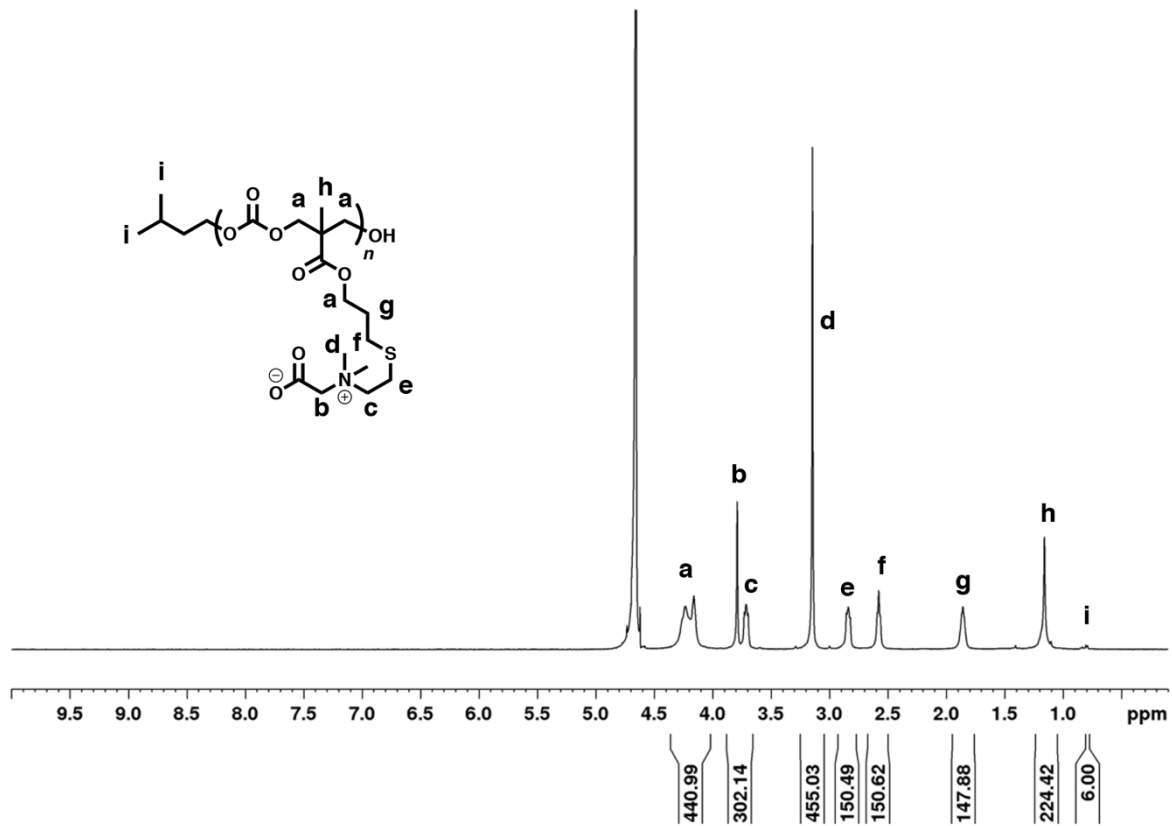


Figure 4-11. ¹H-NMR spectrum of pC-zwitterion (500 MHz, D₂O).

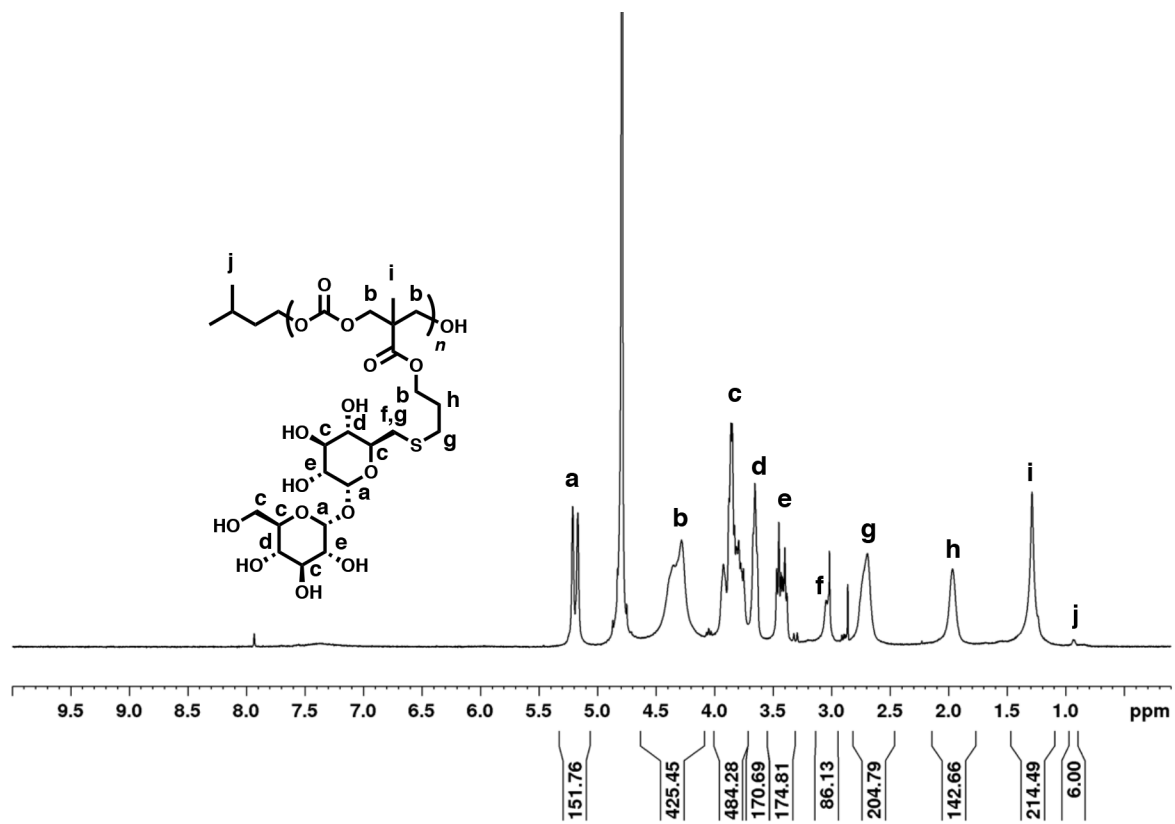


Figure 4-12. ¹H-NMR spectrum of pC-trehalose (500 MHz, D₂O).

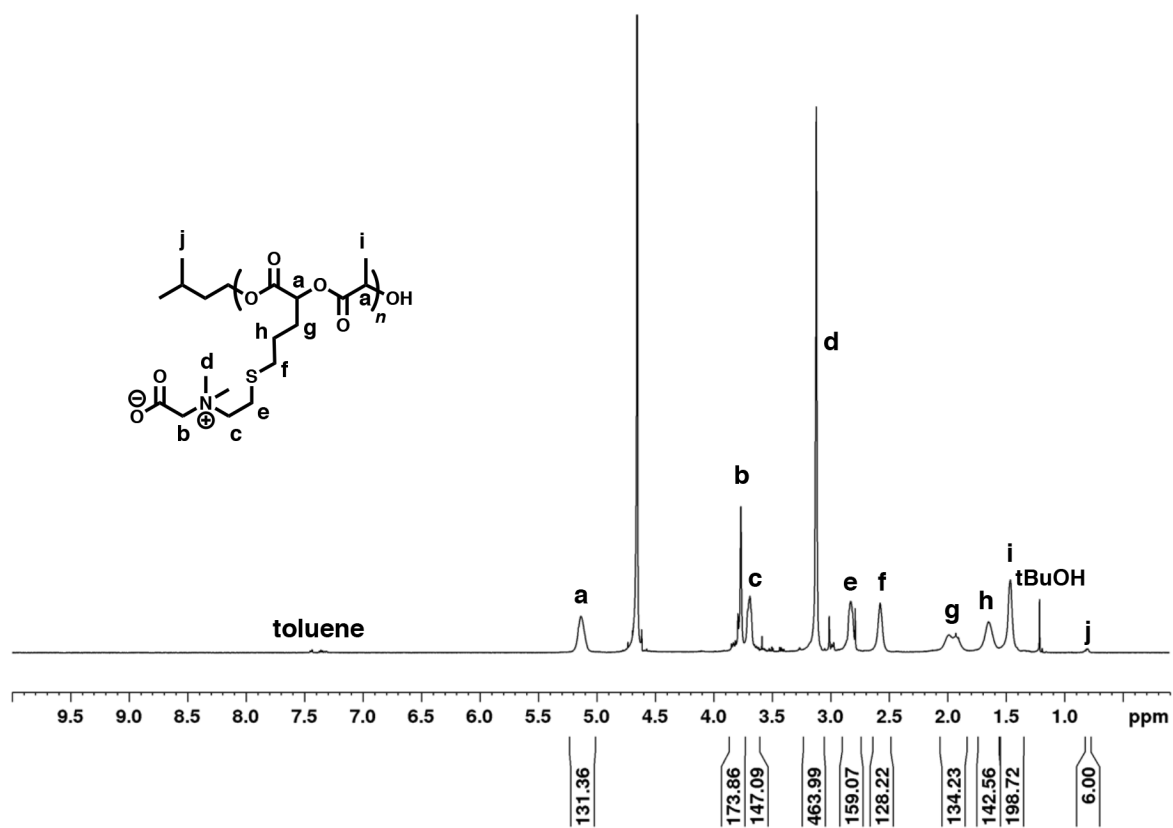


Figure 4-13. $^1\text{H-NMR}$ spectrum of pLA-zwitterion (500 MHz, D_2O).

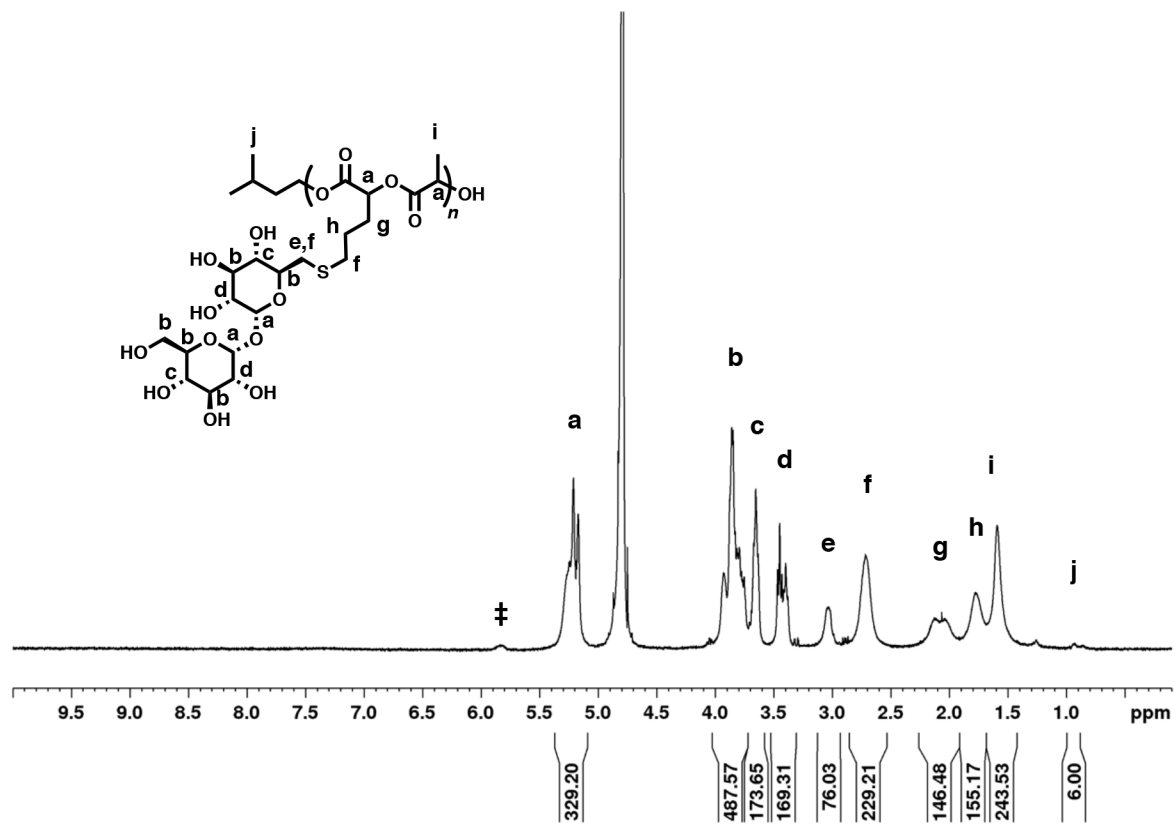


Figure 4-14. ¹H-NMR spectrum of pLA-trehalose (500 MHz, D₂O). ‡ indicates incomplete modification of the starting alkene polymer.

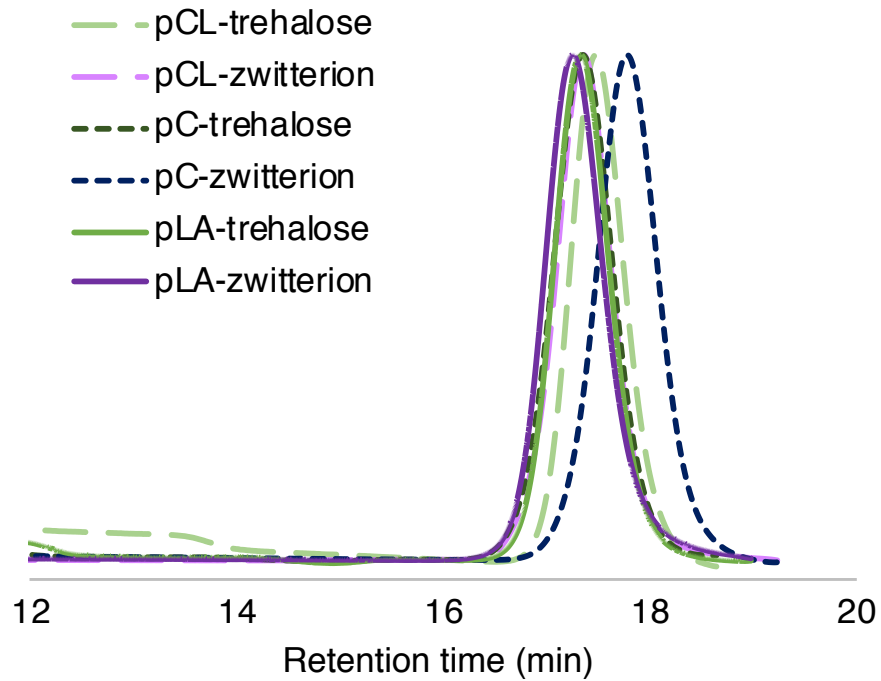


Figure 4-15. SEC overlays of synthesized polyesters and polycarbonates.

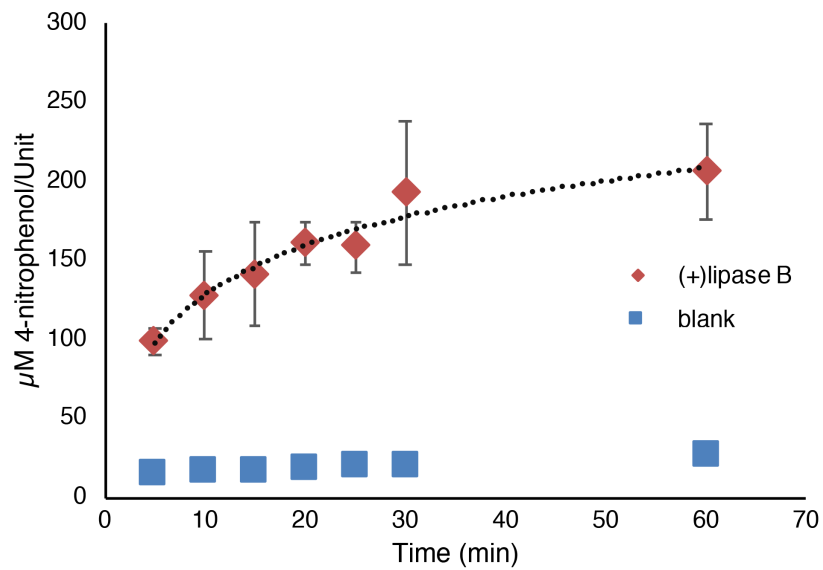


Figure 4-16. Enzymatic hydrolysis of 4-nitrophenyl acetate by immobilized lipase B.

4.6. References

1. Schellekens, H.; Hennink, W. E.; Brinks, V., *Pharm. Res.* **2013**, *30*, 1729.
2. Yang, Q.; Lai, S. K., *Wiley Interdiscip. Rev.: Nanomed. Nanobiotechnol.* **2015**, *7*, 655.
3. Abu Lila, A. S.; Kiwada, H.; Ishida, T., *J. Controlled Release* **2013**, *172*, 38.
4. Ganson, N. J.; Povsic, T. J.; Sullenger, B. A.; Alexander, J. H.; Zelenkofske, S. L.; Sailstad, J. M.; Rusconi, C. P.; Hershfield, M. S., *J. Allergy Clin. Immunol.* **2016**, *137*, 1610.
5. Zhang, P.; Sun, F.; Liu, S. J.; Jiang, S. Y., *J. Controlled Release* **2016**, *244*, 184.
6. Bendele, A.; Seely, J.; Richey, C.; Sennello, G.; Shopp, G., *Toxicol. Sci.s* **1998**, *42*, 152.
7. Pelegri-O'Day, E. M.; Lin, E. W.; Maynard, H. D., *J. Am. Chem. Soc.* **2014**, *136*, 14323.
8. Pelegri-O'Day, E. M.; Maynard, H. D., *Acc. Chem. Res.* **2016**, *49*, 1777.
9. Qi, Y.; Chilkoti, A., *Curr Opin Chem Biol* **2015**, *28*, 181.
10. Pelegri-O'Day, E. M.; Paluck, S. J.; Maynard, H. D., *J. Am. Chem. Soc.* **2017**, *139*, 1145.
11. Ulery, B. D.; Nair, L. S.; Laurencin, C. T., *J. Polym. Sci., Part B: Polym. Phys.* **2011**, *49*, 832.
12. Nair, L. S.; Laurencin, C. T., *Prog. Polym. Sci.* **2007**, *32*, 762.
13. Wolf, T.; Steinbach, T.; Wurm, F. R., *Macromolecules* **2015**, *48*, 3853.
14. Steinbach, T.; Wurm, F. R., *Biomacromolecules* **2016**, *17*, 3338.
15. Moghanizadeh-Ashkezari, M.; Shokrollahi, P.; Zandi, M.; Shokrolahi, F., *Polym. Adv. Technol.* **2018**, *29*, 528.
16. Pang, Y.; Liu, J. Y.; Qi, Y. Z.; Li, X. H.; Chilkoti, A., *Angew. Chem. Int. Ed.* **2016**, *55*, 10296.
17. Hill, M. R.; Guegain, E.; Tran, J.; Figg, C. A.; Turner, A. C.; Nicolas, J.; Sumerlin, B. S., *ACS Macro Lett.* **2017**, *6*, 1071.

18. Tardy, A.; Nicolas, J.; Gigmes, D.; Lefay, C.; Guillaneuf, Y., *Chem. Rev.* **2017**, *117*, 1319.
19. Guegain, E.; Michel, J. P.; Boissenot, T.; Nicolase, J., *Macromolecules* **2018**, *51*, 724.
20. Ko, J. H.; Terashima, T.; Sawamoto, M.; Maynard, H. D., *Macromolecules* **2017**, *50*, 9222.
21. Leemhuis, M.; Kruijtzter, J. A. W.; van Nostrum, C. F.; Hennink, W. E., *Biomacromolecules* **2007**, *8*, 2943.
22. Lohmeijer, B. G. G.; Pratt, R. C.; Leibfarth, F.; Logan, J. W.; Long, D. A.; Dove, A. P.; Nederberg, F.; Choi, J.; Wade, C.; Waymouth, R. M.; Hedrick, J. L., *Macromolecules* **2006**, *39*, 8574.
23. Pratt, R. C.; Lohmeijer, B. G. G.; Long, D. A.; Lundberg, P. N. P.; Dove, A. P.; Li, H. B.; Wade, C. G.; Waymouth, R. M.; Hedrick, J. L., *Macromolecules* **2006**, *39*, 7863.
24. Parrish, B.; Quansah, J. K.; Emrick, T., *J. Polym. Sci., Part A: Polym. Chem.* **2002**, *40*, 1983.
25. Zou, J.; Hew, C. C.; Themistou, E.; Li, Y. K.; Chen, C. K.; Alexandridis, P.; Cheng, C., *Adv. Mater.* **2011**, *23*, 4274.
26. Hu, X. L.; Chen, X. S.; Xie, Z. G.; Liu, S.; Jing, X. B., *J. Polym. Sci., Part A: Polym. Chem.* **2007**, *45*, 5518.
27. Stevens, D. M.; Watson, H. A.; LeBlanc, M.-A.; Wang, R. Y.; Chou, J.; Bauer, W. S.; Harth, E., *Polym. Chem.* **2013**, *4*, 2470.
28. Delcroix, D.; Martin-Vaca, B.; Bourissou, D.; Navarro, C., *Macromolecules* **2010**, *43*, 8828.
29. Burtis, C. A.; Ashwood, E. R. *Tietz Fundamentals of Clinical Chemistry*, 4th ed.; Saunders: Philadelphia, PA, **1996**; p 803
30. Miletic, N.; Abetz, V.; Ebert, K.; Loos, K., *Macromol. Rapid Commun.* **2010**, *31*, 71.

31. Pego, A. P.; Poot, A. A.; Grijpma, D. W.; Feijen, J., *Macromol. Biosci.* **2002**, *2*, 411.
32. Zhu, K. J.; Hendren, R. W.; Jensen, K.; Pitt, C. G., *Macromolecules* **1991**, *24*, 1736.
33. Woodruff, M. A.; Hutmacher, D. W., *Prog. Polym. Sci.* **2010**, *35*, 1217.
34. Chang, S. H.; Lee, H. J.; Park, S.; Kim, Y.; Jeong, B., *Biomacromolecules* **2018**.
35. Dong, B.; Li, N.; Zheng, L. Q.; Yu, L.; Inoue, T., *Langmuir* **2007**, *23*, 4178.

Chapter 5

Protein-Reactive Unsaturated PEG Analogs by ROMP

5.1. Introduction

Covalent conjugation of poly(ethylene glycol) (PEG) to proteins, or protein PEGylation, is known to increase stability, solubility, and *in vivo* circulation lifetimes of proteins.¹⁻³ This strategy has been employed in the development of PEGylated protein therapeutics, which display superior pharmacokinetic properties compared to unmodified proteins.⁴ PEGylation is well established and remains the mainstay in the field of protein therapeutics; there are ten PEGylated protein therapeutics currently approved for human use in the United States.⁴⁻⁵ They are employed to treat a variety of diseases ranging from cancer and chronic gout.

Because of the utility of PEG, there is significant interest in preparing functional or structurally different analogs of the polymer. For instance, PEG-like polymers have been synthesized that contain degradable moieties, and hydrolyzable backbone functionalities, such as esters, have been introduced.⁶⁻⁹ In several early examples, Meijer and coworkers incorporated esters into linear PEG analogs via ring opening polymerization of oxo-crown ethers.⁶⁻⁸ Copolymerization of short PEGs with lactides has been a popular route to obtaining degradable PEG analogs.¹⁰⁻¹³ For example, Hubbell and coworkers demonstrated the formation of degradable hydrogels from acrylate terminated copolymers of oligo(ethylene glycol) and α -hydroxy acids. Hawker and coworkers prepared hydrolytically degradable PEG analogs by introducing vinyl ether moieties into a PEG backbone via chloride elimination in poly(ethylene oxide-*co*-epichlorohydrin).¹⁴ Furthermore, reductively degradable PEG analogs have been prepared by introducing disulfide bridges between oligo(ethylene glycol) units.¹⁵⁻¹⁶

Additionally, backbone-functional alternatives to PEG have been developed based on the ring-opening polymerization of linear polyglycerols and derivatives.¹⁷⁻¹⁸ Some examples include polyglycerols containing hydroxyl, allyl¹⁹, and amine²⁰ functional groups that have been prepared

and can be subsequently modified to include a variety of additional functionalities. Chau and coworkers have also demonstrated the utility of this strategy by reporting a large number of backbone functionalized polyether polyols via post-polymerization modification of poly(ethoxyethyl glycidyl ether-*co*-ethylene oxide).²¹ Ferrocene-functionalized PEG copolymers have been synthesized as redox-switchable thermoresponsive materials.²² Most of the above examples are prepared by ring opening polymerization. In this report, we disclose the use of end-functionalized PEG-like polymers prepared by ROMP.

ROMP is a functional-group-tolerant and well-established method for the development of functional and biocompatible polymers.²³⁻²⁴ Kiessling and coworkers have reported ROMP derived glycopolymers, which are capable of binding proteins.²⁵⁻³³ In an early example, a sulfated neoglycopolymer was prepared *via* ROMP, which was capable of binding P-selectin.²⁶ In another example, ROMP was used for the preparation of glycopolymers capable of binding the lectin concanavalin A.²⁵ Peptide-substituted polynorbornenes prepared by ROMP were additionally used to inhibit cell adhesion to fibronectin.³⁴ Yet to date, there are only several examples of the development of ROMP polymers for protein polymer conjugation.³⁵ Kane and coworkers, have reported the preparation of ROMP polymers containing pendant 2-chloromethylester functionality, which is reactive towards free thiols on cysteine residues at pH 8.0 through a displacement reaction of the chloride.³⁵ Reaction of this cysteine reactive polymer with bovine serum albumin (BSA) resulted in protein multimers.³⁵ In another example of protein-reactive ROMP polymers, Sleiman and coworkers have demonstrated the preparation of block copolymers with biotin end-group functionality, capable of binding streptavidin (SAv).³⁶ Biotin functionality was installed by terminating the ROMP reaction with biotin functionalized vinyl ethers. In aqueous conditions, the biotin-functionalized block copolymers assembled into micelles, which could be crosslinked *via*

the addition of SAV tetramers. Recently, Pokorski and coworkers have reported ROMP based *grafting from* and *grafting to* methods for protein-polymer conjugation.³⁷⁻³⁸ In their *grafting from* approach, lysozyme modified with norbornene functionality was subjected to a Grubbs type ruthenium metathesis catalyst and subsequently used as a macro-catalyst for the polymerization of a PEG-modified norbornene.³⁷ In their *grafting to* approach, Pokorski and coworkers utilized the living nature of ROMP to end-cap a water-soluble PEGylated norbornene polymer with a short block of amine reactive norbornene dicarboxylic anhydride.³⁸ The resulting diblock copolymer could be conjugated to free amines present on lysozyme as well as the coat protein of bacteriophage Q β .³⁸

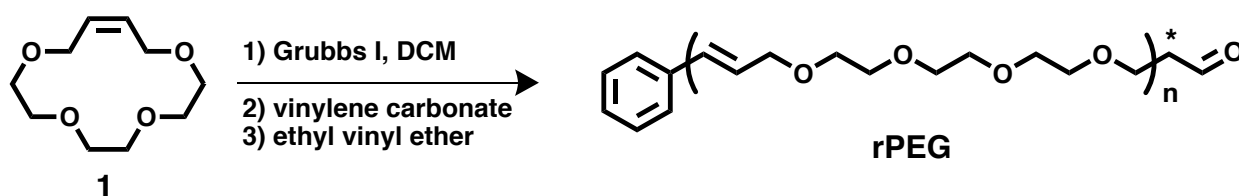
We previously reported the ROMP of unsaturated crown ethers, producing water-soluble unsaturated PEG analogs.³⁹⁻⁴⁰ We prepared polymers with pendant amino acids by copolymerization of the unsaturated crown ether analogs with pendant amino acid unsaturated benzo-crown ethers.⁴⁰ However, these polymers did not have functional end groups for attachment to proteins. In this report, we describe the ROMP synthesis of PEG-analogs (rPEGs) containing ω -aldehyde end-group functionality, for straightforward conjugation to surface exposed amines by reductive amination. Formation of these rPEG-protein conjugates is described, as well as extensive, yet largely unsuccessful, investigation into the thiol-ene modification of the unsaturated alkene-containing backbone.

5.2. Results and Discussion

5.2.1. Polymer Synthesis

Aldehyde end-functionalized PEGs are commonly used for bioconjugation to surface exposed amines on proteins *via* mild and efficient reductive amination reactions.⁴¹⁻⁴³ **rPEG 1-5**

have been prepared by ROMP of the unsaturated crown ether monomer **1** (Scheme 5-1).³⁹⁻⁴⁰ Aldehyde ω -end-group functionality was installed by terminating the ROMP with vinylene carbonate, as previously reported by Kilbinger and coworkers.⁴⁴

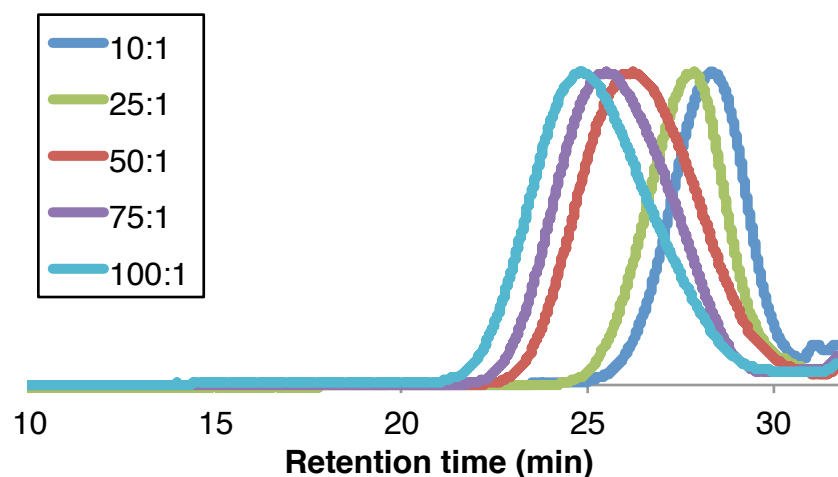


Scheme 5-1. Polymerization of monomer using ROMP. * marks end-group methylene units used for ¹H-NMR analysis.

Polymerizations were carried out in a glovebox under nitrogen atmosphere at 20-23 °C with a ratio of [Grubbs I]:[monomer **1**] = [1]:[10-100]. Polymerizations were analyzed by ¹H-NMR and after the desired conversion was achieved, polymerization was terminated by the addition of an excess of vinylene carbonate. The crude polymers were then purified by repeated precipitation into cold diethyl ether. The resulting polymers were analyzed by ¹H NMR and gel permeation chromatography (GPC) to determine the number average molecular weight (M_n) and dispersity (\mathcal{D}). M_n was determined by ¹H NMR end-group analysis by comparing the integration of the terminal phenyl protons (7.35-7.40 ppm) to the backbone alkenes (5.90-5.65 ppm). Polymers were additionally characterized by GPC using a multiangle light scattering (MALS) detector to determine M_n , M_w and \mathcal{D} (**Figure 5-1**). A total of five rPEGs were prepared with molecular weights between 6 and 20 kDa as measured by GPC (**Table 5-1**).

Table 5-1. Reaction parameters for the synthesis of aldehyde-functional rPEGs

	[M]/[C]	Conv.	Predicted MW	M _n (NMR)	% aldehyde (% methylene)	M _n (GPC)	Đ (GPC)
rPEG 1	10/1	91 %	1.8 kDa	4.3 kDa	58 (67)	6.0 kDa	1.13
rPEG 2	25/1	99 %	5.0 kDa	7.1 kDa	57 (76)	7.4 kDa	1.28
rPEG 3	50/1	95 %	9.6 kDa	11.6 kDa	53 (82)	11.5 kDa	1.54
rPEG 4	75/1	91 %	13.8 kDa	13.9 kDa	46 (65)	17.4 kDa	1.40
rPEG 5	100/1	91 %	18.4 kDa	19.5 kDa	53 (65)	19.9 kDa	1.56

**Figure 5-1.** Gel permeation chromatography (GPC) traces for the synthesized rPEGs

Molecular weight dispersities for the polymers were relatively high ($1.1 > \text{Đ} > 1.6$), which was expected for the non-living polymerization of monomer **1**.³⁹⁻⁴⁰ Furthermore, the presence of the aldehyde (9.79 ppm) could also be confirmed by ¹H NMR and ranged between 50-60% end-group retention. It should be noted that the aldehyde signals may be lower than expected due to hydrogen-deuterium exchange.⁴⁴ Therefore, end-group methylene units (2.5 ppm) resulting from the vinylene carbonate installation (proton marked with * in **Scheme 5-1**) were also compared as evidence of the aldehyde's installation and this led to 65-82% end group retention.

5.2.2. Protein Conjugation

An ω -aldehyde **rPEG** (Mn = 16,800 Da) was conjugated to hen egg-white lysozyme (Lys) *via* reductive amination (**Figure 5-2**). Lys and **rPEG** were incubated in a pH 6.0 100 mM phosphate buffer (PB) at 25 °C using a ratio [Lys]:[**rPEG**] = 1:50. A large excess of polymer was used to ensure complete conjugation to all surface exposed amines on Lys. After 1 h, sodium cyanoborohydride was added to a final concentration of 20 mM in the reaction solution. The conjugation mixture was allowed to incubate for 48 h at 25 °C, before removal of the reducing agent *via* centrifugal filtration.

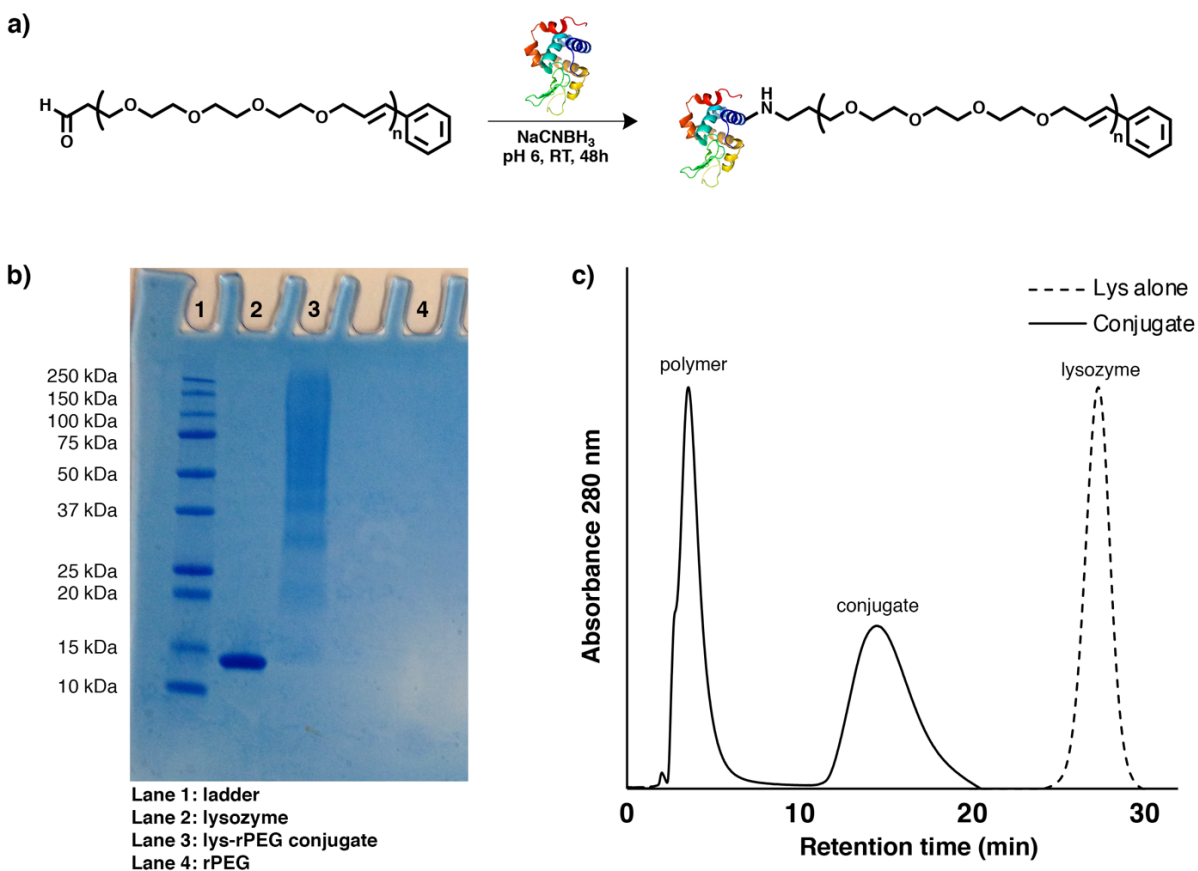


Figure 5-2. a) Conjugation of rPEG to lysozyme b) SDS-PAGE analysis C) IEX purification and analysis.

The resulting Lys-rPEG conjugate was analyzed by sodium dodecyl sulfate polyacrylamide gel electrophoresis (SDS-PAGE) (**Figure 2B**). Conjugation is evident by a high molecular weight smeared band (**Figure 2B, lane 3**), which corresponds to a higher molecular weight than the unmodified Lys (**Figure 2B, lane 2**). The conjugate was also purified and analyzed *via* ion exchange chromatography (IEX) using a fast protein liquid chromatography (FPLC) system (**Figure 2C**). The decreased charge of the conjugate due to PEGylation is apparent by IEX, where a decreased retention time of the conjugate (~14 min) compared to unmodified Lys (~27 min) was observed. Based on the SDS-PAGE and IEX results, we believe the Lys is heterogeneously modified with a high degree of conjugation to the 7 free amines present on the protein surface.⁴⁵

5.2.3. Efforts Toward rPEG Chemical Modification

Given the previous reports of backbone alkene modification on polymers generated by ROMP⁴⁶⁻⁴⁹, we were interested in carrying out the same chemistry on these rPEG analogs. Initial attempts using a single batch of polymer demonstrated clean reaction at the backbone alkenes and complete conversion to the thiol-modified product when measured by ¹H-NMR (**Figure 5-9**) and GPC (**Figure 5-3a**). However, this initial positive result was not reproducible with subsequent batches of polymer. Even with a significant excess of thiol (50 equivalents per alkene) and minimal photoinitiator concentration (0.05 equivalents per alkene), significant increases in molecular weight attributed to crosslinking were observed in the GPC traces (**Figure 5-3b**).

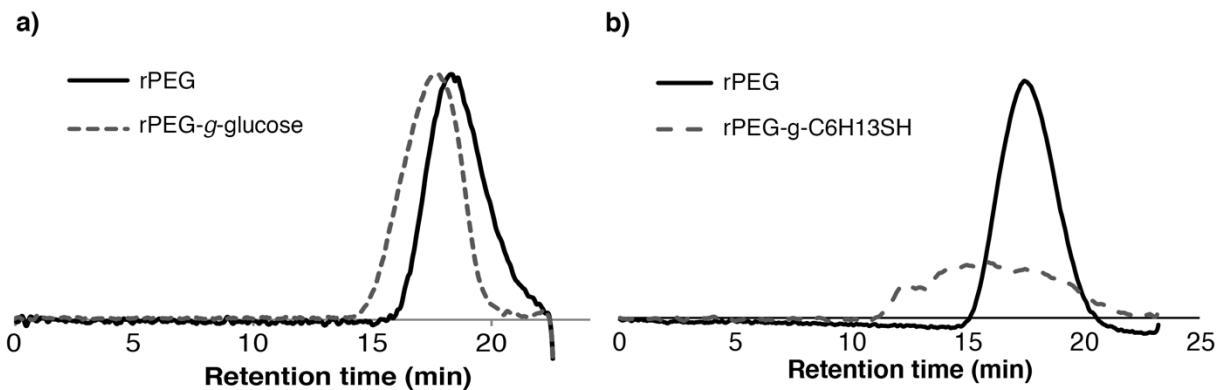
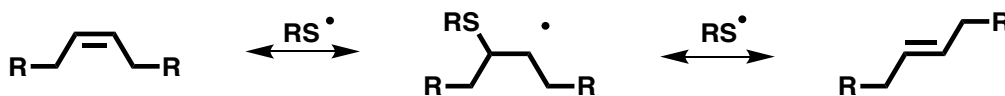


Figure 5-3. GPC trace of a) initial successful rPEG modification using thiolated glucose and b) a representative unsuccessful thiol-ene experiment using hexanethiol.

While there is a wealth of literature on mono-substituted alkene modification using radical thiols,⁵⁰ successful thiol-ene modification of 1,2-disubstituted alkenes has been more challenging. This is due not only to lack of regioselectivity in the case of asymmetrical alkenes, but also to the essential stability of carbon radicals generated during the reactions.⁵¹ Specifically, thiol addition to 1,2-disubstituted alkenes is significantly more reversible than that to terminal alkenes (**Scheme 5-2**).⁵² Some efforts to limit the reverse reaction and improve hydrogen transfer to the carbon-centered radical have been reported, among them the addition of an active hydrogen atom donor such as HBr⁵³ and the reduction of the reaction temperature⁵⁴.

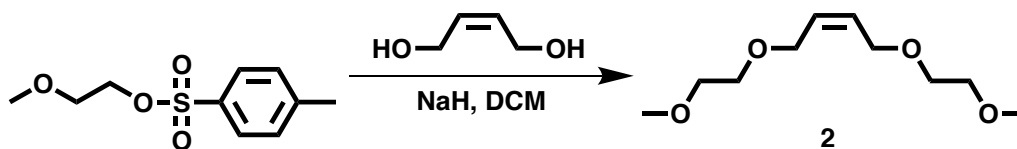


Scheme 5-2. Reversibility and isomerization of thiol-ene addition.

An additional challenge is the presence of the allyl ether functionality. It has been reported that allylic and benzylic ethers are susceptible to undesired hydrogen atom abstraction due to their

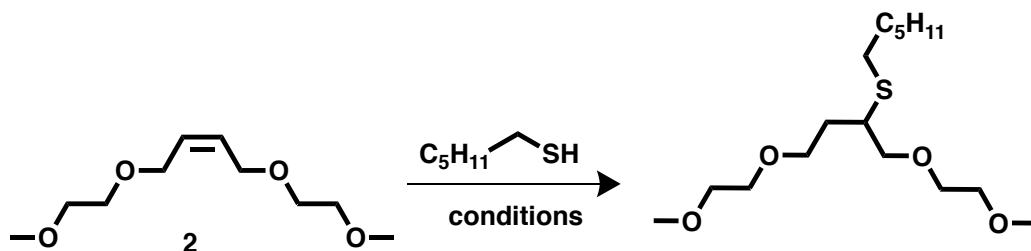
weak carbon-hydrogen bonds.⁵⁵ This structural challenge has led to the development of alternate methods, including triethylborane both with⁵⁵ and without the addition of catechol⁵⁶ as a mild radical source. It seemed likely that the previously observed crosslinking could be due to unwanted stability of carbon-centered radicals in the rPEG structure and therefore could be avoided through appropriate choice of thiol-ene conditions or additives.

Toward these aims, we synthesized a model compound based on the rPEG structure in order to easily screen thiol-ene modification conditions (**Scheme 5-3**). Briefly, tosylated methoxyethanol⁵⁷ was added to 1,4-dihydroxybutene in the presence of sodium hydride at room temperature. Flash column chromatography led to the desired unsaturated oligoethylene glycol analog **2** in 76% yield.



Scheme 5-3. Synthesis of rPEG model compound **2**.

With model compound in hand, we initially screened a variety of conditions with the goal to reduce or eliminate the reversibility of the thiol addition as well as avoid the undesired abstraction of allylic hydrogen atoms (**Table 5-2**). In these studies, hexanethiol was used as a model thiol for ease of purification (**Scheme 5-4**).



Scheme 5-4. Thiol-ene modification of rPEG model compound **2** with hexanethiol.

Table 5-2. Screen of thiol-ene conditions for the modification of rPEG model compound **2**.

Entry	Conditions	Eq. thiol	Temp	Relative percentages (<i>cis</i> - 2 : <i>trans</i> - 2 : product) ^a
1	DMPA	5	25 °C	n.d. ^b
2	DMPA/TTMSS	5	25 °C	86% : 14% : 0%
3	Et ₃ B/catechol	3	25 °C	55% : 45% : 0%
4	DMPA	5	-78 °C	53% : 5% : 42%
5	DMPA	20	-78 °C	27% : 8% : 65%
6	DMPA	100	-78 °C	22% : 2% : 76%

^a As measured by ¹H-NMR. ^b Significant impurities in the crude ¹H-NMR spectrum overlapped with both starting material and product peaks (**Figure 5-12**).

In this initial screen, addition of a hydrogen atom donor, such as tris(trimethylsilyl)silane (TTMSS), resulted in formation of no product, perhaps due to competition of the silyl radicals with the thiol radicals for addition to the alkene. Initiation with triethylborane and complexation with *tert*-butylcatechol resulted only in *cis*/*trans* isomerization and no product formation. However, lowering the temperature resulted in increased conversion to the desired thioether product, presumably by reducing the competing background reversion from the thioether to the *trans*-alkene. Increasing thiol equivalents resulted in improved conversion rates, with 65% conversion observed using 20 equivalents of thiol per alkene and 76% conversion using 100 equivalents of thiol per alkene. In comparison to the thiol-ene reaction at room temperature (**Figure 5-12**), the

¹H-NMR spectrum of the reaction mixture at -78 °C showed clean peaks and minimal byproducts (**Figure 5-13**).

These optimized conditions were then used to modify rPEG with hexanethiol. In this case, while crosslinking was not apparent in the GPC chromatogram (**Figure 5-14**), ¹H-NMR analysis indicated modification had mixed success (**Figure 5-15**). Minimal loss of alkene protons were observed at 5.7 ppm, but significant increase in hexanethiol protons at 0.8 ppm could be measured. Additionally, the molecular weight was smaller after modification, indicating some kind of backbone scission. It is possible that the presence of residual ruthenium in the polymer interferes with the radical thiol-ene reaction, leading to minimal modification or radical-initiated chain scission. Previous attempts to modify tris(hydroxymethyl)phosphine-purified⁵⁸ rPEG also led to crosslinked polymer (data not shown). However, these modifications were carried out at 25 °C. In the future, modification of a ruthenium-free polymer using the low-temperature modification conditions (-78 °C) will be investigated, in the hope that it may lead to high conversion with minimal crosslinking.

5.3. Conclusions

Using ring-opening metathesis polymerization, a series of unsaturated rPEGs of molecular weight 6 and 20 kDa were prepared with protein-reactive aldehyde ω-end-group functionality and end-group retention between 65% and 82%. Subsequent conjugation *via* reductive amination to lysozyme as a model protein was demonstrated and the protein-polymer conjugate was purified using ion exchange chromatography. The characteristic unsaturated ROMP backbone was explored as a method of synthesizing functional PEG polymers. While initial thiol-ene experiments were successful, modification of subsequent polymer batches led to crosslinking and

unreproducible conversion efficiencies. A model compound was synthesized containing similar allyl ether functionality and used to screen a series of conditions for thiol-ene modification, with low temperature (-78 °C) yielding up to 76% conversion. However, these conditions were not successfully translated to modification of rPEG. Currently we are exploring further modification of the material using alternate alkene-reactive chemistries.

5.4. Materials and Methods

5.4.1. Materials

All materials and proteins were purchased from Sigma-Aldrich, Acros, or Fisher Scientific and were used without purification unless noted. Anhydrous toluene was distilled from CaH_2 and stored under argon prior to use. Anhydrous tetrahydrofuran (THF) was distilled from sodium benzophenone and stored under argon prior to use. Anhydrous dichloromethane (DCM) was distilled from CaH_2 and stored under argon prior to use. Cyclic PEG monomer was synthesized as previously described⁴⁰, ruthenium catalyst was removed⁵⁸ and the monomer was distilled under reduced pressure before use. As a precaution, LiClO_4 templated ring-closing metathesis was performed on small scale (<2.5 g) behind a blast shield. Polymerizations were carried out in a Vacuum Atmospheres Genesis stainless steel glove box under anhydrous nitrogen atmosphere.

5.4.2. Analytical Techniques

NMR spectra were obtained on Bruker AV 500 and DRX 500 MHz spectrometers. ^1H -NMR spectra were acquired with a relaxation delay of 2 s for small molecules and 30 s for polymers. Infrared absorption spectra were recorded using a PerkinElmer FT-IR equipped with an ATR accessory. High-resolution mass spectra were obtained on Waters LCT Premier with ACQUITY LC and ThermoScientific Exactive Mass Spectrometers with DART ID-CUBE. Gel Permeation Chromatography (GPC) was conducted on a Shimadzu high performance liquid chromatography (HPLC) system with a refractive index detector RID-10A, one Polymer Laboratories PLgel guard column, and two Polymer Laboratories PLgel 5 μm mixed D columns. Eluent was DMF with LiBr (0.1 M) at 50 °C (flow rate: 0.80 mL/ min). Calibration was performed using near-monodisperse PEG and PMMA standards from Polymer Laboratories. Right-Angle Light Scattering GPC

(RALS-GPC) GPC was conducted on a Shimadzu HPLC Prominence-i system equipped with a UV detector, Wyatt DAWN Heleos-II Light Scattering detector, Wyatt Optilab T-rEX RI detector, one MZ-Gel SDplus guard column, and two MZ-Gel SDplus 100 Å 5µm 300x8.0 mm columns. Eluent was THF at 40 °C (flow rate: 0.70 mL/min). A dn/dc value of 0.067 mL/g for PEG in THF was used (Polymer Source). SDS-PAGE was performed using Bio-Rad Any kD Mini-PROTEAN-TGX gels. SDS-PAGE protein standards were obtained from Bio-Rad (Precision Plus Protein Prestained Standards). For SDS-PAGE analysis, approximately 5 µg of protein was loaded into each lane. SEC was performed on a Bio-Rad BioLogic DuoFlow chromatography system equipped with a HiTrap Heparin HP affinity column. A 10 mM sodium phosphate (pH 7.0) buffer containing was used as the solvent (flow rate: 0.4 mL/min) and the salt strength was increased from 0M to 1M in a linear gradient.

5.4.3. Methods

Representative ROMP polymerization of cyclic monomer 1

Cyclic unsaturated monomer **1** was synthesized as previously described.³⁹ In a nitrogen-filled glovebox, Grubbs I (8 mg, 0.1 mmol) was dissolved in dichloromethane (495 µL) and added to a dram vial with stir bar containing monomer **1** (100 mg, 0.49 mmol). The polymerization solution was stirred rapidly at room temperature for 4 hours before addition of vinylene carbonate (75 µL) and letting stir an additional 60 minutes. The reaction vial was then removed from the box and residual active catalyst was further quenched with ethyl vinyl ether (150 µL) and stirred for an additional 75 minutes. The polymer was then precipitated 2x into cold ether (20 mL) and dried in vacuo to yield a tan oil (76 mg, 76% yield). M_N (¹H-NMR) = 11.6 kDa, M_N (GPC) = 11.5 kDa, M_w (GPC) = 17.8 kDa, \bar{D} = 1.54. ¹H-NMR (500 MHz in CD₃CN) δ : 9.67 (t, J = 2 Hz, 1H), 7.42

(d, $J = 7.5$ Hz, 2H), 7.32 (t, $J = 7.5$ Hz, 2H), 7.24 (t, $J = 7.3$ Hz, 1H), 6.61 (d, $J = 16$ Hz, 1H), 6.32 (dt, $J = 16, 5.8$ Hz, 1H), 5.89-5.55 (m, 112H), 4.14-3.89 (m, 226H), 3.71-3.42 (m, 690H), 2.58 (dt, $J = 1.8, 5.9$ Hz, 2H).

Representative conjugation of rPEG to lysozyme and purification of conjugate

In a LoBind Eppendorf tube, lysozyme (1 mg) was dissolved in 100 mM phosphate buffer, pH 6.0 (400 μ L). **rPEG** ($M_n = 16,800$) was separately dissolved in the same buffer (500 μ L) and combined. The solution was incubated with shaking at 20 °C for fifteen minutes and then a solution of NaCNBH₃ in buffer (200 mM, 100 μ L) was added. The conjugation mixture was incubated at 20 °C for 48 hours before purification. To purify, the crude mixture was exchanged using centrifugal filtration into a 10 mM phosphate buffer, pH 7.0. The solution was divided into 3 runs and the crude separated by FPLC using a HiTrap Heparin HP affinity column as anionic ion exchange column at 0.4 mL/min and a gradient from 0M to 1M HCl. Conjugate-containing fractions were pooled, concentrated using centrifugal filtration, and analyzed by SDS-PAGE to confirm purity.

Representative thiol-ene reaction using DMPA as photoinitiator

In a dram vial with stir bar, **rPEG** (7 mg, 34.6 μ mol alkene units) was dissolved in anhydrous THF (700 μ L). 1-thio- β -D-glucose tetraacetate (554 mg, 1.52 mmol, 50 equivalents relative to alkene) and DMPA (1.56 mg, 6.1 μ mol, 0.2 equivalents relative to alkene) were added and the mixture degassed by sparging for 10 minutes. Then the vial was exposed to 365 nm light for 2.5 hours. To purify, the solution was slightly concentrated in vacuo and precipitated into cold ether four times. M_N (GPC) = 10.7 kDa, M_W (GPC) = 16.3 kDa, $\bar{D} = 1.52$. ¹H-NMR (500 MHz in CD₃CN) δ : 5.72-

5.15 (m, 1H per repeat unit), 5.06-4.93 (m, 1H), 4.92-4.80 (m, 2H), 4.25-4.12 (m, 1H), 4.12-3.97 (m, 1H), 3.89-3.75 (m, 1H), 3.74-3.43 (m, 16H), 3.19-3.04 (m, 1H), 2.08-1.88 (m, 15H), 1.72-1.56 (m, 1H).

Synthesis of rPEG model compound 2

A flame-dried 25 mL round bottom flask with stir bar was charged with NaH (68 mg, 1.70 mmol) and suspended in anhydrous DMF (3 mL). A solution of 1,4-dihydroxybutene (46 μ L, 50 mg, 0.57 mmol) in anhydrous DMF (1 mL) was added and stirred for 5 minutes, followed by the addition of a solution of 2-methoxyethanol tosylate⁵⁷ (392 mg, 1.70 mmol) in anhydrous DMF (1 mL). The reaction was let stir at room temperature for 46 hours. To quench, the mixture was poured into water and extracted 3x with EtOAc. The organic layers were combined, dried over MgSO₄, and solvent was removed in vacuo. The crude material was purified by Biotage using an EtOAc/DCM gradient to yield a colorless oil (67.5 mg, 0.33 mmol, 58%). ¹H-NMR (500 MHz in CDCl₃) δ : 5.74 (ddd, J = 1, 3.7, 4.7 Hz, 2H), 4.10 (dd, 1, 3.7 Hz, 4H), 3.59-3.53 (m, 8H), 3.38 (s, 6H). ¹³C-NMR (500 MHz in CDCl₃) δ : 129.4, 72.0, 69.4, 66.9, 59.1. IR: ν = 2874, 1455, 1367, 1329, 1287, 1244, 1198, 1091, 1038, 982, 882, 849, 708. MS-QTOF (m/z) [M+Na]⁺ calcd for C₁₀H₂₀NaO₄ 227.1259; found 227.1302.

Thiol-ene reaction using Et3B + catechol as radical initiators

In a flame-dried dram vial with stir bar, compound **2** (10 mg, 0.049 mmol), hexanethiol (21 μ L, 0.147 mmol), and *tert*-butyl catechol (10 mg, 0.058 mmol) were dissolved in anhydrous dichloromethane (100 μ L) under argon. Triethylborane (1M in hexanes, 60 μ L) was added and let

stir under argon for 2 h. Volatiles were removed under reduced pressure and conversion was assessed by $^1\text{H-NMR}$.

5.5. Appendix with Supplementary Figures

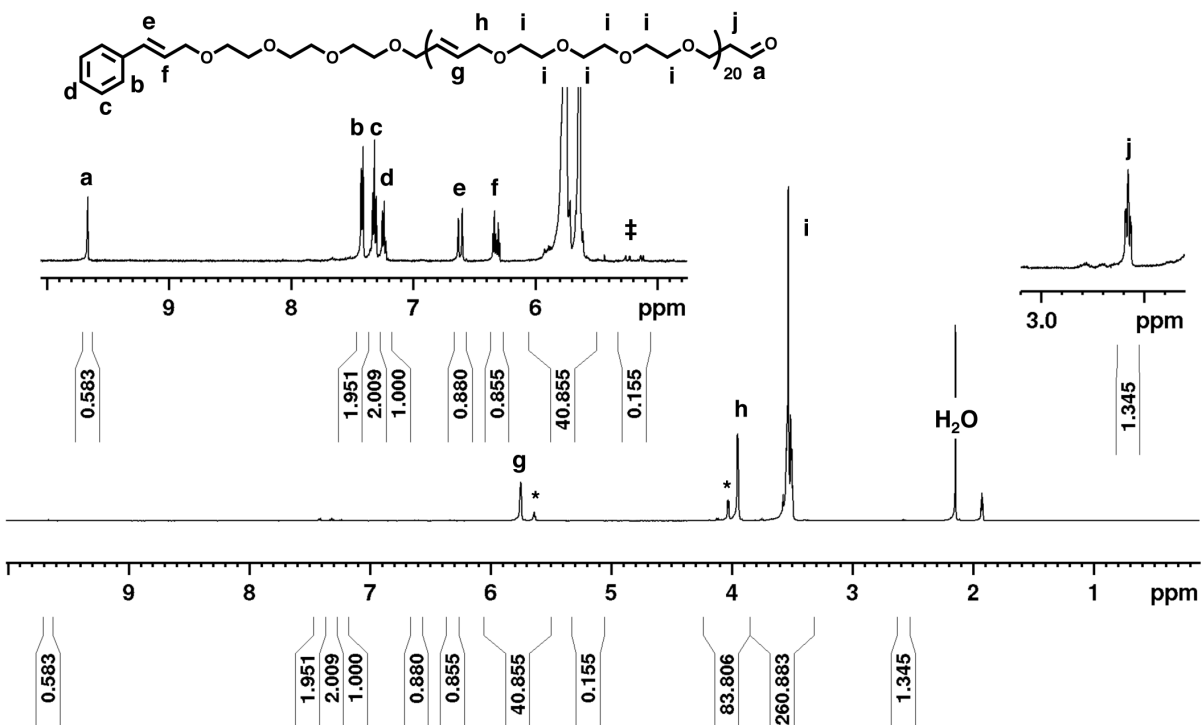


Figure 5-4. ¹H-NMR spectrum of 10:1 rPEG polymer (500 MHz, CD₃CN). * indicates protons corresponding to *cis* backbone alkenes. ‡ indicates protons corresponding to a terminal alkene unit.

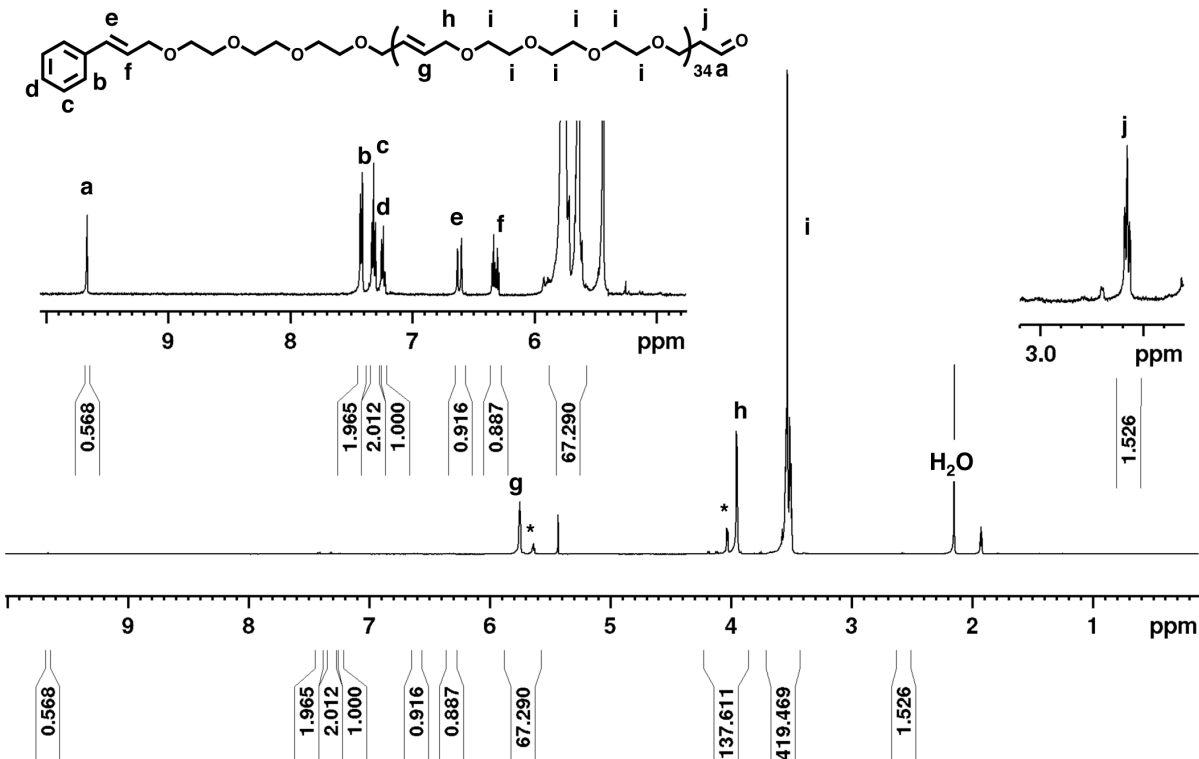


Figure 5-5. ¹H-NMR spectrum of 25:1 rPEG polymer (500 MHz, CD₃CN). * indicates protons corresponding to *cis* backbone alkenes.

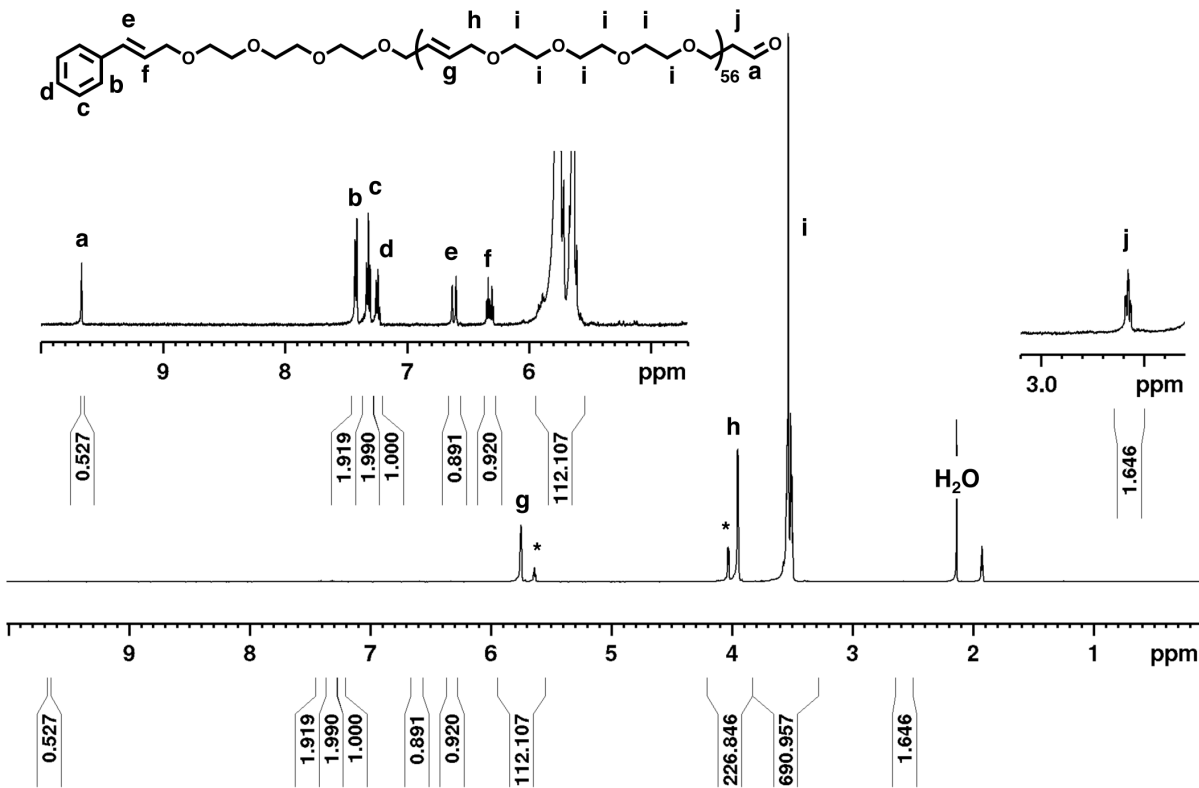


Figure 5-6. ¹H-NMR spectrum of 50:1 rPEG polymer (500 MHz, CD₃CN). * indicates protons corresponding to *cis* backbone alkenes.

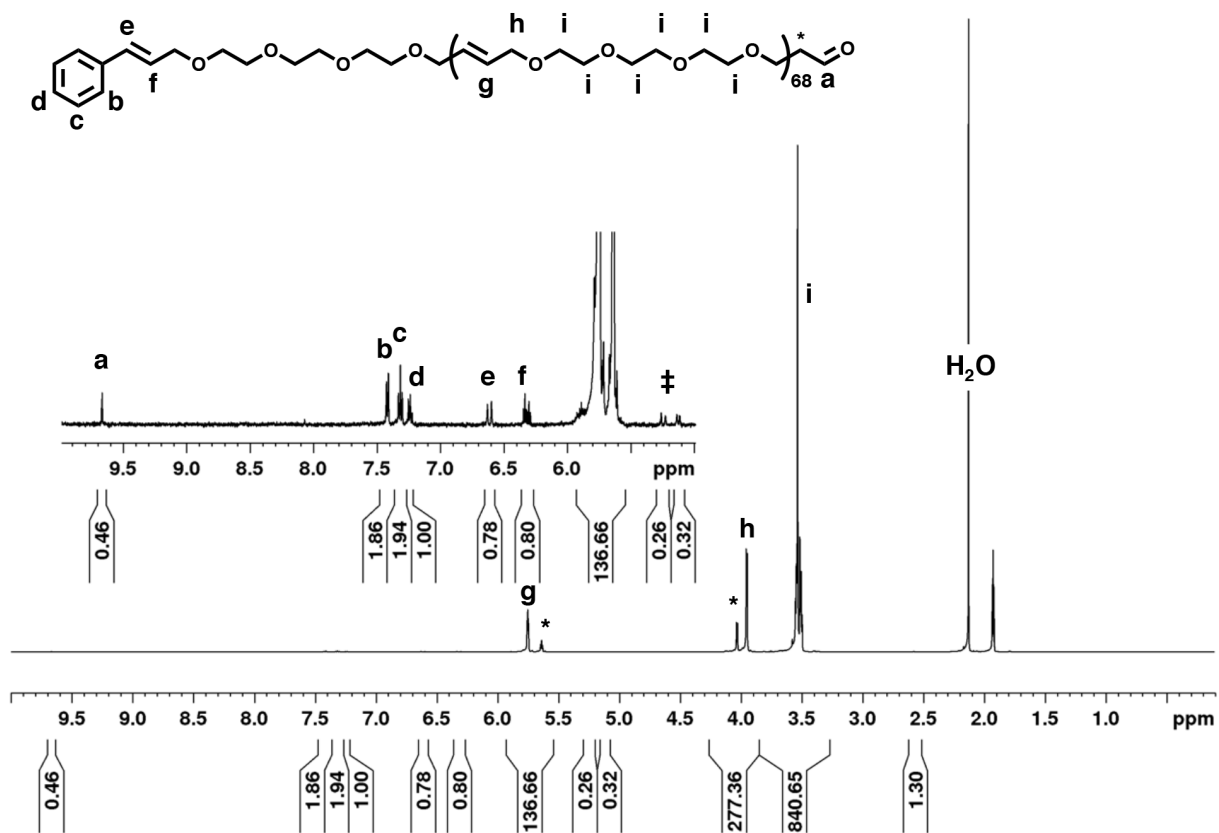


Figure 5-7. ¹H-NMR spectrum of 75:1 rPEG polymer (500 MHz, CD₃CN). * indicates protons corresponding to *cis* backbone alkenes. ‡ indicates protons corresponding to a terminal alkene unit.

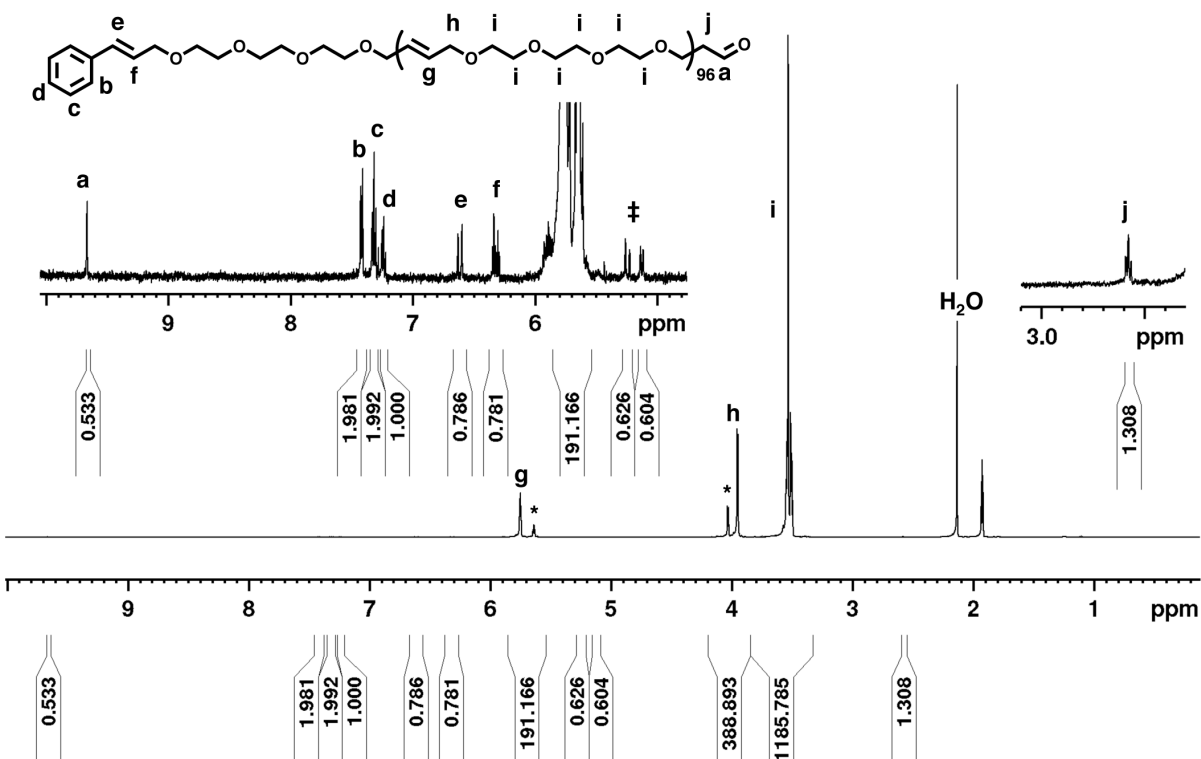


Figure 5-8. $^1\text{H-NMR}$ spectrum of 100:1 rPEG polymer (500 MHz, CD_3CN). * indicates protons corresponding to *cis* backbone alkenes. ‡ indicates protons corresponding to a terminal alkene unit.

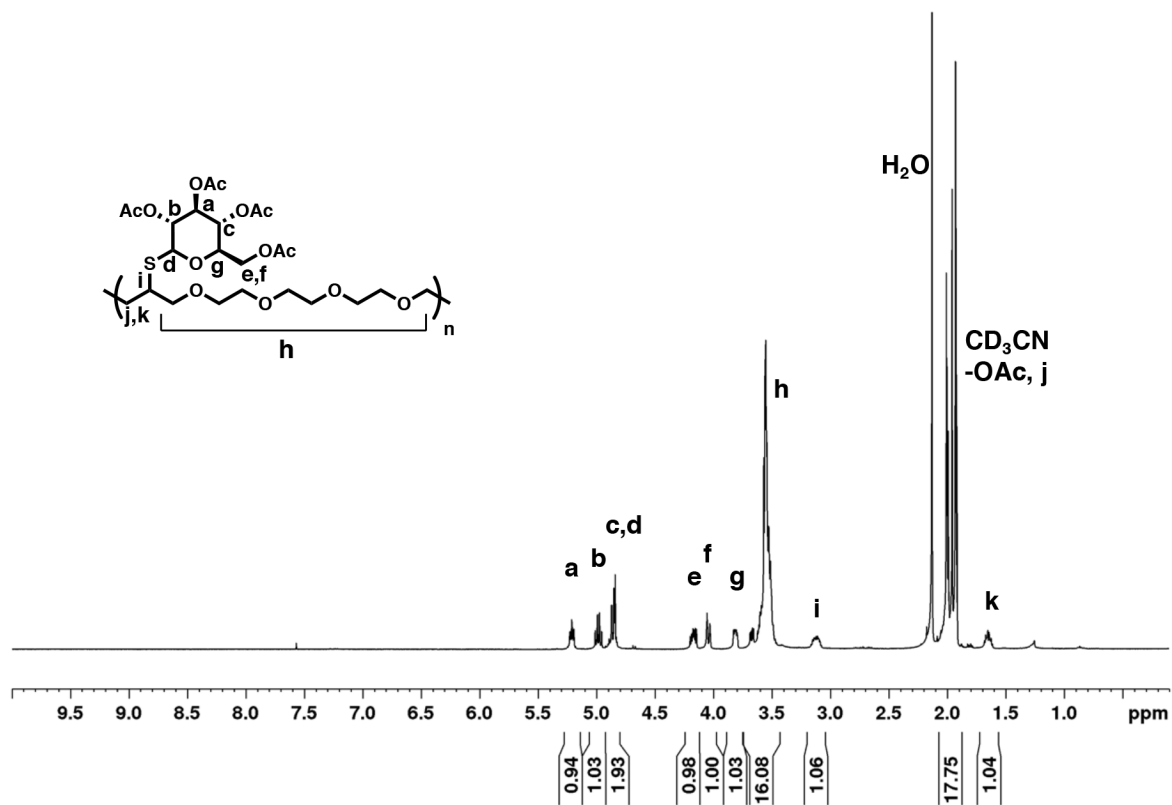


Figure 5-9. ¹H-NMR spectrum of successful thiol-ene product rPEG-g-glucose (500 MHz, CD₃CN).

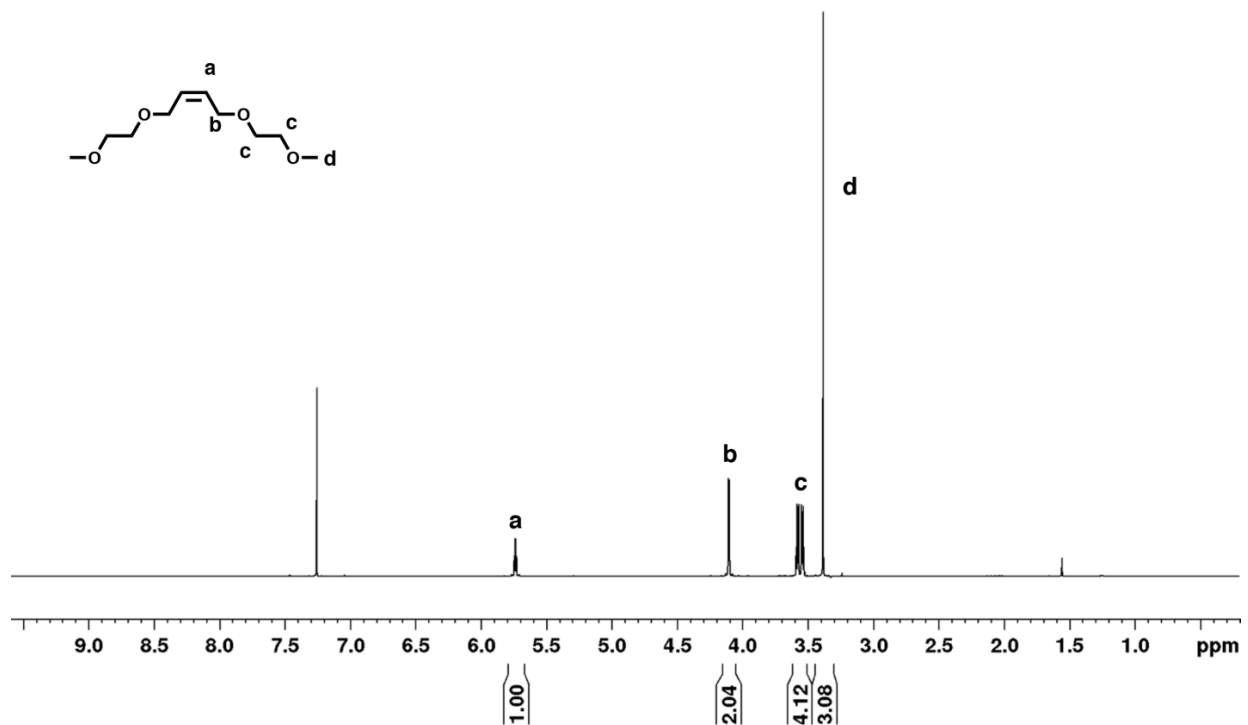


Figure 5-10. ^1H -NMR spectrum of rPEG model 2 (500 MHz, CDCl_3).

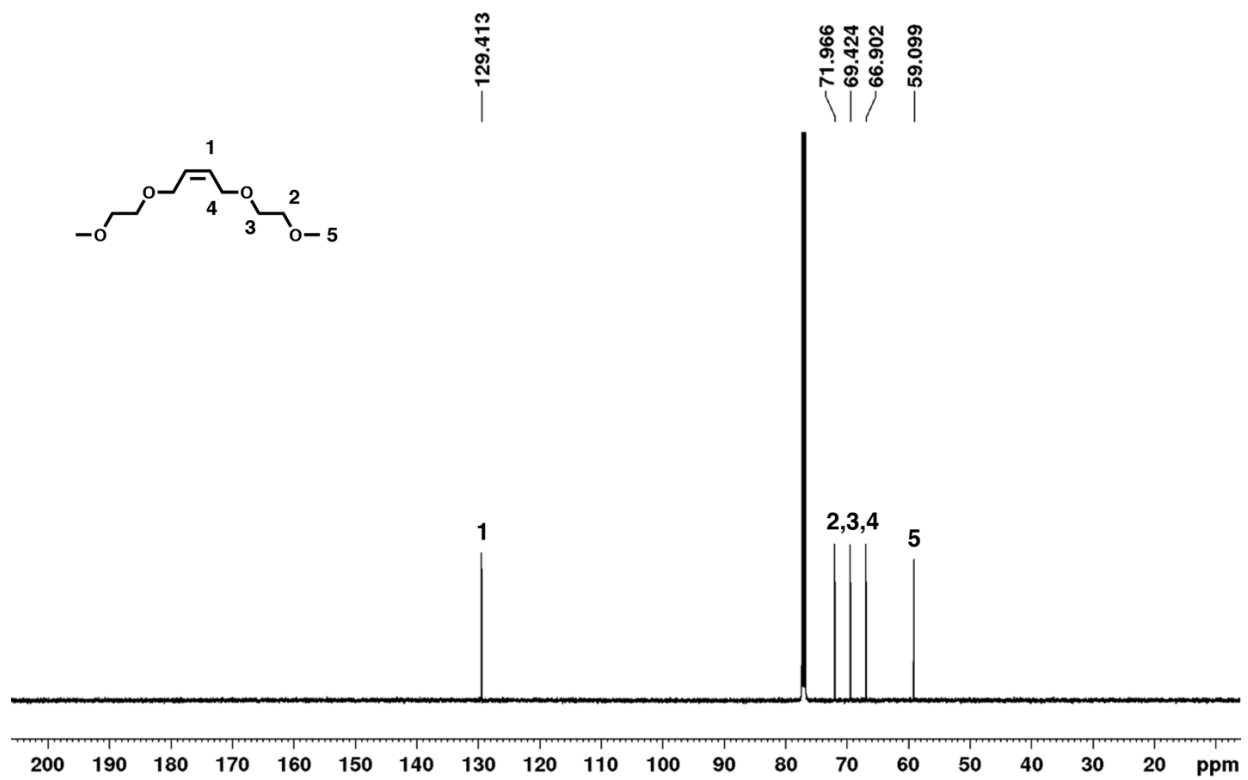


Figure 5-11. ^{13}C -NMR spectrum of rPEG model 2 (500 MHz, CDCl_3).

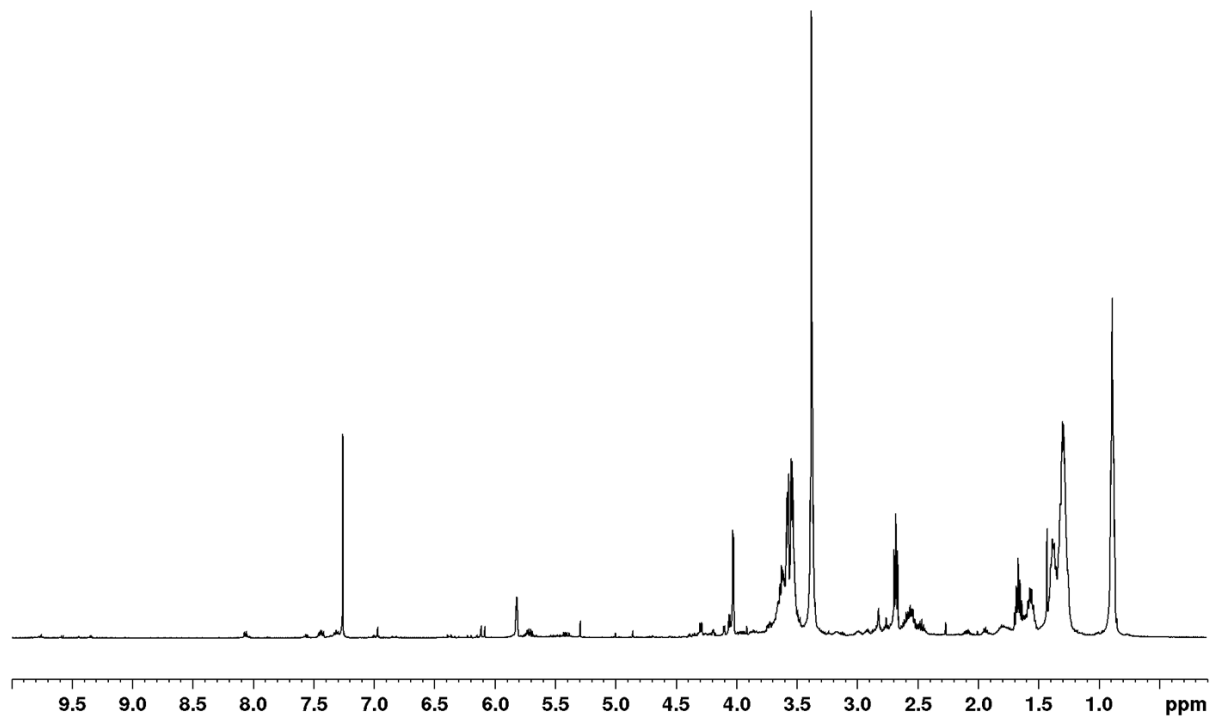


Figure 5-12. Crude $^1\text{H-NMR}$ spectrum of model thiol-ene (Table 5-2, entry 1) (500 MHz, CDCl_3).

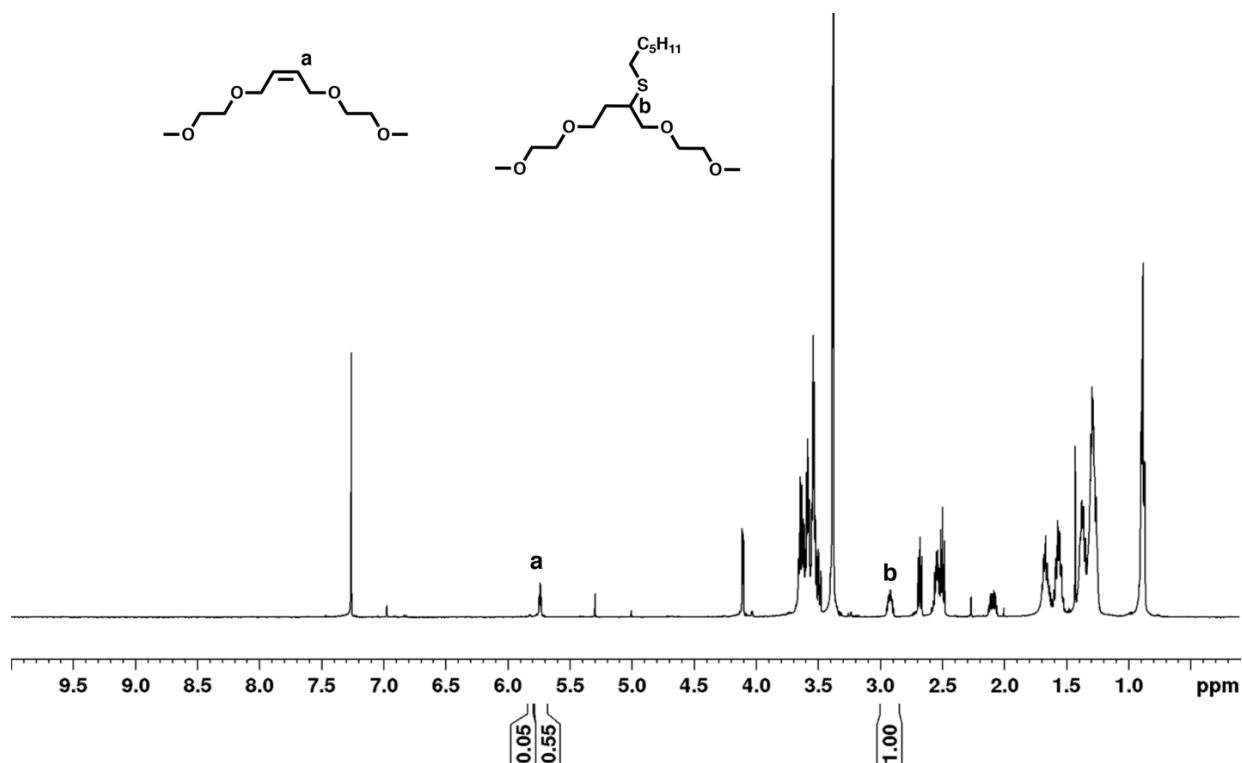


Figure 5-13. Crude $^1\text{H-NMR}$ spectrum of model thiol-ene (Table 5-2, entry 6) (500 MHz, CDCl_3).

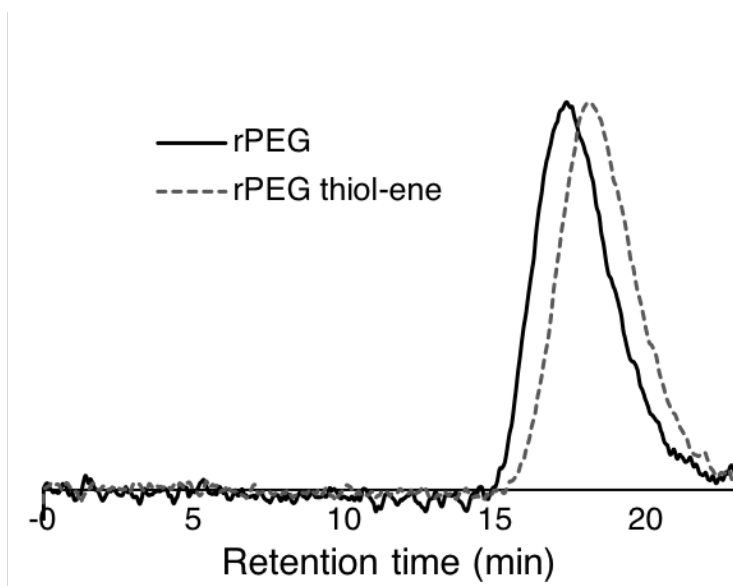


Figure 5-14. DMF GPC trace of rPEG and rPEG using optimized thiol-ene conditions at $-78\text{ }^\circ\text{C}$.

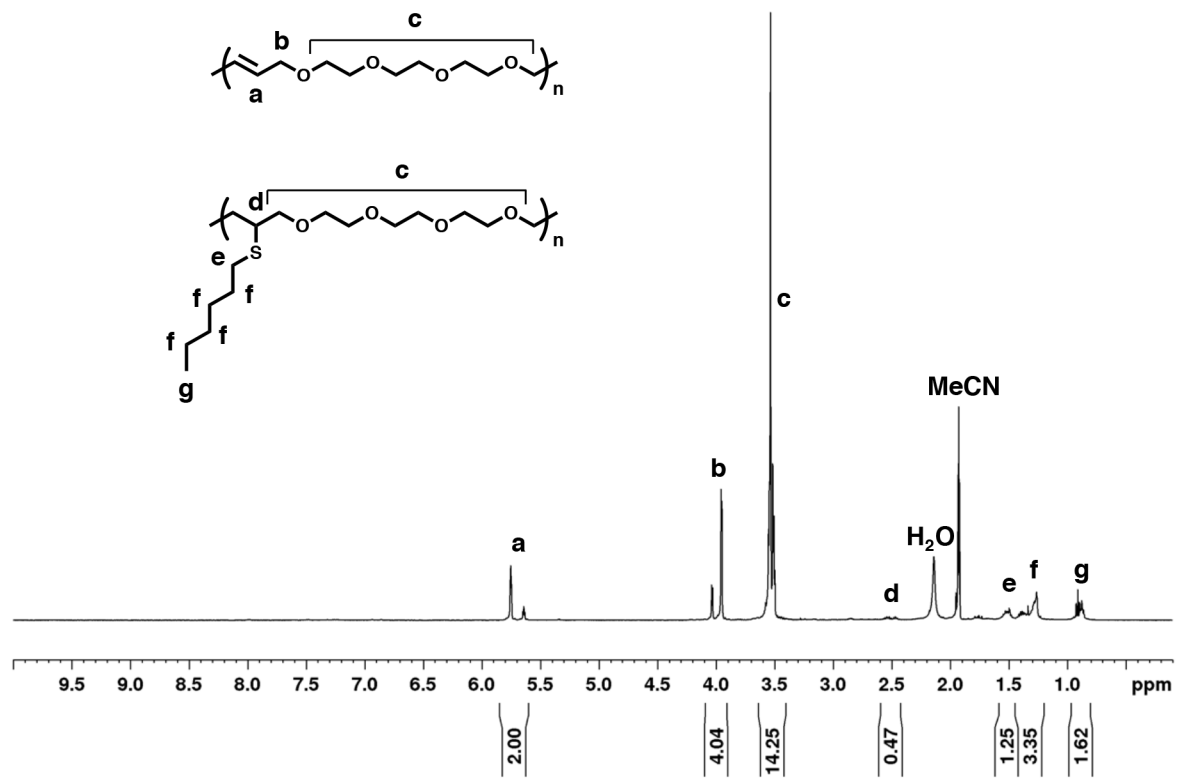


Figure 5-15. ¹H-NMR spectrum of thiol-ene using optimized conditions at -78 °C (500 MHz, CD₃CN).

5.6. References

1. Abuchowski, A.; McCoy, J. R.; Palczuk, N. C.; Vanes, T.; Davis, F. F., *J. Biol. Chem.* **1977**, *252*, 3582.
2. Abuchowski, A.; Vanes, T.; Palczuk, N. C.; Davis, F. F., *J. Biol. Chem.* **1977**, *252*, 3578.
3. Harris, J. M.; Chess, R. B., *Nat. Rev. Drug Discov.* **2003**, *2*, 214.
4. Alconcel, S. N. S.; Baas, A. S.; Maynard, H. D., *Polym. Chem.* **2011**, *2*, 1442.
5. Pelegri-O'Day, E. M.; Lin, E.-W.; Maynard, H. D., *J. Am. Chem. Soc.* **2014**, *136*, 14323.
6. Janssen, H. M.; Peeters, E.; van Zundert, M. F.; van Genderen, M. H. P.; Meijer, E. W., *Macromolecules* **1997**, *30*, 8113.
7. Janssen, H. M.; Peeters, E.; van Zundert, M. F.; van Genderen, M. H. P.; Meijer, E. W., *Angew. Chem. Int. Ed.* **1997**, *36*, 122.
8. Peeters, E.; Janssen, H. M.; van Zundert, M. F.; van Genderen, M. H. P.; Meijer, E. W., *Acta Polym.* **1996**, *47*, 485.
9. Illy, N.; Taylan, E.; Brissault, B.; Wojno, J.; Boileau, S.; Barbier, V.; Penelle, J., *Eur. Polym. J.* **2013**, *49*, 4087.
10. Li, S. M.; Rashkov, I.; Espartero, J. L.; Manolova, N.; Vert, M., *Macromolecules* **1996**, *29*, 57.
11. Metters, A. T.; Anseth, K. S.; Bowman, C. N., *Polymer* **2000**, *41*, 3993.
12. Sawhney, A. S.; Pathak, C. P.; Hubbell, J. A., *Macromolecules* **1993**, *26*, 581.
13. Zhu, K. J.; Xiangzhou, L.; Shilin, Y., *J. Appl. Polym. Sci.* **1990**, *39*, 1.
14. Lundberg, P.; Lee, B. F.; van den Berg, S. A.; Pressly, E. D.; Lee, A.; Hawker, C. J.; Lynd, N. A., *ACS Macro Lett.* **2012**, *1*, 1240.

15. Lee, Y.; Koo, H.; Jin, G. W.; Mo, H. J.; Cho, M. Y.; Park, J. Y.; Choi, J. S.; Park, J. S., *Biomacromolecules* **2005**, *6*, 24.
16. Sun, K. H.; Sohn, Y. S.; Jeong, B., *Biomacromolecules* **2006**, *7*, 2871.
17. Obermeier, B.; Wurm, F.; Mangold, C.; Frey, H., *Angew. Chem. Int. Ed.* **2011**, *50*, 7988.
18. Herzberger, J.; Niederer, K.; Pohlit, H.; Seiwert, J.; Worm, M.; Wurm, F. R.; Frey, H., *Chem. Rev.* **2016**, *116*, 2170.
19. Obermeier, B.; Frey, H., *Bioconj. Chem.* **2011**, *22*, 436.
20. Reuss, V. S.; Obermeier, B.; Dingels, C.; Frey, H., *Macromolecules* **2012**, *45*, 4581.
21. Li, Z.; Chau, Y., *Bioconj. Chem.* **2009**, *20*, 780.
22. Tonhauser, C.; Alkan, A.; Schomer, M.; Dingels, C.; Ritz, S.; Mailander, V.; Frey, H.; Wurm, F. R., *Macromolecules* **2013**, *46*, 647.
23. Trnka, T. M.; Grubbs, R. H., *Acc. Chem. Res.* **2001**, *34*, 18.
24. Hilf, S.; Kilbinger, A. F. M., *Nat Chem* **2009**, *1*, 537.
25. Kanai, M.; Mortell, K. H.; Kiessling, L. L., *J. Am. Chem. Soc.* **1997**, *119*, 9931.
26. Manning, D. D.; Hu, X.; Beck, P.; Kiessling, L. L., *J. Am. Chem. Soc.* **1997**, *119*, 3161.
27. Allen, M. J.; Raines, R. T.; Kiessling, L. L., *J. Am. Chem. Soc.* **2006**, *128*, 6534.
28. Asgatay, S.; Franceschi-Messant, S.; Perez, E.; Vicendo, P.; Rico-Lattes, I.; Phez, E.; Rols, M. P., *Int. J. Pharm.* **2004**, *285*, 121.
29. Biagini, S. C. G.; Davies, R. G.; Gibson, V. C.; Giles, M. R.; Marshall, E. L.; North, M.; Robson, D. A., *Chem. Commun.* **1999**, 235.
30. Carrillo, A.; Yanjarappa, M. J.; Gujraty, K. V.; Kane, R. S., *J. Polym. Sci. Pol. Chem.* **2006**, *44*, 928.

31. Madkour, A. E.; Koch, A. H. R.; Lienkamp, K.; Tew, G. N., *Macromolecules* **2010**, *43*, 4557.
32. Maynard, H. D.; Okada, S. Y.; Grubbs, R. H., *Macromolecules* **2000**, *33*, 6239.
33. Owen, R. M.; Gestwicki, J. E.; Young, T.; Kiessling, L. L., *Org. Lett.* **2002**, *4*, 2293.
34. Maynard, H. D.; Okada, S. Y.; Grubbs, R. H., *J. Am. Chem. Soc.* **2001**, *123*, 1275.
35. Carrillo, A.; Gujraty, K. V.; Rai, P. R.; Kane, R. S., *Nanotechnology* **2005**, *16*, S416.
36. Chen, B.; Metera, K.; Sleiman, H. F., *Macromolecules* **2005**, *38*, 1084.
37. Isarov, S. A.; Pokorski, J. K., *ACS Macro Lett.* **2015**, *4*, 969.
38. Isarov, S. A.; Lee, P. W.; Pokorski, J. K., *Biomacromolecules* **2016**, *17*, 641.
39. Marsella, M. J.; Maynard, H. D.; Grubbs, R. H., *Angew. Chem.-Int. Edit. Engl.* **1997**, *36*, 1101.
40. Maynard, H. D.; Grubbs, R. H., *Macromolecules* **1999**, *32*, 6917.
41. Bentley, M. D.; Roberts, M. J.; Harris, J. M., *J. Pharm. Sci.* **1998**, *87*, 1446.
42. Pound, G.; McKenzie, J. M.; Lange, R. F. M.; Klumperman, B., *Chem. Commun.* **2008**, 3193.
43. Tao, L.; Mantovani, G.; Lecolley, F.; Haddleton, D. M., *J. Am. Chem. Soc.* **2004**, *126*, 13220.
44. Hilf, S.; Grubbs, R. H.; Kilbinger, A. F. M., *J. Am. Chem. Soc.* **2008**, *130*, 11040.
45. Masuda, T.; Ide, N.; Kitabatake, N., *Chem. Senses* **2005**, *30*, 667.
46. Lowe, A. B.; Liu, M. N.; van Hensbergen, J. A.; Burford, R. P., *Macromol. Rapid Commun.* **2014**, *35*, 391.
47. van Hensbergen, J. A.; Burford, R. P.; Lowe, A. B., *J. Polym. Sci., Part A: Polym. Chem.* **2013**, *51*, 487.

48. Wolfberger, A.; Rupp, B.; Kern, W.; Griesser, T.; Slugovc, C., *Macromol. Rapid Commun.* **2011**, *32*, 518.
49. Xiao, Z. Y.; Bennett, C. W.; Connal, L. A., *J. Polym. Sci. Pol. Chem.* **2015**, *53*, 1957.
50. Hoyle, C. E.; Bowman, C. N., *Angew. Chem. Int. Ed.* **2010**, *49*, 1540.
51. Claudino, M.; Johansson, M.; Jonsson, M., *Eur. Polym. J.* **2010**, *46*, 2321.
52. Griesbaum, K., *Angew. Chem. Int. Ed.* **1970**, *9*, 273.
53. Skell, P. S.; Allen, R. G., *J. Am. Chem. Soc.* **1960**, *82*, 1511.
54. Eszenyi, D.; Kelemen, V.; Balogh, F.; Bege, M.; Csavas, M.; Herczegh, P.; Borbas, A., *Chem. - Eur. J* **2018**, *24*, 4532.
55. Povie, G.; Tran, A. T.; Bonnaffe, D.; Habegger, J.; Hu, Z. Y.; Le Narvor, C.; Renaud, P., *Angew. Chem. Int. Ed.* **2014**, *53*, 3894.
56. Gorges, J.; Kazmaier, U., *Eur. J. Org. Chem.* **2015**, 8011.
57. Hooper, R.; Lyons, L. J.; Mapes, M. K.; Schumacher, D.; Moline, D. A.; West, R., *Macromolecules* **2001**, *34*, 931.
58. Maynard, H. D.; Grubbs, R. H., *Tetrahedron Lett.* **1999**, *40*, 4137.